KINEMATIC ANALYSIS AND SIMULATION STUDIES OF INTERVERTEBRAL MOTION

By

AVINASH GAJANAN PATWARDHAN

Bachelor of Engineering
Nagpur University
Nagpur, India
1972

Master of Engineering
Indian Institute of Science
Bangalore, India
1974

Submitted to the Faculty of the Graduate College
of the Oklahoma State University
in partial fulfillment of the requirements
for the Degree of
DOCTOR OF PHILOSOPHY
May, 1980

KINEMATIC ANALYSIS AND SIMULATION STUDIES

OF INTERVERTEBRAL MOTION

Thesis Approved:

Thesis Adviser

Dean of the Graduate College

ACKNOWLEDGMENTS

I take this opportunity to express my sincere gratitude to all who have helped in any way to make this study possible. In particular, I am grateful to Dr. A. H. Soni, chairman of my advisory committee, for his continuous encouragement and guidance which were instrumental in the successful completion of this research. I wish to express my sincere appreciation of his confidence in my ability and personal counsel throughout the course of my graduate study. I wish to thank Dr. J. Andy Sullivan, of the University of Oklahoma Health Sciences Center, for providing me with the necessary human spine specimens and for his willingness to spend several hours of his time with me during the experimental work. I am also thankful to my other committee members, Dr. R. L. Lowery, Dr. L. D. Zirkle, and Dr. P. F. Duvall, for their encouragement and helpful suggestions.

I am thankful to my friends, Dr. Jack Lee, Dr. Amnon Vadasz, and Dr. Malladi Siddhanty, for providing encouragement during the early part of my graduate study.

I wish to thank Mr. Preston Wilson and Mr. Arlen Harris of the Mechanical Engineering Laboratory for fabricating the experimental setup.

Financial assistance from the School of Mechanical Engineering and the Orthopaedic Research and Education Foundation is gratefully acknowledged.

I wish to thank Ms. Charlene Fries for doing an excellent job in typing this thesis, and Mr. Y. C. Tsai and Dr. T. S. Kale for drawing the figures for this thesis.

I am particularly indebted to my parents, whose spiritual, material, and inspirational encouragement made this goal possible. I am grateful to my wife Vandana whose love and understanding helped me pull through the last year of my work, and to my daughter Jennifer for letting me work during these past few months.

TABLE OF CONTENTS

LIST OF TABLES

LIST OF FIGURES

CHAPTER I

INTRODUCTION

1.1 Anatomy of the Human Spine

The human spinal column consists of 24 mobile bones, called vertebrae. These vertebrae are designated symbolically from top to bottom as C1-C7 (cervical or neck region), T1-T12 (thoracic or chest region), and L1-L5 (lumbar or low back region). The skull articulates with C1, and the column is supported on the fused vertebrae S1-S5, constituting the sacrum which is part of the pelvis. An intervertebral disc joins two adjacent vertebrae. Each disc consists of a peripheral annulus fibrosus which surrounds a nucleus pulposus, capped on its superior and inferior aspects by the dome-shaped cartilaginous end plates. The posterior elements of the two vertebrae are joined together through articular facet joints arising from the articular processes. In the sagittal plane (lateral view), the normal erect spine has four curves. The cervical and lumbar regions are curved convex anteriorly, and the thoracic and sacral regions are curved convex posteriorly. In the frontal plane, the normal erect spine appears straight and symmetrical with the exception of a slight right thoracic curve which is said to be due to the position of the aorta or right handedness. A motion segment which is constituted by two adjacent vertebrae and their intervening soft tissues can, in general, exhibit six components of motion, i.e., translation along and rotation

about three mutually perpendicular axes. Figure 1 shows the components of an intervertebral joint.

1.2 Scope of Kinematic Research as Applied to the Human Spine

During the period following World War II, an active interest was developed among researchers to study the phenomenon of pilot ejection which caused vertebral fractures in some of the pilots ejected from wrecked aircraft. It was then that the first mathematical model of a human spine was developed to study the accelerations and stresses induced in the spinal column due to the acceleration pulse of the seat. The study was motivated to predict the injuries to the vertebrae. With the advent of high speed ground transportation, a new class of problems is being faced. These include injuries to the thoracolumbar spine due to a sudden deceleration, the whiplash injury to the cervical spine, and the general gross motion study of the human body involved in a crash impact. The seriousness of these injuries cannot be overstated. For example [65, 66, 68] in a whiplash situation, injuries to the spinal column range from damage to the soft tissue only (ligaments, discs, etc.) to combined soft tissue and bony damage (fracture and dislocation). The nerve roots and spinal cord can be damaged in any injury which causes fracture or dislocation. The structural and physiological aspects of the spine also pose some interesting problems. Probably the most important among these are related to the static deformity of the spine, known as scoliosis. Although a great deal of work has been done toward identifying or classifying different types of these deformities and their treatment, the true nature of the causes leading to these

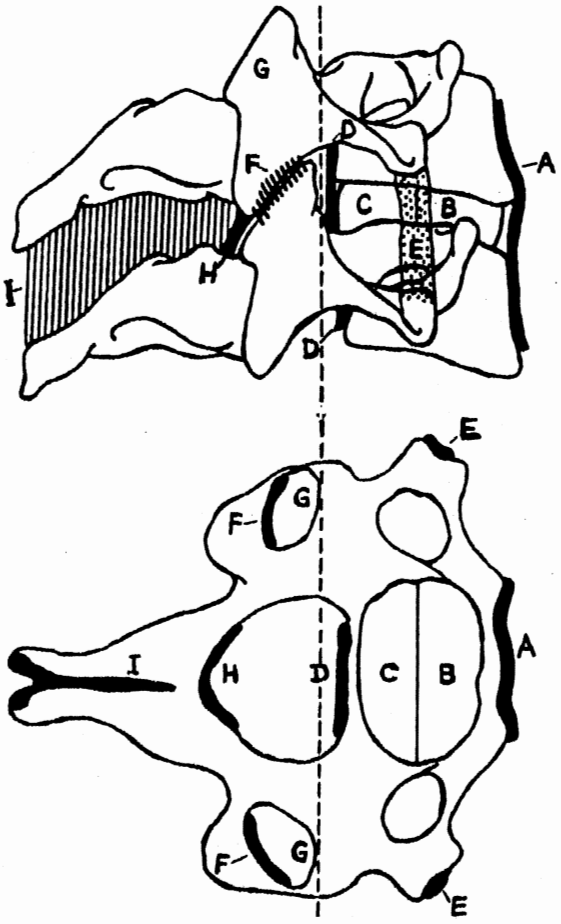

A : ANTERIOR LONGITUDINAL LIGAMENT.

B : ANNULUS FIBROSUS-ANTERIOR HALF.

C : ANNULUS FIBROSUS-POSTERIOR HALF.

D : POSTERIOR LONGITUDINAL LIGAMENT.

E : INTERTRANSVERSE LIGAMENT.

F : FACET JOINT CAPSULES.

G : FACET JOINTS.

H : LIGAMENTUM FLAVUM

I : INTERSPINOUS AND SUPRASPINOUS LIGAMENTS.

Figure 1. Components of an Intervertebral Joint

deformities has not been completely revealed. Application of kinematic research tools to the mechanics of the human spine has much to contribute in terms of the basic understanding of intervertebral motion characteristics which, in turn, will provide tools for understanding injuries which occur in automobile crashes or sports, and will enable medical researchers to achieve a better insight into the mechanics of various deformities.

The science of kinematics studies the relative motion of one rigid body relative to another rigid body. The manner in which the rigid body executes this relative motion defines the kinematic constraints. The relative motion of a rigid body may be described in terms of infinitesimal motion or finite motion. However, the science of kinematics places more emphasis on infinitesimal motion. This is due to the fact that all the higher order motion properties of the body can be examined with ease and can be directly related to the dynamic behavior of the rigid body. The first order kinematic properties that describe a rigid body motion are the instantaneous screw axis (ISA) and its associated pitch value. The instantaneous screw axis is also the generator of the axode. The second order kinematic properties of the relative rigid body motion are the first order properties of the axode which is a ruled (geometric) surface. The second order properties of the axode generated by the ISA describe the third order properties of the rigid body motion. Any higher order motion of a rigid body can be studied by examining the higher order properties of the axode. The advantages of studying the axode properties to analyze the rigid body motion should be obvious. The motion is a time dependent quantity. The axode, on the other hand, is a geometric property. Thus, with the study of the axode, the motion

is studied in an absolute frame of references where time dependency is eliminated.

A mechanical system may be considered as one or more rigid bodies connected together by one or both the following types of connectivities: (1) elastic or flexible connection which may consist of linear or non-linear elastic elements, and (2) mechanical joints or couplings which govern the characteristics of the relative motion permitted between the connected rigid bodies.

There are twelve well-accepted and physically realizable pairs with one or more degrees of freedom of motion. In building a mechanical system, the rigid bodies may be connected using these physically realizable kinematic pairs. Such a system of rigid bodies connected by kinematic pairs may have constrained or unconstrained relative motion. The manner in which connectivity is established between rigid bodies using the kinematic pairs will describe the degrees of freedom of the rigid-body motion.

The biological system performing relative motion, however, is different from the mechanical system. The rigid bodies in a biological system are in general deformable. The joints connecting the rigid bodies do not appear to conform to the well-defined geometry of mechanical kinematic pairs. Furthermore, there is usually a shock-absorber or a cushion imbedded in a biological joint.

The scope of kinematic research in studying such biological joints may be visualized in the following two parts:

1. Analysis of the relative motion at such joints using the advanced kinematic theories without being concerned as to the mechanics of this motion; and

2. Synthesis of the actual relative motion at these joints by combining in a rational manner the kinematic constraints and motion characteristics of the joint with the elastic restraints of the biological tissue and other supporting structures.

The following sections examine the state of the art in studying the intervertebral motion followed by a critical analysis and the existing methodology.

1.3 Review of Literature

There has been considerable interest in studying the kinematics of intervertebral motion of the human spine since the earliest significant contribution to the subject by Jacob Winslow. In the year 1730, he reported a scientific study meticulously describing the apophyseal facets of the vertebrae and their constrained motion during movements of the head, neck, and the rest of the spinal column. Since then, many investigators have owrked with live subjects or autopsy specimens to determine the range of motion, in terms of relative displacement due to intervertebral motion of the human spine. Significant contributions by several researchers are reported in References [1-40]. A brief analysis of the significant studies related to the kinematics of the human spine follows.

There are four general categories that an investigator chooses from before he proceeds to study the kinematic behavior of intervertebral motion. These four categories are type of study, segment of the spine, data collection procedure, and data analysis:

1. Type of study: There are two reported ways to study the kinematics of the human spine. These are either in-vivo study or in-vitro

study. The basic objective of such kinematic studies appears to be similar. In an in-vitro kinematic study, the investigator is preferably aiming to extrapolate information on the kinematics of motion characterized by an in-vivo spine.

2. Segment of the spine: The human spine consists of 24 vertebrae distributed in three segments: (a) cervical (C_1 - C_7), (b) thoracic (T_1 - T_{12}), and (c) lumbar (L_1 - L_5). An investigator may either select any one of these three segments of the spine or investigate the entire spine.

3. Data collection procedure: The data describing the kinematics of intervertebral motion are collected by designing a suitable laboratory experiment. An in-vivo laboratory experiment and data collection involve utilization of bubble goniometer, shadow technique, and the roentgenograph technique for recording discrete positions of the spine or the cineroentgenograph for recording continuous motion. An in-vitro experimental procedure for data collection appears to have more freedom to record detailed descriptions of the relative motion of the vertebrae.

Planar motion data on the intervertebral joint motion were obtained [37-39] using single roentgenograph measurement. Simultaneous data from two roentgenographs taken in intersecting planes were used [20, 21, 40, 48] to measure the spatial motion of vertebrae. Externally applied electronic transducer systems were used [18, 20] to measure axial rotation of vertebral bodies. Their study represents a single component of motion measurement. An electro-mechanical motion transducer system was developed [36] to measure the motion of the lumbar spine using liquid mercury-filled tubes as strain elements. Motion transducer systems to measure space motion have been also used in studies of other anatomical joints.

For example, a multiloop instrument system was used [41] to measure jaw motion. An instrumented linkage was developed [42] to study the mandibular motion. Single and multiloop linkage instrumented measurement techniques were developed [43-45] to measure the spatial motion of the canine shoulder and the human knee joint [46]. Cineradiography was used [47] to measure the motion at the wrist.

4. Data analysis: Many of the data analysis procedures depend upon the way the data are collected. The reported studies on kinematics of the human spine may be distributed into one of the following six groups: (a) simple observation on the range of motion, (b) simple statistical analysis giving mean and standard deviations of the range of motion, (c) location of instant centers of velocity assuming that the motion is a planar motion especially in the sagittal plane, (d) locating instantaneous screw axes (in a limited sense), and (e) developing a mathematical procedure to determine centroidal curvature or calculating relative displacements of the vertebrae.

Distribution of the reported research studies, classified into twelve groups based on the analysis above, is presented in Table IX.* Table X presents the methodology and data collection procedures utilized by these investigators. Table XI presents the summary of results of their investigations. The isolated attempts made on determining the spine configuration under static mode and with non-kinematic tools are summarized in Table XII. Table XIII presents an analysis of the instrumentation techniques for collecting the in-vitro data on the relative motion of synovial joints.

---

*Tables IX through XIV are included in Appendix A.

The significance of motion simulation models as research tools in contributing to physiological research on the human spine has been recognized in the literature. A three-dimensional elasto-static model of the thoraco lumbar spine has been proposed and its application demonstrated on the response of the spine to compressive and lateral loads [52]. Functions of individual cervical muscles were analyzed to study their effectiveness in producing specified head motion by a three-dimensional elasto-static model of the cervical spine [54]. A three-dimensional model was developed [53] to calculate forces in muscles and reactions at intervertebral joints in static postures. A comprehensive three-dimensional elasto-static model simulating the thoraco-lumbar spine with interactive role of sacrum, sternum and ribs was developed to study the response of the rib cage to lateral compressive and bending loads, and to study the stabilizing effect of the rib cage on the vertebral column [55, 56].

Table XIV summarizes the state of the art in some of the key motion simulation models of a spine subjected to static loading conditions. These motion-simulation models have the following attributes:

1. Intervertebral motion is simulated in three dimensions using either an isolated spinal segment [52, 53, 54] or using the entire thoracic cage [55, 56].

2. The elements of the intervertebral joint, such as disc and ligaments, are represented by using springs and beam elements [52, 55].

3. The vertebrae are treated as rigid bodies.

4. The equations of equilibrium of forces are written using the stiffness matrix approach [52, 56] or using the reaction forces [53].

5. The motion simulation models are validated using the available data in the literature.

6. These models are developed using the discrete parameter approach.

1.4 A Critical Analysis

The instant center location as reported in References [7, 8, 10, 18, 21, 22, 24, 26] is achieved by obtaining two finitely separated positions of a vertebra moving relative to another vertebra. The motion about this instant center is expected to describe the instantaneous velocities of any point within the vertebra. But the "instant center" obtained by finite position analysis only provides a pole point--which approximates the higher-order infinitesimal motion properties using finite motion theories. Therefore, much of the information based on the present way of obtaining the instant center is approximate and must be analyzed or interpreted with care before conducting the kinematic studies on the mobility of the human spine. The locus of the instant center, when it is located in an instantaneous kinematic sense, will provide a centrode. The relative motion of two vertebrae can then be described truly with mathematical precision by means of the centrode and its conjugate centrode. On the other hand, the instant center, as reported in the references cited above, represents a pole; the locus of such pole points will describe a polode which is not capable of describing the true relative motion of the vertebrae.

The concept of instant center location to describe vertebral motion assumes a planar motion of the vertebrae. However, it is well known that intervertebral motion is truly a three-dimensional spatial motion having all six components of motion.

The intervertebral motion in three dimensions can be described by locating instantaneous screws, obtaining the axodes and conjugate axodes as the locus of the instantaneous screws. However, as in the case of instant center location, the instantaneous screws have been located [22, 24] using the finitely separated positions of the moving vertebrae. Furthermore, no attempt is made to establish the relationship between the true location of the instantaneous screw and the approximately located instantaneous screw. Also, the screw by itself does not provide a complete kinematic criterion for conducting comparative study as it is stated by Panjabi and White [24]. The screw contributes only first-order property of rigid-body motion, provided it is obtained using infinitesimally separated positions of the rigid body.

With the basic deficiency in applying instrumentation techniques and data collection in the past, it has not been possible to locate the instant centers or instantaneous screw axes and centrodes or axodes in their true instantaneous kinematic sense. The data collected via roentgenographs are for the finite positions of the vertebrae. As a consequence, the data analysis follows the basic drawbacks of the data collection technique. Since at present there is no reported study that will predict the error involved in extrapolating information from finite-position motion to instantaneous motion, there is no theoretical basis for the number of roentgenographs needed and the incremental values of angular positions of the spine necessary for the follow-up data analysis to: (1) best approximate the motion at every instant, and (2) provide techniques to interpolate information corresponding to vertebral positions for which no roentgenograms are available. Due to this lack of suitable developments in data collection and analysis, one cannot

evaluate and compare the characteristic motion (position, velocity, and acceleration of the vertebrae) in an absolute frame of reference.

The analysis above and the data summarized in Tables IX through XIV (Appendix A) show that the three-dimensional kinematic theories have not been fully applied in mobility studies of the human spine beyond determining "instantaneous centers" of velocity or locating "instantaneous screws" based on a discrete set of observations.

The geometry of the facet joint has an important bearing on several physiological aspects of the human spine. The location and orientation of facets and the geometry of the surface of contact at each facet joint govern the components of motion and the functional relationships between these components of motion at each facet joint. These geometric characteristics of the facet joint interact with the stiffness properties of the individual ligaments and intervertebral disc to generate a specific pattern of motion at each intervertebral joint due to a mode of motion of the entire human spine. The role of these geometrical characteristics of facet joints in contributing to the physiological aspects of the human spine has been recognized in the literature. The variation in range and pattern of intervertebral motion at the lumbar, thoracic, and cervical spine has been attributed to the location and orientation of the facets at these vertebral levels [1]. A reversed coupling between the lateral bending and axial rotation sometimes found in the thoraco lumbar region has been cited [24] as a probable cause of scoliotic deformity of the spine caused by the imbalance of motion components in that region. A deviation from the normal geometric characteristics of facet joints in the lower lumbar region has been thought of as a cause of above normal torsional strain leading to the degeneration of

intervertebral discs [20]. There has been an extensive experimental work [21] on the partial or total fusion of facet joints at various vertebral levels in order to investigate the effect of fusion on the range and pattern of motion of intervertebral joints and the entire spine. However, even today theoretical models are not available to predict the change in the intervertebral motion and the motion of the entire spine due to partial or total fusion without going through the extensive experimental work.

In order to investigate on a scientific basis the characteristic motion of intervertebral joints and the kinematic function of the facet joints at each vertebral level, we need to develop human spine-motion simulation model which incorporates the total kinematic influence along with the stiffness properties of the vertebral joints. Such a motion simulation model must be developed using the following criteria:

1. The simulation model must predict within acceptable tolerance limits the three-dimensional motion response of a human spine subjected to static loading conditions.

2. The simulation model must incorporate the kinematic as well as geometric characteristics (e.g., location, orientation, surface properties) of the facet joints at each vertebral level.

3. The simulation model must identify and include the kinematically equivalent intervertebral joint.

4. The kinematic equivalent of intervertebral joint must incorporate parameters that permit one to examine the function of facet joints in controlling the characteristic intervertebral motion.

The existing simulation models [52-56] do not incorporate the above features which are very essential in studying the spinal motion under a

variety of loading conditions. Some of the reasons for this inadequacy are presented below:

1. The equivalent stiffness matrix representation [58] of the coupling effect created by the functional relationships induced by the facet joints on the intervertebral motion is inadequate because it represents the constraints, at the most, at a few discrete positions.

2. The technique of representing the articular facet joint by two springs--one of high stiffness perpendicular to the plane of the joint and the other a spring of low stiffness along the facet [52, 60]--also fails to provide the appropriate functional description of the joint. This technique has two drawbacks: (a) there is no kinematic representation of the three-dimensional curvature of the facets, and (b) it does not ensure a continuous contact between the superior and inferior facet elements.

3. The significance of the kinematic influence of facet joints in governing intervertebral motion is recognized to a degree [54, 59]; however, no kinematic thoery is developed to describe the three-dimensional motion of the joint by an equivalent kinematic pair capable of describing the exact intervertebral motion in three dimensions.

4. A systematic kinematic approach which involves determining degrees of freedom, components of motion, and their functional relationships has not been developed to model the spinal joint on the basis of its experimental data.

An examination of the reported studies and their analysis reveals that the importance of the three-dimensional kinematic theories for describing kinematically equivalent intervertebral joints has been recognized [54, 59] but has not been fully exploited in developing motion

simulation models of the human spine. Hence some of the key questions on the mobility of the intervertebral joint and spine still remain to be answered. For example, such questions are:

1. How to describe quantitatively the intervertebral motion and develop procedures to compare the motion characteristics?

2. How many degrees of freedom do the facet joints have at each vertebral level?

3. What are the components of motion of the facet joints associated with each pair of vertebrae?

4. What are the functional relationships between the components of motion of the facet joints at each vertebral level?

5. How to develop a systematic, kinematic approach that will permit one to synthesize mathematically the equivalent kinematic pair that will simulate the intervertebral motion at each vertebral level?

6. How to integrate the function of the equivalent kinematic pair along with the stiffness properties of disc and ligaments at each vertebral level in developing a motion simulation model?

In the present work, methodology is developed for data collection and data analysis which attempts to answer some of the key questions raised above. The next chapter presents the specific research objectives of this research program.

CHAPTER II

RESEARCH OBJECTIVES

It is proposed to develop a methodology to perform a three-dimensional kineto-elasto-static analysis of the human spine by testing cadaver specimens of the lumbar spine. The specific objectives of this proposed research are presented below:

1. To develop a methodology to describe quantitatively the three-dimensional intervertebral motion. The activities to meet this aim include the development of stepwise procedures for:

   a. Data collection of the three-dimensional intervertebral relative motion of each vertebra as the spine executes motion in sagittal plane, frontal plane, and planes in between.

   b. Calculation of parameters of instantaneous screws of motion. These parameters include the direction cosines of the screw axes, the location of these axes, and the pitch values associated with them.

   c. Determination of an analytical form of axode. Such an axode will be a mathematical ruled surface which will approximate the locus of the instantaneous screw axes as the vertebra executes a mode of relative motion with reference to a fixed frame of reference.

   d. Interpolation on the parameters of the instantaneous screw

axes. The axode approximation as developed in section 1(c) above will be used as a mathematical basis for the interpolation procedure.

2. To develop a methodology for the purpose of conducting simulation studies on the three-dimensional intervertebral motion of a human spine subjected to static loading conditions. This research objective will be met by undertaking the following activities:

a. Development of a discrete parameter model simulating the three-dimensional relative motion of rigid bodies which constitute an open loop kinematically constrained elastic system. The simulation model developed in this section will be a generalized model which will simulate the motion characteristics of a given system with known parameters describing the elastic and kinematic constraints of the system.

b. Development of a stepwise procedure to adapt the generalized simulation model developed in section 2(a) above to the biological system consisting of intervertebral joints. This will involve evaluating, for the human spine, the parameters describing the elastic and kinematic constraints at each intervertebral joint. The activities to meet this aim will require the development of stepwise procedures to:

(1) Determine experimentally the stiffness matrix at each intervertebral joint.

(2) Simulate the kinematic constraints of the intervertebral joint by selecting a kinematic pair from the set of 12 physically realizable kinematic pairs (joints).

(3) Determine the parameters describing (in the best possible manner) the kinematic constraints at each of the intervertebral joints. The relative merit of a kinematic pair simulating the actual facet joint will be evaluated by combining an experimentally determined stiffness matrix (2.b(1)) with the motion characteristics of a kinematic pair (2.b(2)) selected one at a time. By comparing with the experimental data, the motion performance of the human spine as predicted by each combination, the parameters which come closest to describing the kinematic constraints of the intervertebral joints will be determined.

The methodology to carry out the proposed research objectives is presented in the following chapters.

CHAPTER III

DESIGN OF EXPERIMENT AND DATA COLLECTION

3.1 Design of Experiment

In order to meet the objectives of this research program, it is required to collect data describing the three-dimensional intervertebral motion under a controlled set of conditions. The equipment designed especially for the purpose of collecting such data include: (1) a spine fixture, and (2) a linkage transducer.

In the following a brief functional description of the spine fixture and the linkage transducer is presented.

1. The spine fixture: The fixture, shown in Figure 2, holds the spine specimen centrally with the lowest vertebral body clamped in a removable cup. The clamping method is designed such that it allows easy mounting and dismounting of the spine specimen. The specially designed spine fixture has the following functional features:

   a. The spine specimen is able to execute its normal mode of motion in the sagittal plane, the frontal plane, and in any other plane in between.

   b. The gross motion of the entire spine specimen in any of the planes mentioned above can be tracked as a function of an independent parameter, namely the angular rotation of a vector joining the center of the clamped vertebra with the center of the topmost vertebra.

Figure 2. The Spine Fixture

c. A known amount of axial twist can be imparted to the top-most vertebra.

d. External static loads can be applied in known increments to any one or more vertebrae. These loads include three forces and three moments along and about a set of three mutually perpendicular axes, which constitute the fixed frame of reference. Reference axes are located on the frame of the fixture at the center of the cup which holds the spine specimen.

2. The linkage transducer: A linkage transducer with seven links and six rotary potentiometers, as shown in Figure 3, is designed to measure the three-dimensional intervertebral motion. The design requirements for the linkage transducer included:

a. Minimum weight of the transducer so as not to load and interfere with the actual intervertebral motion to be measured.

b. Ease of fabrication and installation on the spine specimen.

c. Small overall size of the transducer so that it can be mounted within the limited space available. Four such linkage transducers are required to collect data describing the three-dimensional intervertebral motion of the lumbar spine (L_1-L_5).

The coordinate systems located on each of the seven links of the spatial linkage transducer are shown in Figure 4. The coordinate system 1 is attached to the upper vertebra and coordinate system 7 is attached to the lower vertebra. The axes of the coordinate systems 1 and 7 are aligned and located with respect to the reference blocks used for

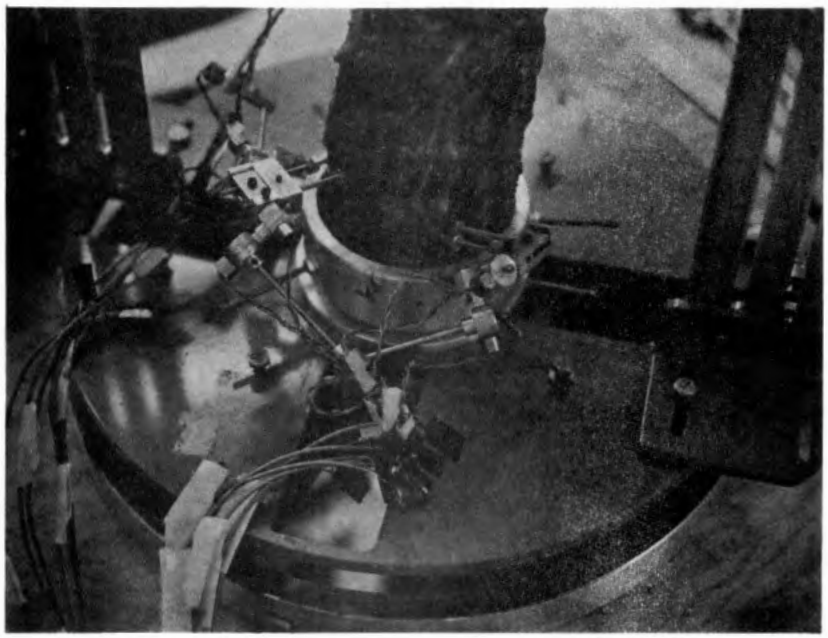

Figure 3. Linkage Transducer

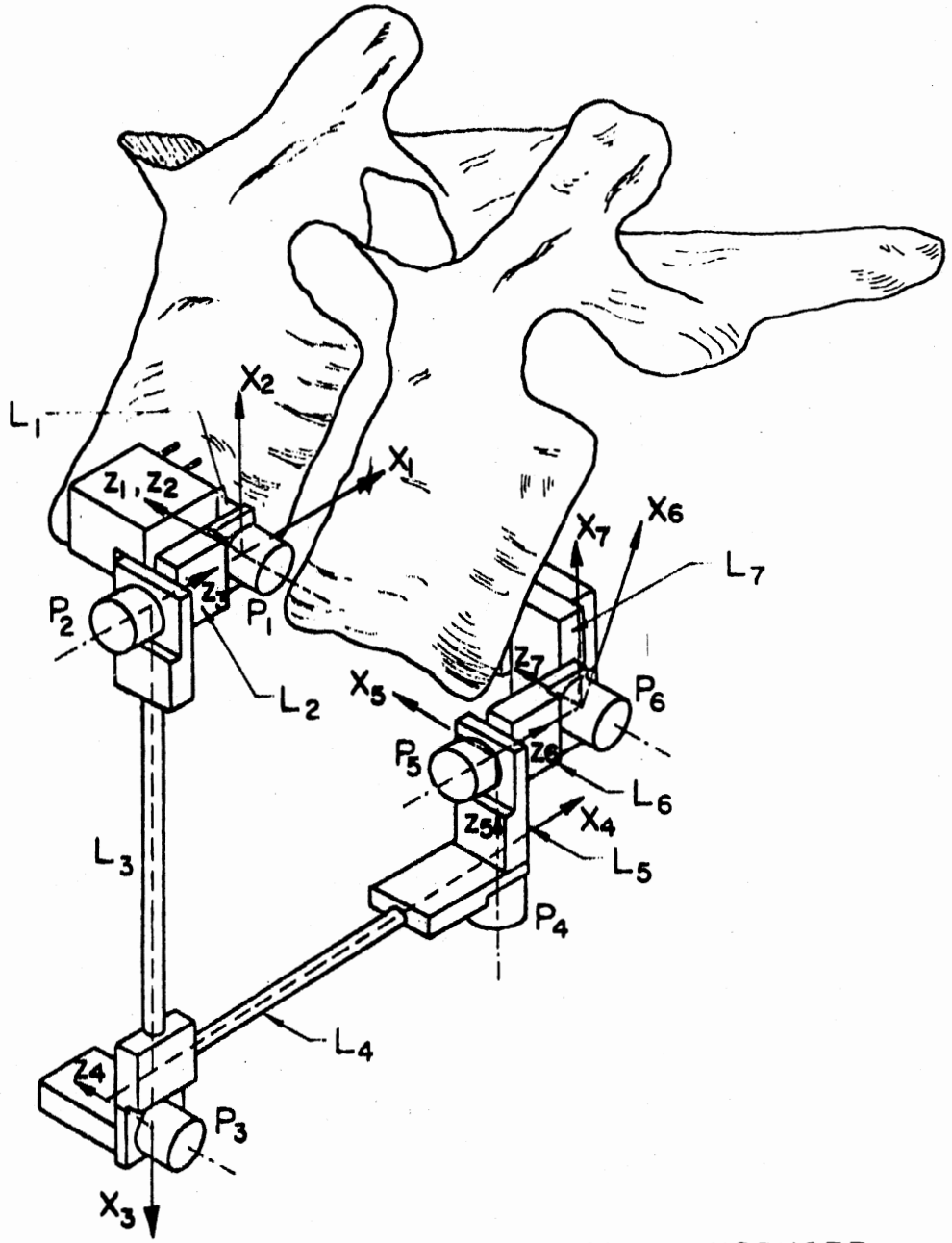

Figure 4. Coordinate Systems on the Linkage Transducer

mounting the linkage transducer between the two vertebral bodies. The parameter A_i is the perpendicular distance between the axes Z_i and Z_{i+1} and is positive if measured in the positive direction of X_i. The twist angle α_i is the rotation about the X_i axis that is required to make the Z_i axis parallel to the Z_{i+1} axis. S_i is the distance along the Z_{i+1} axis from the origin O_i to O_{i+1}. The variable θ_i is the angle of rotation about the Z_{i+1} axis required to make the X_i axis parallel to the X_{i+1} axis. Since the linkage transducer is instrumented to measure only angular rotations at the six joints, α_i, A_i, and S_i (i = 1, 6) are constants. Table I presents these data for the four linkage transducers used in this research program.

The small size of the linkage transducer imposes a constraint on the design of rotary potentiometers that are expected to measure the relative angular displacements of the links of the spatial linkage. Such small angular-displacement potentiometers were fabricated by a commerical producer according to a given set of specifications, listed in Table II. The mounting design for the potentiometers on the linkage transducer provided an additional bushing with a tolerance of +0.001 inch, to offset the effect of radial and end play in the shaft of each potentiometer.

Each potentiometer was calibrated using a special fixture. This setup allowed the potentiometer shaft to be rotated through one-half (0.5) degree rotation each time. A D.C. voltage of 10.000 ($\pm$0.001) volts was maintained at the supply terminals of the potentiometer. A least square technique was used to fit a straight line to the voltage versus angular rotation data obtained for each potentiometer. Table III presents for each potentiometer the results of this analysis in

TABLE I

LINKAGE TRANSDUCER DATA

Transducer No.	$\alpha(I)$, I - 1, 6 Degrees	A(1), I = 1, 6 Inches	S(I), I = 1, 6 Inches
1	0.0	0.0	0.0
	270.0	0.0	-0.786
	270.0	2.715	0.99
	90.0	2.415	0.793
	90.0	0.0	0.769
	90.0	0.0	0.0
2	0.0	0.0	0.0
	270.0	0.0	-0.82
	270.0	2.876	0.875
	90.0	2.519	1.031
	90.0	0.0	0.772
	90.0	0.0	0.0
3	0.0	0.0	0.0
	270.0	0.0	-0.801
	270.0	2.762	0.902
	90.0	2.412	0.799
	90.0	0.0	0.789
	90.0	0.0	0.0
4	0.0	0.0	0.0
	270.0	0.0	-0.787
	270.0	2.663	0.886
	90.0	2.412	0.746
	90.0	0.0	0.744
	90.0	0.0	0.0

TABLE II

SPECIFICATIONS OF THE ROTARY POTENTIOMETERS
(MANUFACTURED BY MAUREY INSTRUMENT
CORPORATION, CHICAGO, ILLINOIS)

Type	37-M 42
Linearity (independent)	±1%
Weight	< 1 gm
Diameter	0.375 inch
Height	0.28125 inch
Length of Shaft	0.625 inch, 10-32 bushing
Shaft Diameter	0.125 inch ±0.001
Starting Torque	< 1.0 oz-inch
Power	0.02 watt
Electrical Travel (Theoretical)	350° ±5°
Mechanical Travel	360° continuous
Total Resistance	5 K-ohms ±10%
Life	20,000 revolutions at 40 RPM

TABLE III

CALIBRATION DATA OF POTENTIOMETERS

POT No.	Calibration Constant (V/θ)	Linear Range in Voltage	Linearity ± Degrees
1	0.028300	0.50-9.50	+1.17 -1.15
2	0.029197	0.25-9.50	+1.13 -0.93
3	0.029221	0.50-9.80	+0.72 -0.76
4	0.028909	0.50-9.75	+1.17 -1.12
5	0.028579	0.50-9.75	+1.03 -1.00
6	0.029156	0.25-7.50	+1.21 -0.75
7	0.028733	0.60-9.75	+1.12 -0.93
8	0.028787	6.75-9.50	+0.96 -0.32
9	0.028917	1.30-9.50	+1.15 -0.92
10	0.028760	0.25-9.60	+0.91 -0.98
11	0.028606	0.50-4.50	+0.61 -0.96
12	0.028273	2.25-7.25	+0.92 -1.40
13	0.029239	0.25-7.50	+0.64 -0.56
14	0.029048	0.75-9.50	+0.99 -1.03
15	0.028800	2.25-9.50	+0.85 -0.83
16	0.028501	0.50-9.85	+0.65 -0.89
17	0.028982	0.75-9.90	+0.63 -0.96
18	0.029589	2.50-9.80	+0.67 -0.91

TABLE III (Continued)

POT No.	Calibration Constant (V/θ)	Linear Range in Voltage	Linearity ± Degrees
19	0.028302	2.00-9.40	+0.88 -0.77
20	0.028824	1.15-6.50	+1.02 -0.84
21	0.028177	3.00-7.00	+0.71 -0.73
22	0.028733	0.20-8.20	+0.92 -0.78
23	0.029814	2.50-9.85	+1.03 -0.95
24	0.029335	3.50-8.80	+0.57 -0.90
25	0.029311	0.25-9.50	+0.83 -0.41
26	0.029241	0.25-9.75	+0.62 -0.17

terms of the calibration constant, linear range of operation in voltage, and the linearity of the calibration curve. Figure 5 shows a typical plot of voltage versus angle of rotation data for a potentiometer.

After mounting the potentiometers on the linkage transducer, each potentiometer was initialized. This involved measuring the voltage at each potentiometer corresponding to the known values of the angles (preferably multiples of 90°). Potentiometers 1 through 24 were used for measuring relative angular displacements in the linkage transducers (six potentiometers per linkage transducer). The error analysis of the linkage transducer showed that the error in the measurement of motion components is a function of the overall configuration of the linkage transducer. The maximum error in the measurement of rotational motion of a vertebra was found to be ±0.3 degrees.

3. Preparation of the spine specimen: The following procedure was used in the preparation of the specimen:

a. Store the spine specimen in the deep freeze at -20° to preserve the physical properties of the specimen.

b. Prior to performing the experiment, thaw the specimen at 20°C.

c. Relative humidity of 96 percent should be maintained while performing the experiment. This was accomplished by spraying saline solution on the specimen every hour.

d. X-rays in the AP (frontal), lateral (sagittal), and oblique planes should be taken for checking the quality of the specimen.

e. Remove the majority of the paraspinous muscle mass, keeping the ligaments and facet capsules intact. Leave a small

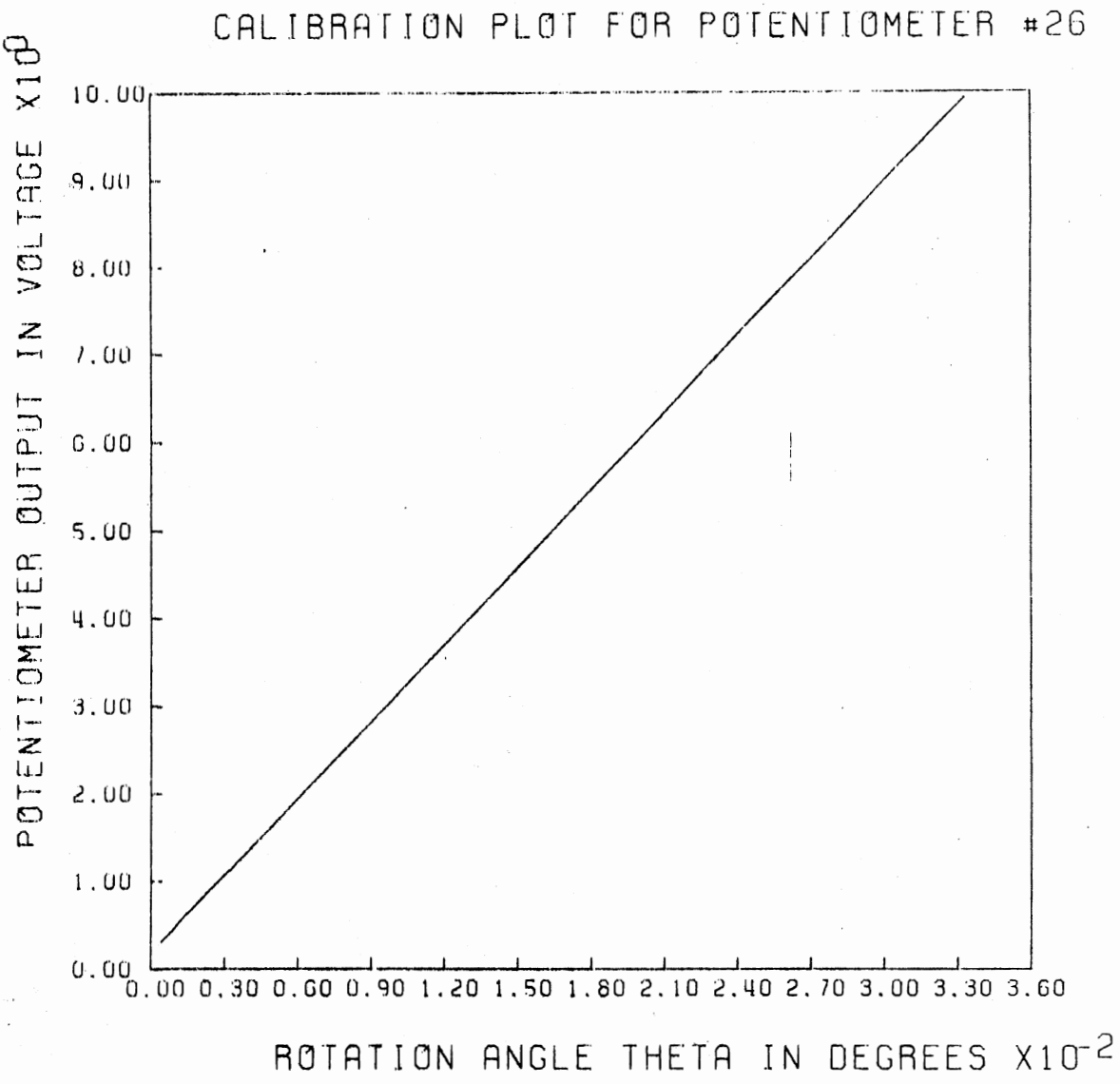

Figure 5. A Typical Calibration Plot

amount of tissue as an additional protection against dehydration of the deeper structure.

3.2 Data Collection

In order to meet the objectives of this research program, the following experimental data were collected:

1. Data describing the three-dimensional intervertebral relative motion as the spine specimen executes its normal mode of motion in the sagittal plane, frontal plane, and planes in between.

2. Data describing the stiffness properties of ligaments, disc, and supporting structure at each intervertebral joint.

3. Data describing the three-dimensional intervertebral relative motion as the spine executes a mode of motion caused by a set of static loads applied in increments.

Figure 6 shows schematically the entire setup used for the experimental data collection. The output from the linkage transducers is fed into a 32-channel analog-to-digital converter device which converts the voltage output in digital form. The digitized data are stored on a magnetic disc for later use and are also printed on the line printer for user interaction. The data collection procedure is controlled by the mini-computer with interaction from the user. In the following a stepwise procedure is presented which was used to collect the three types of data mentioned above:

1. Data describing the three-dimensional intervertebral motion in the normal mode of motion:

   a. Mount the spine specimen on the spine fixture with the bottom vertebral body fixed rigidly in the cup.

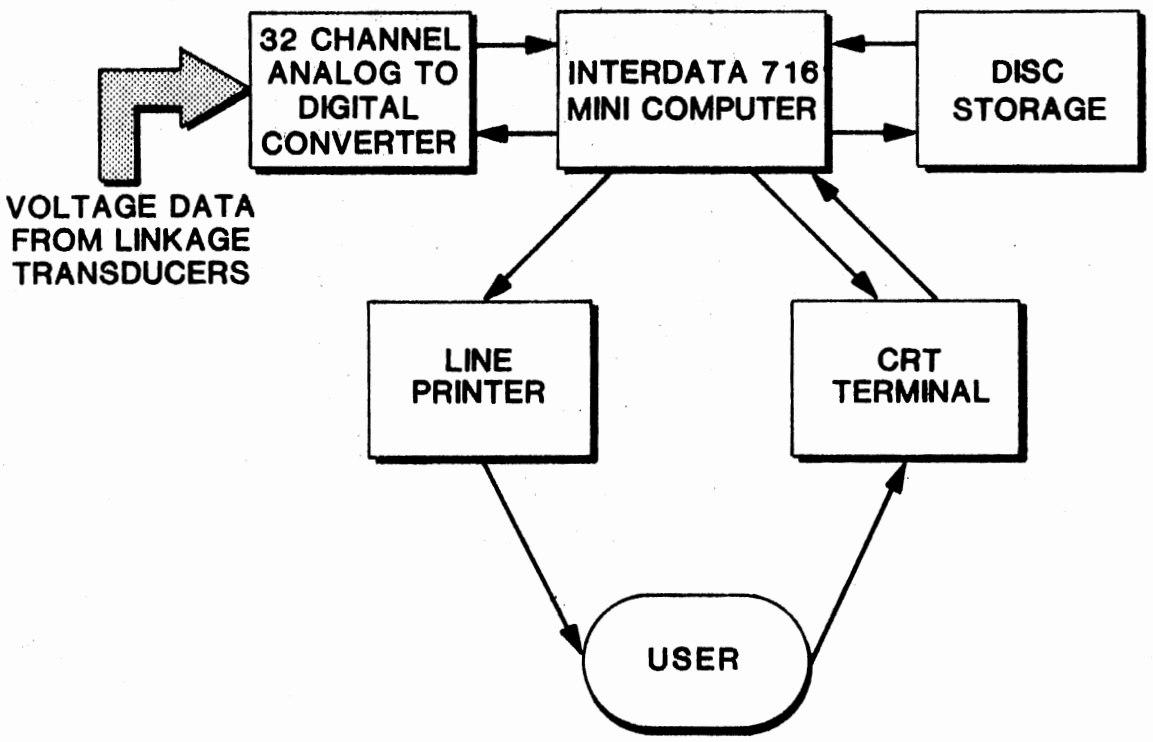

Figure 6. A Schematic Representation of the Experimental Setup

b. Locate the spine specimen in its sagittal plane.

c. Keep the twist angle of the top vertebra at zero value.

d. Move the spine specimen from its extreme extension position to its extreme flexion position in small increments. At each increment, collect voltage data from the potentiometers of the linkage transducer.

e. Rotate the vertical plane of motion of the spine specimen through an increment of 15° and repeat step d.

f. Repeat steps d and e until the entire mobility range of the spine specimen is exhausted.

g. Give a small increment to the twist angle of the top vertebra and repeat steps d through f.

h. Repeat steps d through g until maximum left axial-rotation is achieved for the top vertebra. Repeat for the maximum right axial-rotation.

2. Data describing the stiffness properties at each intervertebral joint.

Consider a pair of vertebrae, say L1 - L2, for which the stiffness matrix is to be determined. For the vertebra L1, the system coordinates are defined as U_1, U_2, . . ., U_6, which represent the possible six components of relative motion of body L1 with respect to body L2. If P_1, P_2, . . . , P_6 are the system forces along the system coordinates, then the force deflection relationship is given by the matrix below. The matrix [A] is called the flexibility matrix. The following stepwise procedure will be used to obtain the flexibility matrix experimentally for each pair of vertebrae:

$$\begin{bmatrix} U_1 \\ U_2 \\ \cdot \\ \cdot \\ \cdot \\ U_6 \end{bmatrix} = \begin{bmatrix} a_{11} & a_{12} & \cdot & \cdot & \cdot & a_{16} \\ a_{21} & a_{22} & \cdot & \cdot & \cdot & a_{26} \\ \cdot & & & & & \\ \cdot & & & & & \\ \cdot & & & & & \\ a_{61} & a_{62} & \cdot & \cdot & \cdot & a_{66} \end{bmatrix} \begin{bmatrix} P_1 \\ P_2 \\ \cdot \\ \cdot \\ \cdot \\ P_6 \end{bmatrix}$$

a. Isolate a pair of vertebrae and fix the bottom vertebra to the fixture. Cut the facet joint off the vertebral body, so that stiffness matrix data reflect only the elastic constraints of the ligaments and intervertebral disc.

b. Attach a linkage transducer between the pair of vertebrae.

c. Identify the system coordinates U_1, U_2, . . ., U_6 for the moving vertebra. U_1, U_2, U_3 define the translations along, and U_4, U_5, U_6 define the rotation about three mutually perpendicular system axes.

d. Apply a unit load $P_1 = 1$ along coordinate U_1 and measure the displacements U_1, U_2, . . ., U_6. This yields the first column of the flexibility matrix. Alternatively, the coefficients a_{11}, a_{21}, . . ., a_{61} are the slopes of the straight lines approximating the P_1 versus U_1, P_1 versus U_2, . . ., P_1 versus U_6 curves, respectively.

e. Repeat the procedure in item d with $P_k = 1$ and $P_i = 0$, $i \neq k$ to obtain the kth column of the flexibility matrix.

Having obtained the flexibility matrix [A], the stiffness matrix can be determined by $[K] = [A]^{-1}$.

3. Data describing the equilibrium configuration of the spine subjected to a set of static loads.

The three-dimensional intervertebral motion data describing the

successive equilibrium configuration of the specimen subjected to specified loading conditions is collected using the following procedure:

a. Choose a system of external static forces.

b. Attach the loading hook to each of the vertebrae to be subjected to external loads.

c. Attach steel wires to the loading hook and pass them over a set of adjustable pulleys which can be fixed on the loading frame of the spine fixture (Figure 7).

d. Place static weights at the other ends of the steel wires to simulate the system of forces.

e. After the spine attains an equilibrium position, collect the voltage data from the potentiometers of the linkage transducers.

f. Repeat steps d and e with known increments of loads to obtain the data describing the successive equilibrium configuration of the spine specimen subjected to the chosen system of static loads.

4. Data describing the geometry of components of the spine system.

In addition to the three types of data described above, the following geometric data are needed:

a. Data describing the location and direction cosines of the fixed frame of reference with respect to the coordinate system 7 of each linkage transducer.

b. Coordinates of the point of application of loads used to evaluate the stiffness matrix of each intervertebral joint. These coordinates are located in the coordinate system 7 of each linkage transducer.

c. Coordinates of the points of application of loads used to evaluate the stiffness matrix of each intervertebral joint.

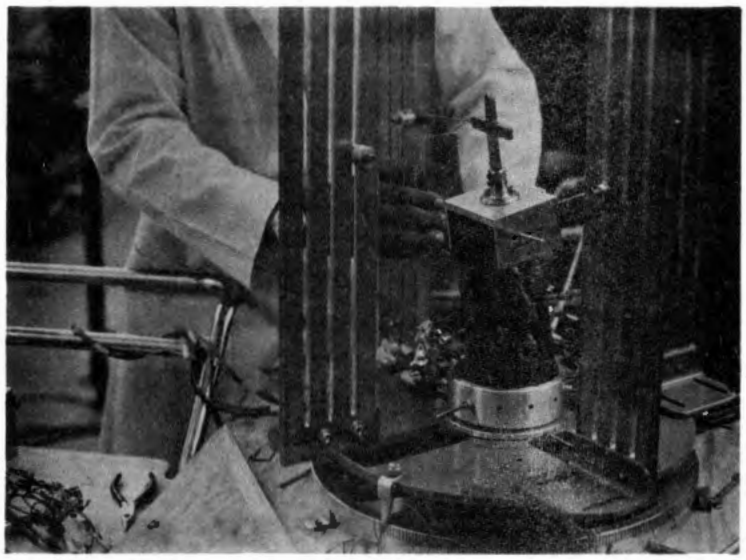

Figure 7. Loading Frame for Stiffness Data Collection

These coordinates are located in the coordinate system 7 of each linkage transducer.

d. Coordinates of the center of the facet joint for each intervertebral joint. These coordinates are located in the coordinate system 7 of each linkage transducer.

e. Data describing the direction cosines of a set of reference axes erected at the center of each facet joint. These data are collected with reference to the coordinate system 7 of each linkage transducer.

In order to locate a point in the reference system 7 of the linkage transducer, a pointer must be affixed to the coordinate system 1 of the transducer. The coordinates of the pointer are known in the reference system 1. The data from the potentiometers of the linkage transducers are collected when the end of the pointer is coincident with the point to be located. Using the matrix transformation (Equation 2, Chapter IV), the coordinates of the point can be calculated in the reference system 7 of the linkage transducer.

In order to locate a line in the reference system 7 of the linkage transducer, the coordinates of any two points on this line must be calculated in reference system 7 using the procedure described above. The principles of three-dimensional coordinate geometry can then be used to determine the direction cosines of the line in coordinate system 7 of the linkage transducer.

The next chapter presents in detail the methodology of kinematic analysis of the data describing the three-dimensional intervertebral motion of the human spine.

CHAPTER IV

SIGNATURE ANALYSIS OF INTERVERTEBRAL MOTION

The relative motion of a vertebra with respect to a fixed frame of reference can be described using an instantaneous screw of motion which is described by a line and associated pitch value. The locus of instantaneous screw obtained as a result of intervertebral motion in a finite range is called an axode. The axode is a mathematical ruled surface. Associated with the ruled surface are the characteristic scalar parameters which describe the geometric properties of the ruled surface. These characteristic parameters of the ruled surface or of the axode due to the relative intervertebral motion provide the data for signature analysis of the intervertebral motion. By performing the signature analysis in this manner, it becomes possible to compare on a quantitative basis the intervertebral motion within a given spine or between two spine specimens. However, since in reality such axode data for intervertebral motion are available in discrete form, a method needs to be developed to fit a ruled surface having an nth degree approximation with the continuous axode generated by a pair of vertebrae. Once such a functional form of axode is available, it becomes possible to interpolate and obtain characteristic parameters describing the instantaneous kinematic properties of the intervertebral motion at any desired location of the vertebra.

This chapter presents in detail the methodology developed for:

1. Calculation of parameters of instantaneous screw axes.

2. Analytical formulation of the axode of intervertebral motion.

3. Interpolation using the axode approximation.

4.1 Calculation of Parameters of Instantaneous Screw Axes

Motion of a rigid body Σ from a position Σ_1 to a position Σ_2 in a fixed frame of reference can be uniquely defined by a screw $\bar{S}_{12}$. A total of six parameters is required to define this displacement. These include the two parameters required to define the location of the screw axis, two more to define its direction, and the translation τ and the rotation ϕ. The pitch of the screw is given by $\rho = \frac{\tau}{\phi}$. If we consider the vertebra as a rigid body, then the motion of a vertebra relative to the vertebra fixed to the reference system is obtained in terms of the geometric parameters of the spatial linkage transducer attached between the two vertebrae. It therefore becomes necessary to obtain the parameters of screw $\bar{S}_{12}$ from such geometric data of the linkage transducer using successive transformation of coordinates. For the coordinate system shown in Figure 8, the matrix of transformation from the Kth to the (K + 1)th coordinate system is [47]:

$$[B'] \begin{bmatrix} 1 & 0 & 0 & 0 \\ -a_k\cos\theta_k & \cos\theta_k & \cos\alpha_k\sin\theta_k & \sin\alpha_k\sin\theta_k \\ a_k\sin\theta_k & -\sin\theta_k & \cos\alpha_k\cos\theta_k & \sin\alpha_k\cos\theta_k \\ -S_k & 0 & -\sin\alpha_k & \cos\alpha_k \end{bmatrix} \tag{1}$$

where a_k and S_k are the linear geometric parameters of the Kth link of

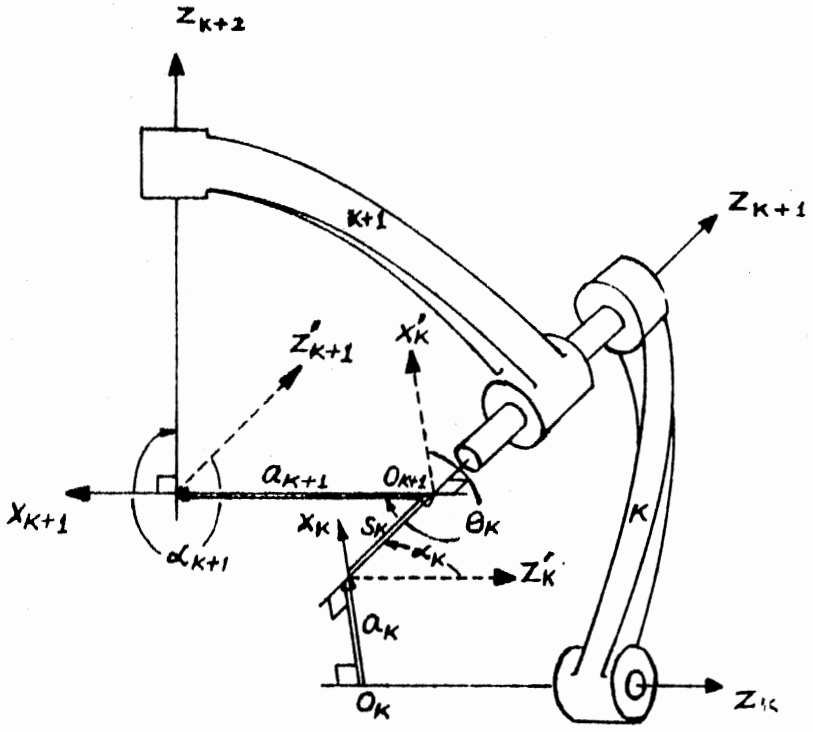

Figure 8. A Coordinate System for a Linkage With Revolute Pairs

the mechanism, and θ_k is the rotation angle as measured by the rotary potentiometer at the joint corresponding to the Z_{k+1} axis. For position Σ_1 of the rigid body, the overall transformation matrix from the moving to the fixed coordinate system is given by:

$$[B']_1 = [B'_6]\ [B'_5]\ [B'_4]\ [B'_3]\ [B'_2]\ [B'_1] \tag{2}$$

Two consecutive positions of the moving vertebra with respect to the fixed one would be defined by matrices $[B']_1$, $[B']_2$. This displacement of the moving vertebra can be represented by a rotation about and a translation along a screw axis located in the fixed vertebra. The matrix defining this screw displacement is obtained as:

$$[A'] = [B']_2\ [B']_1^{-1} = \begin{bmatrix} 1 & 0 & 0 & 0 \\ S_x & a_{11} & a_{12} & a_{13} \\ S_y & a_{21} & a_{22} & a_{23} \\ S_z & a_{31} & a_{32} & a_{33} \end{bmatrix} \tag{3}$$

From this matrix [A'], the required information to define screw $\bar{S}_{12}$ is obtained in the following manner:

$$\frac{\mu y}{\mu x} = [a_{23}\cdot a_{31} - a_{21}(a_{33-1})]/D$$

$$\frac{\mu z}{\mu x} = [a_{21}\cdot a_{32} - a_{31}(a_{22-1})]/D \tag{4}$$

$$\mu_x^2 + \mu_y^2 + \mu_z^2 = 1$$

$$D = (a_{22-1})\ (a_{33-1}) - a_{23}\cdot a_{32}$$

$$\cos\phi = (a_{11} - \mu_x^2)/(1 - \mu_x^2) \tag{5}$$

$$\sin\phi = \frac{\mu x \cdot \mu y}{\mu z}(1 - \cos\phi) - \frac{a_{12}}{\mu z}$$

$$\tau = \frac{-e_3}{d_3} \tag{6}$$

where

$$e_3 = \frac{S_x \cdot a_{31}}{a_{11}-1} - S_z - \left(a_{32} - \frac{a_{31} \cdot a_{12}}{a_{11}-1}\right) \frac{[S_x \cdot a_{21} - S_y(a_{11}-1)]}{[(a_{22}-1)(a_{11}-1) - a_{12} \cdot a_{21}]}$$

$$d_3 = \mu_z - \frac{a_{31} \cdot \mu_x}{a_{11}-1} - \left(a_{32} - \frac{a_{31} \cdot a_{12}}{a_{11}-1}\right) \frac{[\mu_y \cdot (a_{11}-1) - \mu_x \cdot a_{21}]}{[(a_{22}-1)(a_{11}-1) - a_{12} \cdot a_{21}]}$$

$$g_y = d_2 \cdot \tau + e_2 - C_{23} \cdot g_z$$

$$g_x = d_1 \cdot \tau + e_1 - C_{12} \cdot g_y - C_{13} \cdot g_z \tag{7}$$

$$C_{12} = \frac{a_{12}}{(a_{11}-1)}$$

$$C_{13} = \frac{a_{13}}{(a_{11}-1)}$$

$$C_{23} = \frac{[a_{23}(a_{11}-1) - a_{13} \cdot a_{21}]}{[(a_{22}-1)(a_{11}-1) - a_{12} \cdot a_{21}]}$$

$$d_1 = \frac{\mu_x}{(a_{11}-1)}$$

$$d_2 = \frac{[\mu_y \cdot (a_{11}-1) - \mu_x \cdot a_{21}]}{[(a_{22}-1)(a_{11}-1) - a_{12} \cdot a_{21}]}$$

$$e_1 = \frac{-S_x}{(a_{11}-1)}$$

$$e_2 = \frac{[S_x \cdot a_{21} - S_y \cdot (a_{11}-1)]}{[(a_{22}-1)(a_{11}-1) - a_{12} \cdot a_{21}]}$$

μ_x, μ_y, μ_z are the direction cosines of the screw axis, and g_x, g_y, g_z locate this axis in the fixed reference system. τ is the translation

along and ϕ is the rotation about this screw axis. Hence, Equations (1) through (7) define completely the parameters of screw $\bar{S}_{12}$. If the two positions Σ_1 and Σ_2 of the rigid body are taken sufficiently close together, they can be treated as infinitesimally separated and the screw $\bar{S}_{12}$ becomes the instantaneous velocity screw $\bar{S}$ at position Σ_1. The instant pitch of this instantaneous screw is then defined as:

$$S_{I.P.} = \frac{\dot{t}}{\dot{\phi}} = \frac{\Delta\tau/\Delta t}{\Delta\phi/\Delta t} = \frac{\Delta t}{\Delta\phi} = \rho_{\bar{S}_{12}}$$

4.2 Calculation of Parameters of Screw Axes in the Anatomical Frame of Reference

Equations (1) through (7) of section 4.1 can be used to calculate the parameters of screw axes of motion. These parameters are, however, defined in the reference system $x_7y_7z_7$ of the linkage transducer used to collect motion data between an intervertebral joint. In order to obtain the components of this relative motion in terms of the flexion angle, lateral bending, and axial twist, an anatomical reference system, $x_oy_oz_o$, is defined as shown in Figure 9. The plane x_oz_o defines the sagittal plane, the plane y_oz_o defines the frontal plane, and the plane x_oy_o defines the horizontal plane of the human spine. The x_o axis of this anatomical reference system is pointed posteriorly and the y_o axis is pointed to the right, looking posteriorly at the spine. The reference system $x_oy_oz_o$ is a right-handed reference system. The rotation about axis y_o is called the flexion angle, the rotation about axis x_o is called the lateral bending, and the rotation about axis z_o is called the axial twist. In order to obtain the components of the intervertebral relative motion about the axes of the anatomical reference system, the

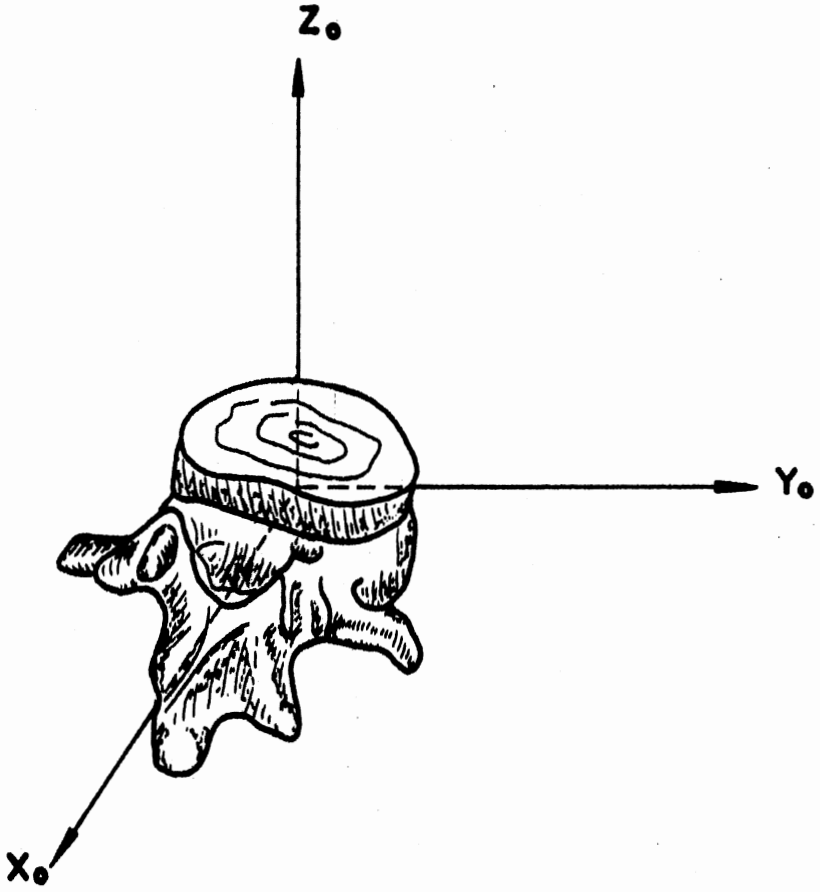

Figure 9. Anatomical Reference System

transformation from the transducer reference $X_7Y_7Z_7$ to the anatomical reference $X_oY_oZ_o$ must be known. As explained in Chapter III, voltage data describing, in the reference system $X_7Y_7Z_7$, the location of two points (P_1 and P_2) on the X_o axis and two points (P_3 and P_4) on the Y_o axis was obtained during the experimental data collection for each pair of vertebrae. If the coordinates of the pointer P in the $X_1Y_1Z_1$ reference of the transducer are X_p, Y_p, Z_p, then using the transformation [B'] (Equation (2), Chapter IV), we can write the following:

$$\begin{bmatrix} 1 \\ X_{p_i} \\ Y_{p_i} \\ Z_{p_i} \end{bmatrix} = [B'] \begin{bmatrix} 1 \\ X_p \\ Y_p \\ Z_p \end{bmatrix}, \qquad i = 1, 4$$

where $[B']_i$ is a function of the voltage data corresponding to the location of the p_ith point. Then the direction cosines of the axes X_o and Y_o with respect to the reference system $X_7Y_7Z_7$ can be obtained by the following relationships:

$$\ell_{7_{x_o}} = (x_{p_2} - x_{p_1})/r_x$$

$$m_{7_{x_o}} = (y_{p_2} - y_{p_1})/r_x$$

$$n_{7_{x_o}} = (z_{p_2} - z_{p_1})/r_x$$

$$\ell_{7_{y_o}} = (x_{p_4} - x_{p_3})/r_y$$

$$m_{7_{y_o}} = (y_{p_4} - y_{p_3})/r_y$$

$$n_{7_{y_o}} = (z_{p_4} - z_{p_3})/r_y$$

where

$$r_x = [(x_{p_2} - x_{p_1})^2 + (y_{p_2} - y_{p_1})^2 + (z_{p_2} - z_{p_1})^2]^{1/2}$$

and

$$r_y = [(x_{p_4} - x_{p_3})^2 + (y_{p_4} - y_{p_3})^2 + (z_{p_4} - z_{p_3})^2]^{1/2}$$

The direction cosines of the Z_o axis can be obtained by taking the cross product:

$$\hat{U}_{z_o} = \hat{U}_{x_o} \cdot \hat{U}_{y_o}$$

The transformation matrix from the coordinate system $X_7Y_7Z_7$ to the anatomical reference $X_oY_oZ_o$ is given by the following relationship:

$$[F] = \begin{bmatrix} \ell_{7_{x_o}} & m_{7_{x_o}} & n_{7_{x_o}} \\ \ell_{7_{y_o}} & m_{7_{y_o}} & n_{7_{y_o}} \\ \ell_{7_{z_o}} & m_{7_{z_o}} & n_{7_{z_o}} \end{bmatrix}$$

Using the above transformation, the parameters of the screw axis can now be transformed from the transducer reference $X_7Y_7Z_7$ to the anatomical reference $X_oY_oZ_o$ by the following equations:

$$\begin{bmatrix} \mu'_x \\ \mu'_y \\ \mu'_z \end{bmatrix} = [F] \begin{bmatrix} \mu_x \\ \mu_y \\ \mu_z \end{bmatrix}$$

$$\begin{bmatrix} g'_x \\ g'_y \\ g'_z \end{bmatrix} = [F] \begin{bmatrix} g_x - x_c \\ g_y - y_c \\ g_z - z_c \end{bmatrix}$$

where x_c, y_c, z_c are the coordinates of the origin of $X_o Y_o Z_o$ reference in the $X_7 Y_7 Z_7$ coordinate system. μ'_x, μ'_y, μ'_z are the direction cosines of the screw axis, and g'_x, g'_y, g'_z are the coordinates of a point on the screw axis referred to the anatomical reference $X_o Y_o Z_o$. The magnitude of the translation τ and the rotation ϕ about the screw axis remains invariant during the above transformation. Using the newly defined direction cosines (μ'), the components of the intervertebral relative motion about the axes of the anatomical reference system can be obtained as follows:

$$\theta_{x_o} = \mu'_x \cdot \phi$$

$$\theta_{y_o} = \mu'_y \cdot \phi$$

$$\theta_{z_o} = \mu'_z \cdot \phi$$

$$\tau_{x_o} = \mu'_x \cdot \tau$$

$$\tau_{y_o} = \mu'_y \cdot \tau$$

$$\tau_{z_o} = \mu'_z \cdot \tau$$

where θ_{y_o} is the flexion angle, θ_{x_o} is the lateral bending, and θ_{z_o} is the axial twist.

4.3 Calculation of Parameters of Screw $\overline{S}_{23}$ Using the Parameters of Screw $\overline{S}_{12}$ and $\overline{S}_{13}$

The data describing the three-dimensional intervertebral motion may be analyzed in two ways to obtain the parameters of:

1. Successive screws $\overline{S}_{1,2}$; $\overline{S}_{2,3}$; $\overline{S}_{(n-1),n}$; describing the motion of a vertebra with respect to its previous position, or

2. Screws $\overline{S}_{1,2}$; $\overline{S}_{1,3}$; $\overline{S}_{1,n}$; describing the motion of a vertebra with respect to its first position.

Due to limitations on the accuracy of the data collection procedure, errors are introduced in the data describing the location of a vertebra in its positions 1, 2, . . . , n. In order to analyze such data, it therefore becomes necessary to refer to a common reference, namely, the first position of the vertebra, and calculate the screws $\overline{S}_{1,2}$; $\overline{S}_{1,3}$; . . .; $\overline{S}_{1,n}$. The parameters of the successive screws must, however, be calculated not from the original vertebral position data, but from the parameters of the screws $\overline{S}_{1,2}$; $\overline{S}_{1,3}$; . . . ; $\overline{S}_{1,n}$. It is therefore necessary to devise a mathematical procedure to calculate the parameters of screw $\overline{S}_{2,3}$ using the screws $\overline{S}_{1,2}$ and $\overline{S}_{1,3}$; and so on.

The matrix $[A']_{21}$ (Equation 3) defines the screw displacement of a vertebra moving from position 1 to 2. If a matrix [D] is formulated using augmented vectors as columns, whose components define the coordinates of four non-coplanar points in the vertebral reference system, then

$$[D]_2 = [A']_{21}\,[D]_1 \tag{8a}$$

where

$$[D] = \begin{bmatrix} 1 & 1 & 1 & 1 \\ x^{(1)} & x^{(2)} & x^{(3)} & x^{(4)} \\ y^{(1)} & y^{(2)} & y^{(3)} & y^{(4)} \\ z^{(1)} & z^{(2)} & z^{(3)} & z^{(4)} \end{bmatrix}$$

The components of matrix $[D]_2$ define in the fixed reference system the coordinates of the four non-coplanar points on the moving vertebra in its second position. Using the same principle, the following equations can be written:

$$[D]_3 = [A']_{31} [D]_1 \tag{8b}$$

$$[D]_3 = [A']_{32} [D]_2 \tag{8c}$$

Equations (8a), (8b), and (8c) yield:

$$[A']_{32} = [A']_{31} [A']_{21}^{-1} \tag{9}$$

Equation (9) defines the screw displacement matrix $[A']_{32}$ which can be used to calculate the parameters of screw $\overline{S}_{2,3}$ using the methodology presented in section 4.1.

4.4 Analytical Formulation of the Axode of Intervertebral Motion

The choice of a mathematical ruled surface used for approximating the axode of motion between two or more finitely separated positions of a vertebra depends upon the kinematic boundary conditions to be satisfied at these positions. For this investigation, it was decided to formulate a generalized analytical form of the axode which would satisfy any of the following three boundary conditions:

1. Velocity of the vertebra at three finitely separated positions: (V-V-V).

2. Velocity and acceleration of the vertebra at position 1 and velocity at position 2: (V, A-V).

3. Velocity at position 1, and velocity and acceleration at position 2: (V-V, A).

In order to satisfy any of the above boundary conditions the generalized axode must pass through three instantaneous (or velocity) screws of motion. Once such a generalized form is available, the boundary condition 2, (V, A-V), can be satisfied by choosing two consecutive velocity screws at position 1 and the third velocity screw at position 2. In the same manner, the boundary condition 3, (V-V, A), can be satisfied by the generalized axode which will pass through a velocity screw at position 1 and two consecutive velocity screws at position 2.

Among the second degree ruled surfaces, the most general one is the hyperboloid of one sheet which can be completely specified by three non-intersecting lines. In the following the details of a methodology is presented which can be used to obtain a generalized form of the axode passing through three velocity or instantaneous screw axes.

1. The three instantaneous screw axes are defined in a fixed frame of reference $(X_oY_oZ_o)$ by their direction cosines (ℓ_i, m_i, n_i) and by the coordinates $(\alpha_i, \beta_i, \gamma_i)$ of a point lying on each screw axis:

   a. S_1: $\ell_1, m_1, n_1; \alpha_1, \beta_1, \gamma_1$

   b. S_2: $\ell_2, m_2, n_2; \alpha_2, \beta_2, \gamma_2$

   c. S_3: $\ell_3, m_3, n_3; \alpha_3, \beta_3, \gamma_3$.

2. Coordinate system for the hyperboloid of one sheet: Define a

plane passing through axes 1 and parallel to axes 2. The equation to this plane is given by [84]:

$$(m_2n_1 - m_1n_2)x + (\ell_1n_2 - \ell_2n_1)y + (\ell_2m_1 - m_2\ell_1)z$$
$$= \alpha_1(m_2n_1 - m_1n_2) + \beta_1(\ell_1n_2 - \ell_2n_1) + \gamma_1(\ell_2m_1 - m_2\ell_1)$$

In general, the equation to a plane (P_{ij}) containing line i and parallel to line j is given by:

$$ax + by + cz = d \tag{10}$$

where

$$a = m_jn_i - m_in_j$$

$$b = \ell_in_j - \ell_jn_i$$

$$c = \ell_jm_i - m_j\ell_i$$

$$d = \alpha_ia + \beta_ib + \gamma_ic$$

If three axes are not parallel to the same plane, planes drawn through each axis parallel to the other two form a parallelopiped. For the six planes of the parallelopiped, Equation (10) can be written as:

$$P_{12}: \quad a_1x + b_1y + c_1z = d_1$$

$$P_{13}: \quad a_2x + b_2y + c_2z = d_2$$

$$P_{23}: \quad a_3x + b_3y + c_3z = d_3$$

$$P_{21}: \quad a_1x + b_1y + c_1z = d_4$$

$$P_{31}: \quad a_2x + b_2y + c_2z = d_5$$

$$P_{32}: \quad a_3x + b_3y + c_3z = d_6$$

Since the planes P_{12} and P_{21} are parallel to each other, the coefficients in the equations defining the two planes are identical, and so on.

The plane parallel to P_{12} and P_{21} and halfway between them is given by:

$$PP_{12-21}: \quad a_1x + b_1y + c_1z = \frac{d_1 + d_4}{2} = e_1 \tag{11}$$

Similarly,

$$PP_{13-31}: \quad a_2x + b_2y + c_2z = \frac{d_2 + d_5}{2} = e_2$$

and

$$PP_{23-32}: \quad a_3x + b_3y + c_3z = \frac{d_3 + d_6}{2} = e_3$$

The three planes defined by Equation (11) intersect at a point c which is the center of the parallelopiped. The coordinates of this point of intersection c in the fixed frame of reference are given by:

$$\begin{bmatrix} x_c \\ y_c \\ z_c \end{bmatrix} = \begin{bmatrix} a_1 & b_1 & c_1 \\ a_2 & b_2 & c_2 \\ a_3 & b_3 & c_3 \end{bmatrix}^{-1} \begin{bmatrix} e_1 \\ e_2 \\ e_3 \end{bmatrix} \tag{12}$$

The center c of the parallelopiped is now chosen as the origin of a new coordinate system. The cx', cy', and cz' axes of the new coordinate system are taken parallel to the edges 1, 2, and 3 of the parallelopiped, respectively. The direction cosines of the new reference axes are then defined in the fixed frame of reference as:

$$x'(\ell_1, m_1, n_1); \; y'(\ell_2, m_2, n_2); \; z'(\ell_3, m_3, n_3)$$

Figure 10 shows the coordinate system for the hyperboloid of one sheet. The coordinate system cx'y'x' is an oblique coordinate system.

3. Analytical form of axode: The lengths of the three sides of the parallelopiped are given by [84]:

$$h_{ij} = \frac{\begin{vmatrix} \alpha_i - \alpha_j, & \beta_i - \beta_j, & \gamma_i - \gamma_j \\ \ell_i & m_i & n_i \\ \ell_j & m_j & n_j \end{vmatrix}}{\begin{vmatrix} \ell_1 & m_1 & n_1 \\ \ell_2 & m_2 & n_2 \\ \ell_3 & m_3 & n_3 \end{vmatrix}} \tag{13a}$$

where h_{ij} is the distance between axes i and j, and is measured along a line parallel to the third axis.

In the new coordinate system defined for the hyperboloid of one sheet, the three instantaneous (velocity) screw axes can be redefined as:

a. $y' = b,\ z' = -c$

b. $z' = c,\ x' = -a$

c. $x' = a,\ y' = -b$

where

$$a = h_{23/2}$$

$$b = h_{13/2}$$

$$c = h_{12/2} \tag{13b}$$

The analytical form of axode approximated by the hyperboloid of one

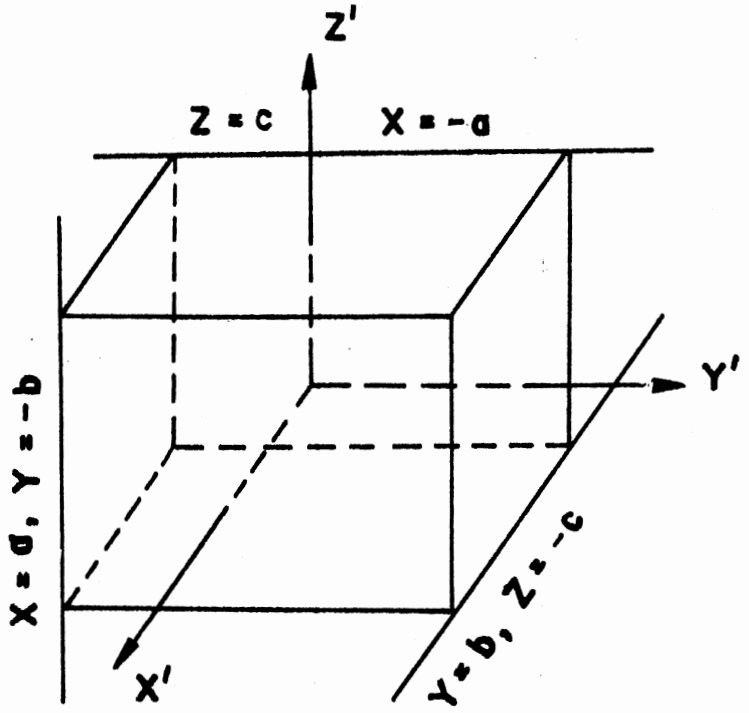

Figure 10. A Coordinate System for the Hyperboloid of One Sheet

sheet (a second degree ruled surface) passing through these three axes is given by:

$$ay'z' + bz'x' + cx'y' + abc = 0 \tag{14}$$

4. Stepwise procedure: The following stepwise procedure, based upon the methodology developed above, should be used to formulate the analytical form of axode approximated by a second degree ruled surface passing through three non-intersecting screw axes:

a. Using the direction cosines of the three screw axes, and the coordinates of a point lying on each screw axis, evaluate coefficients $a_1 - a_3$, $b_1 - b_3$, $c_1 - c_3$, and $e_1 - e_3$ of Equation (11).

b. Calculate the coordinates of the center c of the parallelopiped using Equation (12). These coordinates are defined in the fixed frame of reference OXYZ.

c. Define an oblique coordinate system CX'Y'Z' for the ruled surface (hyperboloid of one sheet). The origin C of this new coordinate system coincides with the center of the parallelopiped. The direction cosines of the oblique axes CX', CY', CZ' referred to the rectangular frame of reference OXYZ are ℓ_1, m_1, n_1; ℓ_2, m_2, n_2; ℓ_3, m_3, n_3.

d. Calculate the lengths h_{12}, h_{13}, h_{23} of the three sides (or edges) of the parallelopiped by solving Equation (13a).

e. In the new coordinate system CX'Y'Z', redefine the three screw axes using Equation (13b):

(1) $y' = b$, $z' = -c$

(2) $z' = c$, $x' = -a$

(3) $x' = a$, $y' = -b$.

f. In the new coordinate system CX'Y'Z', the analytical form of the axode approximated by the hyperboloid of one sheet (a second degree ruled surface) passing through the three screw axes redefined in step e is then given by:

$$ay'z' + bz'x' + cx'y' + abc = 0$$

4.5 Interpolation Using the Axode Approximation

The analytical form of the axode as derived in section 4.4 approximates the true axode of intervertebral motion by a second degree ruled surface. In the following, a methodology is developed which utilizes this second degree ruled surface to interpolate on the direction cosines of the instantaneous screw axis of motion:

1. The coordinates of a point on the screw axis referred to the hyperboloid coordinate system: The new coordinate system (CX'Y'Z') defined for the hyperboloid of one sheet is an oblique coordinate system. The direction cosines of the axes CX', CY', CZ' referred to the fixed frame of reference (OXYZ) are ℓ_1, m_1, n_1; ℓ_2, m_2, n_2; ℓ_3, m_3, n_3. The angles y'cz', x'cz', x'cy' are λ, μ, ν, where

$$\cos \lambda = \ell_2\ell_3 + m_2m_3 + n_2n_3$$

$$\cos \mu = \ell_1\ell_3 + m_1m_3 + n_1n_3$$

$$\cos \nu = \ell_1\ell_2 + m_1m_2 + n_1n_2$$

If α, β, γ are the coordinates of a point P lying on a screw axis referred to the fixed frame of reference, then the coordinates (α', β', γ') of the same point P referred to the new coordinate system (cx'y'z') are given by:

$$\begin{bmatrix} \alpha' \\ \beta' \\ \gamma' \end{bmatrix} = \begin{bmatrix} 1 & \cos\nu & \cos\mu \\ \cos\nu & 1 & \cos\lambda \\ \cos\mu & \cos\lambda & 1 \end{bmatrix}^{-1} \begin{bmatrix} r\cos\theta \\ r\cos\phi \\ r\cos\psi \end{bmatrix} \tag{15}$$

where

$$\cos\theta = \ell_r \cdot \ell_1 + m_r \cdot m_1 + n_r \cdot n_1$$

$$\cos\phi = \ell_r \cdot \ell_1 + m_r \cdot m_2 + n_r \cdot n_2$$

$$\cos\psi = \ell_r \cdot \ell_3 + m_r \cdot m_3 + n_r \cdot n_3$$

$$\ell_r = \frac{(\alpha - x_c)}{r}$$

$$m_r = \frac{(\beta - y_c)}{r}$$

$$n_r = \frac{(\gamma - z_c)}{r}$$

$$r = [(\alpha - x_c)^2 + (\beta - y_c)^2 + (\gamma - z_c)^2]^{1/2}$$

2. Condition for a line to lie entirely on the ruled surface: Let ℓ', m', n' be the direction cosines of a line referred to the oblique coordinate system CX'Y'Z'. Let $P_1'(\alpha', \beta', \gamma')$ be the coordinates of a point on this line. Let $P_2'(x', y', z')$ be another point on the same line, and let the measure $P_1' P_2'$ be r. Then the coordinates x', y', z' are given by:

$$\begin{bmatrix} X' \\ Y' \\ Z' \end{bmatrix} = \begin{bmatrix} \alpha' \\ \beta' \\ \gamma' \end{bmatrix} + \begin{bmatrix} C_{11} & C_{12} & C_{13} \\ C_{21} & C_{22} & C_{23} \\ C_{31} & C_{32} & C_{33} \end{bmatrix} \begin{bmatrix} \ell' r \\ m' r \\ n' r \end{bmatrix} \tag{16}$$

where

$$[C] = \begin{bmatrix} 1 & \cos\nu & \cos\mu \\ \cos\nu & 1 & \cos\lambda \\ \cos\mu & \cos\lambda & 1 \end{bmatrix}^{-1}$$

The point P_2' (x', y', z') will lie on the ruled surface (hyperboloid of one sheet defined by Equation (14)) if the following condition is satisfied:

$$\begin{aligned} a[\beta' + (C_{21}\ell' + C_{22}m' + C_{23}n')r]\,[\gamma' + (C_{31}\ell' + C_{32}m' \\ + C_{33}n')r] + b[\gamma' + (C_{31}\ell' + C_{32}m' + C_{33}n')r]\,[\alpha' \\ + (C_{11}\ell' + C_{12}m' + C_{13}n')r] + c[\alpha' + (C_{11}\ell' + C_{12}m' \\ + C_{13}n')r]\,[\beta' + (C_{21}\ell' + C_{22}m' + C_{23}n')r] \\ + a\,b\,c = 0 \end{aligned}$$

If the above equation holds good for all values of r, then the entire line (ℓ', m', n') will lie on the ruled surface. This yields the following three conditions:

$$a\beta'\gamma' + b\gamma'\alpha' + c\alpha'\beta' + a\,b\,c = 0 \tag{17}$$

$$u_1\ell' + u_2m' + u_3n' = 0 \tag{18}$$

$$v_1\ell'^2 + v_2m'^2 + v_3n'^2 + v_4\ell'm' + v_5m'n' + v_6\ell'n' = 0 \tag{19}$$

where

$$u_1 = a(\beta'C_{31} + \gamma'C_{21}) + b(\gamma'C_{11} + \alpha'C_{31}) + c(\alpha'C_{21} + \beta'C_{11})$$

$$u_2 = a(\beta'C_{32} + \gamma'C_{22}) + b(\gamma'C_{12} + \alpha'C_{32}) + c(\alpha'C_{22} + \beta'C_{12})$$

$$u_3 = a(\beta'C_{33} + \gamma'C_{23}) + b(\gamma'C_{13} + \alpha'C_{33}) + c(\alpha'C_{23} + \beta'C_{13})$$

$$v_1 = aC_{21}C_{31} + bC_{31}C_{11} + C\cdot C_{11}C_{21}$$

$$v_2 = aC_{22}C_{32} + bC_{32}C_{12} + C\cdot C_{12}C_{22}$$

$$v_3 = aC_{23}C_{33} + bC_{33}C_{13} + C\cdot C_{13}C_{23}$$

$$v_4 = a(C_{21}C_{32} + C_{22}C_{31}) + b(C_{31}C_{12} + C_{32}C_{11}) + C\cdot(C_{11}C_{22} + C_{12}C_{21})$$

$$v_5 = a(C_{22}C_{33} + C_{23}C_{32}) + b(C_{32}C_{13} + C_{33}C_{12}) + C\cdot(C_{12}C_{23} + C_{13}C_{22})$$

$$v_6 = a(C_{21}C_{33} + C_{23}C_{31}) + b(C_{31}C_{13} + C_{33}C_{11}) + C\cdot(C_{11}C_{23} + C_{13}C_{21})$$

3. Relationship between the direction cosines ℓ', m', n': Since ℓ', m', n' are the direction cosines of a line referred to the oblique set of axes cx', cy', cz', the following relationship [84] must be satisfied by the direction cosines (ℓ', m, n'):

$$\begin{vmatrix} 1 & \cos\nu & \cos\mu & \ell' \\ \cos\nu & 1 & \cos\lambda & m' \\ \cos\mu & \cos\lambda & 1 & n' \\ \ell' & m' & n' & 1 \end{vmatrix} = 0$$

which yields the following equation:

$$\ell'^2(1 - \cos^2\lambda) + m'^2(1 - \cos^2\mu) + n'^2(1 - \cos^2\nu) - 2\ell'm'(\cos\nu - \cos\lambda\cos\mu) - 2m'n'(\cos\lambda - \cos\mu\cos\nu) - 2\ell'n'(\cos\mu - \cos\lambda\cos\nu) = (1 - \cos^2\lambda - \cos^2\mu - \cos^2\nu + 2\cos\lambda\cos\mu\cos\nu) \quad (20)$$

4. Direction cosines of the interpolated screw axis in the fixed frame of reference (OXYZ): Equations (18), (19), and (20) define the

direction cosines (ℓ', m', n') of a line passing through a point α', β', and γ' and lying entirely on the ruled surface (hyperboloid of one sheet), referred to the oblique coordinate system CX'Y'Z'. As mentioned earlier in section 4.5, the direction cosines of the axes CX', CY', CZ' referred to the fixed frame of reference OXYZ are ℓ_1, m_1, n_1; ℓ_2, m_2, n_2; ℓ_3, m_3, n_3. If P_1' (α', β', γ') and P_2' are two points on the line (ℓ', m', n') such that the measure $P_1'P_2'$ along this line is unity, then the coordinates (X_{p1}, Y_{p1}, Z_{p1}) and (X_{p2}, Y_{p2}, Z_{p2}) of these two points referred to the fixed frame OXYZ are given by:

$$\begin{bmatrix} X_{p1} \\ Y_{p1} \\ Z_{p1} \end{bmatrix} = \begin{bmatrix} \ell_1 & \ell_2 & \ell_3 \\ m_1 & m_2 & m_3 \\ n_1 & n_2 & n_3 \end{bmatrix} \begin{bmatrix} \alpha' \\ \beta' \\ \gamma' \end{bmatrix}$$

$$\begin{bmatrix} X_{p2} \\ Y_{p2} \\ Z_{p2} \end{bmatrix} = \begin{bmatrix} \ell_1 & \ell_2 & \ell_3 \\ m_1 & m_2 & m_3 \\ n_1 & n_2 & n_3 \end{bmatrix} \begin{bmatrix} 1 & \cos\nu & \cos\mu \\ \cos\nu & 1 & \cos\lambda \\ \cos\mu & \cos\lambda & 1 \end{bmatrix}^{-1} \begin{bmatrix} \ell' \\ m' \\ n' \end{bmatrix} + \begin{bmatrix} X_{p1} \\ Y_{p1} \\ Z_{p1} \end{bmatrix}$$

If ℓ, m, n are the direction cosines of the same line referred to the fixed frame of reference OXYZ, then

$$\begin{bmatrix} \ell \\ m \\ n \end{bmatrix} = \begin{bmatrix} \ell_1 & \ell_2 & \ell_3 \\ m_1 & m_2 & m_3 \\ n_1 & n_2 & n_3 \end{bmatrix} \begin{bmatrix} 1 & \cos\nu & \cos\mu \\ \cos\nu & 1 & \cos\lambda \\ \cos\mu & \cos\lambda & 1 \end{bmatrix}^{-1} \begin{bmatrix} \ell' \\ m' \\ n' \end{bmatrix} \qquad (21)$$

5. Stepwise procedure: The following stepwise procedure, based upon the methodology developed above, should be used to interpolate on the direction cosines of the instantaneous screw axis of motion passing

through a point α, β, γ.

a. Using the oblique coordinate system CX'Y'Z' as determined in section 4.4 and Equation (15), calculate the coordinates (α', β', γ') of the point referred to CX'Y'Z'.

b. Since the actual axode of motion is approximated by a second degree ruled surface, the point (α', β', λ') may not lie on the ruled surface. Therefore, using Equation (17) (condition for a point to lie on the ruled surface), locate a point (α^*, β^*, γ^*) on the ruled surface such that the new point is closest to the actual point (α', β', γ'). Redefine $\alpha' = \alpha^*$, $\beta' = \beta^*$, $\gamma' = \gamma^*$.

c. Using the redefined coordinates α', β', γ', solve Equations (18), (19), and (20) to obtain the direction cosines (ℓ', m', n') of the interpolated screw axis passing through the point (α', β', γ') referred to the oblique coordinate system CX'Y'Z'. There are two families of straight lines which can generate the same ruled surface. Therefore, the correct set must be identified which is consistent with the original three screw axes of motion.

d. Calculate the direction cosines of the interpolated screw axis referred to the fixed frame of reference OXYZ, by using Equation (21).

The methodology developed in sections 4.1 through 4.5 can now be applied to perform kinematic analysis of data describing three-dimensional intervertebral motion. The next section presents demonstrative examples of such kinematic analysis of the experimental data.

4.6 Kinematic Analysis of Experimental Data Describing Three-Dimensional Intervertebral Motion

In sections 4.1 through 4.5 a methodology was developed to perform analysis of the data describing the three-dimensional intervertebral motion of the spine. Using the mathematical procedures presented in the above sections, the intervertebral motion data can be analyzed to obtain:

1. Parameters of the screw axes of motion as the intervertebral joint executes a mode of relative motion.

2. Analytical form of the axode approximating the locus of the instantaneous screw axes as the intervertebral joint executes a mode of relative motion.

3. Interpolation on the parameters of the instantaneous screw axes using the axode approximation developed above.

The methodology for kinematic data analysis or signature analysis of intervertebral motion was applied to the experimental data collected by testing four human spine specimens consisting of lumbar segments L1 through L5. The results of this kinematic analysis of intervertebral motion are presented in the following.

4.6.1 Range and Pattern of Motion of Intervertebral Joints

As a spine executes a mode of motion, there is relative motion at each intervertebral joint of the spine. The parameters of the successive screws of this motion describe the pattern of motion of the intervertebral joint for the particular mode of spine motion. The limiting values of this intervertebral relative motion in terms of the rotational

and translational components describe the range of motion of the intervertebral joint for the particular mode of spine motion.

Table IV presents a sample of the results of the kinematic analysis performed on the experimental data describing the parameters of the screw axes of motion. Intervertebral motion data were collected for each spine specimen as the spine was flexed from full extension to full flexion in the sagittal plane, frontal plane, and in planes in between (15^{o} apart). Figure 11(a) through (m) shows the plots of range of motion as a function of plane of motion. After careful examination of these plots, the following observations were made:

1. The flexion angle (θ_{y_o}) decreases as the plane of motion shifts from the sagittal plane ($\theta_p = 0$) to the frontal plane ($\theta_p = 90^{o}$) and then it increases again as the plane shifts to the sagittal plane ($\theta_p = 180^{o}$).

2. The angle of lateral bending (θ_{x_o}) increases as the plane of motion shifts from the sagittal plane ($\theta_p = 0$) to the frontal plane ($\theta_p = 90^{o}$) and then it reduces again as the plane shifts to the sagittal plane ($\theta_p = 180^{o}$).

3. The axial twist increases as the plane of motion shifts from the sagittal plane to the frontal plane.

4. Eliminating the governing effect of the facet joints increased, in general, the total intervertebral relative motion.

5. Some intervertebral joints displayed somewhat symmetric behavior as the plane of motion was shifted from sagittal ($\theta_p = 0$) to frontal ($\theta_p = 90^{o}$) and from frontal to sagittal ($\theta_p = 180^{o}$).

TABLE IV

PARAMETERS OF SCREW AXES OF MOTION L2-L3 SPECIMEN 2: SAGITTAL PLANE, EXTREME EXTENSION TO EXTREME FLEXION

Direction Cosines of Screw			Rotation About Screw (Degrees)	Translation Along Screw (Inches)	Coordinates of a Point on Screw		
μ_x	μ_y	μ_z			g_x	g_y	g_z
0.392	0.916	0.089	-1.317	0.007	-0.349	0.479	1.570
0.227	0.957	-0.182	-1.358	0.008	0.771	1.852	1.201
0.087	0.991	-0.099	-2.853	0.010	0.492	1.567	1.530
0.035	0.993	-0.113	-4.186	0.051	-0.142	0.796	1.772
0.134	0.990	-0.041	-4.725	0.061	-0.219	0.719	1.870
0.141	0.979	-0.145	-5.213	0.047	-0.599	0.218	1.857

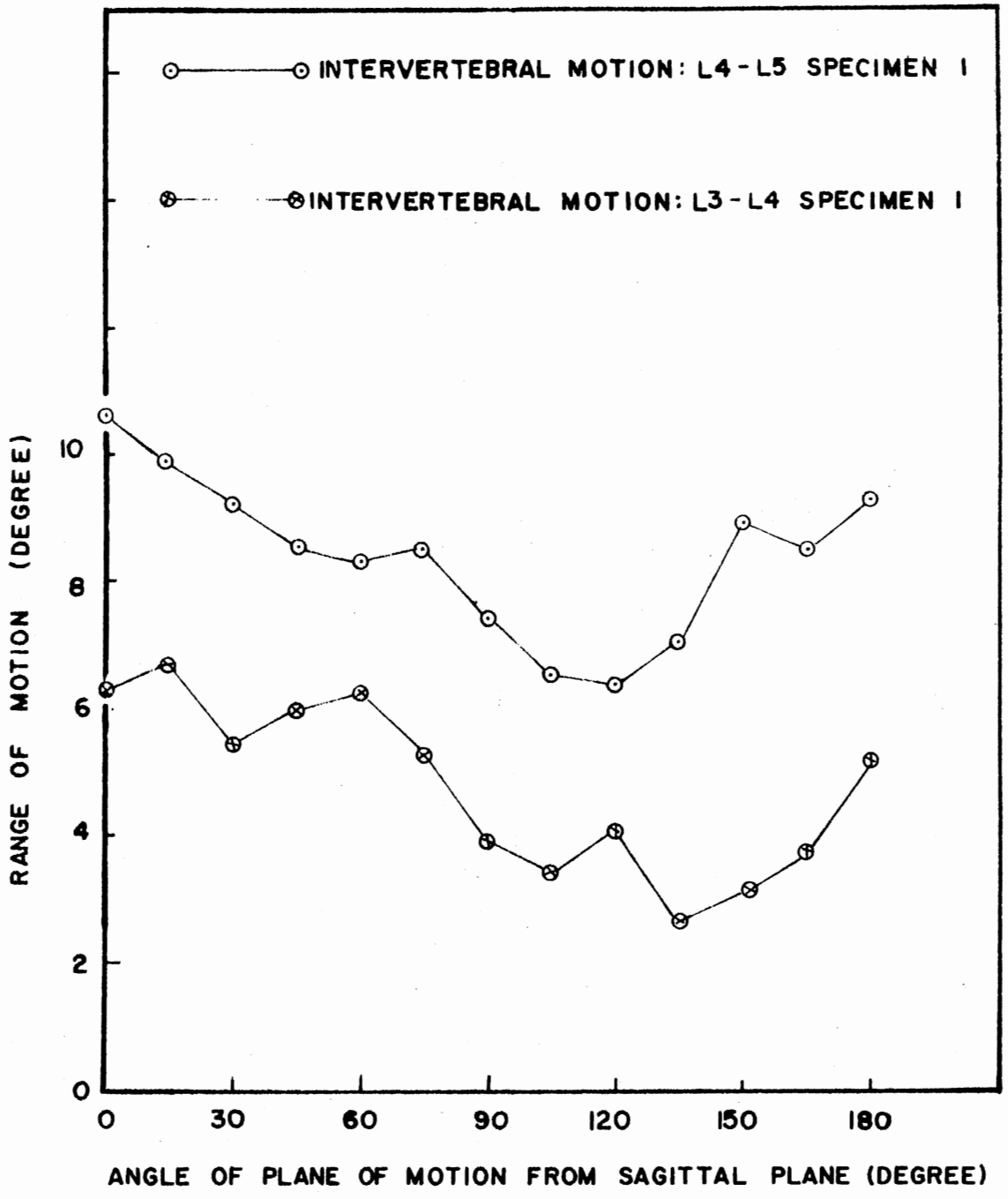

(a) L3-L4, L4-L5, Specimen 1

Figure 11. Range of Motion as a Function of Plane of Motion

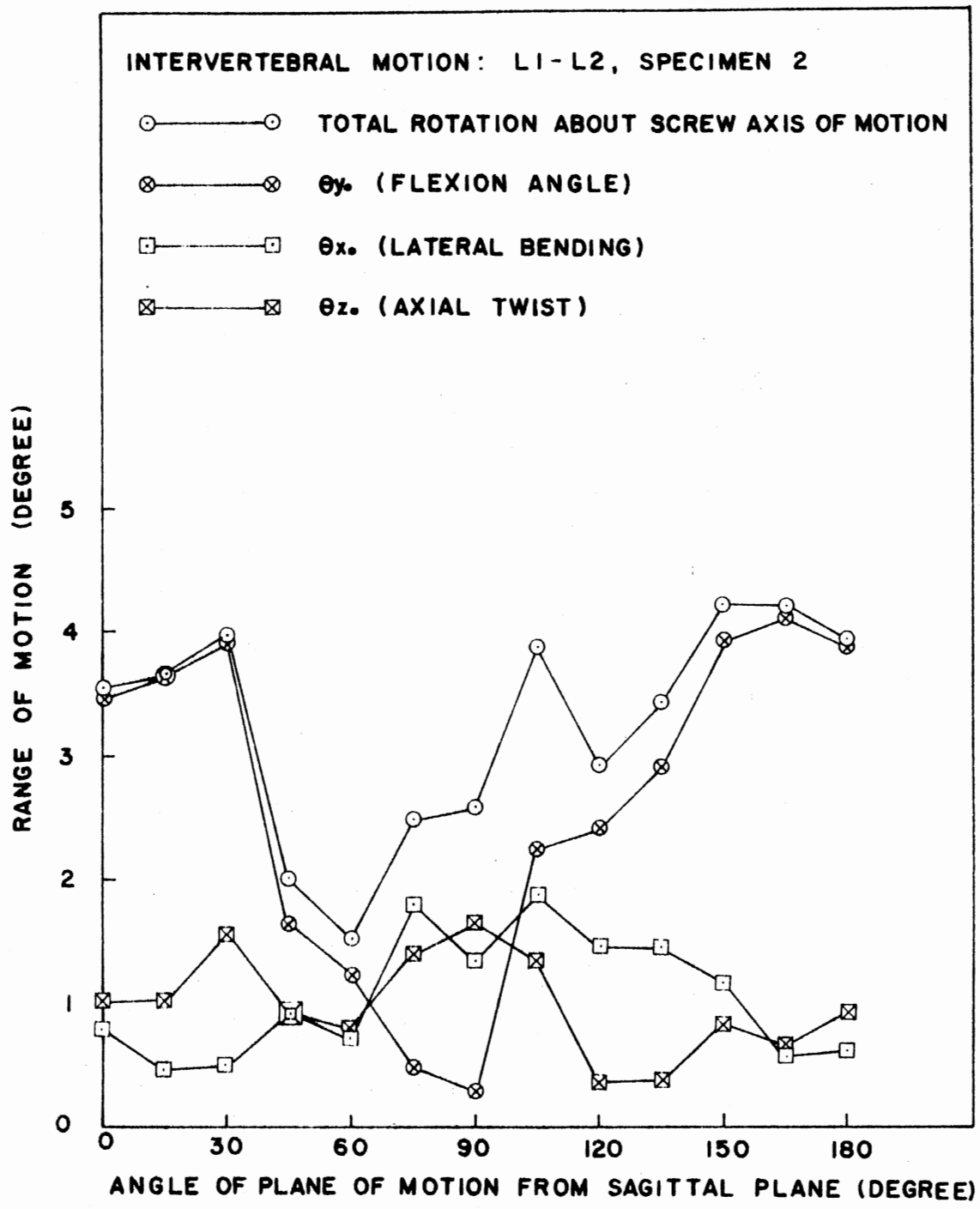

(b) L1-L2, Specimen 2

Figure 11. (Continued)

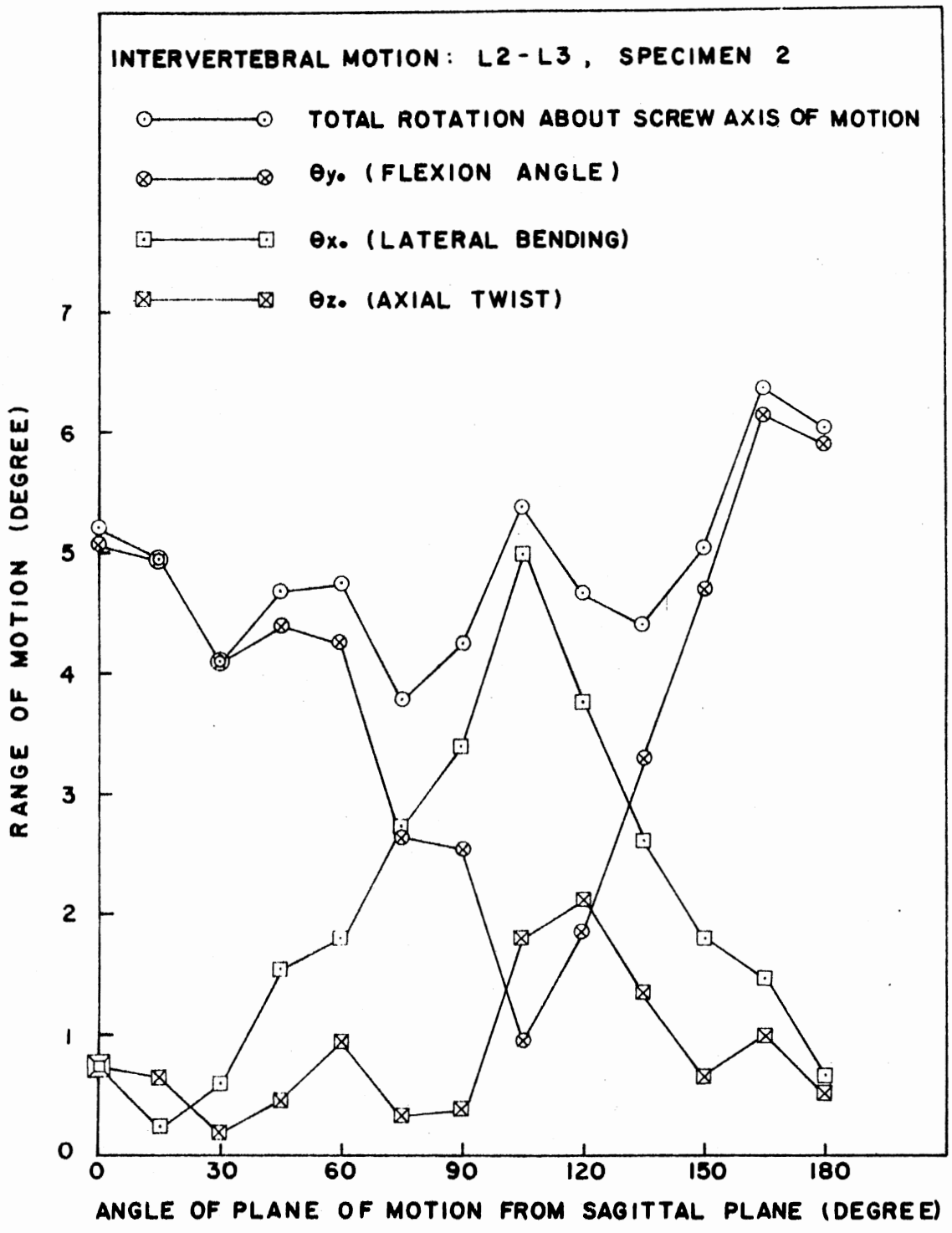

(c) L2-L3, Specimen 2

Figure 11. (Continued)

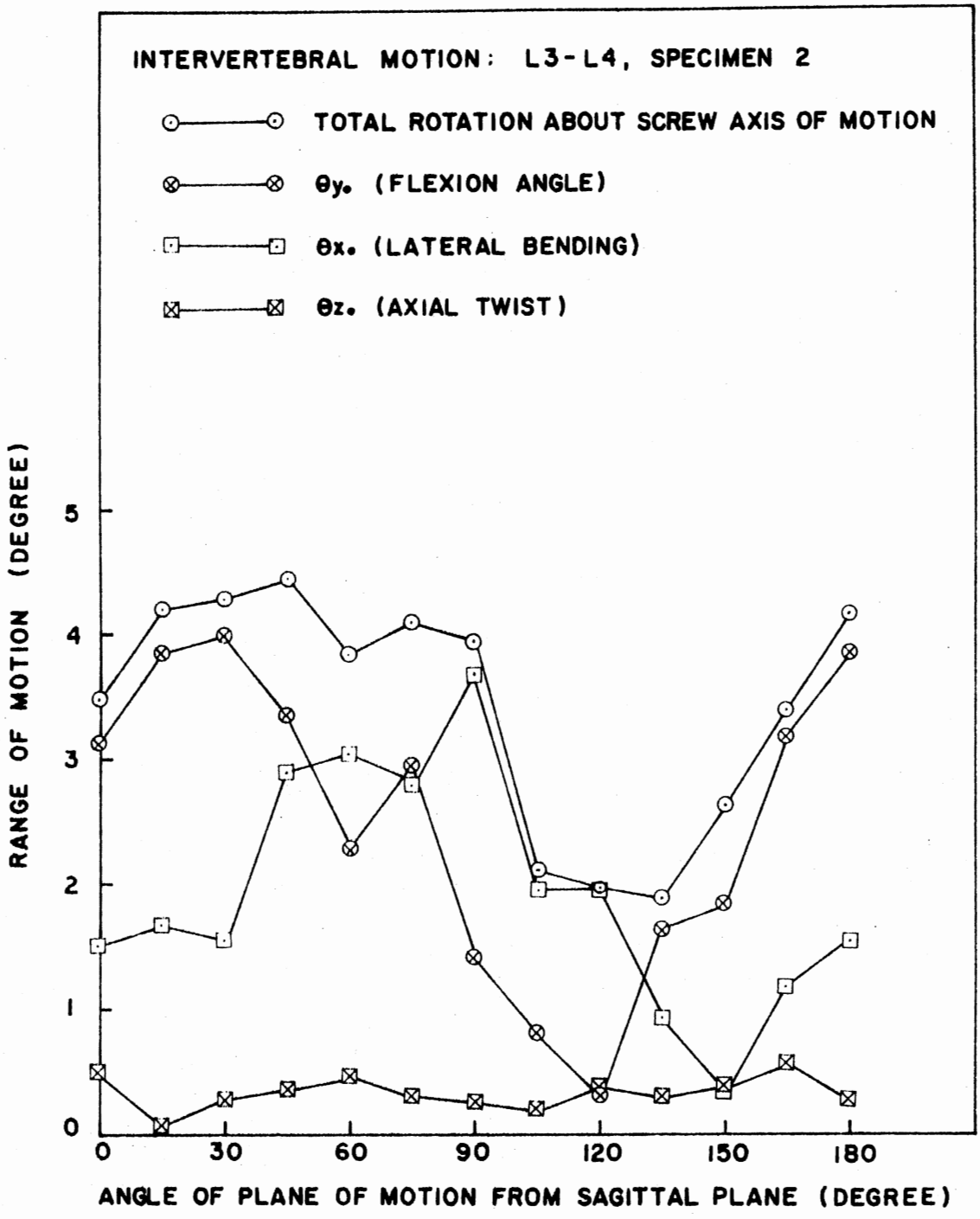

(d) L3-L4, Specimen 2

Figure 11. (Continued)

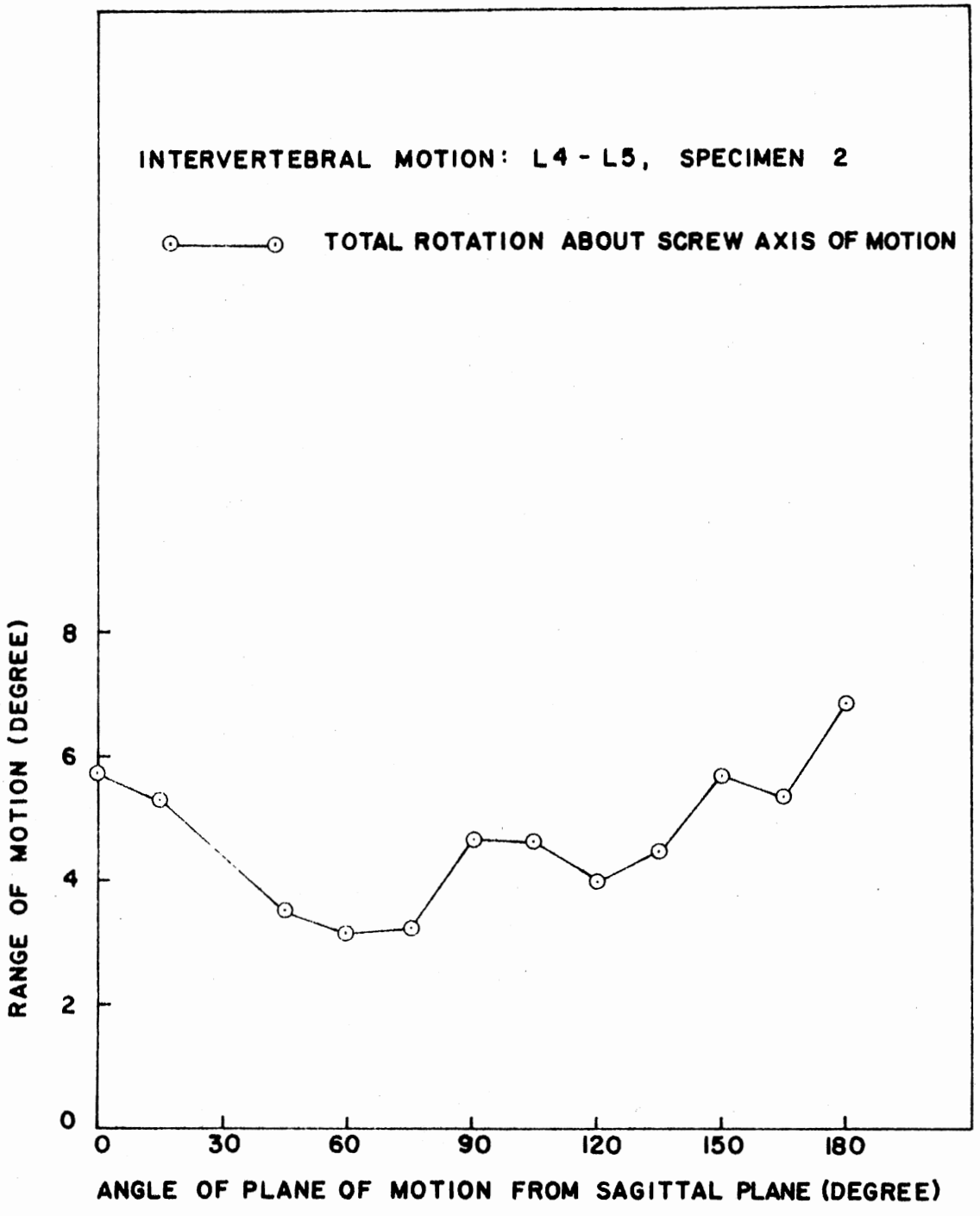

(e) L4-L5, Specimen 2

Figure 11. (Continued)

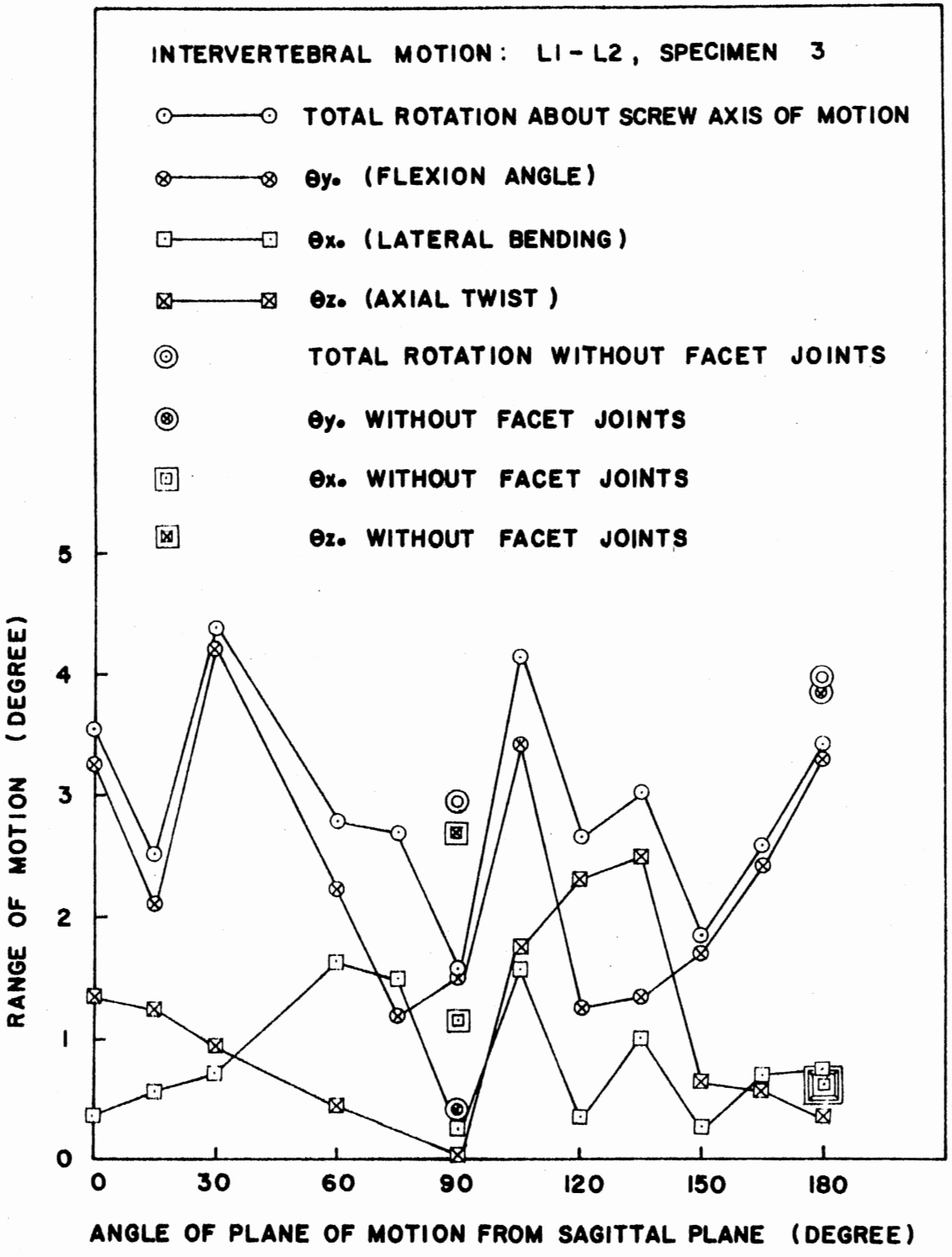

(f) L1-L2, Specimen 3

Figure 11. (Continued)

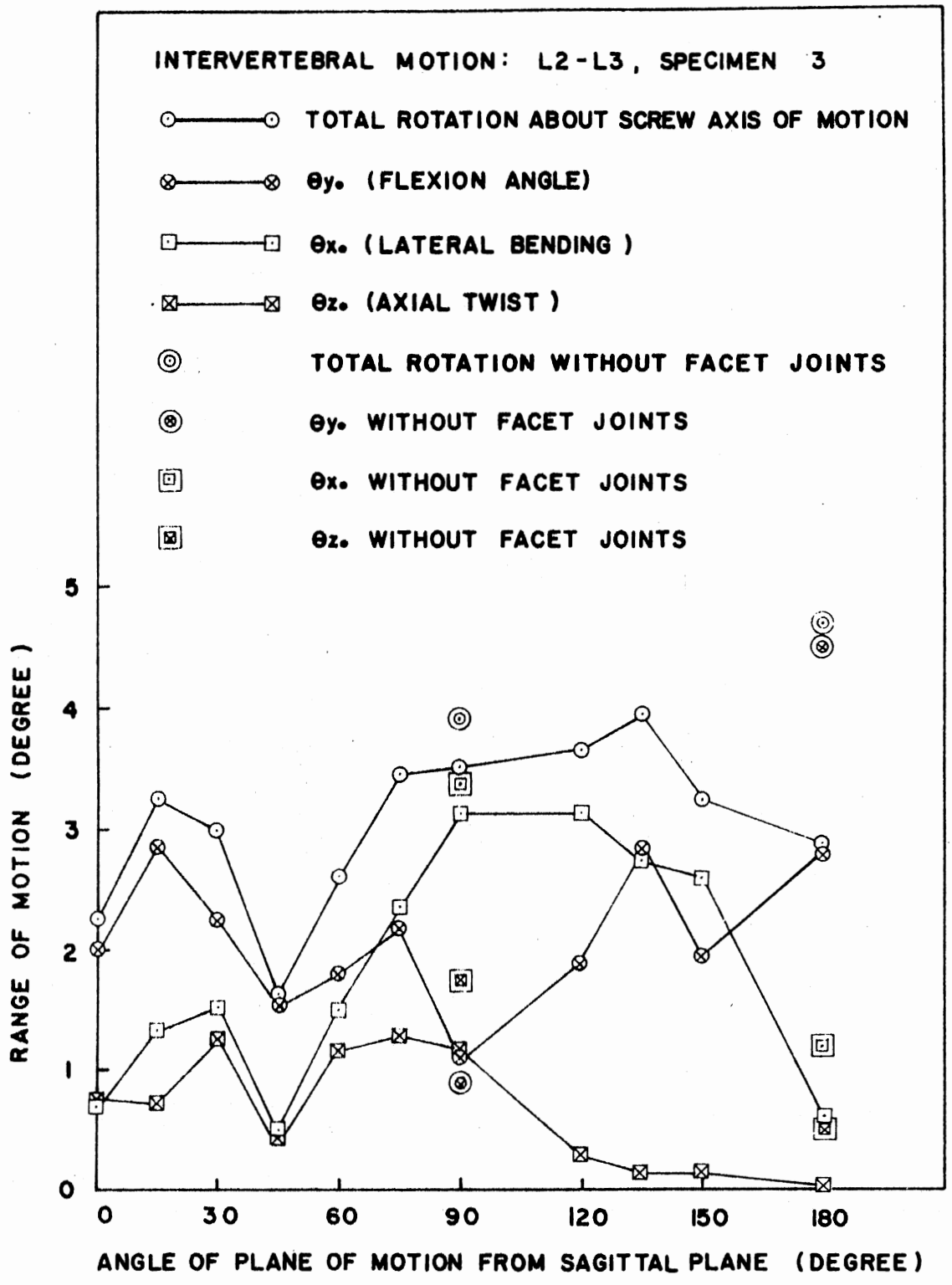

(g) L2-L3, Specimen 3

Figure 11. (Continued)

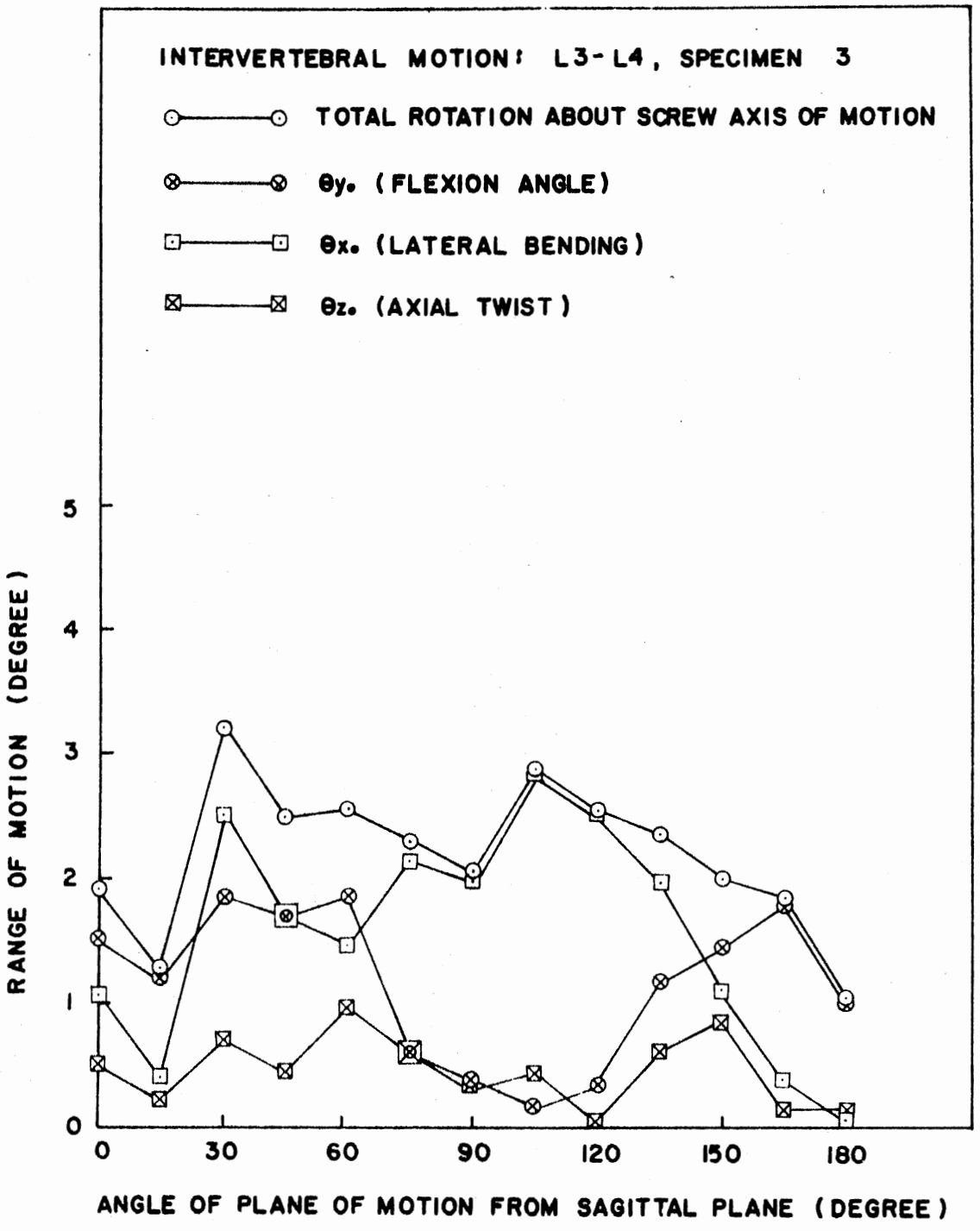

(h) L3-L4, Specimen 3

Figure 11. (Continued)

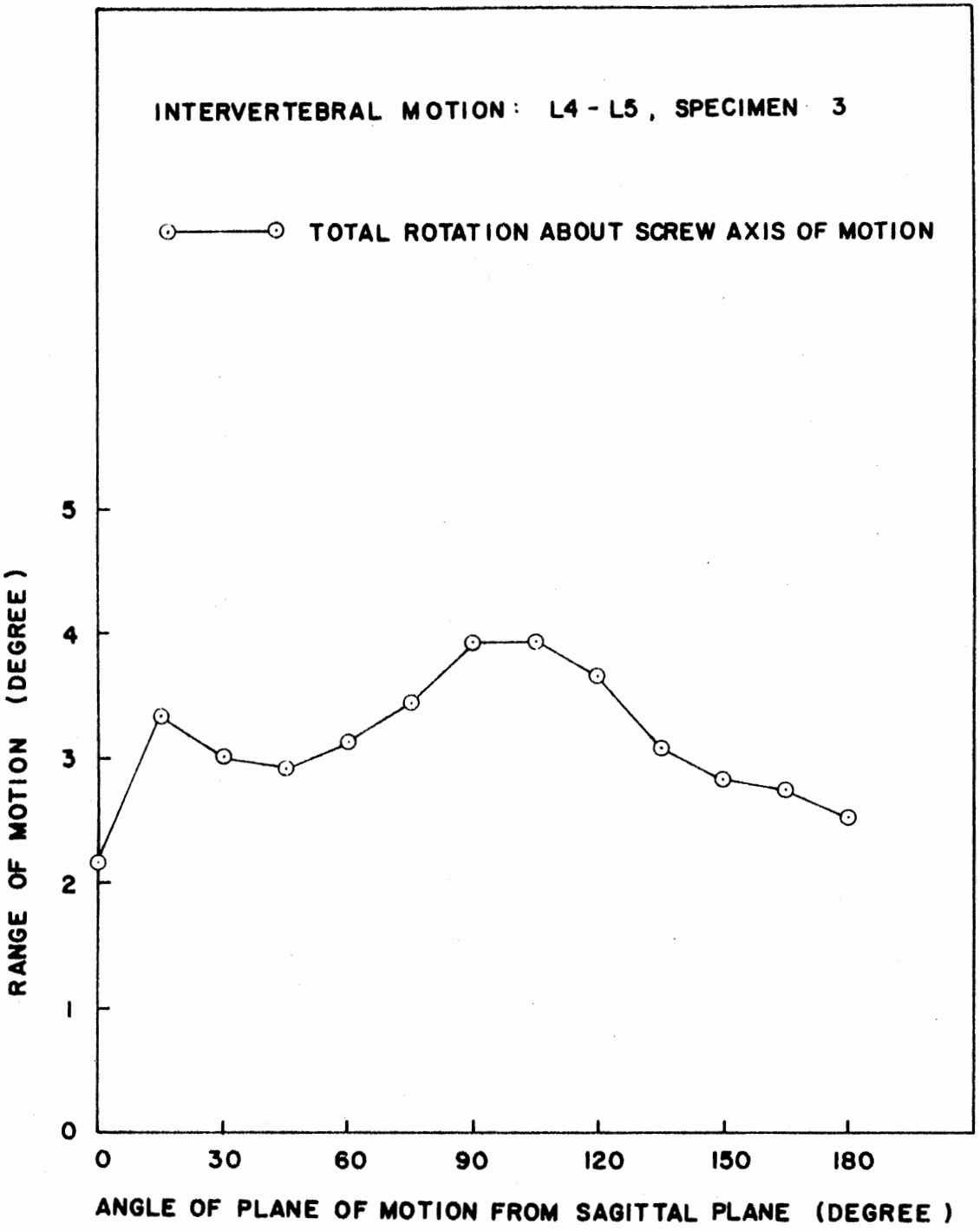

(i) L4-L5, Specimen 3

Figure 11. (Continued)

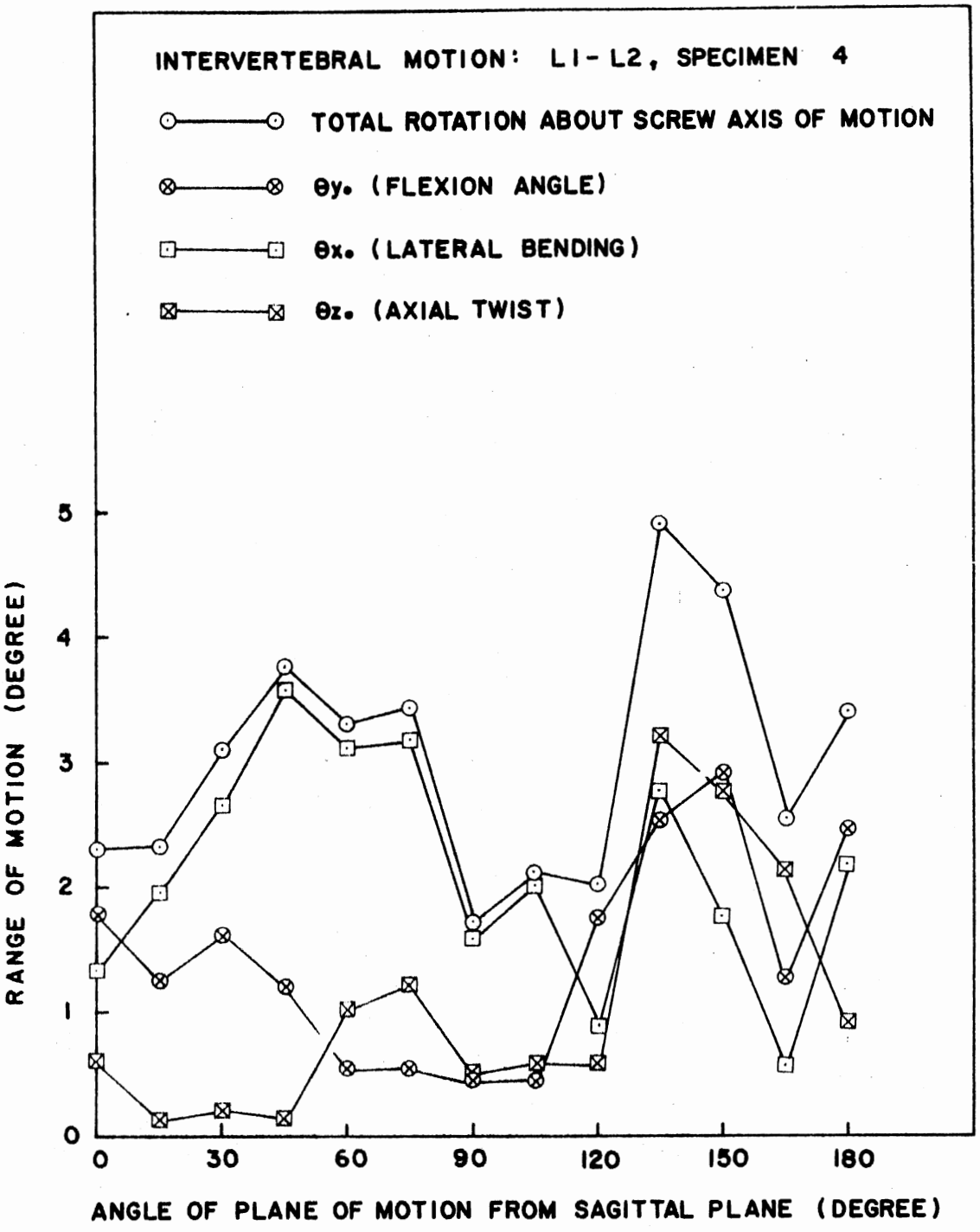

(j) L1-L2, Specimen 4

Figure 11. (Continued)

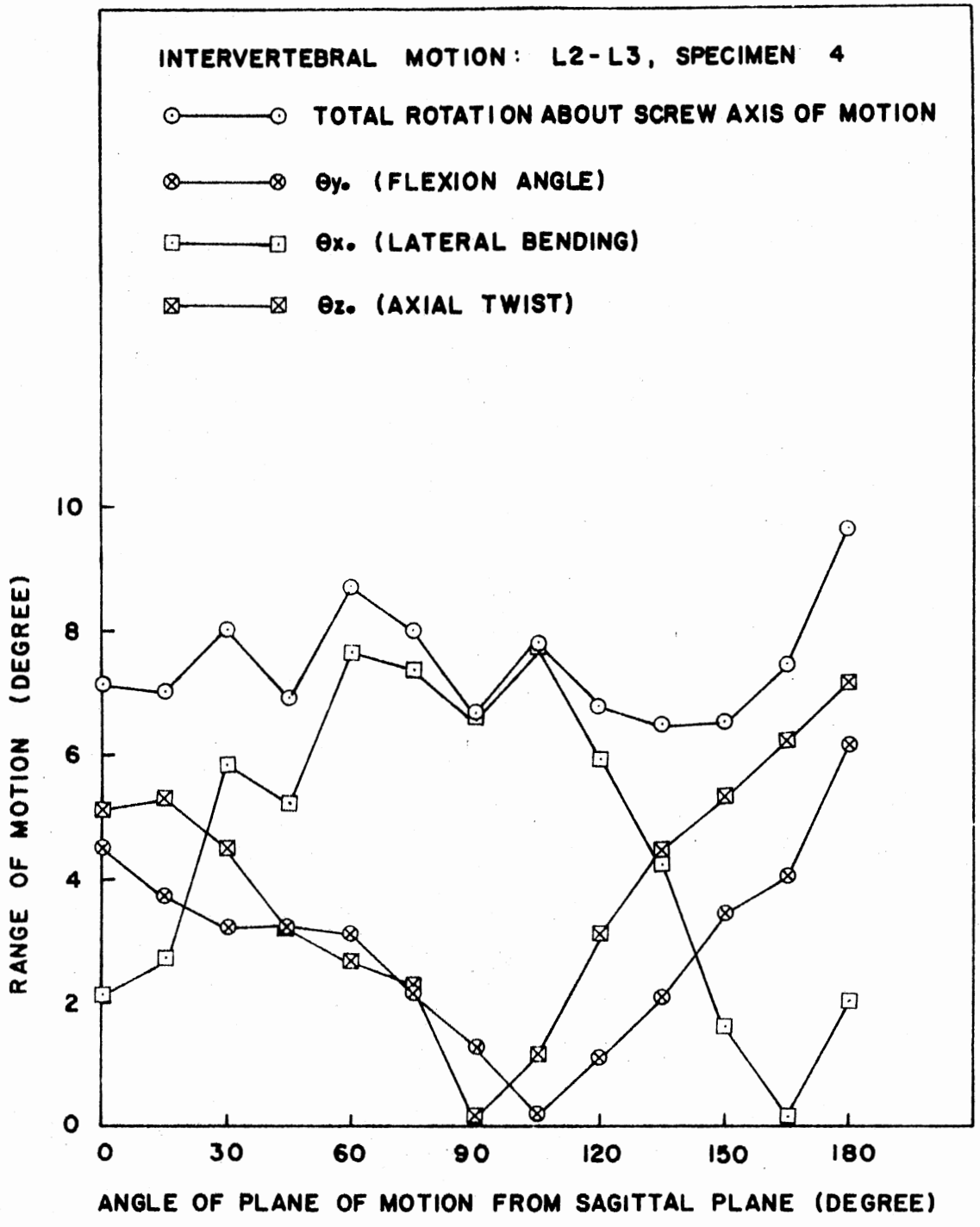

(k) L2-L3, Specimen 4

Figure 11. (Continued)

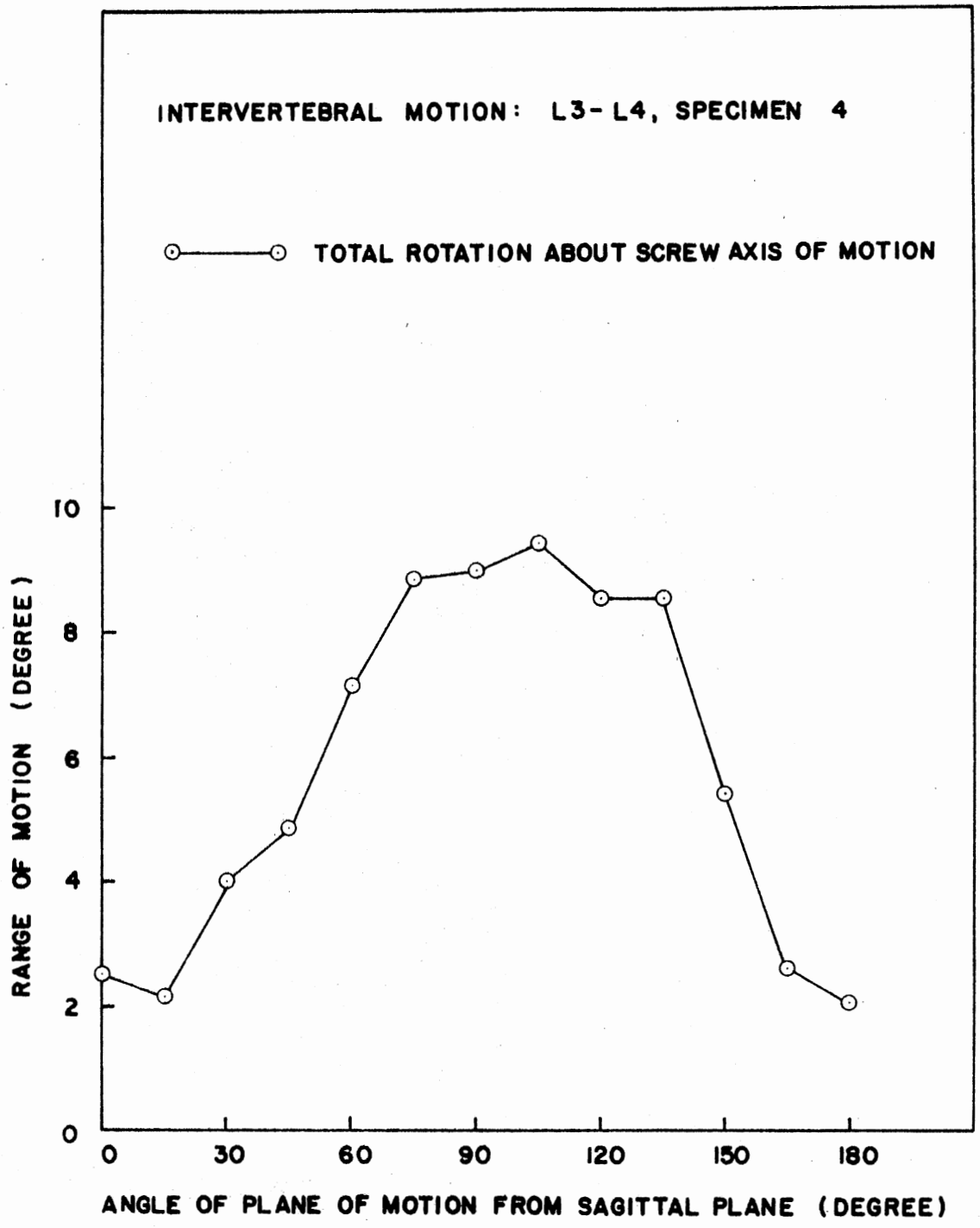

(1) L3-L4, Specimen 4

Figure 11. (Continued)

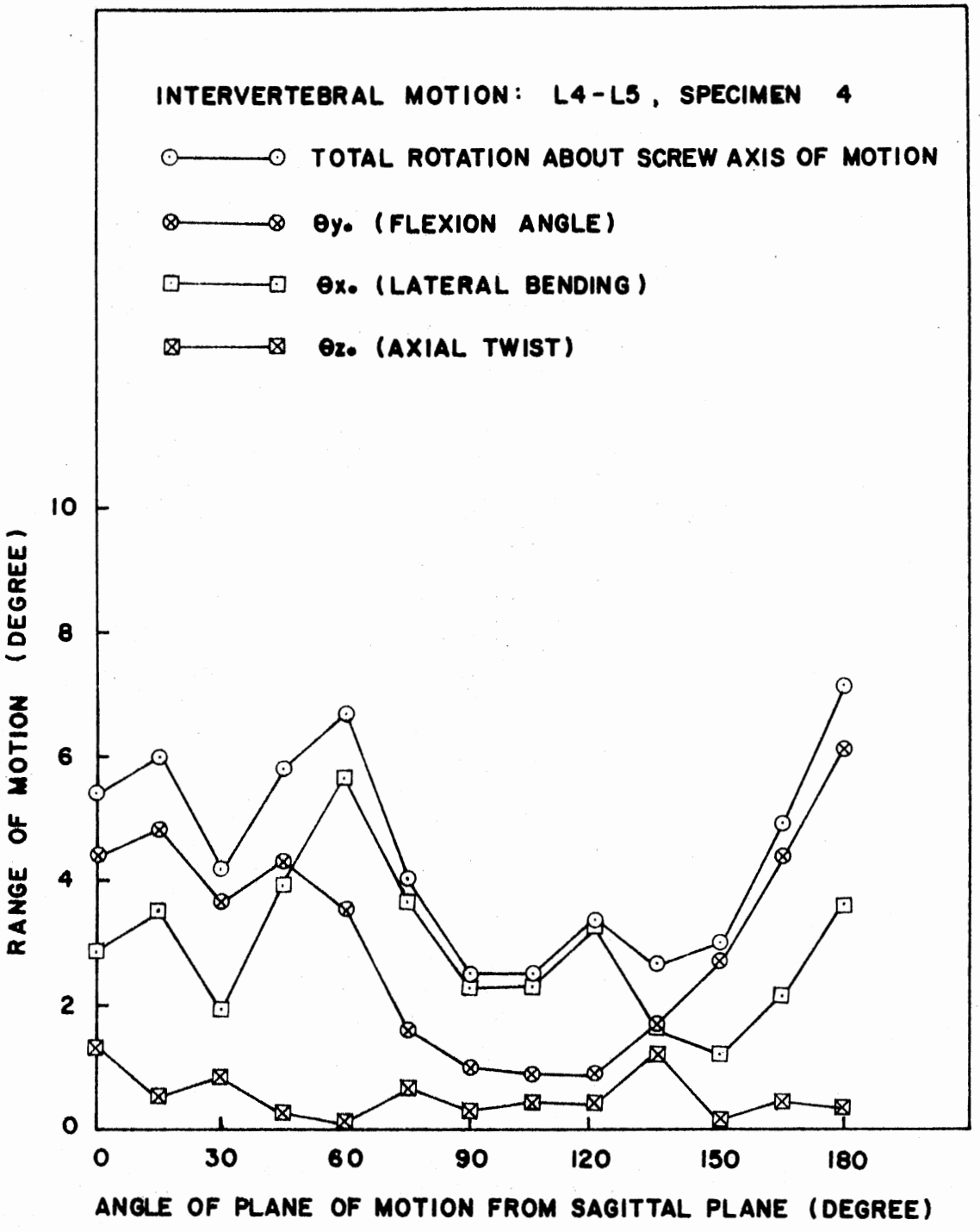

(m) L4-L5, Specimen 4

Figure 11. (Continued)

The results of the range of motion study performed on the spine specimen are subject to the following limitations:

1. The motion (from full extension to full flexion) of the spine specimen in each plane was produced by loads applied to the specimen by hand. Human judgment was employed to determine whether the spine had reached its limiting range of motion in any given plane of motion.

2. The gross motion of the spine specimen in a given plane was ensured by a special guiding fixture. However, because of the initial curvature of the spine specimen (which was quite pronounced in some cases), some out-of-plane forces may have been applied to the spine, thus affecting the resultant motion.

3. The spine specimen did not belong to a close age group.

4. Each spine specimen was physiologically different from the other. Some of the specimens belonged to normal human beings, while others had undergone arthritic degeneration.

The above limitations must be kept in mind while interpreting the results of this study of the range of motion of intervertebral joints.

The sources of error in the above kinematic analysis are:

1. Limited resolution of the rotary potentiometers to measure small rotations.

2. Error in measuring the parameters (α_i, a_i, S_i) of the transducers.

3. Interference to the normal motion of the spine due to the linkage transducer.

4. Error in locating the anatomical frame of reference.

An examination of the results of the kinematic analysis showed that the translational component of the intervertebral motion is very small as compared to the rotational components for all the intervertebral joints examined in this study. This may be attributed to the following two reasons:

1. The intervertebral joints of the lumbar segment of a human spine have very small translatory motion. Their major contribution to the gross motion of the spine is the rotational motion about the three anatomical axes.

2. Insensitivity of the linkage transducer to measure small translatory components of motion.

The latter of the two reasons mentioned above will be discussed in Chapter VI. Since for the present study experimental data were collected only on the lumbar segment of the human spine, it was decided to consider only the rotational components of the intervertebral relative motion for further analysis.

4.6.2 Axode Approximation and Interpolation

The methodology developed in sections 4.4 and 4.5 provides stepwise procedures for formulating a mathematical ruled surface approximating the locus of instantaneous screw axes of motion, and to interpolate, using this axode approximation, on the parameters of the screw axis of motion. This section presents two example problems demonstrating the application of the above methodology.

The first example problem takes a system of three non-intersecting lines to formulate the equation of the second degree ruled surface passing through them. The validity of the methodology for interpolation is

checked by interpolating on the direction cosines of one of the known lines using the equation of the ruled surface. The data for this example problem are as follows:

1. Direction cosines of three generators and coordinates of a point on each generator are listed in Table V.

TABLE V

DATA FOR AXODE APPROXIMATION AND INTERPOLATION

ℓ	m	n	X_p	Y_p	Z_p
0.0	1.0	0.0	4.0	0.0	0.0
0.0	0.0	1.0	0.0	2.0	0.0
0.8660254	0.0	0.5	2.0	0.0	0.0

2. Coordinates of the point P to be used for interpolating the direction cosines of the line passing through that point and lying on the ruled surface are: 2.0, 0.0, 0.0.

Using Equations (12), (13a), and (13b) of section 4.4, the coefficients a, b, and c of Equation (14) defining the second degree ruled surface (hyperboloid of one sheet) are evaluated:

$$a = 1.0,\ b = 0.577350,\ c = 2.309401$$

Hence the equation of the ruled surface passing through the three lines is given by:

$$Y'Z' + 0.577350\ Z'X' + 2.309401\ X'Y' + 1.333333 = 0$$

This equation is defined in an oblique frame of reference CX'Y'Z'. The coordinates of the origin C of this oblique frame are:

$$X_c = 2.0,\ Y_c = 1.0,\ Z_c = -0.577350$$

The direction cosines of the axes of the oblique frame CX'Y'Z' referred to the rectangular frame of reference OXYZ are (0, 1, 0); (0, 0, 1); (0.8660254, 0, 0.5).

Using Equation (15), the coordinates of point P referred to the oblique reference frame CX'Y'Z' are calculated. These coordinates are:

$$\alpha' = -1.0,\ \beta' = 0.577350,\ \gamma' = 0.0$$

Using the redefined coordinates α', β', γ', Equations (18), (19), and (20) are solved to obtain the ratios (ℓ'/n'), (m'/n') of the interpolated line passing through the point $(\alpha', \beta', \gamma')$ referred to the oblique coordinate system CX'Y'Z'. There are two families of generators that can generate the same ruled surface. The ratios of the direction cosines of the interpolated generator belonging to the set of three given lines are obtained as:

$$\ell'/n' = 0.0,\ m'/n' = 0.5$$

The direction cosines of the interpolated generator referred to the rectangular frame of reference OXYZ are obtained by solving Equation (21). These direction cosines are:

$$\ell = 0.8660254,\ m = 0.0,\ n = 0.5$$

The above example problem proves the validity of the methodology developed in sections 4.4 and 4.5.

The above procedure is now applied to the actual data describing the intervertebral relative motion.

1. Direction cosines of three generators and coordinates of a point on each generator are listed in Table VI.

TABLE VI

EXPERIMENTAL DATA FOR AXODE APPROXIMATION AND INTERPOLATION

ℓ	m	n	X_p	Y_p	Z_p
-0.929006	0.296382	0.221597	10.405794	-2.876803	0.0
-0.933871	0.309166	0.179733	18.234073	-5.726150	0.0
-0.943458	0.290690	0.159332	23.395055	-6.793991	0.0

2. Coordinates of point P used for interpolation:

$$X_p = 16.1253884,\ Y_p = -4.7300684,\ Z_p = 0.0$$

3. Equation of the axode passing through the three screw axes is:

$$-3.085799\ Y'Z' - 7.202464\ Z'X' + 2.468024\ X'Y' + 54.852712 = 0$$

4. The above equation of the axode is defined in the oblique frame CX'Y'Z'. The coordinates of the center C are:

$$X_c = -13.72086,\ Y_c = 4.7649,\ Z_c = 6.227071$$

5. The direction cosines of the interpolated screw axis passing through the point P are:

$$\ell = -0.932318,\ m = 0.301409,\ n = 0.195864$$

Since the actual axode of motion is approximated by a second degree ruled surface, the point P (α', β', γ') may not lie on the ruled surface. A new point P* (α^*, β^*, γ^*) on the ruled surface is chosen such that it is closest to the actual point P. The interpolation is actually performed using this new point P* instead of P. Because of this approximation, an error is introduced in interpolation of the parameters of the screw axis. Thus the accuracy of the interpolated parameters is a strong function of the degree of the true axode of motion.

CHAPTER V

SIMULATION STUDIES OF THE HUMAN SPINE SUBJECTED TO STATIC LOADS

The components of an intervertebral joint can be classified according to their functional role into three categories:

1. The vertebral bodies can be treated as rigid bodies.

2. The intervertebral disc, ligaments, and soft tissues behave as elastic elements contributing internal elastic forces towards the equilibrium of the intervertebral joint system subjected to external static forces.

3. The facet joint and the intervertebral disc together provide kinematic constraints to the intervertebral motion, thus governing the motion characteristics of this relative motion. The kinematic constraints imposed by the facet joint are a function of the orientation of the facets, the surface geometry of the facets, and the type of contact between the two facets of a facet joint.

The motion response of an intervertebral joint to a set of externally applied static forces can therefore be studied as the combined response of the elastic elements such as the intervertebral disc, ligaments, soft tissues, etc., and the kinematic constraints of the facet joint. A human spine with N number of vertebrae is functionally equivalent to an open loop elastic system consisting of N number of rigid bodies connected to each other through elastic and kinematic constraints.

The methodology for the development of a motion simulation model of the human spine subjected to static loads consists of two steps:

1. Development of a general discrete parameter model simulating the three-dimensional relative motion of an open loop kinematically constrained elastic system consisting of N rigid bodies connected together by (N - 1) joints, and elastic (spring) elements.

2. Application of the above theoretical simulation model to predict the response of a human spine subjected to external static loads.

5.1 Development of a General Discrete Parameter Model of an Open Loop Kinematically Constrained Elastic System

Consider an open loop mechanical system consisting of N number of rigid bodies. The connectivity at each pair of rigid bodies consists of:

1. Equivalent springs which constitute the equivalent stiffness matrix between the pair of rigid bodies.

2. A kinematic pair whose class and type govern the characteristics of the relative motion between the pair of rigid bodies.

Figure 12 shows two pairs of rigid bodies denoted by (i + 1), (i), and (i - 1). A body reference system $X_i\ Y_i\ Z_i$ is embedded in the ith body. The geometry of the rigid body i can be defined in the local reference system $X_i\ Y_i\ Z_i$. Let $\vec{V}_i$ be the vector locating in the reference system $X_i\ Y_i\ Z_i$ the point at which the equivalent internal elastic reactions between pair (i) and (i - 1) would occur when the system is subjected to external static forces. Let $\vec{a}_{ik}$ be the vector locating, in $X_i\ Y_i\ Z_i$, the point of application of the external static force $\vec{P}_{ik}$

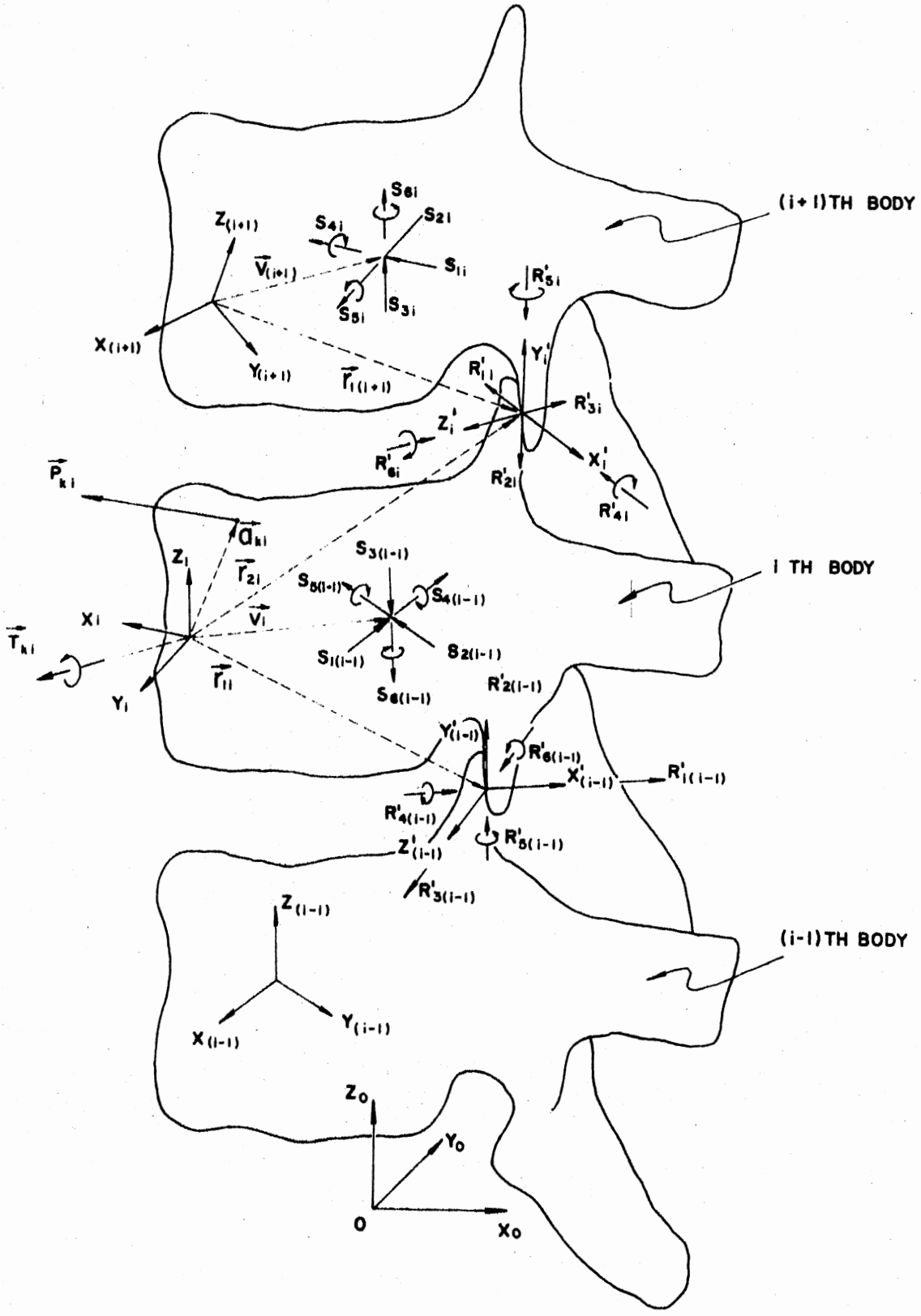

Figure 12. Freebody Diagram of an Ith Body

applied to the ith body. Let $\overline{r_{1i}}$ be the vector locating, in $X_i\ Y_i\ Z_i$, the center of the kinematic pair between bodies (i) and (i - 1). Let $\overline{r_{2i}}$ be the vector locating, in $(XYZ)_i$, the point of contact at the kinematic pair between bodies (i) and (i + 1) in the current configuration. The reaction forces due to physical contact between two bodies at each kinematic pair are assumed to act at the center of each kinematic pair.

The ith body is in a state of equilibrium under the influence of the following external forces and internal reactions:

1. $R_{j_{(i-1)}}$; $j = 1, \ldots, 6$: The six possible reaction forces (three forces and three moments) due to the physical contact at the kinematic pair between the ith and (i - 1)th rigid bodies. These reaction forces are defined in the reference system $(XYZ)_{(i-1)}$, which is a local reference system in body (i - 1).

2. R_{j_i}; $j = 1, \ldots, 6$: The six possible reaction forces due to the physical contact at the kinematic pair between the ith and (i + 1)th rigid bodies. These reaction forces are defined in the reference system $(XYZ)_i$, which is a local reference system in body i.

3. $S_{j_{(i-1)}}$; $j = 1, \ldots, 6$: The six possible internal elastic forces (three forces and three moments) due to the stiffness properties of the joint between bodies i and (i - 1). These elastic reaction forces are defined in $(XYZ)_{(i-1)}$.

4. S_{j_i}; $j = 1, \ldots, 6$: The six possible internal elastic forces due to the stiffness properties of the joint between bodies i and (i + 1). These elastic reaction forces are defined in $(XYZ)_i$.

5. $P_{i,k}$; $k = 1, \ldots, NP_i$: The set of external static forces applied to the rigid body i.

6. $T_{i,k}$; $k = 1, \ldots, NT_i$: The set of external moments applied to the rigid body i.

Let $O_o\ X_o\ Y_o\ Z_o$ be the fixed frame of reference. The direction cosines of the axis $O_i\ X_i$, $O_i\ Y_i$, O_i, Z_i referred to the fixed frame of reference $O_o\ X_o\ Y_o\ Z_o$ are l_{ox_i}, m_{ox_i}, n_{ox_i}; l_{oy_i}, m_{oy_i}, n_{oy_i},; l_{oz_i}, m_{oz_i}, n_{oz_i}. The configuration of rigid bodies will be defined completely in the fixed frame of reference once these direction cosines are known for a given configuration.

Since the body i is in a state of equilibrium, the following six equations of static equilibrium can be written in the reference system $(XYZ)_{(i-1)}$.

$\Sigma F_{x_{(i-1)}} = 0$:

$$R_{1_{(i-1)}} - S_{1_{(i-1)}} + R_{1i_{x_{(i-1)}}} + R_{2i_{x_{(i-1)}}} + R_{3i_{x_{(i-1)}}} + S_{1i_{x_{(i-1)}}} + S_{2i_{x_{(i-1)}}} + S_{3i_{x_{(i-1)}}} + \sum_{k=1}^{NP_i} P_{k_{x_{(i-1)}}} = 0 \quad (22)$$

$\Sigma F_{y_{(i-1)}} = 0$:

$$R_{2_{(i-1)}} - S_{2_{(i-1)}} + R_{1i_{y_{(i-1)}}} + R_{2i_{y_{(i-1)}}} + R_{3i_{y_{(i-1)}}} + S_{1i_{y_{(i-1)}}} + S_{2i_{y_{(i-1)}}} + S_{3i_{y_{(i-1)}}} + \sum_{k=1}^{NP_i} P_{k_{y_{(i-1)}}} = 0 \quad (23)$$

$\Sigma F_{z_{(i-1)}} = 0$:

$$R_{3_{(i-1)}} - S_{3_{(i-1)}} + R_{1i_{z_{(i-1)}}} + R_{2i_{z_{(i-1)}}} + R_{3i_{z_{(i-1)}}}$$

$$+ S_{1i_{z_{(i-1)}}} + S_{2i_{z_{(i-1)}}} + S_{3i_{z_{(i-1)}}} + \sum_{k=1}^{NP_i} P_{k_{z_{(i-1)}}} = 0$$

$\Sigma M_{x_{(i-1)}} = 0$:

$$S_{2_{(i-1)}} Z_{(i-1)_{v_i}} - S_{3_{(i-1)}} Y_{(i-1)_{v_i}} + R_{3_{(i-1)}} Y_{(i-1)_{r_{1_i}}}$$

$$- R_{2_{(i-1)}} Z_{(i-1)_{r_{1_i}}} + R_{i_{z_{(i-1)}}} Y_{(i-1)_{r_{2_i}}}$$

$$- R_{i_{y_{(i-1)}}} Z_{(i-1)_{r_{2_i}}} + S_{i_{z_{(i-1)}}} Y_{(i-1)_{r_{t_i}}}$$

$$- S_{i_{y_{(i-1)}}} Z_{(i-1)_{r_{t_i}}} - S_{4_{(i-1)}} + R_{4_{(i-1)}} + R_{4_{i_{x_{(i-1)}}}}$$

$$+ R_{5_{i_{x_{(i-1)}}}} + R_{6_{i_{x_{(i-1)}}}} + S_{4_{i_{x_{(i-1)}}}} + S_{5_{i_{x_{(i-1)}}}}$$

$$+ S_{6_{i_{x_{(i-1)}}}} + \sum_{k=1}^{NT_i} T_{k_{x_{(i-1)}}} + \sum_{k=1}^{NP_i} Y_{(i-1)_{a_k}} P_{k_{z_{(i-1)}}}$$

$$- \sum_{k=1}^{NP_i} Z_{(i-1)_{a_k}} P_{k_{y_{(i-1)}}} = 0 \qquad (25)$$

$\Sigma M_{y_{(i-1)}} = 0$:

$$-S_{1_{(i-1)}} Z_{(i-1)_{v_i}} + S_{3_{(i-1)}} X_{(i-1)_{v_i}} - R_{3_{(i-1)}} X_{(i-1)_{r_{1_i}}}$$

$$+ R_{1_{(i-1)}} Z_{(i-1)_{r_{1_i}}} + R_{i_{z_{(i-1)}}} X_{(i-1)_{r_{2_i}}}$$

$$+ R_{i_{x_{(i-1)}}} Z_{(i-1)_{r_{2_i}}} - X_{(i-1)_{r_{t_i}}} S_{i_{z_{(i-1)}}}$$

$$+ Z_{(i-1)r_{t_i}} S_{i_{x_{(i-1)}}} - S_{5_{(i-1)}} + R_{5_{(i-1)}} + R_{4_{i_{y_{(i-1)}}}}$$

$$+ R_{5_{i_{y_{(i-1)}}}} + R_{6_{i_{y_{(i-1)}}}} + S_{4_{i_{y_{(i-1)}}}} + S_{5_{i_{y_{(i-1)}}}}$$

$$+ S_{6_{i_{y_{(i-1)}}}} + \sum_{k=1}^{NT_i} T_{k_{y_{(i-1)}}} + \sum_{k=1}^{NP_i} Z_{(i-1)a_k} P_{k_{x_{(i-1)}}}$$

$$- \sum_{k=1}^{NP_i} X_{(i-1)a_k} P_{k_{z_{(i-1)}}} = 0 \qquad (26)$$

$\underline{\Sigma M_{z_{(i-1)}} = 0:}$

$$S_{1_{(i-1)}} Y_{(i-1)v_i} - S_{2_{(i-1)}} X_{(i-1)v_i} + R_{2_{(i-1)}} X_{(i-1)r_{1_i}}$$

$$- R_{1_{(i-1)}} Y_{(i-1)r_{1_i}} + R_{i_{y_{(i-1)}}} X_{(i-1)r_{2_i}}$$

$$- R_{i_{x_{(i-1)}}} Y_{(i-1)r_{2_i}} + X_{(i-1)r_{t_i}} S_{i_{y_{(i-1)}}}$$

$$- Y_{(i-1)r_{t_i}} S_{i_{x_{(i-1)}}} - S_{6_{(i-1)}} + R_{6_{(i-1)}} + R_{4_{i_{z_{(i-1)}}}}$$

$$+ R_{5_{i_{z_{(i-1)}}}} + R_{6_{i_{z_{(i-1)}}}} + S_{4_{i_{z_{(i-1)}}}} + S_{5_{i_{z_{(i-1)}}}} + S_{6_{i_{z_{(i-1)}}}}$$

$$+ \sum_{k=1}^{NT_i} T_{k_{z_{(i-1)}}} + \sum_{k=1}^{NP_i} X_{(i-1)a_k} P_{k_{y_{(i-1)}}}$$

$$- \sum_{k=1}^{NP_i} Y_{(i-1)a_k} P_{k_{x_{(i-1)}}} = 0 \qquad (27)$$

The terms in Equations (22) through (27) represent the components, along the $(XYZ)_{(i-1)}$ reference system, of the external forces, internal reactions, and moments due to these external forces and internal reactions.

The internal reactions and applied forces can be expressed as functions of direction cosines of axes $(XYZ)_i$ and $(XYZ)_{(i-1)}$ referred to the fixed reference cystem $X_o\ Y_o\ Z_o$. These functional relationships (which are derived in Appendix B) may be expressed as:

$$R_{i_{\zeta_{(i-1)}}} = C_{1_{R_i}} L_{o_{\zeta_{(i-1)}}} + C_{2_{R_i}} M_{o_{\zeta_{(i-1)}}} + C_{3_{R_i}} N_{o_{\zeta_{(i-1)}}} \tag{28}$$

where

$$C_{1_{R_i}} = -R_{1_i} \ell_{o_{x_i}} - R_{2_i} \ell_{o_{y_i}} - R_{3_i} \ell_{o_{z_i}}$$

$$C_{2_{R_i}} = -R_{1_i} m_{o_{x_i}} - R_{2_i} m_{o_{y_i}} - R_{3_i} m_{o_{z_i}}$$

$$C_{3_{R_i}} = -R_{1_i} n_{o_{x_i}} - R_{2_i} n_{o_{y_i}} - R_{3_i} n_{o_{z_i}}$$

$$\begin{aligned} S_{i_{\zeta_{(i-1)}}} = {} & L_{o_{\zeta_{(i-1)}}} \left(S_{1_i} L_{o_{x_i}} + S_{2_i} L_{o_{y_i}} + S_{3_i} L_{o_{z_i}} \right) \\ & + M_{o_{\zeta_{(i-1)}}} \left(S_{1_i} M_{o_{x_i}} + S_{2_i} M_{o_{y_i}} + S_{3_i} M_{o_{z_i}} \right) \\ & + N_{o_{\zeta_{(i-1)}}} \left(S_{1_i} N_{o_{x_i}} + S_{2_i} N_{o_{y_i}} + S_{3_i} N_{o_{z_i}} \right) \end{aligned} \tag{29}$$

$$\begin{aligned} R_{1_{i_{\zeta_{(i-1)}}}} = -R_{1_i} \Big(& L_{o_{x_i}} L_{o_{\zeta_{(i-1)}}} + M_{o_{x_i}} M_{o_{\zeta_{(i-1)}}} \\ & + N_{o_{x_i}} N_{o_{\zeta_{(i-1)}}} \Big) \end{aligned}$$

$$R_{2_{i\zeta_{(i-1)}}} = -R_{2_i}\left(L_{o_{y_i}} L_{o\zeta_{(i-1)}} + M_{o_{y_i}} M_{o\zeta_{(i-1)}} + N_{o_{y_i}} N_{o\zeta_{(i-1)}}\right)$$

$$R_{3_{i\zeta_{(i-1)}}} = -R_{3_i}\left(L_{o_{z_i}} L_{o\zeta_{(i-1)}} + M_{o_{z_i}} M_{o\zeta_{(i-1)}} + N_{o_{z_i}} N_{o\zeta_{(i-1)}}\right)$$

$$R_{4_{i\zeta_{(i-1)}}} = -R_{4_i}\left(L_{o_{x_i}} L_{o\zeta_{(i-1)}} + M_{o_{x_i}} M_{o\zeta_{(i-1)}} + N_{o_{x_i}} N_{o\zeta_{(i-1)}}\right)$$

$$R_{5_{i\zeta_{(i-1)}}} = -R_{5_i}\left(L_{o_{y_i}} L_{o\zeta_{(i-1)}} + M_{o_{y_i}} M_{o\zeta_{(i-1)}} + N_{o_{y_i}} N_{o\zeta_{(i-1)}}\right)$$

$$R_{6_{i\zeta_{(i-1)}}} = -R_{6_i}\left(L_{o_{z_i}} L_{o\zeta_{(i-1)}} + M_{o_{z_i}} M_{o\zeta_{(i-1)}} + N_{o_{z_i}} N_{o\zeta_{(i-1)}}\right) \tag{30}$$

Similar equations can be written for components of the internal elastic forces $S_{1_i}, \ldots, S_{6_i}$.

$$P_{k_{\zeta_{(i-1)}}} = P_k\left(L_{o_{p_k}} L_{o\zeta_{(i-1)}} + M_{o_{p_k}} M_{o\zeta_{(i-1)}} + N_{o_{p_k}} N_{o\zeta_{(i-1)}}\right) \tag{31}$$

$$T_{k_{\zeta_{(i-1)}}} = T_k\left(L_{o_{T_k}} L_{o\zeta_{(i-1)}} + M_{o_{T_k}} M_{o\zeta_{(i-1)}} + N_{o_{T_k}} N_{o\zeta_{(i-1)}}\right) \tag{32}$$

The dummy variable ζ in Equations (28) through (32) can be replaced by X, Y, and Z successively, thus yielding the components of internal reactions, external forces, and moments along the axes of the reference system $(XYZ)_{(i-1)}$.

The components of the vector $\vec{v}_i$ locating the point of application of the internal elastic forces between bodies i and (i - 1) are given by:

$$\begin{aligned}
\zeta_{(i-1)_{v_i}} = {} & L_{o_{\zeta_{(i-1)}}} \left(L_{o_{x_i}} X_{i_{v_i}} + L_{o_{y_i}} Y_{i_{v_i}} + L_{o_{z_i}} Z_{i_{v_i}} \right) \\
& + M_{o_{\zeta_{(i-1)}}} \left(M_{o_{x_i}} X_{i_{v_i}} + M_{o_{y_i}} Y_{i_{v_i}} + M_{o_{z_i}} Z_{i_{v_i}} \right) \\
& + N_{o_{\zeta_{(i-1)}}} \left(N_{o_{x_i}} X_{i_{v_i}} + N_{o_{y_i}} Y_{i_{v_i}} + N_{o_{z_i}} Z_{i_{v_i}} \right)
\end{aligned} \tag{33}$$

where

$$X_{i_{v_i}} = v_i \cdot L_{i_{v_i}}$$

$$Y_{i_{v_i}} = v_i \cdot M_{i_{v_i}}$$

$$Z_{i_{v_i}} = v_i \cdot N_{i_{v_i}}$$

are the components of vector $\vec{v}_i$ referred to the local reference system $(XYZ)_i$ of body i.

The components of the vector $\vec{a}_k$, locating the point of application of force $\vec{P}_k$ on body i, are given by:

$$\zeta_{(i-1)_{a_k}} = L_{o_{\zeta_{(i-1)}}} \left(L_{o_{x_i}} X_{i_{a_k}} + L_{o_{y_i}} Y_{i_{a_k}} + L_{o_{z_i}} Z_{i_{a_k}} \right)$$

$$+ M_{o_{\zeta_{(i-1)}}} \left(M_{o_{x_i}} X_{i_{a_k}} + M_{o_{y_i}} Y_{i_{a_k}} + M_{o_{z_i}} Z_{i_{a_k}} \right)$$

$$+ N_{o_{\zeta_{(i-1)}}} \left(N_{o_{x_i}} X_{i_{a_k}} + N_{o_{y_i}} Y_{i_{a_k}} + N_{o_{z_i}} Z_{i_{a_k}} \right) \tag{34}$$

where

$$X_{i_{a_k}} = a_k \cdot L_{i_{a_k}}$$

$$Y_{i_{a_k}} = a_k \cdot M_{i_{a_k}}$$

$$Z_{i_{a_k}} = a_k \cdot N_{i_{a_k}}$$

are the components of vector $\vec{a}_k$ referred to the body reference system $(XYZ)_i$ of body i.

The components of the vector $\vec{r}_{l_i}$, locating the center of the kinematic pair between bodies i and (i-1), are given by:

$$\zeta_{(i-1)_{r_{l_i}}} = L_{o_{\zeta_{(i-1)}}} \left(L_{o_{x_i}} X_{i_{r_{l_i}}} + L_{o_{y_i}} Y_{i_{r_{l_i}}} + L_{o_{z_i}} Z_{i_{r_{l_i}}} \right)$$

$$+ M_{o_{\zeta_{(i-1)}}} \left(M_{o_{x_i}} X_{i_{r_{l_i}}} + M_{o_{y_i}} Y_{i_{r_{l_i}}} + M_{o_{z_i}} Z_{i_{r_{l_i}}} \right)$$

$$+ N_{o_{\zeta_{(i-1)}}} \left(N_{o_{x_i}} X_{i_{r_{l_i}}} + N_{o_{y_i}} Y_{i_{r_{l_i}}} + N_{o_{z_i}} Z_{i_{r_{l_i}}} \right) \tag{35}$$

where

$$X_{i_{r_{l_i}}} = r_{l_i} \cdot L_{i_{r_{l_i}}}$$

$$Y_{i_{r_{1_i}}} = r_{1_i} \cdot M_{i_{r_{1_i}}}$$

$$Z_{i_{r_{1_i}}} = r_{1_i} \cdot N_{i_{r_{1_i}}}$$

are the components of vector $\vec{r}_{1_i}$ referred to the local reference system $(XYZ)_{(i)}$ of body i.

The components of the vector $\vec{r}_{2_i}$, locating the point of contact at the kinematic pair between bodies i and (i+1) in the current configuration, are given by:

$$\begin{aligned}\zeta_{(i-1)_{r_{2_i}}} = {} & L_{o\zeta_{(i-1)}}\left(L_{ox_i} X_{i_{r_{2_i}}} + L_{oy_i} Y_{i_{r_{2_i}}} + L_{oz_i} Z_{i_{r_{2_i}}}\right) \\ & + M_{o\zeta_{(i-1)}}\left(M_{ox_i} X_{i_{r_{2_i}}} + M_{oy_i} Y_{i_{r_{2_i}}} + M_{oz_i} Z_{i_{r_{2_i}}}\right) \\ & + N_{o\zeta_{(i-1)}}\left(N_{ox_i} X_{i_{r_{2_i}}} + N_{oy_i} Y_{i_{r_{2_i}}} + N_{oz_i} Z_{i_{r_{2_i}}}\right)\end{aligned} \tag{36}$$

where

$$X_{i_{r_{2_i}}} = r_{2_i} \cdot L_{i_{r_{2_i}}}$$

$$Y_{i_{r_{2_i}}} = r_{2_i} \cdot M_{i_{r_{2_i}}}$$

$$Z_{i_{r_{2_i}}} = r_{2_i} \cdot N_{i_{r_{2_i}}}$$

Note that the point of contact on body i at the kinematic pair between bodies i and (i+1) may change in each configuration due to the translation (if any) at that kinematic pair. On the other hand, the

the point of contact on body i at the kinematic pair between bodies i and (i-1) remains at the center of that kinematic pair.

The components of the vector $\vec{r}_{t_i}$, locating the points of application of the internal elastic reactions between bodies i and (i+1), are given by:

$$\zeta_{(i-1)_{r_{t_i}}} = \zeta_{(i-1)_{r_{2_i}}} - \zeta_{(i-1)_{r_{1_{(i+1)}}}} + \zeta_{(i-1)_{V_{(i+1)}}}$$

where

$$\begin{aligned}\zeta_{(i-1)_{r_{1_{(i+1)}}}} &= L_{o_{\zeta_{(i-1)}}}\left(L_{o_{x_{(i+1)}}} X_{(i+1)_{r_1}} + L_{o_{y_{(i+1)}}} Y_{(i+1)_{r_1}}\right. \\ &\quad \left. + L_{o_{z_{(i+1)}}} Z_{(i+1)_{r_1}}\right) \\ &\quad + M_{o_{\zeta_{(i-1)}}}\left(M_{o_{x_{(i+1)}}} X_{(i+1)_{r_1}} + M_{o_{y_{(i+1)}}} Y_{(i+1)_{r_1}}\right. \\ &\quad \left. + M_{o_{z_{(i+1)}}} Z_{(i+1)_{r_1}}\right) \\ &\quad + N_{o_{\zeta_{(i-1)}}}\left(N_{o_{x_{(i+1)}}} X_{(i+1)_{r_1}} + N_{o_{y_{(i+1)}}} Y_{(i+1)_{r_1}}\right. \\ &\quad \left. + N_{o_{z_{(i+1)}}} Z_{(i+1)_{r_1}}\right)\end{aligned} \tag{37}$$

where

$$X_{(i+1)_{r_1}} = r_{1_{(i+1)}} L_{(i+1)_{r_{1_{(i+1)}}}}$$

$$Y_{(i+1)_{r_1}} = r_{1_{(i+1)}} M_{(i+1)_{r_{1_{(i+1)}}}}$$

$$Z_{(i+1)_{r_1}} = r_{1_{(i+1)}} N_{(i+1)_{r_{1_{(i+1)}}}}$$

are the components of vector $\vec{r}_{1_{(i+1)}}$ referred to the local reference system $(XYZ)_{(i+1)}$ of body $(i+1)$; and

$$\begin{aligned}
\zeta_{(i-1)_{v_{(i+1)}}} = {} & L_{o_{\zeta_{(i-1)}}}\left(L_{o_{x_{(i+1)}}} X_{(i+1)_{v_{(i+1)}}}\right. \\
& \left. + L_{o_{y_{(i+1)}}} Y_{(i+1)_{v_{(i+1)}}} + L_{o_{z_{(i+1)}}} Z_{(i+1)_{v_{(i+1)}}}\right) \\
& + M_{o_{\zeta_{(i-1)}}}\left(M_{o_{x_{(i+1)}}} X_{(i+1)_{v_{(i+1)}}}\right. \\
& \left. + M_{o_{y_{(i+1)}}} Y_{(i+1)_{v_{(i+1)}}} + M_{o_{z_{(i+1)}}} Z_{(i+1)_{v_{(i+1)}}}\right) \\
& + N_{o_{\zeta_{(i-1)}}}\left(N_{o_{x_{(i+1)}}} X_{(i+1)_{v_{(i+1)}}}\right. \\
& \left. + N_{o_{y_{(i+1)}}} Y_{(i+1)_{v_{(i+1)}}} + N_{o_{z_{(i+1)}}} Z_{(i+1)_{v_{(i+1)}}}\right)
\end{aligned} \tag{38}$$

The dummy variable ζ in Equations (33) through (38) can be replaced by X, Y, and Z successively, thus yielding the equations defining the components of the geometric vectors $\vec{r}_{1_i}$, $\vec{r}_{2_i}$, $\vec{r}_{t_i}$, $\vec{v}_i$, and $\vec{a}_k$ referred to the reference system $(XYZ)_{(i-1)}$. An examination of Equations (28) through (38) shows that the terms appearing in Equations (22) through (27) are functions of the direction cosines of reference systems $(XYZ)_{(i+1)}$, $(XYZ)_i$, and $(XYZ)_{(i-1)}$ referred to the fixed frame of reference $O_o X_o Y_o Z_o$. The location and orientation of reference system $(XYZ)_i$ can be uniquely defined in reference system $(XYZ)_{(i-1)}$ by a set of generalized coordinates whose number may vary from 1 to 6 depending

upon the kinematic degrees of freedom between the two rigid bodies i and (i-1). However, since the pair of rigid bodies is assumed to be kinematically constrained due to a kinematic pair between them, these generalized coordinates are nothing but the parameters of the kinematic pair, and equal the number of degrees of freedom of the kinematic pair. Therefore, in order to incorporate the parameters of the kinematic pair in the equations of static equilibrium of the ith rigid body, the terms in Equations (22) through (27) must be made functions of direction cosines referred to reference system $(XYZ)_{(i-1)}$ and so on. This is accomplished by using the following relationships (derived in Appendix B) between the direction cosines:

$$
\begin{aligned}
L_{o_{\zeta_i}} &= L_{(i-1)_{\zeta_i}} L_{o_{x_{(i-1)}}} + M_{(i-1)_{\zeta_i}} L_{o_{y_{(i-1)}}} \\
&\quad + N_{(i-1)_{\zeta_i}} L_{o_{z_{(i-1)}}} \\
M_{o_{\zeta_i}} &= L_{(i-1)_{\zeta_i}} M_{o_{x_{(i-1)}}} + M_{(i-1)_{\zeta_i}} M_{o_{y_{(i-1)}}} \\
&\quad + N_{(i-1)_{\zeta_i}} M_{o_{z_{(i-1)}}} \\
N_{o_{\zeta_i}} &= L_{(i-1)_{\zeta_i}} N_{o_{x_{(i-1)}}} + M_{(i-1)_{\zeta_i}} N_{o_{y_{(i-1)}}} \\
&\quad + N_{(i-1)_{\zeta_i}} N_{o_{z_{(i-1)}}}
\end{aligned}
\tag{39}
$$

The dummy variable ζ in Equation (39) can be replaced by X, Y, and Z to obtain relationships for the direction cosines of axes O_iX_i, O_iY_i, and O_iZ_i.

The direction cosines of the axes of the reference system $(XYZ)_i$ referred to the reference system $(XYZ)_{(i-1)}$ are functions only of the parameters of the kinematic pair between rigid bodies i and (i - 1). Let the reference system $(XYZ)_i$ be connected to the reference system $(XYZ)_{(i-1)}$ through a kinematic pair which has an instantaneous screw axis of rotation denoted by $\hat{u}r$. If the direction cosines of the axis of rotation, $\hat{u}r$, referred to the reference system $(XYZ)_{(i-1)}$ are $L_{(i-1)_{ur}}$, $M_{(i-1)_{ur}}$, and $N_{(i-1)_{ur}}$, then (as shown in Appendix C) we may write:

$$\Delta L_{(i-1)_{\zeta_i}} = \left(-N_{(i-1)_{ur}} \cdot M_{(i-1)_{\zeta_i}} + M_{(i-1)_{ur}} \cdot N_{(i-1)_{\zeta_i}}\right) \Delta q_r$$

$$\Delta M_{(i-1)_{\zeta_i}} = \left(N_{(i-1)_{ur}} \cdot L_{(i-1)_{\zeta_i}} - L_{(i-1)_{ur}} \cdot N_{(i-1)_{\zeta_i}}\right) \Delta q_r$$

$$\Delta N_{(i-1)_{\zeta_i}} = \left(-M_{(i-1)_{ur}} \cdot L_{(i-1)_{\zeta_i}} + L_{(i-1)_{ur}} \cdot M_{(i-1)_{\zeta_i}}\right) \Delta q_r \tag{40}$$

where Δq_r is a rotation about $\hat{u}r$. The dummy variable ζ in Equation (40) can be replaced by X, Y, and Z to obtain the small change in the direction cosines of O_iX_i, O_iY_i, and O_iZ_i axes, referred to the $(XYZ)_{(i-1)}$ reference system, as a result of a small rotation Δq_r about the instantaneous axis of rotation $\hat{u}r$ at the kinematic pair between the rigid bodies i and (i - 1).

Application of Equation (40) to Equation (39) yields the following relationships:

$$\Delta L_{o_{\zeta_i}} = L_{(i-1)_{\zeta_i}} \Delta L_{o_{x_{(i-1)}}} + M_{(i-1)_{\zeta_i}} \Delta L_{o_{y_{(i-1)}}}$$

$$+ N_{(i-1)_{\zeta_i}} \Delta L_{o_{z_{(i-1)}}} + \left(L_{o_{x_{(i-1)}}} A_{(i-1)_{\zeta_i}} \right.$$

$$\left. + L_{o_{y_{(i-1)}}} B_{(i-1)_{\zeta_i}} + L_{o_{z_{(i-1)}}} C_{(i-1)_{\zeta_i}} \right) \Delta q_r$$

$$\Delta M_{o_{\zeta_i}} = L_{(i-1)_{\zeta_i}} \Delta M_{o_{x_{(i-1)}}} + M_{(i-1)_{\zeta_i}} \Delta M_{o_{y_{(i-1)}}}$$

$$+ N_{(i-1)_{\zeta_i}} \Delta M_{o_{z_{(i-1)}}} + \left(M_{o_{x_{(i-1)}}} A_{(i-1)_{\zeta_i}} \right.$$

$$\left. + M_{o_{y_{(i-1)}}} B_{(i-1)_{\zeta_i}} + M_{o_{z_{(i-1)}}} C_{(i-1)_{\zeta_i}} \right) \Delta q_r$$

$$N_{o_{\zeta_i}} = L_{(i-1)_{\zeta_i}} \Delta N_{o_{x_{(i-1)}}} + M_{(i-1)_{\zeta_i}} \Delta N_{o_{y_{(i-1)}}}$$

$$+ N_{(i-1)_{\zeta_i}} \Delta N_{o_{z_{(i-1)}}} + \left(N_{o_{x_{(i-1)}}} A_{(i-1)_{\zeta_i}} \right.$$

$$\left. + N_{o_{y_{(i-1)}}} B_{(i-1)_{\zeta_i}} + N_{o_{z_{(i-1)}}} C_{(i-1)_{\zeta_i}} \right) \Delta q_r \qquad (41)$$

where

$$A_{(i-1)_{\zeta_i}} = -N_{(i-1)_{ur}} \cdot M_{(i-1)_{\zeta_i}} + M_{(i-1)_{ur}} \cdot N_{(i-1)_{\zeta_i}}$$

$$B_{(i-1)_{\zeta_i}} = N_{(i-1)_{ur}} \cdot L_{(i-1)_{\zeta_i}} - L_{(i-1)_{ur}} \cdot M_{(i-1)_{\zeta_i}}$$

$$C_{(i-1)_{\zeta_i}} = -M_{(i-1)_{ur}} \cdot L_{(i-1)_{\zeta_i}} + L_{(i-1)_{ur}} \cdot M_{(i-1)_{\zeta_i}}$$

In order to incorporate the parameters of the kinematic pair into the equations of static equilibrium, the variational principle is applied to Equations (22) through (27) and small variations of each variable quantity is taken with reference to the fixed frame of reference

$O_o X_o Y_o Z_o$. By using Equations (28) through (41), Equations (22) through (27) may be transformed into the following set of six simultaneous linear equations:

$$\underset{(6\times 9)}{[C]} \quad \underset{(9\times 1)}{[\overline{UV}]} = \underset{(6\times 1)}{[\bar{d}]} \tag{42}$$

where the coefficients of [C] and [d] describe the known quantities which are functions of a known configuration of the system. The definitions of the coefficients C_{ij} and d_i are presented in Appendix C. The unknown vector $[\overline{UV}]$ contains the following nine unknowns:

$$[\overline{UV}]^T = \left[\Delta R_{1_{(i-1)}}, \Delta R_{2_{(i-1)}}, \Delta R_{3_{(i-1)}}, \Delta R_{4_{(i-1)}}, \Delta R_{5_{(i-1)}}, \right.$$
$$\left. \Delta R_{6_{(i-1)}}, \Delta q_{r_{(i-1)}}, \Delta q_{\tau 1_{(i-1)}}, \Delta q_{\tau 2_{(i-1)}} \right]$$

$R_{1_{(i-1)}}, \ldots, R_{6_{(i-1)}}$ are the reactions at the kinematic pair between bodies i and (i-1) referred to the reference system $(XYZ)_{(i-1)}$. $q_{r(i-1)}$, $q_{\tau 1_{(i-1)}}$, and $q_{\tau 2_{(i-1)}}$ are the generalized coordinates or the parameters of the kinematic pair representing, respectively, the rotational degree of freedom (about an instantaneous axis of rotation) and two possible translatory degrees of freedom. Since for a kinematic pair the number of degrees of freedom and the number of constraints add up to six, it is clear that the number of reaction forces (due to constraints of the kinematic pair) and the number of generalized coordinates (q's) will always add up to six.

Hence, Equation (42) can be degenerated into a set of six linear equations in six unknowns by a simple transformation of coordinate systems. Let $(X'Y'Z')_{(i-1)}$ be the characteristic frame of reference for a kinematic pair between rigid bodies i and (i - 1). The axes O'X', O'Y',

and O'Z' are the principal axes of the kinematic pair. For example, in the case of a revolute pair constraining motion in the X'Y' plane, the principal axis O'Z' is aligned with the axis of rotation passing through the center of the revolute pair. The transformation between the reference system $(XYZ)_{(i-1)}$ and $(X'Y'Z')_{(i-1)}$ is given by Equation (43) below.

Using the transformation (43), Equation (42) can be written as:

$$[C'] \; [\overline{UV}'] = [\bar{d}'] \tag{44}$$

where the unknown vector $\overline{UV}'$ is given by:

$$[\overline{UV}']^T = \left[\Delta R'_{1(i-1)}, \Delta R'_{2(i-1)}, \Delta R'_{3(i-1)}, \Delta R'_{4(i-1)}, \Delta R'_{5(i-1)}, \Delta R'_{6(i-1)}, \Delta q'_{r(i-1)}, \Delta q_{\tau 1(i-1)}, \Delta q_{\tau 2(i-1)} \right]$$

Since Equation (44) is referred to the characteristic frame of reference $(X'Y'Z')_{(i-1)}$ of the kinematic pair between bodies i and (i - 1), the relationship between the number of degrees of freedom and number of constraints of the kinematic pair can be applied to degenerate Equation (44) into a set of linear equations whose number always equals the number of unknowns. For example, in the case of a revolute pair where the O'Z' axis of the characteristic frame of reference $(X'Y'Z')_{(i-1)}$ is aligned with the axis of rotation, the unknown vector $[\overline{UV}']$ will contain the following three unknowns:

$$[\overline{UV}']^T = \left[R'_{1(i-1)}, \; R'_{2(i-1)}, \; q_{r(i-1)} \right]$$

and Equation (44) will degenerate into:

$$\begin{bmatrix} \Delta R_1{}_{(i-1)} \\ \Delta R_2{}_{(i-1)} \\ \Delta R_3{}_{(i-1)} \\ \Delta R_4{}_{(i-1)} \\ \Delta R_5{}_{(i-1)} \\ \Delta R_6{}_{(i-1)} \end{bmatrix} \begin{bmatrix} L_{(i-1)_{x'}} & L_{(i-1)_{y'}} & L_{(i-1)_{z'}} & 0 & 0 & 0 \\ M_{(i-1)_{x'}} & M_{(i-1)_{y'}} & M_{(i-1)_{z'}} & 0 & 0 & 0 \\ N_{(i-1)_{x'}} & N_{(i-1)_{y'}} & N_{(i-1)_{z'}} & 0 & 0 & 0 \\ 0 & 0 & 0 & L_{(i-1)_{x'}} & L_{(i-1)_{y'}} & L_{(i-1)_{z'}} \\ 0 & 0 & 0 & M_{(i-1)_{x'}} & M_{(i-1)_{y'}} & M_{(i-1)_{z'}} \\ 0 & 0 & 0 & N_{(i-1)_{x'}} & N_{(i-1)_{y'}} & N_{(i-1)_{z'}} \end{bmatrix} \begin{bmatrix} \Delta R'_1{}_{(i-1)} \\ \Delta R'_2{}_{(i-1)} \\ \Delta R'_3{}_{(i-1)} \\ \Delta R'_4{}_{(i-1)} \\ \Delta R'_5{}_{(i-1)} \\ \Delta R'_6{}_{(i-1)} \end{bmatrix} \tag{43}$$

$$\begin{bmatrix} C'_{11} & C'_{12} & C'_{17} \\ C'_{21} & C'_{22} & C'_{27} \\ C'_{61} & C'_{62} & C'_{67} \end{bmatrix} \begin{bmatrix} \Delta R'_{1(i-1)} \\ \Delta R'_{2(i-1)} \\ \Delta q_{r(i-1)} \end{bmatrix} = \begin{bmatrix} d'_1 \\ d'_2 \\ d'_3 \end{bmatrix}$$

The constants $[d'_i]$ are functions of small increments in the externally applied forces and moments, and the geometric parameter of the current configuration of the rigid bodies $(i+1)$, (i), and $(i-1)$. The coefficients $[C'ij]$ are functions of the geometric parameters of the kinematic pair and also the geometric parameters of the current configuration of the rigid bodies. These geometric parameters are expressed in terms of the direction cosines of the reference system $(XYZ)_{(i-1)}$ referred to the fixed frame of reference $O_o X_o Y_o Z_o$.

It is important to note that in Equation (41) the increments $\Delta L_{o\zeta_i}$, $\Delta M_{o\zeta_i}$, and $\Delta N_{o\zeta_i}$ were decomposed into two stages:

$$\left(\Delta L_{(i-1)\zeta_i}, \Delta M_{(i-1)\zeta_i}, \Delta N_{(i-1)\zeta_i}\right)$$

and

$$\left(\Delta L_{o\zeta_{(i-1)}}, \Delta M_{o\zeta_{(i-1)}}, \Delta N_{o\zeta_{(i-1)}}\right)$$

The increments $\Delta L_{(i-1)\zeta_i}$, $\Delta M_{(i-1)\zeta_i}$, and $\Delta N_{(i-1)\zeta_i}$ were then related by Equation (40) to the increments in the generalized coordinates or parameters of the kinematic pair between bodies i and $(i-1)$. However, the increments $\Delta L_{o\zeta_{(i-1)}}$, $\Delta M_{o\zeta_{(i-1)}}$, and $\Delta N_{o\zeta_{(i-1)}}$ were assumed to be constants. This assumption is a critical step in the development of an iterative procedure which simplifies to a great extent the formulation

of equations of equilibrium for a system with N rigid bodies. With the aid of this assumption, the equation of equilibrium for an ith rigid body contains only the unknown generalized coordinates (or variable parameters) of the kinematic pair between bodies i and (i - 1), thus simplifying the task of developing analytically the equations of equilibrium as well as reducing the order (from N x N to a maximum of 6 x 6) of the set of linear equations to be solved to evaluate the increments in generalized coordinates as a result of increments in the external forces and moments.

In order to obtain a generalized simulation model for a system consisting of N rigid bodies, the following iterative process is developed. For a small increment in the externally applied forces and moments:

1. Set the increments $\Delta L_{o_\zeta(i-1)}$, $\Delta M_{o_\zeta(i-1)}$, $\Delta N_{o_\zeta(i-1)}$ to zero for i = 1, N. This initialization will decouple all the bodies in the sense that equations of equilibrium can be written for the ith body referred to the $(X'Y'Z')_{(i-1)}$ reference system associated with the (i-1)th body and further assuming that the $(X'Y'Z')_{(i-1)}$ reference system is invariant or fixed.

2. Calculate, using Equation (44), the increments in the generalized coordinates (or parameters) of the kinematic pair between bodies i and (i - 1) due to increments in the external forces and moments applied to body i, where i = N, N - 1, N - 2, . . ., 1. Since the equations of equilibrium for the ith body require data describing the configuration of the (i+1)th body, the iterative procedure must be started from the Nth body.

3. Using the increments of the generalized coordinate of the kinematic pair at each joint as calculated in step 2 above, evaluate, using

Equation (41), the increments in the direction cosines $\Delta L_{o\zeta_i}$, $\Delta M_{o\zeta_i}$, and $\Delta N_{o\zeta_i}$ for $i = 1, N$. For $i = 1$, $\Delta L_{o\zeta_{(i-1)}}$, $\Delta M_{o\zeta_{(i-1)}}$, and $\Delta N_{o\zeta_{(i-1)}}$ are zero, since the $(i-1)$th reference system is the fixed reference $X_o Y_o Z_o$.

4. Calculate the differences

$$\left|\Delta L_{o\zeta_i}^{(j)} - \Delta L_{o\zeta_i}^{(j-1)}\right|, \quad \left|\Delta M_{o\zeta_i}^{(j)} - \Delta M_{o\zeta_i}^{(j-1)}\right|, \quad \left|\Delta N_{o\zeta_i}^{(j)} - \Delta N_{o\zeta_i}^{(j-1)}\right|$$

for $i = 1, \ldots, N$, where (j) denotes the current iteration.

5. If the differences as calculated in step 5 above are within an allowable tolerance limit, stop the iteration. Otherwise, repeat steps 2 through 5 for the $(j+1)$th iteration. Note that in the $(j+1)$th iteration for the Nth body,

$$\Delta L_{o\zeta_{(n-1)}} = \Delta L_{o\zeta_i}^{(j)} \qquad \text{with } i = (n-1)$$

$$\Delta M_{o\zeta_{(n-1)}} = \Delta M_{o\zeta_i}^{(j)} \qquad \text{with } i = (n-1)$$

$$\Delta N_{o\zeta_{(n-1)}} = \Delta N_{o\zeta_i}^{(j)} \qquad \text{with } i = (n-1)$$

and so on.

With the successful completion of the check on the increment of direction cosines:

$$\Delta L_{o\zeta_i}^{(j)} - \Delta L_{o\zeta_i}^{(j-1)} \leq \varepsilon$$

$$\Delta M_{o\zeta_i}^{(j)} - \Delta M_{o\zeta_i}^{(j-1)} \leq \varepsilon$$

$$\Delta N_{o\zeta_i}^{(j)} - \Delta N_{o\zeta_i}^{(j-1)} \leq \varepsilon$$

the iterations are terminated. Update values of the direction cosines $L_{o\zeta_i}^{(j)}$, $M_{o\zeta_i}^{(j)}$, and $N_{o\zeta_i}^{(j)}$ for i = 1, N using the following equation:

$$
\begin{aligned}
L_{o\zeta_i}^{(j)} &= L_{o\zeta_i}^{(j-1)} + \Delta L_{o\zeta_i}^{(j)} \\
M_{o\zeta_i}^{(j)} &= M_{o\zeta_i}^{(j-1)} + \Delta M_{o\zeta_i}^{(j)} \\
N_{o\zeta_i}^{(j)} &= N_{o\zeta_i}^{(j-1)} + \Delta N_{o\zeta_i}^{(j)}
\end{aligned}
\tag{45}
$$

The updated values of the direction cosines $L_{o\zeta_i}$, $M_{o\zeta_i}$, and $N_{o\zeta_i}$ define the equilibrium configuration of the system with N rigid bodies subjected to the incremental external forces and moments $\Delta P_{i_k}, \Delta T_{i_k}$. Figure 13 shows a flow chart explaining the comprehensive iterative procedure involved in the methdology of determining the successive equilibrium configuration of a kinematically constrained elastic system consisting of N rigid bodies subjected to a set of externally applied static forces and moments.

5.2 Verification of the Theoretical Simulation Model Using a Known Mechanical System

Let us consider a mechanical system consisting of three bodies connected together by two cylinder pairs as shown in Figure 14. $X_iY_iZ_i$ constitutes a body reference system for the ith body. Since body 1 is held fixed, the reference system $X_1Y_1Z_1$ becomes the fixed reference for this mechanical system. A cylinder pair C_i connects two consecutive bodies i and i + 1. A system of characteristic axes $(X_pY_pZ_p)_i$ is

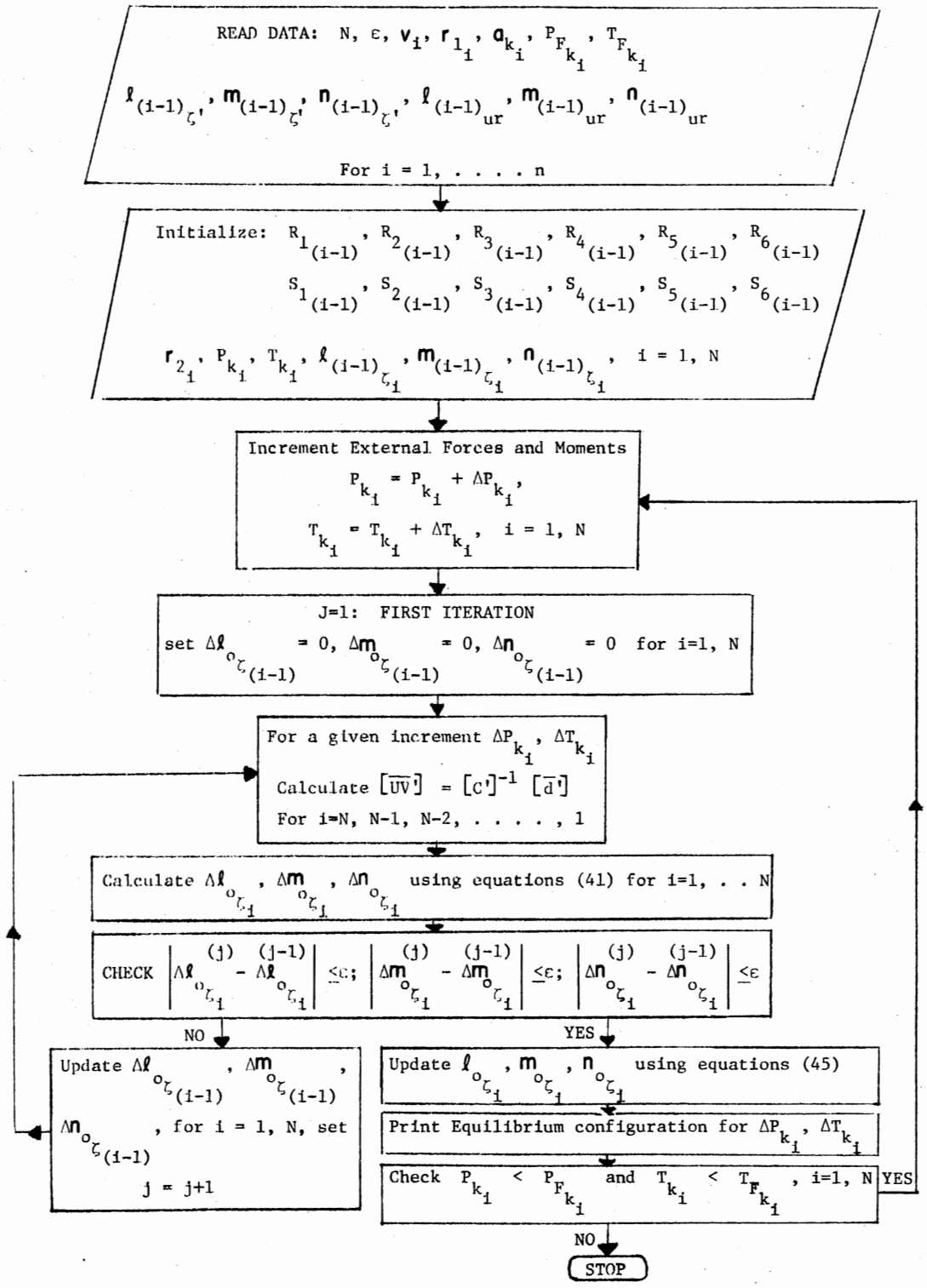

Figure 13. Flow Chart for the Simulation Model

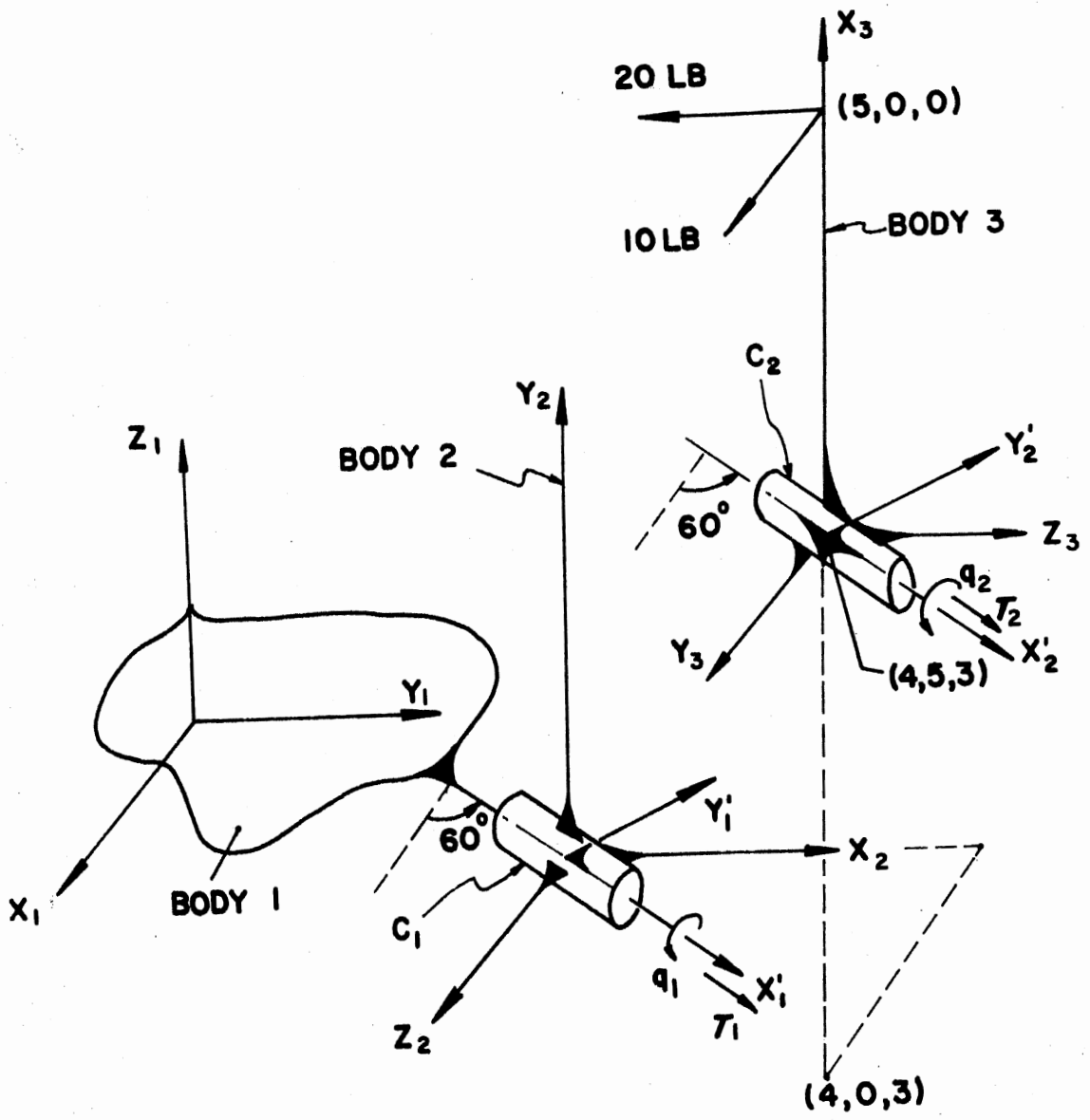

$K_{T_1} = K_{T_2} = 18.03$ lb/in

$K_{\theta_1} = K_{\theta_2} = 378.98$ in-lb/rad

Figure 14. Simulation of a Mechanical System

associated with the cylinder pair C_i and is defined in the body reference $(XYZ)_i$ of body i. The X_{p_i} axis is aligned with the axis of the cylinder pair C_i. The system is subjected to a set of external static loads applied to the third body as shown in Figure 14. In order to predict, using the theoretical simulation model, the equilibrium configuration achieved by such a system under the influence of the external loads, the following data must be prepared:

1. NBODY, TOL, NSTEP:

   3, 0.001, 100

The external loads are applied in small increments of one hundredths of the total load. For each set of incremental loads the equilibrium configuration is evaluated using an iterative procedure until the check on the direction cosines defining the configuration is satisfied. The tolerance data (0.001) controls the number of iterations at each incremental stage.

2. V(I), ELIV(I), EMIV(I), ENIV(I), I = 2, NBODY: $\vec{V}_i$ defines the point of application of internal elastic reactions in the body reference $(XYZ)_i$ due to relative motion between bodies i and i-1. For the system defined in Figure 14, we can write the following data:

   0.0, 0.0, 0.0, 0.0

   0.0, 0.0, 0.0, 0.0

3. RR1(I), ELIRR1(I), EMIRR1(I), ENIRR1(I), I = 2, NBODY: $\vec{r}_{1_i}$ defines the center of a kinematic pair between bodies i and i-1. $\vec{r}_{1_i}$ is defined in body reference $(XYZ)_i$ of body i.

   0.0, 0.0, 0.0, 0.0

   0.0, 0.0, 0.0, 0.0

4. NROTL(I), IROTDR(I), ELUR(I), EMUR(I), ENUK(I), I = 1, (NBODY-1): NROTL(I) defines the number of rotational degrees of freedom at the kinematic pair between bodies i and i-1. IROTDR(I) selects the axis of rotation from the set of characteristic axes associated with the kinematic pair.

IROTDR: 1; Axis of Rotation: X_p

: 2; : Y_p

: 3; : Z_p

ELUR(I), EMUR(I), ENUR(I) define the direction cosines of the axis of rotation of the kinematic pair between bodies i and i-1 with respect to the body reference $(XYZ)_{i-1}$. Thus for the system under consideration, the following data can be written:

1, 1, 0.5, 0.8660254, 0.0

1, 1, 0.8660254, 0.0, 0.5

5. NTRAN(I); I = 1, NBODY-1: NTRAN(I) defines the number of translational degrees of freedom of the kinematic pair between bodies i and (i-1).

1, 1

6. ITAUDR(I, K); K = 1, NTRAN(I), I = 1, NBODY-1: ITAUDR(I, K) defines the axis of translation from the set of characteristic axes of the kinematic pair:

1

1

7. ELIMUT(I, K), EMIMUT(I, K), ENIMUT(I, K), K = 1, NTRAN(I), I = 1, NBODY-1: define the direction cosines of the axis of translation

of the kinematic pair with respect to the body reference $(XYZ)_{(i-1)}$ of body (i-1).

0.5, 0.8660254, 0.0

0.8660254, 0.0, 0.5

8. IOPLN(I), IPPLN(I), I = 1, NBODY-1:

IOPLN = 0: Three-dimensional motion

1: Motion in the XY plane

2: Motion in the YZ plane

3: Motion in the XZ plane

IPPLN = 0: Three-dimensional motion

1: Motion in the X_pY_p plane

2: Motion in the Y_pZ_p plane

3: Motion in the X_pZ_p plane

For the system under consideration, we have

0, 0

0, 0

9. ELIMXP(I), EMIMXP(I), ENIMXP(I), I = 1, NBODY-1: defines in the $(XYZ)_{(i-1)}$ reference system the direction cosines of the axes X_p associated with the kinematic pair between bodies i and (i-1). Thus we have the data:

0.5, 0.8660254, 0.0

0.8660254, 0.0, 0.5

In the same manner the following data can be written.

10. ELIMYP(I), EMIMYP(I), ENIMYP(I), I = 1, NBODY-1:

-0.8660254, 0.5, 0.0

0.5, 0.0, -0.8660254

11. ELIMZP(I), EMIMZP(I), ENIMZP(I), I = 1, NBODY-1:

0.0, 0.0, 1.0

0.0, 1.0, 0.0

12. AK(I, J, K); K = 1, 6; J = 1, 6; I = 1, NBODY-1: defines the stiffness matrix between bodies i and (i-1). The stiffness matrix is defined with respect to the body reference $(XYZ)_{i-1}$ of body (i-1). Thus we have the following data:

10.0, 0.0, 0.0, 0.0, 0.0, 0.0

0.0, 20.0, 0.0, 0.0, 0.0, 0.0

0.0, 0.0, 0.0, 0.0, 0.0, 0.0

0.0, 0.0, 0.0, 572.9578, 0.0, 0.0

0.0, 0.0, 0.0, 0.0, 286.4789, 0.0

0.0, 0.0, 0.0, 0.0, 0.0, 0.0

20.0, 0.0, 0.0, 0.0, 0.0, 0.0

0.0, 0.0, 0.0, 0.0, 0.0, 0.0

0.0, 0.0, 10.0, 0.0, 0.0, 0.0

0.0, 0.0, 0.0, 286.4789, 0.0, 0.0

0.0, 0.0, 0.0, 0.0, 0.0, 0.0

0.0, 0.0, 0.0, 0.0, 0.0, 572.9578

13. NP(I), NT(I); I = 2, NBODY: define the number of external forces and moments acting on each body.

0, 0

2, 0

14. PF(I, K), EL1P(I, K), EM1P(I, K), EN1P(I, K); K = 1, NP(I); I = 2, NBODY: PF(I, K) is the magnitude of the applied Kth load on the ith body. EL1P(I, K), EM1P(I, K), and EN1P(I, K) define the direction of the load in the fixed reference system.

0.0, 0.0, 0.0, 0.0

10.0, 1.0, 0.0, 0.0

20.0, 0.0, -1.0, 0.0

15. A(I, K), ELIA(I, K), EMIA(I, K), ENIA(I, K); K = 1, NPI, I = 2, NBODY: $\vec{A}$(I, K) defines the location of point of application of external loads in the body reference $(XYZ)_i$ of body i.

0.0, 0.0, 0.0, 0.0

5.0, 1.0, 0.0, 0.0

5.0, 1.0, 0.0, 0.0

In the same manner one can write the following data regarding the external moments.

16. TF(I, K), EL1T(I, K), EM1T(I, K), EN1T(I, K); K = 1, NT(I); I = 2, NBODY:

0.0, 0.0, 0.0, 0.0

0.0, 0.0, 0.0, 0.0

17. R1(I), R2(I), R3(I), R4(I), R5(I), R6(I), I = 1, NBODY-1: define the values of internal reactions at the kinematic pair between bodies i and (i-1) in the initial configuration.

0.0, 0.0, 0.0, 0.0, 0.0, 0.0

0.0, 0.0, 0.0, 0.0, 0.0, 0.0

18. S1(I), S2(I), S3(I), S4(I), S5(I), S6(I); I = 1, NBODY-1: define the internal elastic reactions between bodies i and i-1 in the initial configuration.

0.0, 0.0, 0.0, 0.0, 0.0, 0.0

0.0, 0.0, 0.0, 0.0, 0.0, 0.0

19. RR2(I), XIRR2(I), YIRR2(I), ZIRR2(I); I = 2, NBODY: vector $\vec{r}_{2_i}$ defines the location of the kinematic pair between bodies i and i+1 with respect to the body reference $(XYZ)_i$ of body i.

5.0, 0.0, 5.0, 0.0

0.0, 0.0, 0.0, 0.0

20. ELIMX(I), EMIMX(I), ENIMX(I); I = 2, NBODY: define the direction cosines of the X_i (body reference of body i) axis with respect to the reference system $(XYZ)_{i-1}$ of body (i-1).

0.0, 1.0, 0.0

0.0, 1.0, 0.0

In the same manner we can write the following data.

21. ELIMY(I), EMIMY(I), ENIMY(I); I = 2, NBODY:

0.0, 0.0, 1.0

0.0, 0.0, 1.0

22. ELIMZ(I), EMIMZ(I), ENIMZ(I); I = 2, NBODY:

1.0, 0.0, 0.0

1.0, 0.0, 0.0

23. QR(I), QTRAN(I, 1), QTRAN(I, 2); I = 1, NBODY-1: define the initial values of the generalized coordinates of the kinematic pair between bodies i and (i-1).

0.0, 0.0, 0.0

0.0, 0.0, 0.0

The simulation analysis of such a mechanical system yields incremental equilibrium configurations which shows the successive positions through which the three bodies move under the influence of external static loads before reaching the final equilibrium configuration.

The resultant equilibrium configuration of the above system was found to be:

q_1 = 19.5757456 deg.

q_2 = 12.7353072 deg.

τ_1 = -0.5334272 in.

τ_2 = -0.7040290 in.

The internal reactions at the kinematic pair between bodies 1 and 2 and between bodies 2 and 3 in the final equilibrium configuration were found to be, respectively:

R1(1) = 0.0 lbs ; R1(2) = 0.0 lbs

R2(1) = 0.5959802 lbs ; R2(2) = 14.6103786 lbs

R3(1) = 16.5120698 lbs ; R3(2) = -5.9710634 lbs

R4(1) = 0.0 in.-lbs ; R4(2) = 0.0 in.-lbs

R5(1) = -70.2024452 in.-lbs; R5(2) = 32.5868525 in.-lbs

R6(1) = 51.6903911 in.-lbs ; R6(2) = 13.4596755 in.-lbs

It should be noted that these reaction forces are applied at the kinematic pair and are defined with respect to the characteristic axes $X_p Y_p Z_p$ of the kinematic pairs. Since the cylinder pair has two degrees of freedom, namely the rotational and translational motion along its axis, the reaction force along and the reaction moment about this axis

must be zero. This information may be checked from the above results.

The validity of the above solution can easily be demonstrated by checking the equations of static equilibrium of bodies 2 and 3 in their resultant equilibrium configuration.

A graphical representation of the results of the above simulation analysis is shown in Figure 15. The figure shows the successive equilibrium configurations of bodies 2 and 3 in terms of rotation and translation along the axes of the cylinder pairs as a function of the incremental loads applied to body 3. It is important to note that the system is treated as linear during each increment of the externally applied static loads. However, an examination of the overall load versus displacement curve shows nonlinearity. This is due to the fact that as the system undergoes successive equilibrium configurations, the relative geometry between the rigid bodies changes due to the rotational and translational motion at kinematic pairs between the rigid bodies. This, in turn, changes the moment arms of the externally applied forces and the point of application of internal reactions between bodies 2 and 3, thus inducing the nonlinearity in the overall response of bodies 2 and 3 subjected to external forces.

5.3 Application of the Simulation Model to the Human Spine Subjected to Static Loads

5.3.1 A Rational Approach

A theoretical motion simulation model for a kinematically constrained elastic system consisting of N rigid bodies subjected to a set of externally applied static loads was developed in section 5.1. This section

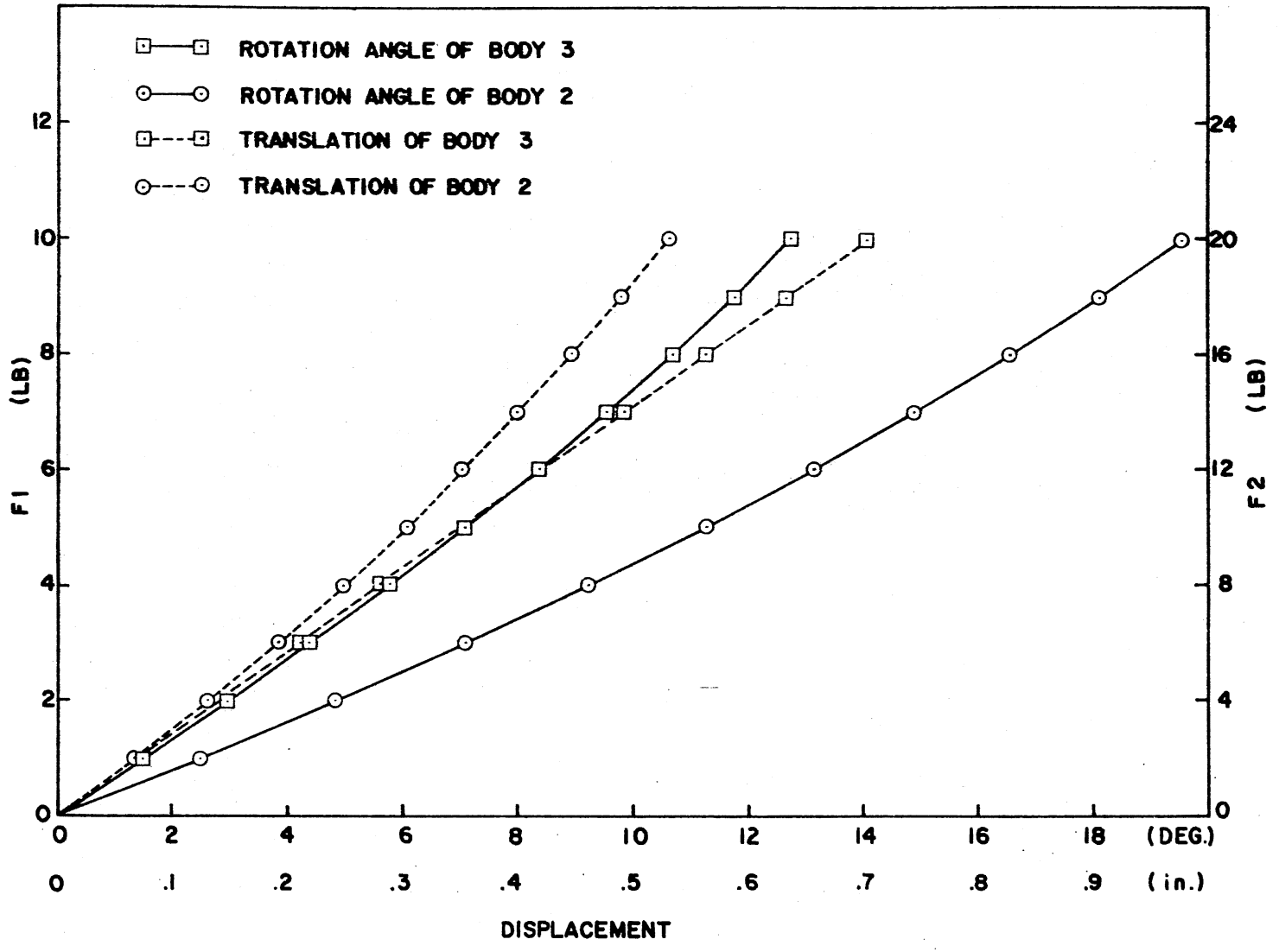

Figure 15. Successive Equilibrium Configuration of the Mechanical System

presents a methodology developed for the purpose of adapting this generalized motion simulation model to the biological system of a human spine consisting of intervertebral joints.

As explained at the beginning of this chapter, the role played by facet joints in controlling the pattern of motion of intervertebral joints is analogous to the function of kinematic pairs in the kinematically constrained elastic system of section 5.1. The orientation of the facet joint at each vertebral level, the geometric characteristics of the surface of contact and type of contact govern the components of motion at each intervertebral joint, the functional relationships between these components of motion, and the overall pattern of the intervertebral motion of a human spine subjected to static loads. The total intervertebral motion, however, is a function of the disc, ligaments, muscles, and facet joint geometry.

In order to formulate the motion simulation model of the spine, it is therefore necessary to arrive at the kinematically equivalent intervertebral joint which can be used in the generalized motion simulation model developed in section 5.1. A rational approach developed in the present work for the purpose of arriving at the kinematically equivalent intervertebral joint is based upon the set of physically realizable kinematic pairs.

There are twelve physically realizable kinematic pairs. Each of these kinematic pairs must be examined critically before arriving at the kinematically equivalent intervertebral joint. These kinematic pairs are classified according to their degrees of freedom and the components of relative motion permitted at each pair. Table VII presents this

TABLE VII

CLASSIFICATION OF PHYSICALLY REALIZABLE KINEMATIC PAIRS AND THEIR PARAMETERS

Class of K.P.	D.F.	Name and Form-Closed			Generalized Parameter Coordinates
1	1	Revolute (a)	Prismatic (b)	Helical (c)	(a) $q_1 = q_r = \theta$ (b) $q_1 = q_{\tau_1} = \tau$ (c) $q_1 = q_r$; $P = \tau/\theta$
2	2	Slotted-Sphere (a)	Cylinder (b)	Cam (c)	(a) $q_1 = \theta$, $q_2 = \phi$ (b) $q_1 = \theta$, $q_2 = \tau$ (c) $q_1 = \theta$, $q_2 = \tau$
3	3	Sphere (a)	Sphere Slotted-Cylinder (b)	Plane (c)	(a) $q_1 = \theta$, $q_2 = \phi$, $q_3 = \psi$ (b) $q_1 = \theta$, $q_2 = \phi$, $q_3 = \tau$ (c) $q_1 = \theta$, $q_2 = \tau_1$, $q_3 = \tau_2$
4	4	Sphere Groove (a)		Cylinder Plane (b)	(a) $q_1 = \theta$, $q_2 = \phi$, $q_3 = \psi$, $q_4 = \tau$ (b) $q_1 = \theta$, $q_2 = \phi$, $q_3 = \tau$, $q_4 = \tau$
5	5		Sphere-Plane (a)		(a) $q_1 = \theta$, $q_2 = \phi$, $q_3 = \psi$, $q_4 = \tau$ $q_5 = \tau_2$

classification along with the characteristic (or principal) set of axes and generalized coordinates for each kinematic pair.

The identification of the characteristic or principal set of axes and the generalized coordinates for each kinematic pair provide sufficient information to define completely the kinematic constraints of a kinematic pair. However, when such a kinematic pair is used in the theoretical simulation model developed in section 5.1, the parametric vector of the kinematic pair includes:

1. The vector $\vec{r}_{1_i}$ locating the center of the kinematic pair.
2. The direction cosines of the axes X'Y'Z' referred to the reference system $(XYZ)_{(i-1)}$: $L_{(i-1)_\zeta'}$, $M_{(i-1)_\zeta'}$, and $N_{(i-1)_\zeta'}$.
3. The generalized coordinates (q's) of the kinematic pair.

The data describing the vector $\vec{r}_{1_i}$ and the direction cosines $L_{(i-1)_\zeta'}$, $M_{(i-1)_\zeta'}$, and $N_{(i-1)_\zeta'}$ are obtained as explained in the chapter on experimental data collection.

Using the parametric vector defined above, the kinematic constraints of each of the twelve physically realizable kinematic pairs shown in Table IX can be incorporated in the theoretical simulation model along with stiffness data describing the elastic properties of each intervertebral joint.

Thus, by replacing the actual intervertebral joints by the equivalent kinematic pairs selected one at a time from the set shown in Table VII it becomes possible to study the response of the human spine subjected to external static loads. Such a study will yield twelve different sets of motion responses for the same set of external static loads. In order to arrive at a kinematic pair best describing the kinematic constraints of the actual intervertebral joints, it is therefore necessary

to formulate a criterion to evaluate the relative merits of each kinematic pair. One such criterion is based upon the comparison of the axodes generated by the motion simulation model with the axodes generated by the actual spine specimen subjected to the same set of external static loads.

This evaluation procedure forms the quantitative basis for selecting from the set of twelve physically realizable pairs the kinematic pair which best describes the kinematic constraints of the actual intervertebral joint. Thus, having arrived at the kinematic equivalent of the intervertebral joint, the theoretical motion simulation model developed in section 5.1 now becomes the motion simulation model for the human spine subjected to external static loads.

The methodology developed in sections 5.1 and 5.3.1 for the purpose of developing a simulation model for the human spine is now applied to the experimental data collected in section 3.2. The results of this analysis are presented in the next section.

5.3.2 Simulation Studies of the Human Spine Using Experimental Data

In order to apply the theoretical motion simulation model to the biological system of intervertebral joints, the following assumptions are made:

1. The coefficients of the equivalent stiffness matrix between a pair of vertebrae are assumed constant over the entire range of intervertebral motion.

2. The equivalent kinematic pair representing the kinematic constraints of an intervertebral joint is assumed to be a spherical joint,

thus simulating only the rotational motion components at the intervertebral joint.

The data required by the theoretical motion simulation model to simulate a kinematically constrained elastic system must be prepared as demonstrated in section 5.2. The data describing the geometric parameters and the stiffness properties of the biological system consisting of intervertebral joints must, however, be prepared by processing the raw experimental data. A stepwise procedure to set up such data for the theoretical motion simulation model is demonstrated in the following by taking an example case of the intervertebral joint, L2-L3 (specimen 4), subjected to a load applied along the $-X_o$ direction:

1. NBODY, TOL, NSTEP:

   2, 0.001, 100

2. RR1(I), ELIRR1(I), EMIRR1(I), ENIRR1(I): As explained earlier, the vector $\vec{r}_{1_i}$ defines, in the body reference $(XYZ)_i$ of body i, the location of the kinematic pair between bodies i and (i-1). Since the kinematic pair between a pair of vertebrae is assumed to be a spherical joint, the center of this spherical joint must be first located with respect to the body reference of one of the vertebrae. Since the load is applied along the $-X_o$ direction, vertebra L2 is flexed with respect to vertebra L3. Table VIII shows the parameters of instantaneous screws of motion of vertebra L2 with respect to L3 as the intervertebral joint executed motion in the flexion mode during the kinematic data collection. These screw data were calculated with respect to the neutral position of vertebra L2. The parameters of the screw axes are defined in the fixed reference system $X_oY_oZ_o$. Using the least square technique (Appendix B), a cone can be fitted to these screw data. The spherical joint which

TABLE VIII

LOCATION OF SPHERICAL JOINT USING LEAST SQUARE CONE FIT

U_x	U_y	U_z	P_x	P_y	P_z
0.3540262	-0.4313658	-0.8298127	-0.9334235	1.0971191	1.0759394
0.4677333	-0.6779525	-0.5671032	-0.1825692	0.9851212	1.9507478
0.4304682	-0.6984427	-0.5717298	-0.0830322	0.9929570	1.9243803
0.3758692	-0.7384927	-0.5597750	-0.2616016	0.9472326	2.1703959
Coordinates of apex of cone in $X_oY_oZ_o$			-1.2248426	2.3365725	3.1341664
Coordinates of apex of cone in $(XYZ)_2$			0.5226054	0.2206634	-0.0151808

represents the equivalent kinematic pair for the intervertebral joint L2-L3 is located at the apex of the least square cone. Table VIII shows the coordinates of this apex in the fixed reference system $X_oY_oZ_o$ attached to the fixed vertebra L3. In order to find the coordinates of the apex of the cone in the body reference $X_2Y_2Z_2$ of vertebra L2, a transformation matrix between coordinate systems $(X_2Y_2Z_2)$ and $(X_oY_oZ_o)$ must be evaluated first. This can be achieved by using the voltage data from the linkage transducer corresponding to the neutral position of vertebra L2. The linkage transducer is connected between the coordinate systems $X_2Y_2Z_2$ and $X_1Y_1Z_1$. Using the terminology of Chapter IV, the transformation from $X_2Y_2Z_2$ to $X_1Y_1Z_1$ in the neutral position is given by the transformation matrix [B']. In addition, if the transformation from $X_1Y_1Z_1$ to the fixed (or anatomical) coordinate system $X_oY_oZ_o$ is given by the transformation matrix [F], then the resultant transformation is given by:

$$[TR] = [F]\,[B']$$

so that the coordinates of the apex of the least square cone in the reference system $X_2Y_2Z_2$ can be calculated using the following equation:

$$[\vec{r}_1]_{(X_2Y_2Z_2)} = \begin{bmatrix} X_c \\ Y_c \\ Z_c \end{bmatrix}_{(X_2Y_2Z_2)} = \Big[[F]\,[B']\Big]^{-1} \begin{bmatrix} X_c \\ Y_c \\ Z_c \end{bmatrix}_{(X_oY_oZ_o)}$$

For the intervertebral joint L2-L3, the components of vector $\vec{r}_1$ as calculated from the above equation are given in Table VIII.

3. V(I), ELIV(I), EMIV(I), ENIV(I): Vector $\vec{V}_i$ defines, in the reference system $X_2Y_2Z_2$ of vertebra L2, the point of application of the internal elastic reactions due to the relative motion at the intervertebral joint L2-L3. Since the kinematic pair used in the simulation of intervertebral motion permits only the rotational components of motion, the internal elastic reactions will consist of only the resistive moments at the intervertebral joint. Hence in the case of a spherical joint, the vector $\vec{V}_i$ is the same as the vector $\vec{r}_{1_i}$.

4. NROTL, IROTDR, ELUR, EMUR, ENUR: Because of the nature of the spherical joint, the choice of the characteristic axes is completely arbitrary, and for convenience axes $X_pY_pZ_p$ are made parallel to axes $X_oY_oZ_o$, respectively. Since the motion component to be simulated is the rotation about the $-Y_o$ axis (flexion angle), we can write the following data:

1, 2, 0.0, 1.0, 0.0

5. NTRAN:

0

6. ITAUDR:

0

7. ELIMUT, EMIMUT, ENIMUT:

0.0, 0.0, 0.0

8. IOPLN, IPPLN:

0, 0

9. ELIMXP, EMIMXP, ENIMXP:

1.0, 0.0, 0.0

10. ELIMYP, EMIMYP, ENIMYP:

0.0, 1.0, 0.0

11. ELIMZP, EMIMZP, ENIMZP:

0.0, 0.0, 1.0

12. AK(I, J, K): Data describing the elastic (or stiffness) properties of the intervertebral joint are obtained by processing the experimental data collected during the load test of the intervertebral joint L2-L3 with the facet joints totally destroyed. Parameters of the instantaneous screws of motion due to the applied load are first calculated with respect to the fixed reference system $X_oY_oZ_o$. A least square cone is then fitted to these screw data to calculate the location of the equivalent spherical joint in the reference system $X_oY_oZ_o$. Figure 16 shows the relative location of the point of application of load (during the load test) and the location of the equivalent spherical joint with respect to the fixed reference $X_oY_oZ_o$. The location of the point of application of the load is measured with respect to the reference $X_oY_oZ_o$ during the experiment. Using the notation consistent with the coordinate system $X_oY_oZ_o$, the coefficients of the stiffness matrix needed to simulate intervertebral motion due to load along the Y_o axis are calculated using the following equations:

a. Rotational stiffness about the axis X_o:

$$K_{\theta_{xx}} = [F(h_2 - h_1)/\theta_{x_o}] \text{ in.-lb/rad}$$

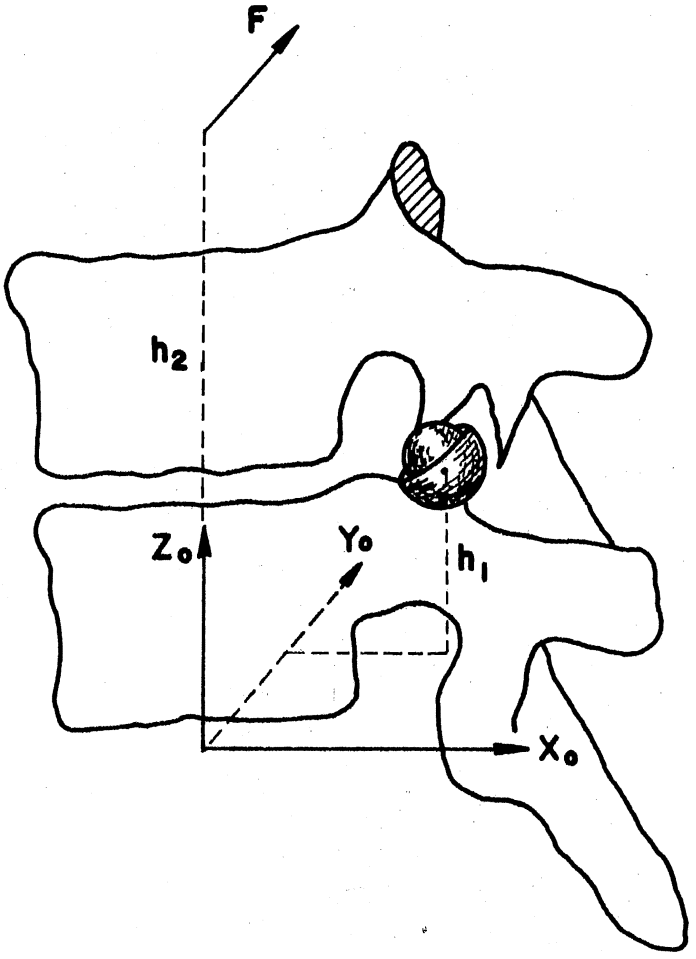

$F = 4.0$ Lbs , $h_1 = 3.32$ in , $h_2 = 10.25$ in.

$\theta_{y_o} = -1.72$ deg. , $\theta_{x_o} = -4.21$ deg. , $\theta_{z_o} = -2.2$ deg.

$K_{\theta_{xy}} = 923.39 \frac{\text{in-lb}}{\text{rad}}$; $K_{\theta_{xx}} = 377.25 \frac{\text{in-lb}}{\text{rad}}$; $K_{\theta_{xz}} = 721.93 \frac{\text{in-lb}}{\text{rad}}$

Figure 16. Calculation of Stiffness Coefficients

b. Rotational stiffness about the Y_o axis due to coupling between the X_o and Y_o axis:

$$K_{\theta_{xy}} = [F(h_2 - h_1)/\theta_{y_o}] \text{ in.-lb/rad}$$

c. Rotational stiffness about the Z_o axis due to coupling between the Z_o and X_o axis:

$$K_{\theta_{xz}} = [F(h_2 - h_1)/\theta_{z_o}] \text{ in.-lb/rad}$$

13. Coupling data:

ICOUPLE = 0: No coupling effect

1: Coupled motion

ICOUPLE1 = 1: Coupling due to M_{x_o}

2: Coupling due to M_{y_o}

3: Coupling due to M_{z_o}

ICOUPLE2 = 1: Coupled motion about the X_o axis

2: Coupled motion about the Y_o axis

3: Coupled motion about the Z_o axis

Since the component of motion to be simulated is rotation about the Y_o axis due to moment M_{y_o}, we can write the following data:

0, 0, 0

14. NP, NT:

1, 0

15. PF, EL1P, EM1P, EN1P: The intervertebral joint L2-L3 was subjected to a load of four pounds (applied in increments of one pound) along the $-X_o$ axis. Hence we have the following data:

kinematic pair between L_i and L_{i+1} (the vertebra above L_i). Using the procedure described earlier, the location of equivalent spherical joints can be calculated for the intervertebral joints $(L_{i+1} - L_i)$ and $(L_i - L_{i-1})$ with respect to the fixed reference $X_oY_oZ_o$. The transformation matrix $[F]_i$ between the coordinate system $(XYZ)_i$ of vertebra L_i and the fixed reference $X_oY_oZ_o$ can then be used to calculate the components of the vector $\vec{r}_{2_i}$. However, since in this example problem the intervertebral motion is being simulated only at the L2-L3 joint, we have the following data:

0.0, 0.0, 0.0, 0.0

21. ELIMXI, EMIMXI, ENIMXI: These define the direction cosines of the axis X_i (of the coordinate system $X_iY_iZ_i$) of vertebra L_i with respect to the coordinate system $(XYZ)_{i-1}$ of vertebra $L_{(i-1)}$. In the example case of the intervertebral joint L2-L3, the fixed reference $X_oY_oZ_o$ is attached to the vertebra L3. The direction cosines of the axis X_2 with respect to the $X_oY_oZ_o$ system are calculated using the following equations:

$$\ell_{o_{x_2}} = X_{c_2} - X_{c_1}$$

$$m_{o_{x_2}} = Y_{c_2} - Y_{c_1}$$

$$n_{o_{x_2}} = Z_{c_2} - Z_{c_1}$$

where

$$\begin{bmatrix} X_{c_2} & X_{c_1} \\ Y_{c_2} & Y_{c_1} \\ Z_{c_2} & Z_{c_1} \end{bmatrix} = [TR] \begin{bmatrix} 1.0 & 0.0 \\ 0.0 & 0.0 \\ 0.0 & 0.0 \end{bmatrix}$$

For the intervertebral joint L2-L3, we have the following data:

0.2739471, -0.9595212, -0.0653601

In the same manner the following data are calculated:

22. ELIMYI, EMIMYI, ENIMYI:

    0.1053506, 0.0974901, -0.9896449

23. ELIMZI, EMIMZI, ENIMZI:

    0.9559573, 0.2642246, 0.1277932

24. QR, QTRAN1, QTRAN2:

    0.0, 0.0, 0.0

The above data are used in the theoretical motion simulation model to predict the successive equilibrium configuration of vertebra L2 with respect to vertebra L3 as the body of L2 is subjected to external static load along the $-X_o$ direction. The results of this simulation analysis are presented in Figure 17(a) and (b), which show the applied load versus angular rotation curves for the flexion angle, lateral rotation, and axial twist of vertebra L2 with respect to L3 in the $X_oY_oZ_o$ (or anatomical) frame of reference.

The simulation studies were conducted on the intervertebral joints using experimental data collected by testing four human lumbar spine

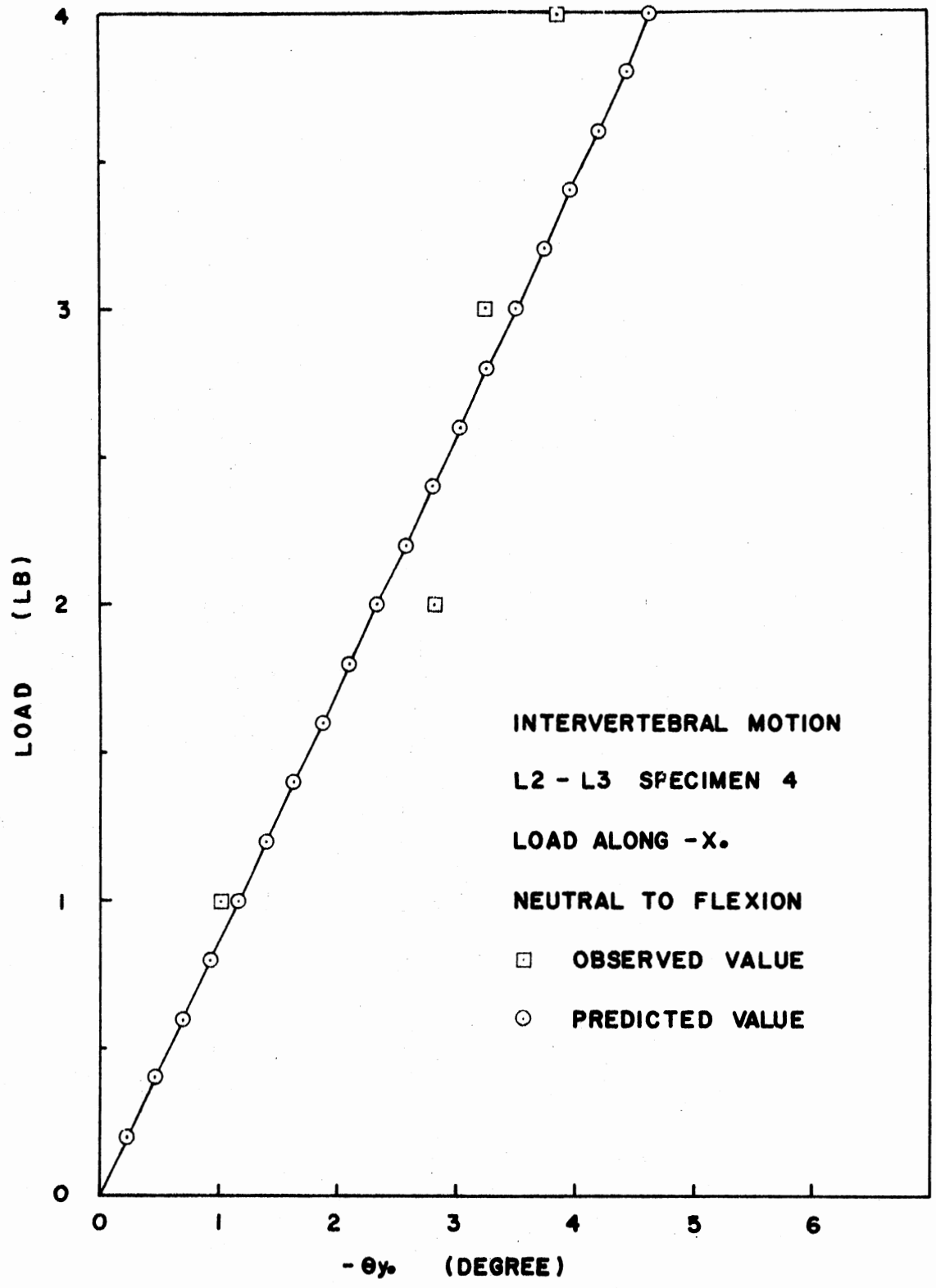

(a) L2-L3, Specimen 4

Figure 17. Successive Equilibrium Configuration of the Intervertebral Joint

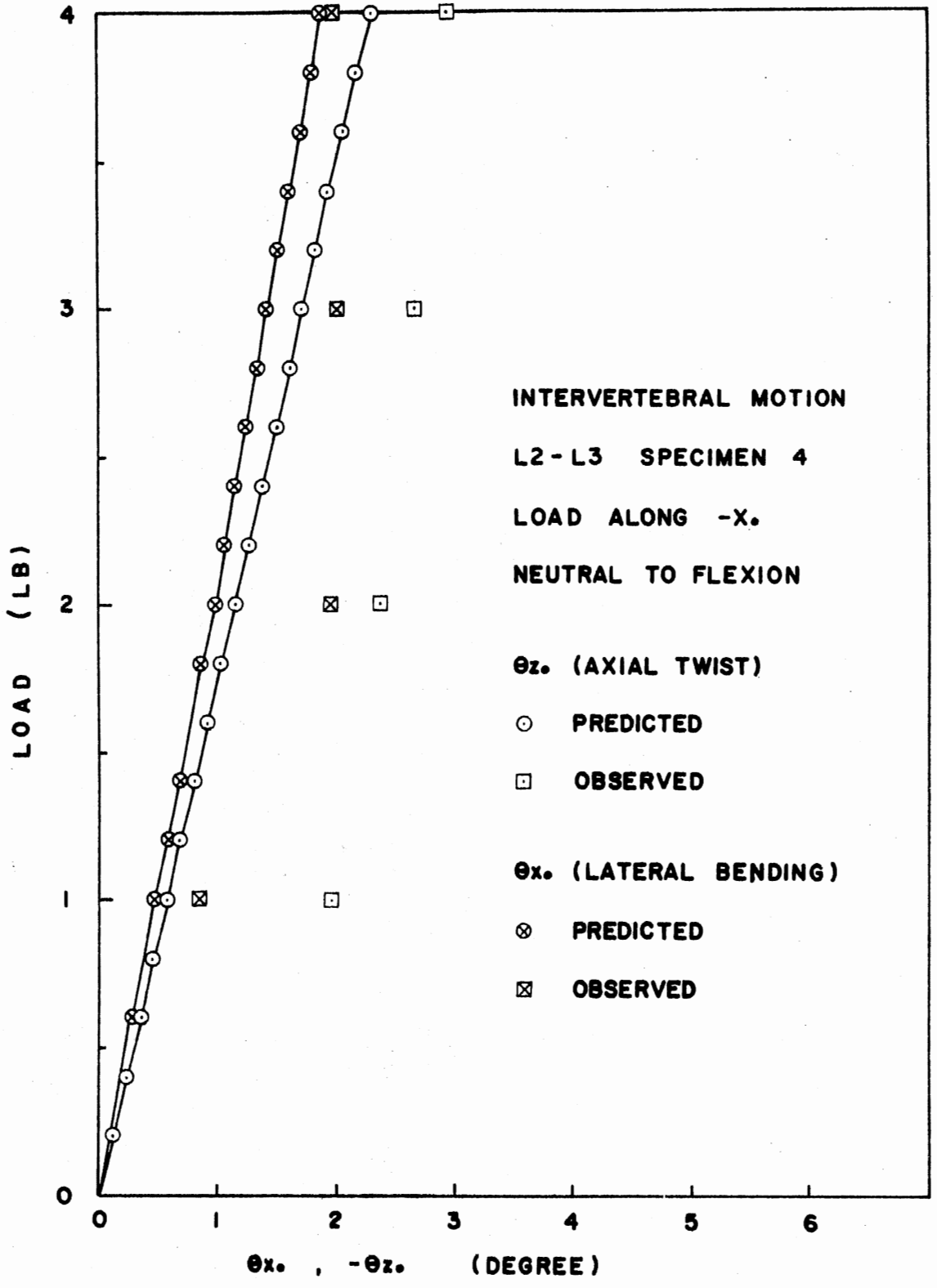

(b) L2-L3, Specimen 4

Figure 17. (Continued)

segments. The results of this simulation analysis are presented in the following Figure 17(a) through (k).

An examination of the above results show that the theoretical motion simulation model of the spine predicts, within reasonable limits, the response of the intervertebral joints of a human spine subjected to external static loads. In general, it was observed that:

1. The predicted response was closer to the observed response in the case of direct rotational components as compared to the coupled rotational components.

2. The response of the intervertebral joints as predicted by the theoretical motion simulation model was very sensitive to the stiffness properties of the intervertebral joint.

3. Since the physiological properties of the spine specimens varied over a wide range (due to the differences in age, degenerative problems in the case of some specimens, and structural problems in some specimens), the stiffness properties of the intervertebral joints may vary considerably from one specimen to the other. Hence the stiffness values from one specimen could not be used in the simulation of other specimens.

4. Stiffness values were in general affected by the removal of facet joints for a pair of vertebrae.

5. The predicted response was a strong function of the location of the equivalent kinematic pair.

The deviation of the predicted response from the observed response of intervertebral joints subjected to external forces can be explained by examining the different sources of errors. The observed response of the intervertebral joint is calculated using the voltage data describing

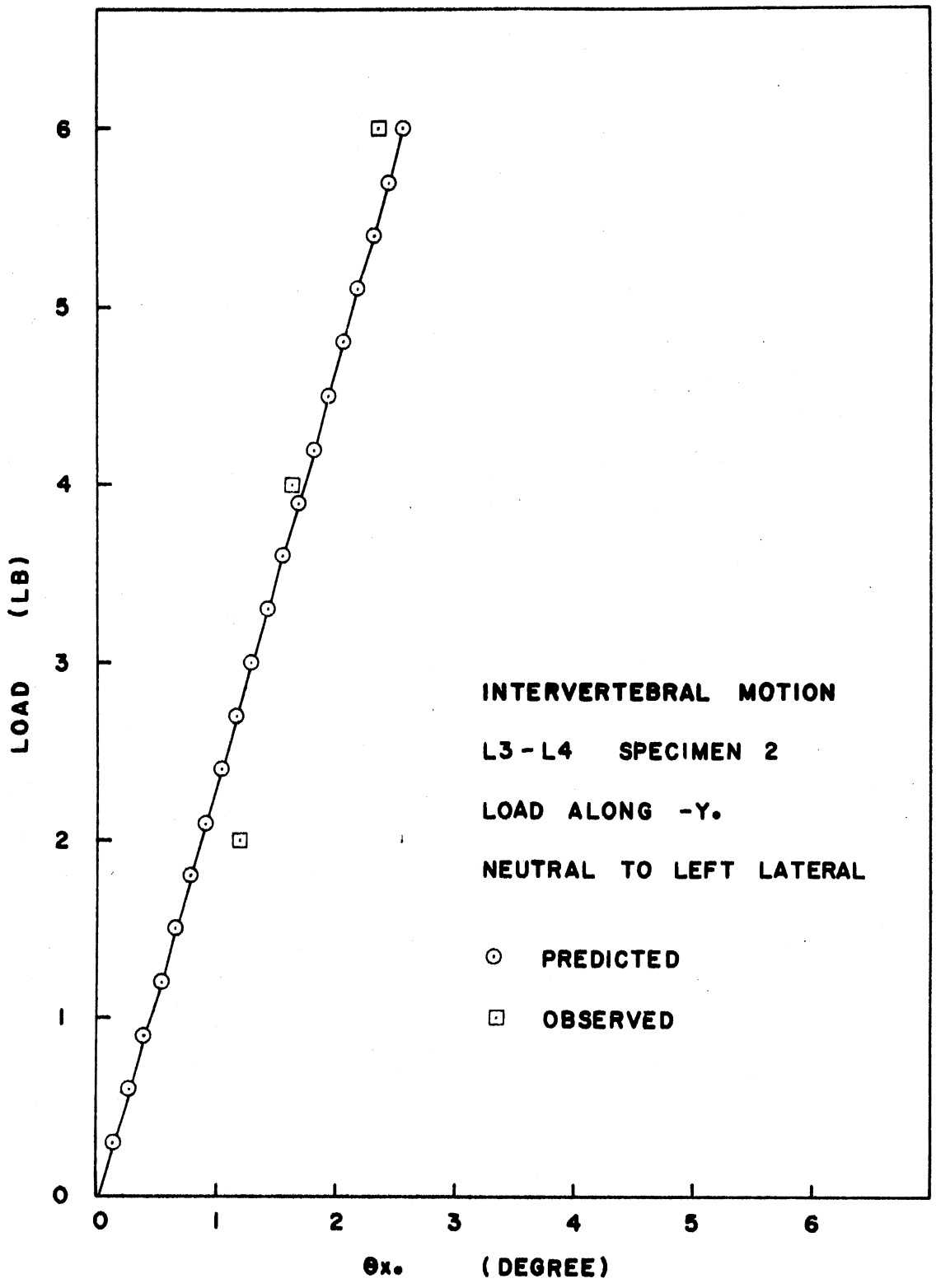

(c) L3-L4, Specimen 2

Figure 17. (Continued)

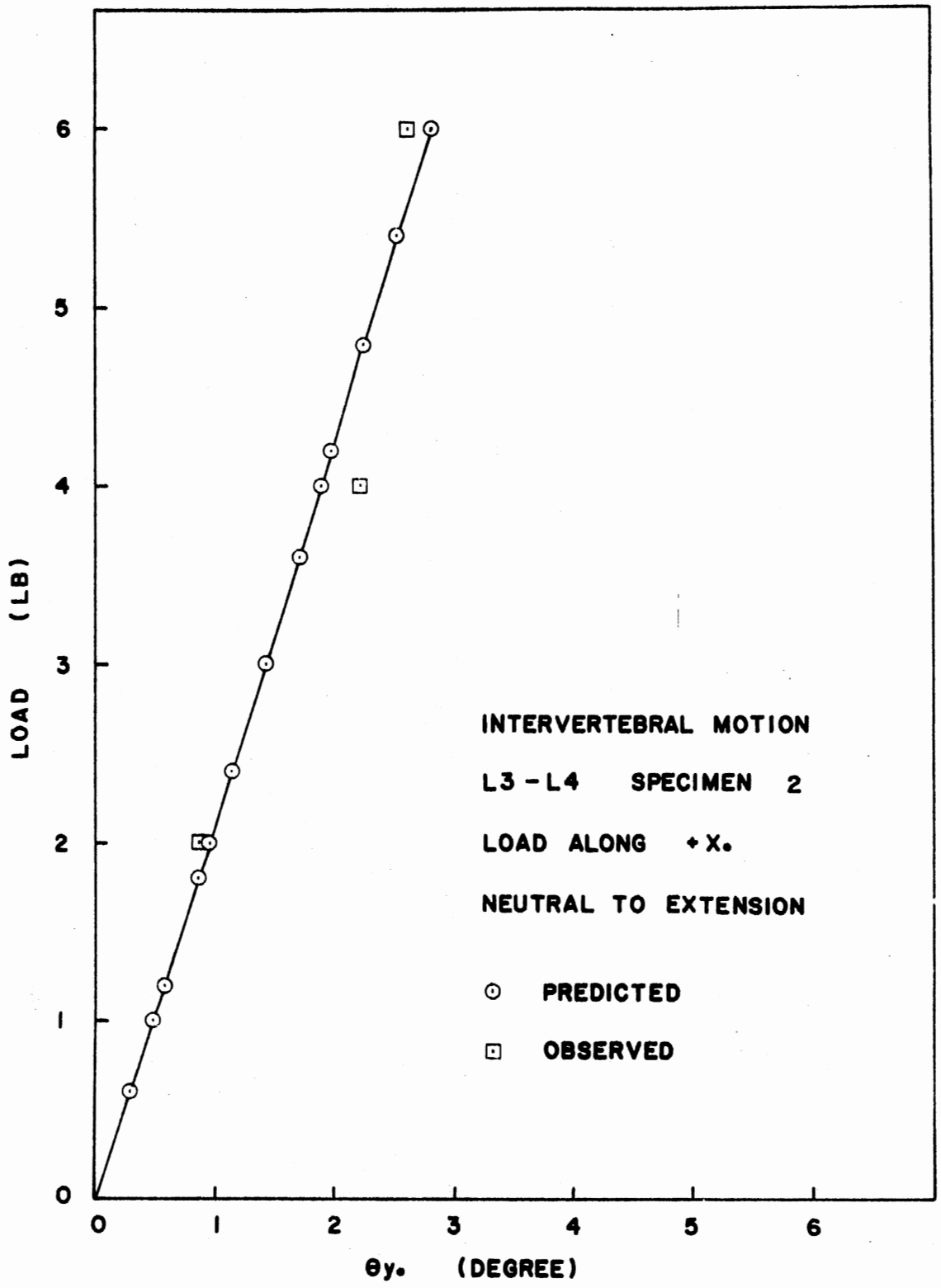

(d) L3-L4, Specimen 2

Figure 17. (Continued)

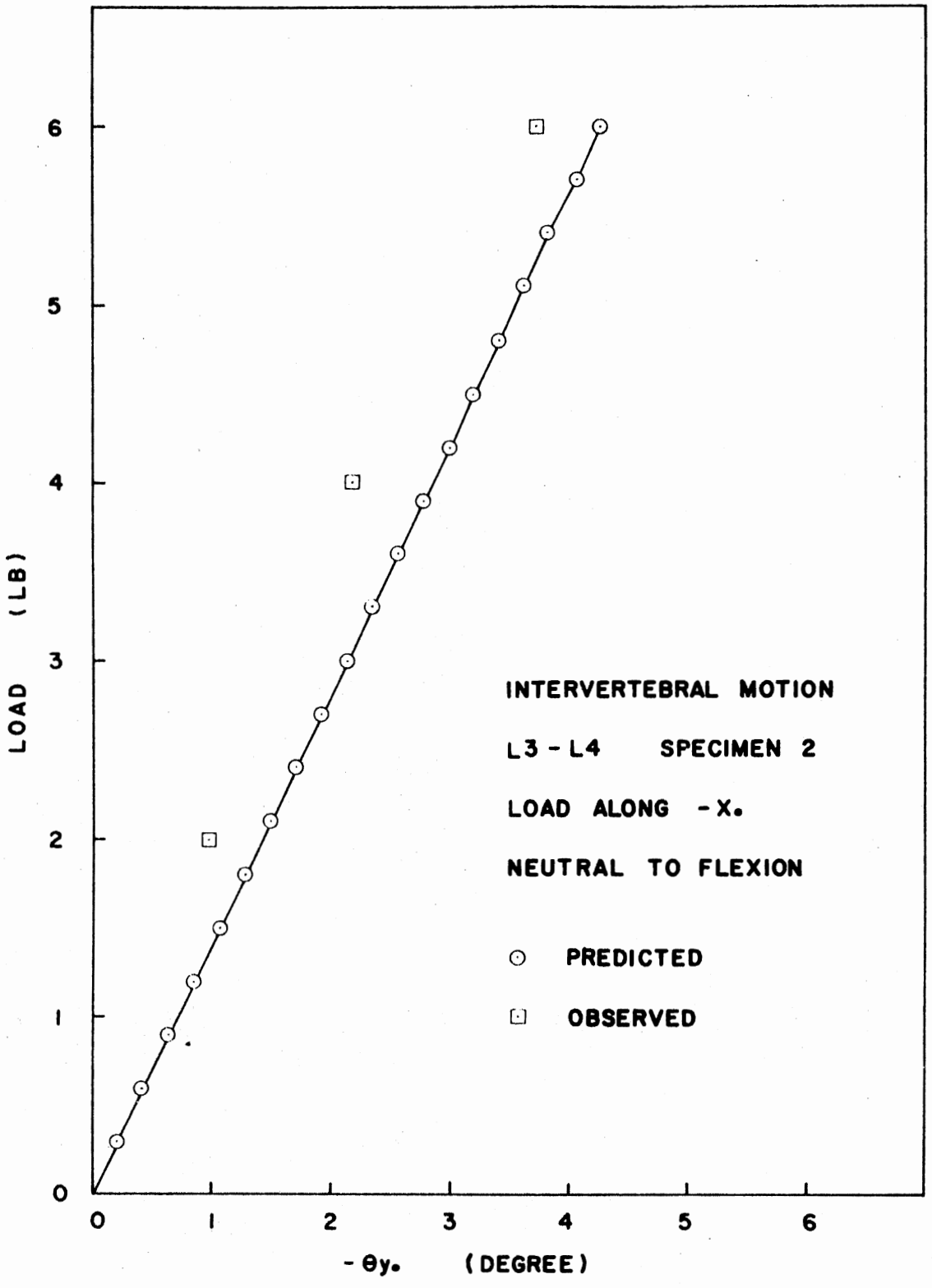

(e) L3-L4, Specimen 2

Figure 17. (Continued)

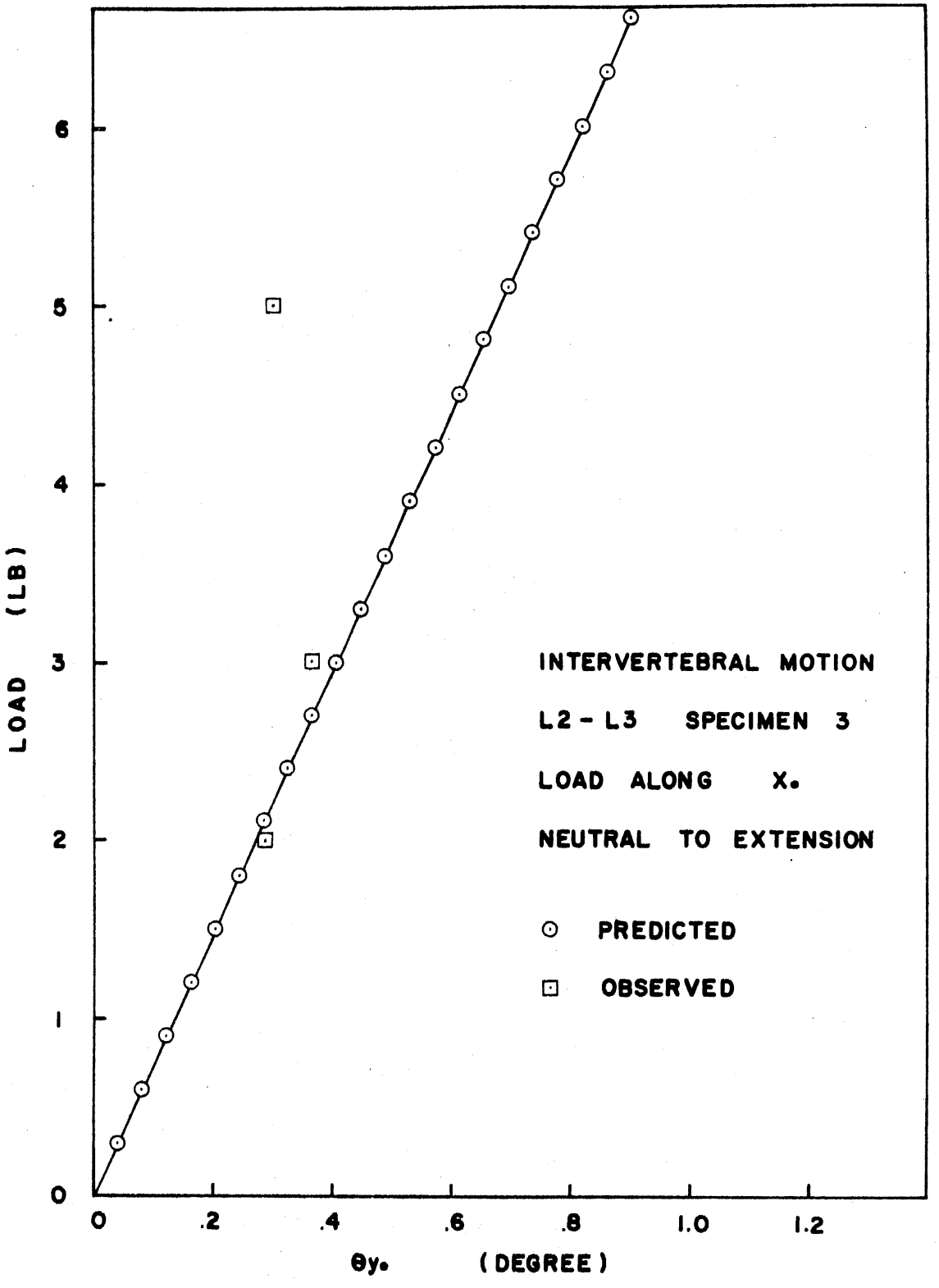

(f) L2-L3, Specimen 3

Figure 17. (Continued)

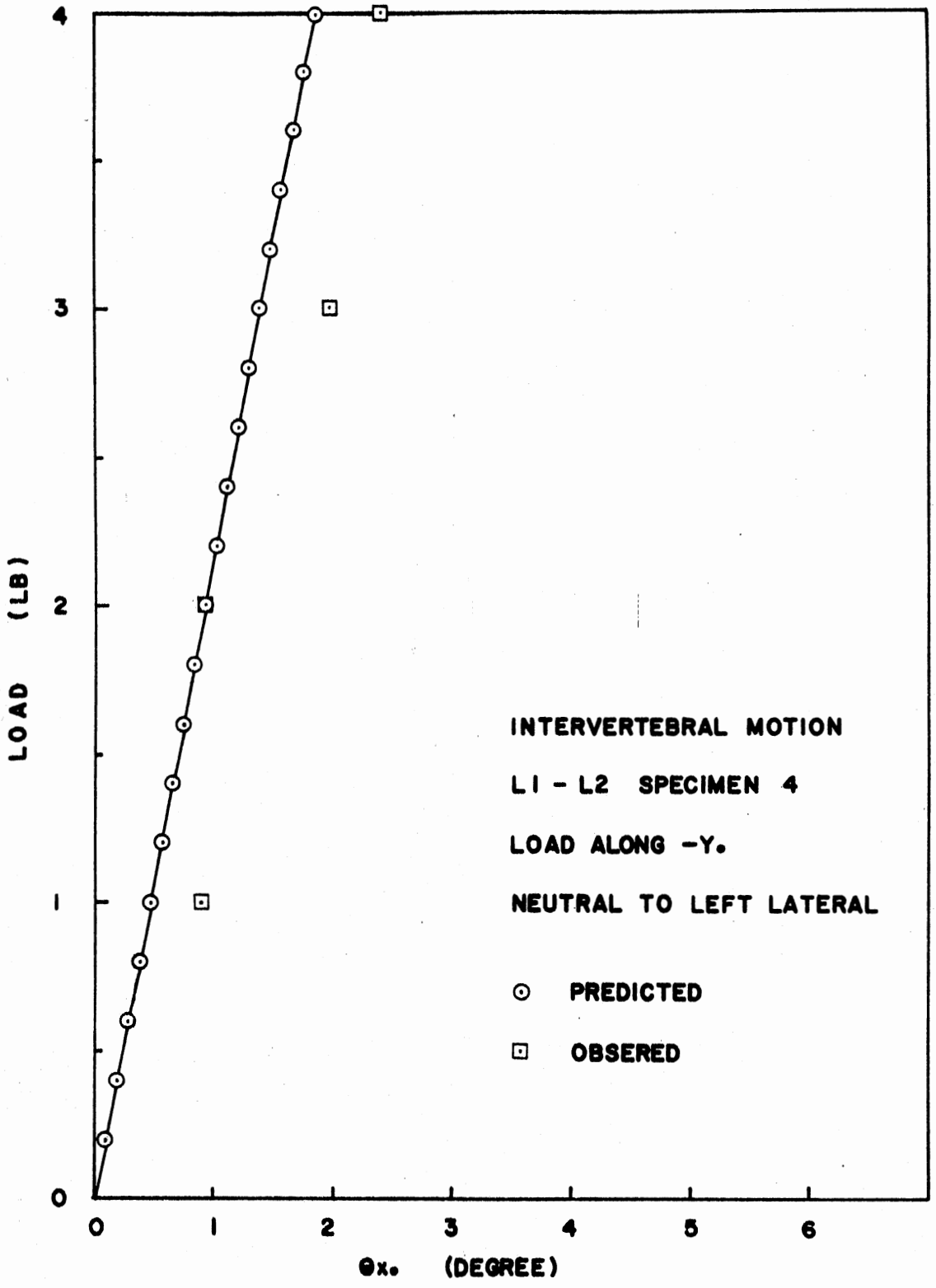

(g) L1-L2, Specimen 4

Figure 17. (Continued)

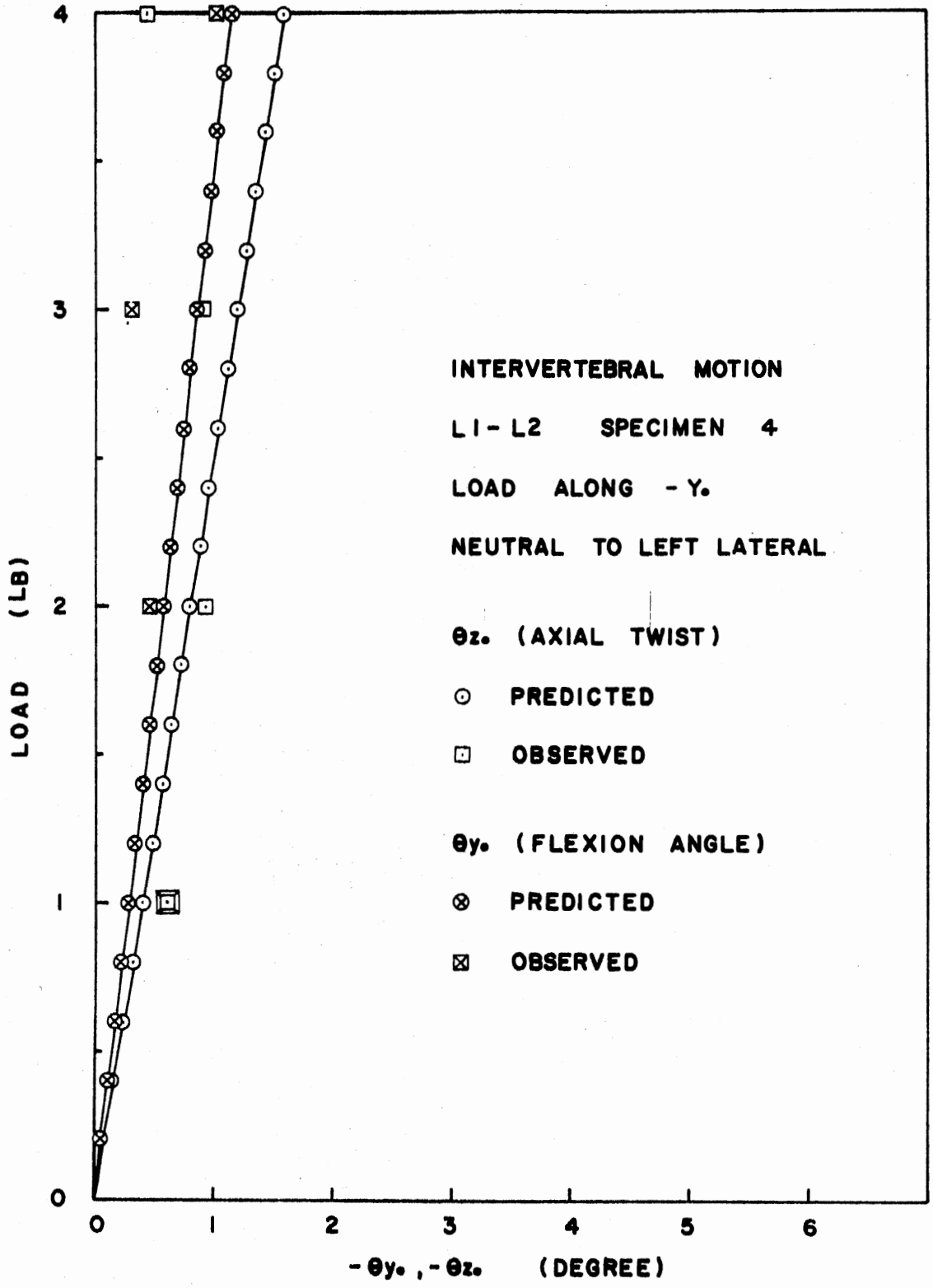

(h) L1-L2, Specimen 4

Figure 17. (Continued)

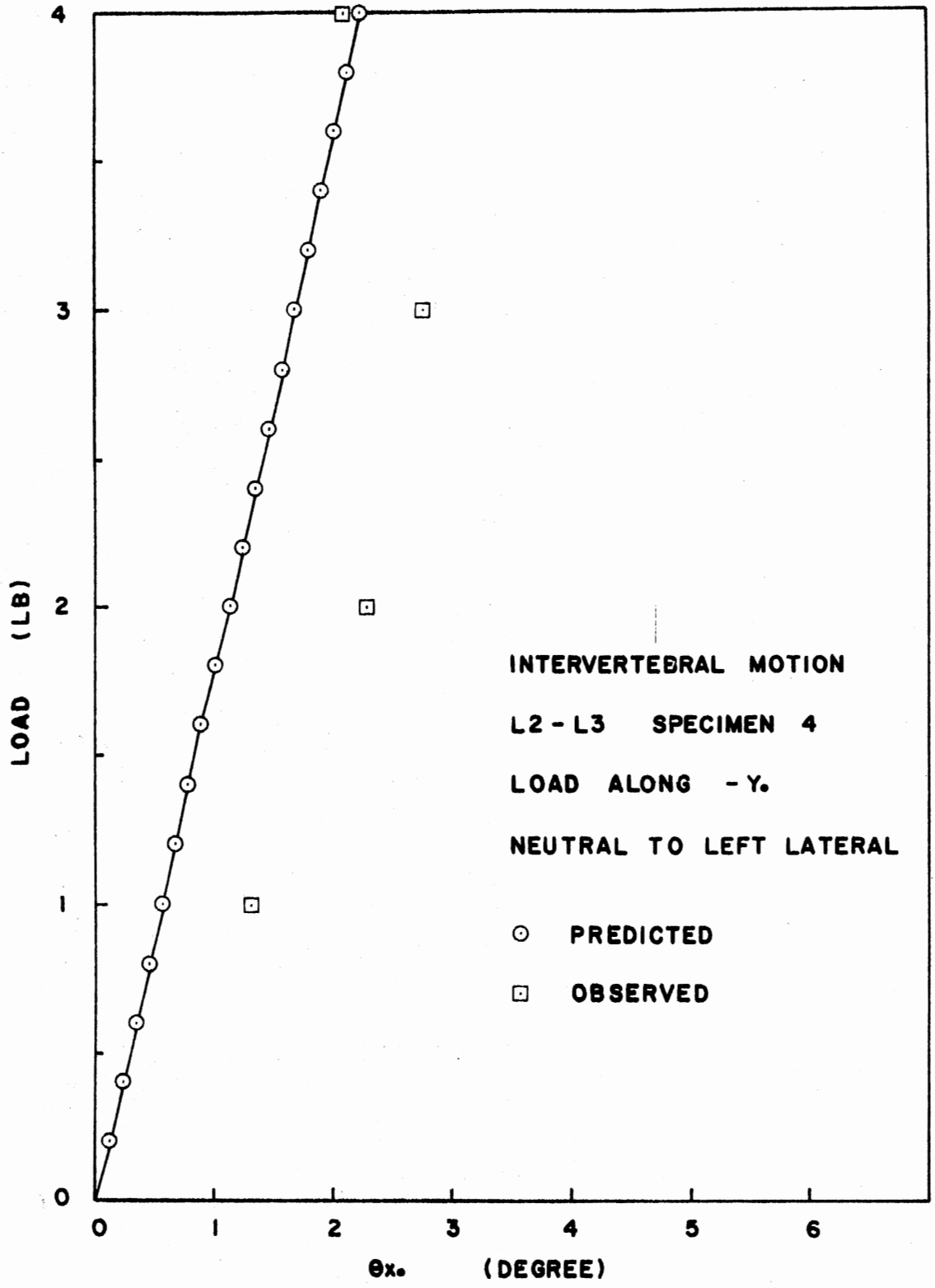

(i) L2-L3, Specimen 4

Figure 17. (Continued)

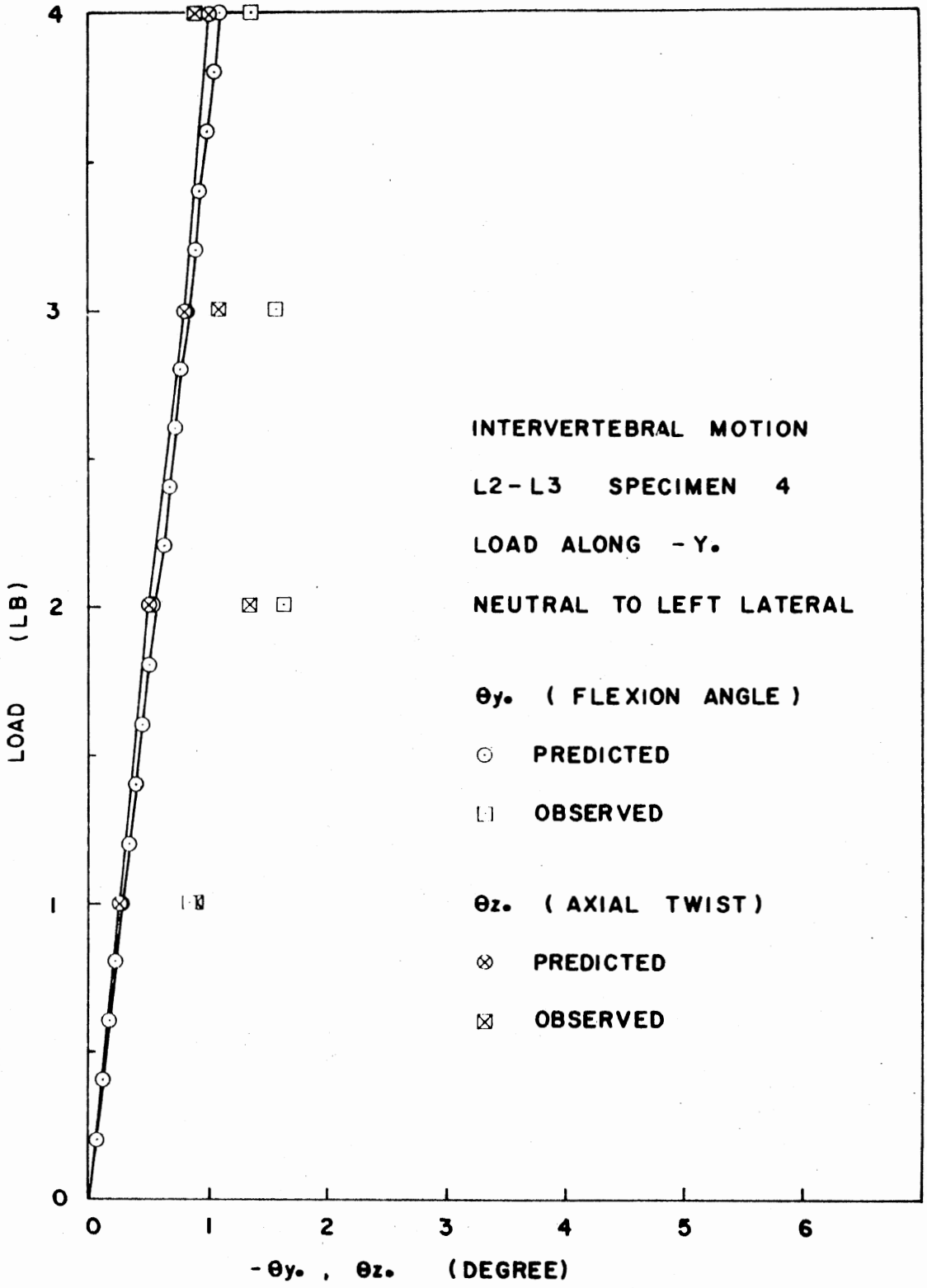

(j) L2-L3, Specimen 4

Figure 17. (Continued)

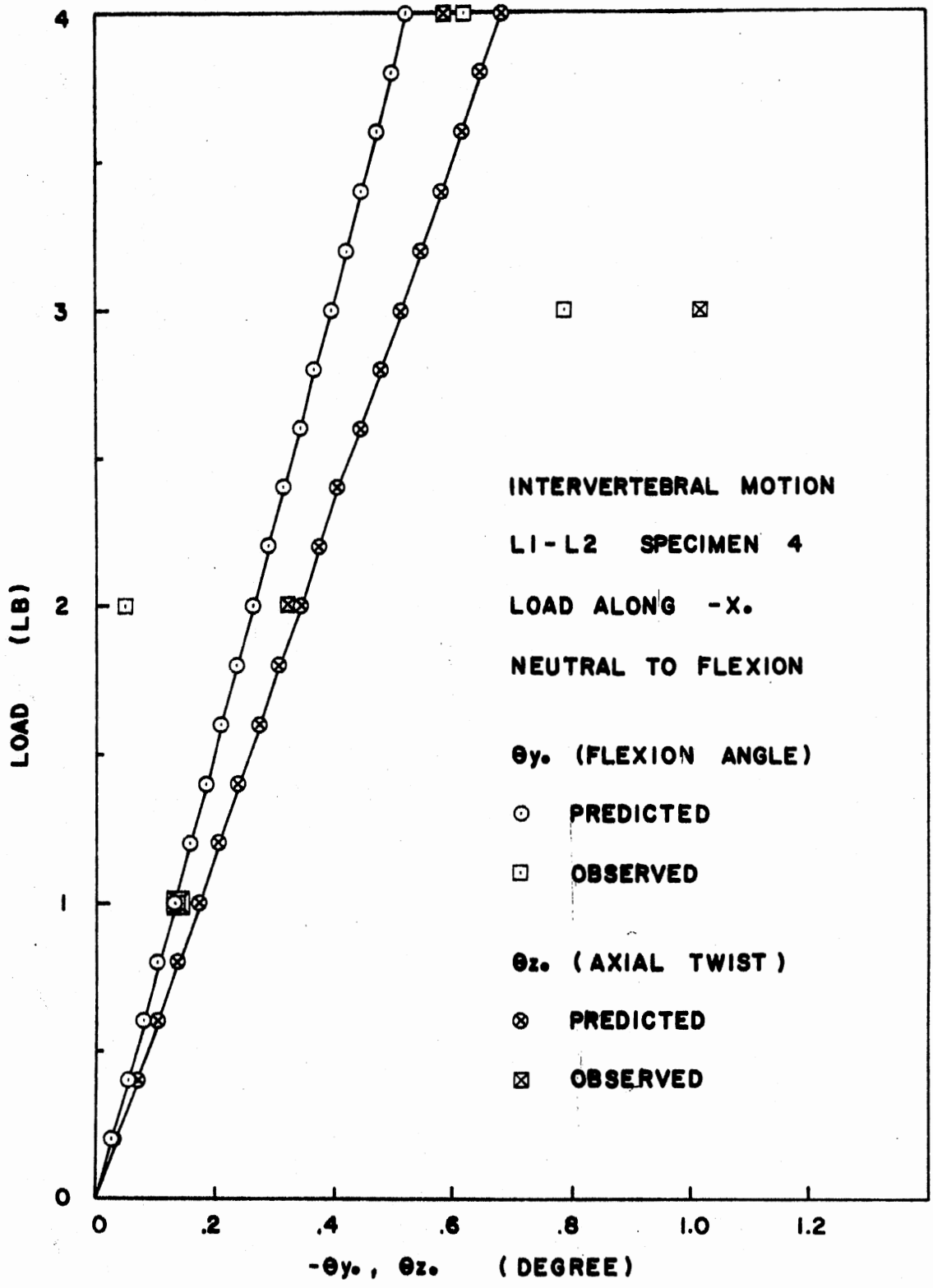

(k) L1-L2, Specimen 4

Figure 17. (Continued)

the equilibrium configuration of the intervertebral joints. The sources of errors in the observed response are:

1. Limited resolution of the rotary potentiometers to measure small rotations.

2. Errors in measuring the parameters (α_i, a_i, S_i) of the transducers.

3. Error in applying the external force in the desired direction.

4. Interference to the normal motion of the spine due to the linkage transducer and restraints of the loading fixture.

5. Frictional effects in the loading fixture.

6. Error in locating the anatomical frame of reference.

In predicting the response of the intervertebral joints to the external static loads, the theoretical motion simulation model uses the voltage data describing the stiffness properties of the intervertebral joint, the geometric parameters of the loading system, and the initial configuration of the intervertebral joints. The sources of errors in the predicted response are:

1. Limited resolution of the rotary potentiometers to measure small rotations.

2. Error in measuring the parameters (α_i, a_i, S_i) of the linkage transducer.

3. Error in locating the anatomical frame of reference.

4. Error in measuring the coordinates of the point of application of external forces.

5. Error in calculating the true stiffness properties of the intervertebral joints. This may be attributed to the following:

a. Error in applying the external forces in the desired direction.

b. Frictional effects in the loading fixture.

c. Interference to the normal motion of the spine due to the linkage transducer and restraints of the loading fixture.

d. Inability to eliminate completely the governing effect of facet joints on the intervertebral motion.

e. The assumption of constant stiffness coefficients for the entire range of mobility of the intervertebral joints.

f. Error in measuring the initial configuration of the intervertebral joints.

g. Error in locating the equivalent kinematic pair--the spherical joint--in the body reference of the moving vertebra. As mentioned earlier, the spherical joint is located at the apex of the least square cone which approximates the true axode of motion of the intervertebral joint. Even though the translational component of the intervertebral motion is negligibly small, the shortest distances from the apex of the least square cone to the actual screws of motion are, in general, large. The approximation involved in locating the spherical joint affects the predicted response of the intervertebral joint.

h. Numerical error introduced due to manipulating small quantities through a large number of matrix operations and transformations.

i. Error due to the iterative nature of the theoretical motion simulation model. The tolerance parameter of the simulation

model governs the number of iterations at each incremental load, thus governing the accuracy of the overall response.

The results of the simulation analysis performed in the present study are very encouraging even though they are subject to some limitations of the theoretical motion simulation model. These limitations are:

1. The motion simulation model simulates only the rotational motion components at the intervertebral joint.

2. The coefficients of the equivalent stiffness matrix between a pair of vertebrae are assumed constant over the entire range of intervertebral motion.

3. The theoretical motion simulation model in its present form can simulate the intervertebral joint with only one equivalent kinematic pair.

In spite of the above limitations of the present work, the basic methodology developed in this dissertation for the purpose of simulating the intervertebral relative motion of a spine subjected to external loads contributes significantly to the state-of-the-art in the kineto-elasto-static analysis of the human spine. The significance and potential applications of the present work are discussed in the next chapter.

CHAPTER VI

CONCLUSIONS, APPLICATIONS, AND SCOPE FOR FURTHER WORK

The present study combines the advanced kinematic theories of rigid body motion with the principles of mechanics to arrive at a rational approach to study the intervertebral motion of a human spine. The scope of the present work involved:

1. Kinematic analysis of the intervertebral relative motion, and
2. Simulation of intervertebral motion of a spine subjected to external static loads.

The kinematic analysis of intervertebral motion involved developing mathematical theories for calculating the parameters of the instantaneous screw axes of motion, the formulation of a mathematical ruled surface approximating the axode of motion, and interpolation using the axode approximation.

The simulation study involved development of a theoretical motion simulation model of a kinematically constrained elastic system, and development of a methodology to apply the theoretical model to the biological system of a human spine consisting of intervertebral joints.

The mathematical tools developed for the kineto-elasto-static analysis of intervertebral motion were then applied to the experimental data collected by testing four lumbar spine specimens consisting of vertebrae L1-L5. An experimental setup consisting of a spine fixture and

instrumented linkage transducers was used to collect the necessary data under controlled sets of conditions.

The results of this analysis have proved the validity of the theories developed in this dissertation. The present study contributes significantly to the state-of-the-art in studying the intervertebral motion of a human spine. Some of the major contributions of the present work are:

1. Development of instrumentation for collecting data describing the true three-dimensional motion of intervertebral joints.

2. Development of mathematical procedures to describe in a quantitative manner the three-dimensional motion of intervertebral joints using axode approximation.

3. Development of mathematical procedures to interpolate on the parameters of screw axes of motion using axode approximation.

4. Study of the range and pattern of motion of intervertebral joints of the human lumbar spine segment.

5. Development of a theoretical motion simulation model of a kinematically constrained open-loop elastic system.

6. Development of a rational approach to simulate the intervertebral motion of a human spine subjected to external static loads.

The methodology developed in this dissertation will permit one to:

1. Conduct a comparative study involving range and pattern of motion by age, sex, race, etc. The axode representation of the three-dimensional intervertebral motion of the human spine as developed in this work provides an absolute frame of reference for describing the intervertebral motion. The characteristic parameters of such an axode

may be used as a basis for comparison of motion characteristics of different intervertebral joints (cervical, thoracic, lumbar).

2. Study the effect of fusion of one or more intervertebral joints on the gross motion of the human spine. Since the simulation model developed in this dissertation isolates the motion characteristics of the actual joint by an equivalent kinematic pair, the parameters of this equivalent kinematic pair can be varied to simulate fusion of joints. In order to demonstrate the potential application of the theoretical motion simulation model as a research tool for studying the phenomenon of fusion, an example problem was used. Figure 18(a) shows a lumbar segment of the spine consisting of vertebral bodies L1-L5 connected to each other by spherical joints. For the purpose of demonstration, only the planar motion in the XY plane is considered. The lumbar spine segment is subjected to two external forces (simulating traction and weight of the upper body) applied to the vertebra L1. Figure 18(b) shows the successive equilibrium configuration of the lumbar segment as the spine achieves the final equilibrium configuration. Figure 18(c) through (f) shows the successive equilibrium configurations of the lumbar spine segment under the same loading conditions with one pair of vertebrae totally fused. The effect of fusing intervertebral joints at different levels on the gross motion of the spine segment is quite apparent from these figures. This example problem demonstrates the potential application of the present work in studying the abnormal motion of the human spine.

3. Study and evaluate the effectiveness of various corrective devices such as the Harington rod, the Dwyer cable, the Luque rod, or external braces in correcting the structural deformities of a scoliotic

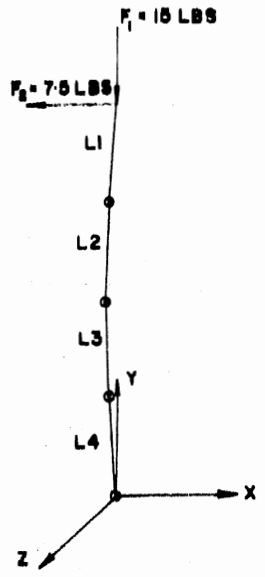

(a) Lumbar Spine Subjected to External Loads

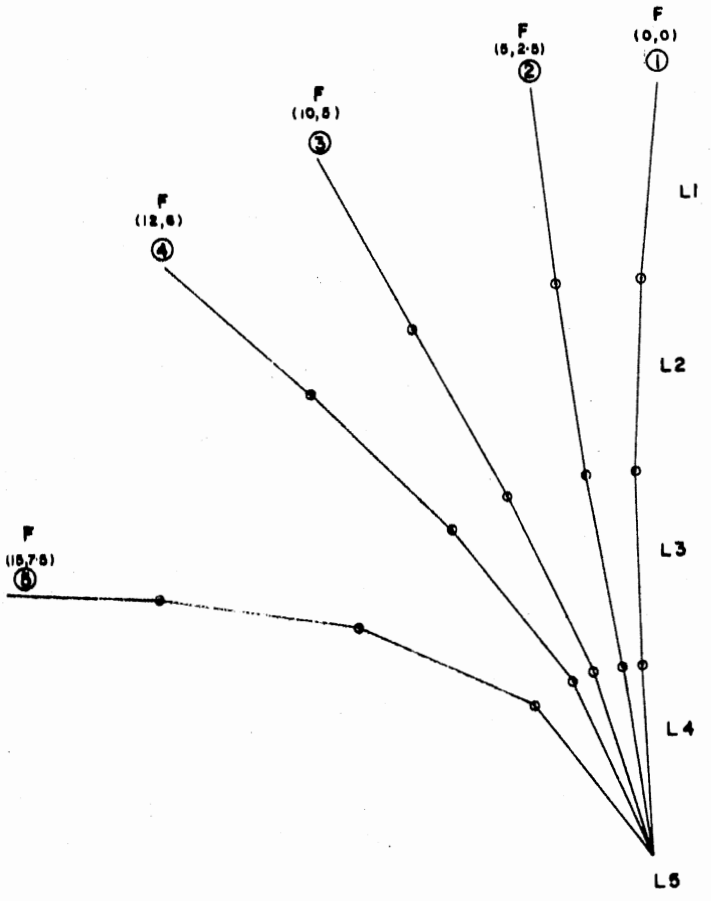

(b) Successive Equilibrium Configuration--No Fused Vertebrae

Figure 18. An Example of Vertebral Fusion

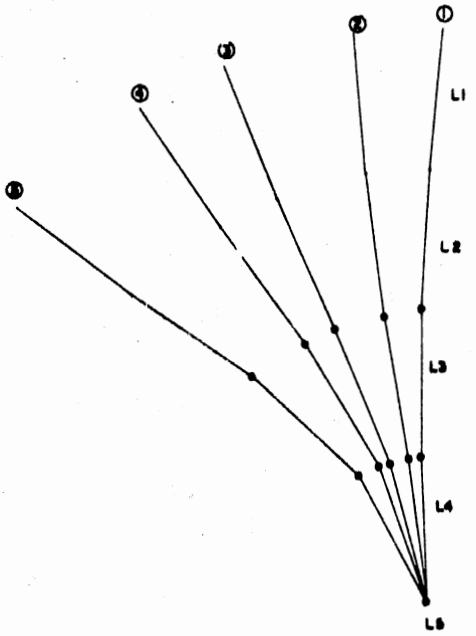

(c) Successive Equilibrium Configuration--L1-L2 Fused

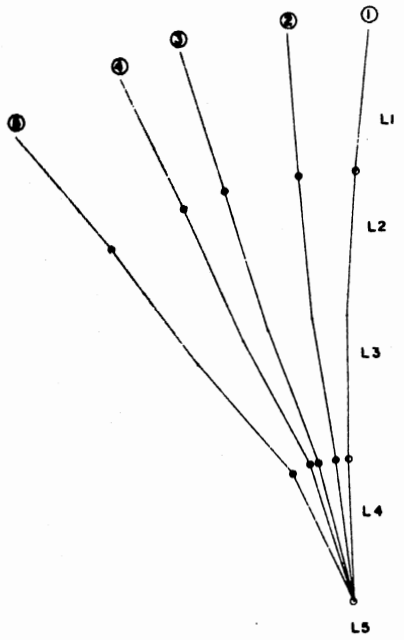

(d) Successive Equilibrium Configuration--L2-L3 Fused

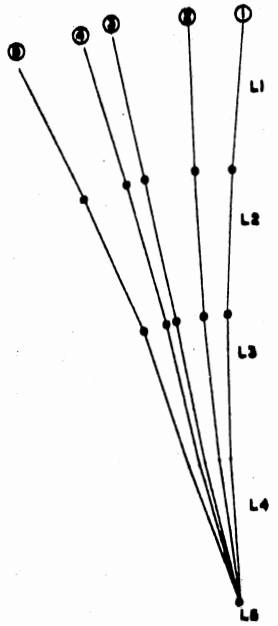

(e) Successive Equilibrium Configuration--L3-L4 Fused

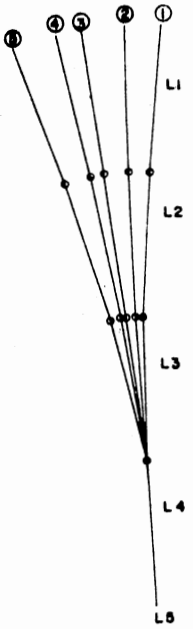

(f) Successive Equilibrium Configuration--L4-L5 Fused

Figure 18. (Continued)

spine. Such an evaluation procedure may involve experimental data collection, using the instrumentation developed in the present work, of data describing the restricted mobility of the spine due to insertion of one of the corrective devices mentioned above. The evaluation may also be done by studying the effect on the gross motion of the spine due to the different systems of forces applied by the various corrective devices. This study can be performed with the help of the motion simulation model of the spine developed in the present work.

4. Synthesize a surrogate (substitute) spine which can be used in a dummy for studying the behavior of a human body involved in a crash situation. The highway safety research institute and other research institutions involved in the "automobile-crash" study are developing tremendous amounts of data on the motion of the human spine using cadaver specimens. Such data can be used to synthesize a surrogate spine for a 95 percentile dummy. The need for the development of such a surrogate spine has been emphasized in the literature. One possible configuration of such a surrogate spine is shown in Figure 19. The present work of simulating the human spine using one equivalent kinematic pair for an intervertebral joint is a step towards the synthesis of such a surrogate spine.

Apart from the application of the present work, there is tremendous scope for doing basic research in investigating the intervertebral motion of the human spine. For example:

1. The present methodology of data collection and analysis can be extended to study the range and pattern of motion of cervical and thoracic segments of the human spine in a truly three-dimensional sense. (The methodology is quite general and can be applied to study other

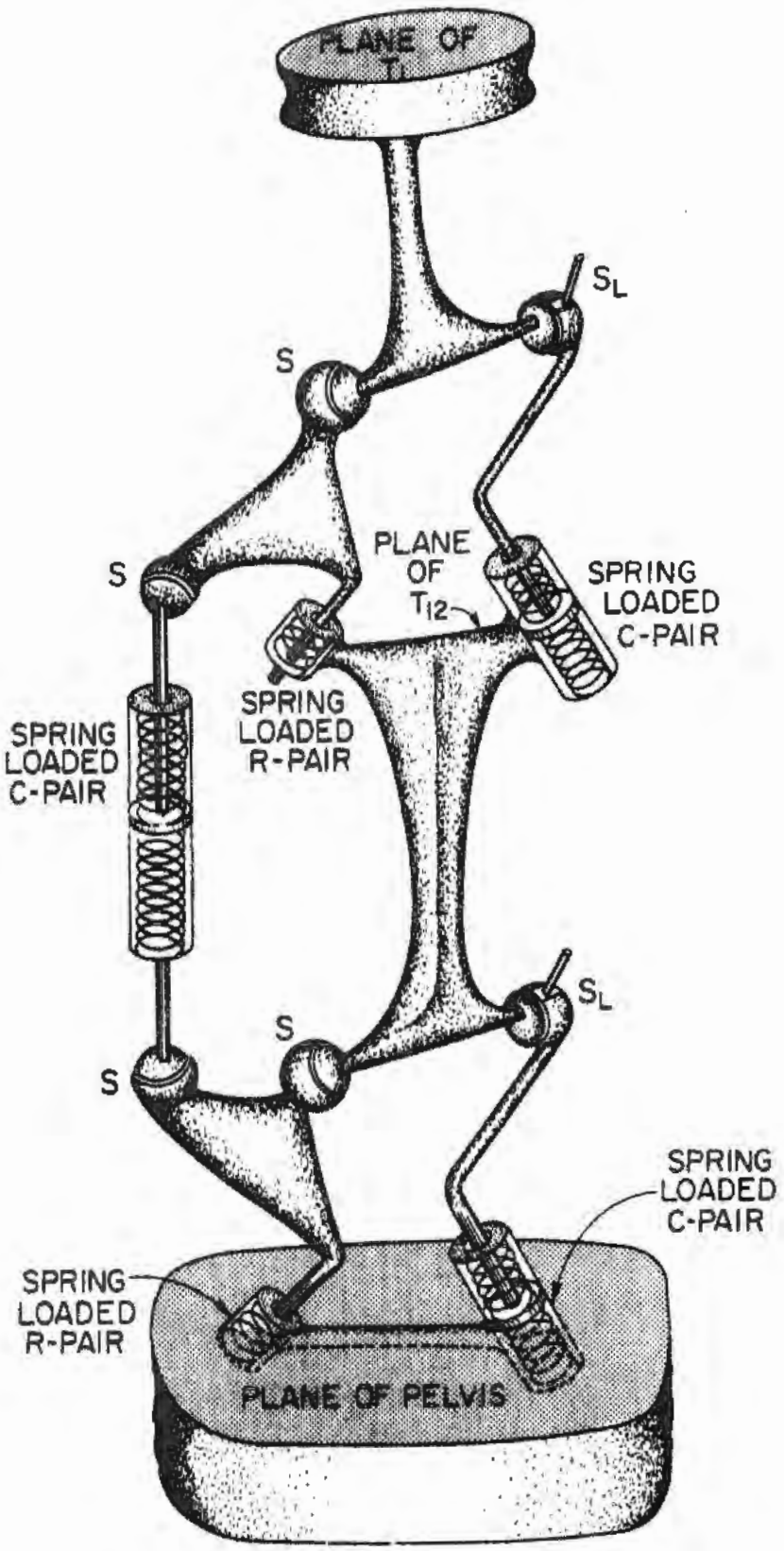

Figure 19. A Surrogate (Substitute) Spine

synovial joints such as the human knee joint, elbow joint, human jaw, etc.)

2. The existing motion simulation model of the spine can be modified to incorporate a spherical pair in combination with one or more slider pairs to simulate the true three-dimensional motion (rotational as well as translational components) of intervertebral joints.

3. The intervertebral motion of a spine can be simulated using nonlinear stiffness properties of intervertebral joints.

4. A study of different kinds of linkage transducers may be performed to investigate the sensitivity of each linkage transducer to different components of motion. The linkage transducer used in this work consisted of six rotary potentiometers. A potentiometer can be used either to measure linear displacements or angular displacements. The corresponding kinematic pairs executing linear or angular displacements are, respectively, the slider or the revolute pair. Using the criterion that the sum of the degrees of freedom of the kinematic pairs of the linkage transducer is six and that the intervertebral joint will at each instant contribute one helical pair, we find a total of 22 linkage transducers with rotary and linear potentiometers. These are schematically shown in Figure 20(a) through (v). The advantage of enumerating all possible linkage transducers is that it becomes possible to systematically search within the enumerated group for a linkage transducer which is most sensitive to a certain combination of motion components. Such a study will involve development of a rational approach and a criterion to perform the sensitivity analysis.

Some of the areas mentioned above are yet to be explored by researchers equipped with the knowledge of advanced kinematic theories.

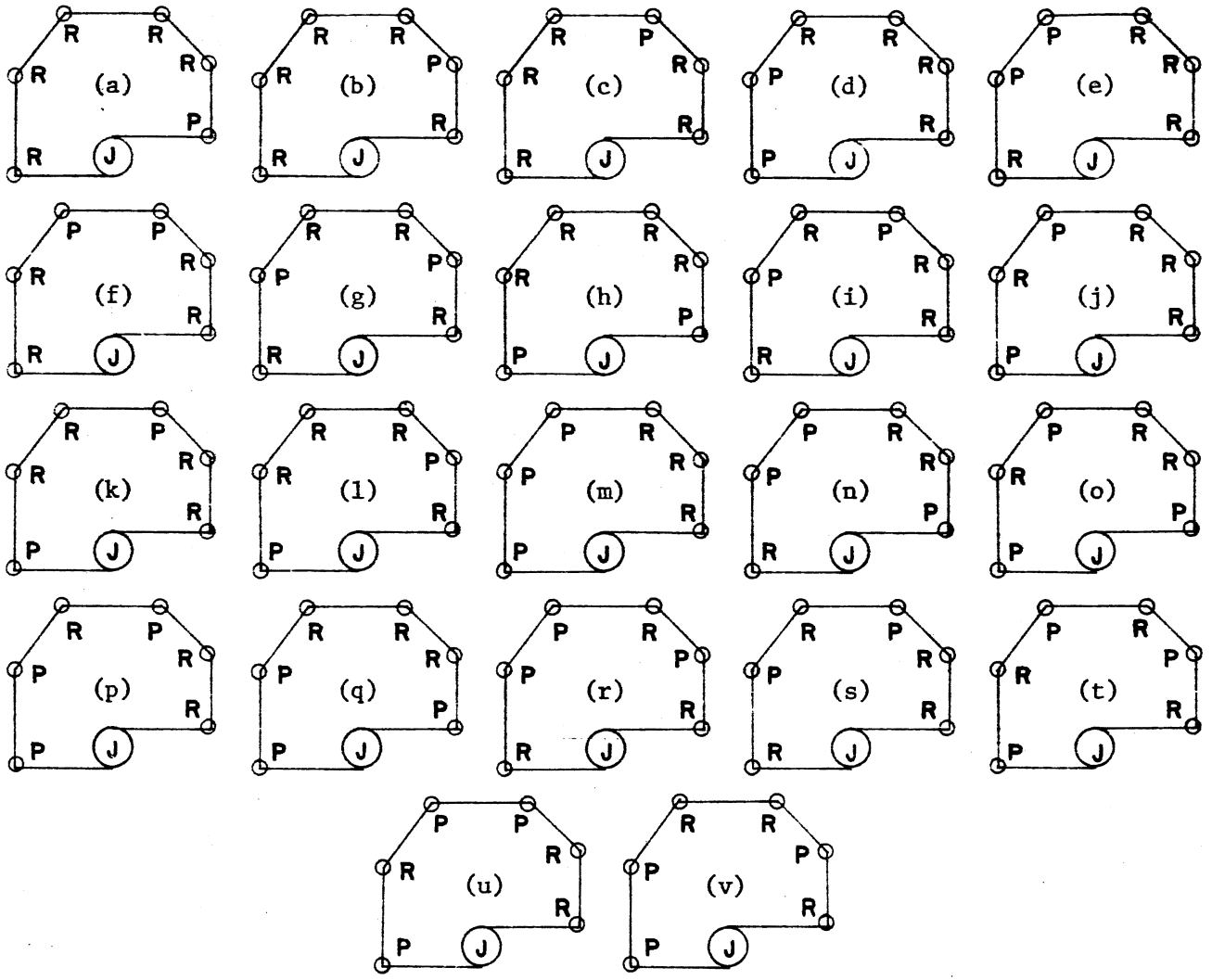

Figure 20. Different Types of Linkage Transducers

The basic and applied research activities in investigating the human spine motion will provide a better understanding of the normal as well as abnormal motion of intervertebral joints and thus will help provide better health care for every individual.

REFERENCES

[1] Elward, J. F. "Motion in the Vertebral Column." The Journal of American Roentgenography, Vol. 42 (1939), pp. 91-99.

[2] Tanz, S. S. "Motion of the Lumbar Spine." The Journal of American Roentgenography, Vol. 69, No. 3 (1953), pp. 399-412.

[3] Aho, A., O. Vartiainen, and O. Salo. "Segmentary Antero-Posterior Mobility of the Cervical Spine." Annales Medicinae Internae Fenniae, Vol. 44 (1955), pp. 287-299.

[4] Fielding, J. W. "Cineroentgenography of the Normal Cervical Spine." The Journal of Bone and Joint Surgery, Vol. 39-A, No. 6 (1957), pp. 1280-1288.

[5] Kottke, F. J., and M. O. Mundale. "Range of Mobility of the Cervical Spine." Archives of Physical Medicine, Vol. 40 (Sept., 1959), pp. 379-382.

[6] Buck, C. A., F. B. Dameron, M. J. Dow, and H. V. Skowlund. "Study of Normal Range of Motion in the Neck Utilizing a Bubble Goniometer." Archives of Physical Medicine, Vol. 40 (Sept., 1959), pp. 390-392.

[7] Hoag, J. M., M. Kosok, and J. R. Moser. "Kinematic Analysis and Classification of Vertebral Motion: Part I." Journal of the American Osteopathic Association, Vol. 59 (July, 1960), pp. 899-908.

[8] Hoag, J. M., M. Kosok, and Moser, J. R. "Kinematic Analysis and Classification of Vertebral Motion: Part II." Journal of the American Osteopathic Association, Vol. 59 (Aug., 1960), pp. 982-986.

[9] Jones, M. D. "Cineradiographic Studies of the Normal Cervical Spine." California Medicine, Vol. 93 (Nov., 1960), pp. 293-296.

[10] Rolander, S. D. "Motion of the Lumbar Spine With Special Reference to Stabilizing Effect of Posterior Fusion." Thesis. Acta Orthopaedica Scandinavica, Supplement, Vol. 90 (1960).

[11] Ferlic, D. "The Range of Motion of the 'Normal' Cervical Spine." Bulletin, Johns-Hopkins Hospital, Vol. 110 (1962), p. 59.

[12] Bennett, J. G., L. E. Bergmanis, J. K. Carpenter, and H. V. Skowlund. "Range of Motion of the Neck." Journal of the American Physical Therapy Association, Vol. 43 (Jan., 1963), pp. 45-47.

[13] Bard, G., and M. D. Jones. "Cineradiographic Recording of Traction of the Cervical Spine." Archives of Physical Medicine and Rehabilitation, Vol. 45 (Aug., 1964), pp. 403-406.

[14] Ball, J., and K. A. E. Meijers. "On Cervical Mobility." Annals of the Rheumatic Diseases, Vol. 23 (Nov., 1964), pp. 429-438.

[15] Fielding, J. W. "Normal and Selected Abnormal Motion of the Cervical Spine From the Second Cervical Vertebra to the Seventh Cervical Vertebra Based on Cineroentgenography." The Journal of Bone and Joint Surgery, Vol. 46-A, No. 8 (Dec., 1964), pp. 1779-1781.

[16] Schoening, H. A., and V. Hannan. "Factors Related to Cervical Spine Mobility: Part 1." Archives of Physical Medicine, Vol. 45 (Dec., 1964), pp. 602-609.

[17] Colachis, S. C., and B. R. Strohm. "Radiographic Studies of Cervical Spine Motion in Normal Subjects: Flexion and Hyperextension." Archives of Physical Medicine, Vol. 46 (Nov., 1965), pp. 753-760.

[18] Gregersen, G. G., and D. B. Lucas. "An In-Vivo Study of the Axial Rotation of the Human Thoracolumbar Spine." The Journal of Bone and Joint Surgery, Vol. 49-A, No. 2 (March, 1967), pp. 247-262.

[19] Loebl, W. Y. "Measurement of Spinal Posture and Range of Spinal Movement." Annals of Physical Medicine, Vol. 9 (Aug., 1967), pp. 103-110.

[20] Lumsden, R. M., and J. M. Morris. "An In-Vivo Study of Axial Rotation and Immobilization of the Lumbosacral Joint." Journal of Bone and Joint Surgery, Vol. 50-A, No. 8 (Dec., 1968), pp. 1591-1602.

[21] Lysell, E. "Motion in the Cervical Spine." Thesis. Acta Orthopaedica Scandinavica, Supplement, Vol. 123, 1969.

[22] White, A. A., III. "Analysis of the Mechanics of the Thoracic Spine in Man." Thesis, Acta Orthopaedica Scandinavica, Supplement, Vol. 127, 1969.

[23] Schultz, A. B., and J. O. Galante. "A Mathematical Model for the Study of the Mechanics of the Human Vertebral Column." Journal of Biomechanics, Vol. 3 (1970), pp. 405-416.

[24] Panjabi, M., and A. A. White, III. "A Mathematical Approach for Three-Dimensional Analysis of the Mechanics of the Spine." Journal of Biomechanics, Vol. 4 (1971), pp. 203-211.

[25] White, A. A., III. "Kinematics of the Normal Spine as Related to Scoliosis." Journal of Biomechanics, Vol. 4 (1971), pp. 405-411.

[26] Cossette, J. W., H. F. Farfan, G. H. Robertson, and R. V. Wells. "The Instantaneous Center of Rotation of the Third Lumbar Intervertebral Joint." Journal of Biomechanics, Vol. 4 (1971), pp. 149-153.

[27] Schultz, A. B., H. Larocca, J. O. Galante, and T. P. Andriacchi. "A Study of Geometrical Relationships in Scoliotic Spines." Journal of Biomechanics, Vol. 5 (1972), pp. 409-420.

[28] Baumgarten, J. R. "A Proposed Prosthesis for the Lumbar Spine." Trans., ASME, Journal of Engineering for Industry, Vol. 95, No. 3, Series B (Aug., 1973), pp. 717-720.

[29] Panjabi, M. M., A. A. White, III, and R. M. Johnson. "Cervical Spine Mechanics as a Function of Transection of Components." Journal of Biomechanics, Vol. 8 (1975), pp. 327-336.

[30] Panjabi, M. M., A. A. White, III, D. Keller, W. O. Southwick, and G. Friedlaender. "Clinical Biomechanics of the Cervical Spine." ASME Paper No. 75-WA/Bio-7, 1975.

[31] McNeice, G. M., J. Koreska, and J. Raso. "Spatial Description of the Spine in Scoliosis." Digest of the 11th International Conference on Medical and Biological Engineering, Ottawa, Canada, 1976.

[32] Schultz, A. B. "A Biomechanical View of Scoliosis." Spine, Vol. 1, No. 3 (Sept., 1976), pp. 162-171.

[33] White, A. A., III, and M. M. Panjabi. "The Clinical Biomechanics of Scoliosis." Clinical Orthopaedics and Related Research, No. 118 (July-Aug., 1976), pp. 100-112.

[34] Cobb, J. R. "The Problem of Primary Curve." The Journal of Bone and Joint Surgery, Vol. 42-A, No. 8 (Dec., 1960), pp. 1413-1425.

[35] Roaf, R. "Rotation Movements of the Spine With Special Reference to Scoliosis." The Journal of Bone and Joint Surgery, Vol. 40-B, No. 2 (May, 1958), pp. 312-332.

[36] Koogle, T. A., R. L. Piziali, D. A. Nagel, and I. Perkash. "A Motion Transducer for Use in the Intact In-Vitro Human Lumbar Spine." Personal communication from Dr. R. L. Piziali, 1977.

[37] Giantiurco, M. C. "A Roentgen Analysis of the Motion of the Lower Lumbar Vertebrae in Normal Individuals and in Patients With Low Back Pain." American Journal of Roentgenology, Vol. 52 (Sept., 1944), pp. 261-268.

[38] Rosenberg, P. "The R-Center Method: A New Method for Analyzing Vertebral Motion by X-Rays." The Journal of the American Osteopathic Association, Vol. 55 (Oct., 1955), pp. 103-111.

[39] Pennal, G. F., and G. S. Conn. "Motion Studies of Lumbar Spine." Journal of Bone and Joint Surgery, Vol. 54-B (Aug., 1972), pp. 442-452.

[40] Suh, C. H. "The Fundamentals of Computer-Aided X-Ray Analysis of the Spine." Journal of Biomechanics, Vol. 7 (1974), pp. 161-169.

[41] Messerman, T. "A Means for Studying Mandibular Movements." The Journal of Prosthetic Dentistry, Vol. 17 (1967), pp. 36-43.

[42] Knapp, F. J., B. L. Richardson, and J. Bogstad. "Study of Mandibular Motion in Six Degrees of Freedom." Journal of Dental Research, Vol. 49 (1970), pp. 289-292.

[43] Kinzel, G. L. "On the Design of Instrumented Linkages for the Measurement of Relative Motion Between Two Rigid Bodies." (Unpublished dissertation, Purdue University, 1973.)

[44] Kinzel, G. L., B. M. Hillberry, and A. S. Hall. "Measurement of the Total Motion Between Two Rigid Body Segments--I Analytical Development." Journal of Biomechanics, Vol. 5, No. 1 (Jan., 1972), pp. 93-105.

[45] Kinzel, G. L., B. M. Hillberry, A. S. Hall, D. C. Van Sickle, and W. M. Harvey. "Measurement of the Total Motion Between Body Segments--II Description of Application." Journal of Biomechanics, Vol. 5, No. 3 (May, 1972), pp. 283-293.

[46] Thompson, C. T. "A System for Determining the Spatial Motions of Arbitrary Mechanisms--Demonstrated on a Human Knee." (Unpublished dissertation, Stanford University, 1972.)

[47] Marsolais, E. G. "A Method for the Kinematic Analysis of an Inaccessible Three-Dimensional Mechanism for Application to Human Skeletal Kinesiology." ASME Paper No. 66-WA/BHF-9, 1966.

[48] Brown, R. H., A. H. Burstein, C. L. Nash, and C. C. Shock. "Spinal Analysis Using a Three-Dimensional Radiographic Technique." Journal of Biomechanics, Vol. 9 (1976), pp. 355-365.

[49] Yang, A. T., Y. Kirschorn, and B. Roth. "On a Kinematic Curvature Theory for Ruled Surfaces." Proc., Fourth World Congress on the Theory of Machines and Mechanisms, Vol. 4, New Castle upon Tyne, England, Sept., 1975, pp. 737-742.

[50] Patwardhan, A. G., and A. H. Soni. "Signature Analysis of Vertebral Motion Data in Discrete Form." Presented at the ACEMB Conference, Atlanta, Georgia, October 21-25, 1978.

[51] Soni, A. H. et al. "Instrumentation for Measuring In-Vitro 3-D Relative Motion of Inter-Vertebral Joints." Presented at the Fifth International Workshop on Human Subjects for Biomedical Research, New Orleans, Louisiana, Oct., 1977.

[52] Belytschko, T. B., T. P. Andriacchi, A. B. Schultz, and J. O. Galante. "Analog Studies of Forces in the Human Spine: Computational Techniques." Journal of Biomechanics, Vol. 6 (1973), pp. 361-371.

[53] Seireg, A., and R. Arvikar. "A Comprehensive Musculeoskeletal Model for the Human Vertebral Column." Advances in Bio-Engineering. New York: ASME, 1975.

[54] Hong, S. W., and C. H. Suh. "A Mathematical Model of the Human Spine and Its Application to the Cercial Spine." Proc., Sixth Annual Biomechanics Conference on the Spine. University of Colorado, Boulder, Colorado, December 6-7, 1975.

[55] Andriacchi, T. P., A. B. Schultz, T. B. Belytschko, and J. O. Galante. "A Model for the Studies of Mechanical Interaction Between the Human Spine and Rib Cage." Journal of Biomechanics, Vol. 7 (1974), pp. 497-507.

[56] Roberts, S. B., and P. H. Chen. "Elastostatic Analysis of the Human Thoracic Skeleton." Journal of Biomechanics, Vol. 3, No. 6 (1970), pp. 527-545.

[57] Schultz, A. B., T. B. Belytschko, T. P. Andriacchi, and J. O. Galante. "Analog Studies of Forces in the Human Spine: Mechanical Properties and Motion Segment Behavior." Journal of Biomechanics, Vol. 6 (1973), pp. 373-383.

[58] Panjabi, M. N. "Three-Dimensional Mathematical Model of the Human Spine Structure." Journal of Biomechanics, Vol. 6 (1973), pp. 671-680.

[59] Aquino, C. F. "A Dynamic Model of the Lumbar Spine." Journal of Biomechanics, Vol. 3 (1970), pp. 473-486.

[60] Prasad, P., and A. I. King. "An Experimentally Validated Dynamic Model of the Spine." Journal of Applied Mechanics, Vol. 41 (1974), pp. 546-550.

[61] Belytschko, T., L. Schwer, and E. Privitzer. "Theory and Application of a Three-Dimensional Model of the Human Spine." Symposium on Biodynamic Models and Their Applications, Dayton, Ohio, February 15-17, 1977, pp. 38-42.

[62] Arvikar, R., and A. Seireg. "A Musculoskeletal Model for Investigating Acceleration Effects on the Disc Pressures in the Human Spine in the Seated Posture." Symposium on Biodynamic Models and Their Applications, Dayton, Ohio, February 15-17, 1977, pp. 43-47.

[63] Schneider, L. W., and B. M. Bowman. "A Prediction of the Dynamic Response of the Head and Neck of Selected Military Subjects to -Gx Acceleration." Symposium on Biodynamic Models and Their Applications, Dayton, Ohio, February 15-17, 1977, pp. 87-91.

[64] Huston, J. C., C. E. Passerello, and R. L. Huston. "Numerical Prediction of Head/Neck Response to Shock-Impact." Measurement and Prediction of Structural and Biodynamic Crash-Impact Response, ASME, 1976, pp. 137-149.

[65] Martinez, J. L., and D. J. Garcia. "A Model for Whiplash." Journal of Biomechanics, Vol. 1 (1968), pp. 23-32.

[66] McKenzie, J. A., and J. F. Williams. "The Dynamic Behavior of the Head and Cervical Spine During Whiplash." Journal of Biomechanics, Vol. 4 (1971), pp. 477-490.

[67] Prasad, P., A. I. King, and C. L. Ewing. "The Role of Articular Facets During +Gz Acceleration." Trans., Journal of Applied Mechanics, ASME, Vol. 96, No. 2 (June, 1974), pp. 321-326.

[68] Orne, D., and Y. K. Liu. "A Mathematical Model of Spinal Reponse to Impact." Journal of Biomechanics, Vol. 4 (1971), pp. 49-71.

[69] "Thoracic Impact Injury Mechanism, Vol. 4." Technical Report No. DOT HS-801710, August, 1975.

[70] Payne, P. R. "Spinal Injury in Crash Environment." Paper presented at the Aircraft Crashworthiness Symposium, Cincinnati, Ohio, October 6-8, 1975.

[71] Vulcan, A. P., and A. I. King. "Forces and Moments Sustained by the Lower Vertebral Column of Seated Human During Seat-to-Head Acceleration." Dynamic Response of Biomechanical Systems. Nicholas Perrone, ed. New York: ASME, 1970, pp. 84-100.

[72] Roberts, D. B. "Intrusion of the Sternum Into the Thoracic Cavity During Frontal Chest Impact and Injury Potential." Paper presented at the Aircraft Crashworthiness Symposium, Cincinnati, Ohio, October 6-8, 1975.

[73] King, A. I. "Survey of the State of the Art of Human Biodynamic Response." Technical Report No. 6. Office of Naval Research, Structural Mechanics Program, Arlington, Virginia, 1977.

[74] Terry, C. T., and V. L. Roberts. "A Viscoelastic Model of the Human Spine Subjected to +Gz Accelerations." Journal of Biomechanics, Vol. 1 (1968), pp. 161-168.

[75] Muskin, R., and C. D. Nash, Jr. "A Model for the Response of Seated Humans to Sinusoidal Displacements of the Seat." Journal of Biomechanics, Vol. 7, No. 3 (1974), pp. 208-215.

[76] Liu, Y. King, and D. U. von Rosenberg. "The Effects of Caudocephalad (+Gz) Acceleration on the Initially Curved Human Spine." Computers in Biology and Medicine, Vol. 4 (1974), pp. 85-106.

[77] Cramer, H. J., Y. King Liu, and D. U. von Rosenberg. "A Distributed Parameter Model of the Inertially Loaded Human Spine." Journal of Biomechanics, Vol. 9 (1976), pp. 115-130.

[78] Soechting, J. F. "Response of the Human Spinal Column to Lateral Deceleration." Trans., Journal of Applied Mechanics, ASME, (Sept., 1973), pp. 643-649.

[79] Soechting, J. F., and P. R. Paslay. "A Model for the Human Spine During Impact Including Musculature Influence." Journal of Biomechanics, Vol. 6 (1973), pp. 195-203.

[80] Smith, D. E., and W. R. Anderson. "A Predictive Model of Dynamic Response of the Human Head/Neck System to -GX Impact Acceleration." Symposium on Biodynamic Models and Their Applications, Dayton, Ohio, February 15-17, 1977.

[81] Schultz, A. B., and J. O. Galante. "A Mathematical Model for the Study of the Mechanics of the Human Vertebral Column." Journal of Biomechanics, Vol. 3 (1970), pp. 405-416.

[82] Beggs, J. S. Advanced Mechanisms. New York: The Macmillan Company, 1966.

[83] Soni, A. H. Mechanism Synthesis and Analysis. New York: McGraw-Hill Book Co., 1974.

[84] Bell, R. J. An Elementary Treatise on Coordinate Geometry of Three Dimensions. 3rd ed. New York: Macmillan Co., Ltd., 1950.

APPENDIX A

LITERATURE REVIEW, TABLES IX THROUGH XIV

TABLE IX

CLASSIFICATION OF REFERENCES

Category Spinal Segment	A	B	C
Cervical	6*, 11*, 12*, 16*	3*, 4*, 5*, 9*, 13*, 14, 15*, 17*, 21, 29, 30*	
Thoracic		22, 24, 25	
		18*, 19*	
Lumbar		2*, 10*, 20*, 26, 40, 42	28
Total Spine		7*, 8*, 31, 34, 35	23, 27

*In vivo study.

Category A: Gross motion measurement with external instrumentation.

Category B: Inter-vertebral motion study:

(i) Range
(ii) Pattern of motion--qualitative and quantitative
(iii) Instantaneous center of rotation--location
(iv) Screw axis representation of three-dimensional motion
(v) Spinal segmental and gross curvature
(vi) Pattern of motion under non-normal conditions.

Category C: Mobility analysis and synthesis of motion.

TABLE X

METHODOLOGY OF EXPERIMENTAL DATA COLLECTION:
ANALYSIS AND COMPARATIVE STUDY

Investigator: Tanz (1953).

In Vivo or In Vitro: In vivo study.

Type of Data Desired: Intersegmental angular motion of lumbar spine in to-and-fro and lateral bending.

Number of Specimens or Subjects: 10 children and 45 adults chosen at random. Subjects with low back pain and suspected discs excluded.

Planes of Measurement: Sagittal and frontal plane studied.

Special Treatment of Specimen Prior to Measurement: Not stated.

Description of Apparatus: Not stated.

Location of Reference System: Not stated.

Positioning of Specimen or Subject During Measurement: Tube was centered over the fourth lumbar vertebra.

Procedure for Measurement: Roentgenograms taken in recumbent positions for to-and-fro and lateral bending.

Parameter Measured: Angle between successive vertebrae.

Sources of Error: Not stated.

Converting Measured Parameters Into Desired Data: Film in flexion and extension was superimposed to match the outline of the sacrum. In this position, a reference line was drawn. Then the two films were adjusted to match the shadows of L5. Another baseline was drawn. Repeat for all vertebrae. Angle between successive lines is intersegmental motion.

Accuracy: Results of repeated observations agreed within 2 degrees.

Hazardous Side Effects: Not stated.

TABLE X (Continued)

Investigator: Aho, Vartiainen, and Salo (1955).

In Vivo or In Vitro: In vivo study.

Type of Data Desired: Intersegmental angular measurements in flexion-extension for C1/2 - C6/7.

Number of Specimens or Subjects: 48 cervical spines were examined.

Planes of Measurement: Sagittal plane.

Special Treatment of Specimens Prior to Measurement: Patients were subjected to conventional radiography in A-P, oblique, lateral positions for radiological diagnosis of pathological symptoms. Intervertebral chondrosis was diagnosed in conjunction with functional radiography.

Description of Apparatus: Not stated.

Location of Reference System: Not stated.

Positioning of Specimen or Subject During Measurements: X-ray tube was directed invariably towards the fifth cervical vertebra.

Procedure for Measurement: Lateral x-rays taken in maximum flexion and extension.

Parameter Measured: Intersegmental angle.

Converting Measured Parameters to the Desired Data: For C1/2 segment angle measured was formed by two lines--one running from odontoid process along inferior articular surface of atlas and the other along superior articular surface of axis. Mobility of C1/2 determined by subtracting the smaller angle from the larger angle.

Sources of Error: Not stated.

Accuracy: Not stated.

Hazardous Side Effects: Not Stated.

TABLE X (Continued)

Investigator: Kottke and Mundale (1959).

In Vivo or In Vitro: In vivo study.

Type of Data Desired: Intersegmental angular displacements from the neutral position of the neck in fully flexed and extended postures.

Number of Specimens or Subjects: 87 normal males, 15 to 30 years of age.

Planes of Measurement: Sagittal plane motion.

Special Treatment of Specimens Prior to Measurement: Not stated.

Description of Apparatus: Not described.

Location of Reference System: Line of atlas from base of the tubercle anteriorly through base of the neural arch used as reference.

Positioning of Specimen or Subject During Measurements: Subject's neck positioned in (1) normal erect, (2) fully flexed, and (3) fully extended postures.

Procedure for Measurement: X-rays taken in three static postures. Lines drawn through the bases of vertebral bodies.

Parameter Measured: Intersegmental angle.

Converting Measured Parameters Into Desired Data: Angles formed by lines through the bases of bodies of lower six cervical vertebrae and the line of reference measured in flexion and extension.

Sources of Error: Not stated.

Accuracy: Intersegmental motion should and must be studied by x-rays. There is inaccuracy in the method of measurement by goniometers since the line of reference shifts giving the wong values of flexion and extension.

Hazardous Side Effects: Not stated.

TABLE X (Continued)

Investigator: Ball and Meijers (1964).

In Vivo or In Vitro: In vitro study.

Type of Data Desired: Intersegmental angular motion in flexion-extension.

Number of Specimens or Subjects: 21 autopsy specimens of cervical spine.

Planes of Measurement: Sagittal plane.

Special Treatment of Specimen Prior to Measurement: Spines were removed by separating occipital condyles from the skull with a chisel and transecting between D2 and D3. Measurements on fresh specimens were kept moist by saline. Steel pins were inserted into the anterior surface of the vertebrae bodies from C2-D1. Lines tied to arches of atlas.

Description of Apparatus: Lines attached to atlas led over a pully attached to a horizontal table. Pulley could be swung through nearly 360 degrees to change direction of load from flexion to extension.

Location of Reference System: Pin inserted into D1 was taken as reference for angular measurements.

Positioning of Specimen or Subject During Measurements: Bodies of D1 and D2 fixed in clamps so that the spine and pins lay in a horizontal plane about one inch above the surface of the table covered with graph paper.

Procedure for Measurement: Static load applied in sagittal plane. X-rays taken when spine was in extreme flexion-extension. Process of loading--x-rays done in duplicate.

Parameter Measured: Intersegmental angle.

Sources of Error: Not stated.

Converting Measured Parameters Into Desired Data: Angle subtended by a pin (say) in C6 vertebra with reference pin measured. Difference between this angle and that calculated for C7 gave movement of C6 on C7 and so on.

Accuracy: Not stated.

Hazardous Side Effects: Not stated.

TABLE X (Continued)

Investigator: Colachis and Strohm (1965).

In Vivo or In Vitro: In vivo study.

Type of Data Desired: Angular displacements of cervical spine from the neutral position.

Number of Specimens or Subjects: Ten normal subjects, age 23 to 34, with no history of neck trauma or cervical complaints.

Planes of Measurement: Sagittal plane.

Special Treatment of Specimens Prior to Measurement: Not stated.

Description of Apparatus: X-ray unit used is Swedish Dynamax 50 used only for head and neck studies.

Location of Reference System: Anterior superior apex of T1 chosen as origin.

Position of Specimen or Subject During Measurements: Subjects were seated with head at a distance of 72 inches from the unit.

Procedure for Measurement: Radiographs taken in neutral, fully flexed, and fully extended positions of the neck.

Parameters Measured: Flexion angle.

Converting Measured Parameters to the Desired Data: Each radiograph was marked with a line joining anterior inferior apex of C2 to the anterior superior apex of T1. Three radiographs were superimposed so that the three lines pivot at the reference point. Angles between lines were measured.

Sources of Error: Not stated.

Accuracy: More objective and precise method of intersegmental and gross motion measurement than the existing cineradiography technique.

Hazardous Side Effects: Not stated.

TABLE X (Continued)

Investigator: Gergersen and Lucas (1967).

In Vivo or In Vitro: In vivo study.

Type of Data Desired: Maximum axial rotation at each level of thoracolumbar spine during standing, sitting, walkine, and lateral bending.

Number of Specimens or Subjects: Seven males, age 21 to 26; no structurally fixed scoliotic curve; 34 pin studies on 17 vertebral levels.

Planes of Measurement: Horizontal plane.

Special Treatment of Specimen Prior to Measurement: Specially tip-threaded Steinmann pins, ϕ = 33 sec of an inch, length = 3.0 to 4.5 inch, inserted into spinous process by a hand drill. Lateral roentgenograms taken to confirm level of pins.

Description of Apparatus: Pelvic fixation device to secure feet, upper extremeties. Axial angular displacement transmitted to a relative rotation transducer (accurate to $\pm$0.1 degrees), then to a Honeywell 1508 visicorder to be traced on a linagraph paper to give total rotation at the pin level.

Location of Reference System: Not stated.

Position of Specimen or Subject During Measurements: During standing--placed in pelvic fixation device in erect position; bicycle seat held tightly against peninium. During sitting--placed in seated position; trunk-thigh angle = 90 degrees. During lateral bending--subject placed standing in pelvic fixation device.

Procedure for Measurement: Subject rotated several times to right and left with maximum effort. Rotation performed as in standing position. During walking subject walked on a treadmill at 4.30 kmph. Each experiment repeated several times.

Parameters Measured: Total angular rotation only in horizontal plane measured at each pin level.

Sources of Error: (1) Steinmann pins can become loose during lateral bending. (2) Individual effort is involved in the maneuvers. (3) A question arises if the motion is normal after pins are inserted.

Converting Measured Parameters Into the Desired Data: Not stated.

Accuracy: Accuracy of results to one degree. Major limitation--motion at only a few vertebrae levels was measured in any one subject.

Hazardous Side Effects: Discomfort to subject. More lasting side effects not stated.

TABLE X (Continued)

Investigator: Loebl (1967).

In Vivo or In Vitro: In vivo study.

Type of Data Desired: A quantitative measure of the curvature of a segment of the spine. Studies on dorsal and lumbar spines.

Number of Specimens or Subjects: 176 normal adults, age 15 to 84.

Planes of Measurement: Sagittal plane flexion-extension.

Special Treatment of Specimens Prior to Measurement: None.

Description of Apparatus: An inclinometer consisting of a dial marked in degrees and fixed to two buttons 9 cm apart.

Location of Reference System: Not stated.

Positioning of Specimen or Subject During Measurements: Subject standing, sitting with spine flexed maximally, and lying prone supported on elbows with spine maximally extended.

Procedure for Measurement: Skin was marked over spinal processes. When two buttons of inclinometer are held against spine markings, weighed needle remains vertical indicating the angle of spinal incline.

Parameters Measured: For a spine segment AB, the angle of spinal incline α (at A) and β (at B) were measured. These angles are formed by tangents at A and B with the vertical.

Converting Measured Parameters to Desired Data: The curvature (γ) of the spinal segment AB is calculated by: $\gamma = \alpha - \beta$.

Sources of Error: (1) Inaccuracy in marking the spinous process; (2) inaccuracy in reading the inclinometer; and (3) variation in spinal flexibility and subject cooperation.

Accuracy: In the great majority of subjects, the method is accurate to within 10 percent of the total range of movement.

Hazardous Side Effects: Not stated.

TABLE X (Continued)

Investigator: Lysell (1969).

In Vivo or In Vitro: In vitro study.

Type of Data Desired: x, y, and z coordinates of the four balls in each vertebra of the spine specimen at each increment of the motion.

Number of Specimens or Subjects: 28 cervical spines (C2 - Th 2 or 3), age 11 to 67 years. Specimens with malignant diseases and past traumatic changes excluded.

Planes of Measurement: Sagittal, frontal, and horizontal planes.

Special Treatment of Specimens Prior to Measurements: Specimen freed from surrounding musculature keeping ligaments, capsules intact, placed in air tight plastic bags and stored at -25°C. Tested at room temperature (22°C) with 100 percent R.H. In each vertebra, four steel balls (ϕ = 0.8 mm) were tested.

Description of Apparatus: Object table and Roenteg tube fixed to stand. Object table rotates about a vertical axis. Specimen can be mounted on object table in front of film holder. Two exposures can be made of the specimen in two preset positions without disturbing the film or specimen between exposures.

Location of Reference System: The two bottom vertebrae were fixed in a brass cup with plastic padding and inserted into the cavity of the object table.

Positioning of Specimen or Subject During Measurement: The sagittal plane of the specimen was made to coincide as closely to that of the primary measurement system. The specimen was in a resting position and was not affected by any loading.

Procedure for Measurement: In the sagittal plane, the specimen was moved from extreme extension to extreme flexion in ten steps and then reversed. Two exposures were made at each step. In the frontal plane, thirteen steps were required and in the horizontal plane seven steps were required.

Parameters Measured: Distances x', x", and y' (y") were measured on the film using a detailed coordinatograph and steroautograph.

Converting Measured Parameters to Desired Data: Based on geometry of the apparatus:

$$\frac{a+b/\cos\upsilon}{a-z/\cos\upsilon} = \frac{x'}{x-z\ \tan\upsilon} = \frac{y'}{y} \quad ; \quad \frac{a+b/\cos\upsilon}{a-z/\cos\upsilon} = \frac{x''}{x+z\ \tan\upsilon} = \frac{y''}{y}$$

a, b, and υ are the known geometric parameters. Coordinates x, y, and z are to be calculated.

TABLE X (Continued)

Sources of Error: (1) Center of ball did not correspond to center of image due to diffusion. (2) Measuring error of the detail coordinatograph. (3) Linear error due to dimensional instability of film. (4) Error in geometry of apparatus.

Accuracy: (1) Discrepancy did not exceed 0.01 mm. (2) Max ±0.05 mm. (3) Max ±0.15 mm. (4) Insignificant.

Hazardous Side Effects: Not stated.

TABLE X (Continued)

Investigator: McNeice (1975).

In Vivo or In Vitro: In vivo study.

Type of Data Desired: Spatial coordinates of each vertebral centroid from L5 to T1. Cervical spine is not included.

Number of Specimens or Subjects: Not stated.

Planes of Measurement: Sagittal and frontal planes.

Special Treatment of Specimens Prior to Measurement: None.

Description of Apparatus: In order to control the taking of radiographs, a special seat was constructed which has back and knee control fixtures.

Location of Reference System: Not stated.

Positioning of Specimen or Subject During Measurement: The subject is secured to the seat to provide proper positioning of pelvis while allowing a typical orientation of the spine.

Procedure for Measurement: The subject is seated on the seat as discussed and for any configuration the A.P. and lateral radiographs are taken.

Parameters Measured: x, y, and z coordinates of the centroids. The z (along the vertical axis) is measured from the lateral radiograph.

Converting Measured Parameters to Desired Data: Not stated.

Sources of Error: (1) there is a possibility of distortion error. (2) Inaccuracy in measurement from x-ray radiographs. (3) Inaccuracy in locating the actual centroid or reference point on the radiographs.

Accuracy: Accuracy* of 1/1000 of an inch in reading from radiographs. Quantitative results on accuracy of this method compared to in vitro method are not available.

Hazardous Side Effects: Not stated.

*Personal communication with the author.

TABLE X (Continued)

Investigator: Panjabi, White, Keller, Southwick, and Friedlaender (1975).

In Vivo or In Vitro: In vivo study.

Type of Data Desired: (1) Angles between two vertebrae. (2) Anterior and superior distances between two vertebrae at each load increment.

Number of Specimens or Subjects: Two cervical spines consisting of eight motion segments.

Planes of Measurement: Sagittal plane testing.

Special Treatment of Specimens Prior to Measurements: Spines were sealed in plastic bags and stored at -20°C. Thawed in water at 37°C for two hours before testing in a Plexiglas chamber with hear 100 percent R.H. at 20°C. All but a thin layer of musculature removed. Needles and balls were attached in each vertebra to serve as well defined markers for measurement.

Description of Apparatus: X-rays taken by a portable unit placed two meters away to give a magnification of 3.2 percent.

Location of Reference System: The base of the spine.

Positioning of Specimen or Subject During Measurement: Not stated.

Procedure for Measurement: The motion segments were loaded one at a time axially and x-rays were taken at each load increment after a four-minute delay to allow for creep.

Parameters Measured: Parameters mentioned in section 3 measured directly on the roentgenographs using simple tools like ruler, protractor, dial caliper, etc.

Converting Measured Parameters to Desired Data: Not stated.

Sources of Error: Not stated.

Accuracy: Sufficiently accurate measurements for clinical purposes.

Hazardous Side Effects: Not Stated.

TABLE X (Continued)

Investigator: Panjabi, White, and Johnson (1975).

In Vivo or In Vitro: In vitro study.

Type of Data Desired: (1) Rotation of the upper vertebra; (2) horizontal translation of its anterior inferior tip.

Number of Specimens or Subjects: Seventeen motion segments from eight cervical spines. Spines from patients with fractures, metabolic diseases, or tumors excluded.

Planes of Measurement: Sagittal plane.

Special Treatment of Specimens Prior to Measurements: Spine cleaned of all musculature except for small intracervical group. Sealed in plastic bag and stored at -20°C. For testing, kept in bag and thawed at 20°C, dissected into three motion segments, each tested at 20°C with 98 percent R.H. Three balls attached to upper vertebra and one ball to lower vertebra.

Description of Apparatus: Loading done by a cord going over a pulley and attached to upper vertebra. The displacements were measured by gauges with flat contacts and a least count of 0.01 mm. The pulley arrangement can be turned 180° to simulate flexion-extension.

Location of Reference System: Lower vertebrae of motion segment as origin.

Positioning of Specimen or Subject During Measurement: Lower vertebra moulded into a quick setting resin and the cast fixed to loading frame. A cord was used to apply loads perpendicular to axis of spine to create flexion-extension.

Procedure for Measurement: Load applied to upper vertebra for four minutes to achieve repeatability and a sufficient time interval permitted to allow for creep. Measurements at each stage of component transection.

Parameters Measured: Two vertical displacements and one horizontal displacement measured from three top balls. Horizontal displacement of lower ball to check rigidity of fixation.

Converting Measured Parameters to Desired Data: Rotation θ in degrees.

$$\theta = \arcsin(\Delta/A + \sin\alpha) - \alpha$$

Δ = difference in two vertical gauge readings

A and α are known geometric parameters.

Sources of Error: (1) Error in displacement gauge reading due to rotation of vertebra. Eliminated due to flat contacts with balls. (2) Effect of any movement between lower vertebra and test stand on the readings eliminated.

TABLE X (Continued)

Accuracy: Not stated.

Hazardous Side Effects: Not stated.

TABLE XI

SUMMARY OF EXPERIMENTAL INVESTIGATION INTO MOBILITY OF HUMAN SPINE
(LAST TWO DECADES)

Investigator	Methodology	Range of Motion									Comment Range of Motion	Pattern of Motion
		Sagittal			Frontal			Horizontal				
		Flexion	Extension	Total	Right Lat.	Left Lat.	Total	Right Rot.	Left Rot.	Total		
Aho et al. (1955)	48 patients were subjected to conventional and functional radiography in A-P, oblique, and lateral positions. Lateral views taken for maximum flexion and extension	Between C1-C7: 107.5°. C5/6 shows max. motion.									15 normal spines In all cases of chondrosis and osteochondrosis mobility reduced	No pathological sliding was detected between vertebrae.
Buck et al. (1959)	Direct measurement on live subjects using bubble goniometer.	69±10 66±8	81±9 73±9	150 139				73±6 72±5	74±4 74±4	147 146	Female Male Neutral position identified as natural position of head. Gross motion studied.	
Kottke et al. (1959)	In vivo study. X-rays of extreme position.	50°	45°	95°							Motion in interspace between vertebrae measured. The greatest amount in f.e. occurs between C5-C6.	In sagittal plane sliding and rotation is coupled because of diagonal inclination of apophyseal facets. Lateral bending is coupled with axial rotation.
		Total range between C1-C7 vertebrae. Range of atlantooccipital motion is 20-35 degrees.										
Jones (1960)	Cine radiographic studies of normal cervical spine on live subjects.	Greater flexion in the lower cervical region. Flexion in lower cervical region less than that for motion I.									Chin motion I Chin motion II	Studied for flexion on extension for 2 different chin motions. In flexion, rotation is coupled with forward glide.
Ferlic (1962)	Direct measurement on live subjects using shadow technique to measure angles between extreme positions.			127 ±19.5 21%			73 ±15.6 35%			142 ±17.1 20%	Range of motion decreases with age. Percent decrease with age.	

TABLE XI (Continued)

Investigator	Methodology	Range of Motion									Comment Range of Motion	Pattern of Motion
		Sagittal			Frontal			Horizontal				
		Flexion	Extension	Total	Right Lat.	Left Lat.	Total	Right Rot.	Left Rot.	Total		
Bennett et al. (1963)	Bubble goniometer used for in vivo measurement.	54.4 ±7.8 25.7 ±6.9 27.2 ±7.2	93.2 ±11.6 66.3 ±15.3 63.5 ±14.0	147.6 ±12.2 92.0 ±18.6 90.7 ±17.8				76.0 ±3.5	75.0 ±4.1	151.0 ±6.1	Also sagittal plane motion while neck was in: (1) max rt. rot., (2) max left rot. There is no correlation between total flexion-extension and total rotation.	
Schoening et al. (1964)	A goniometer used to measure angles described by a wand fixed to the occiput of live subjects.	37.1 42.0	41.6 48.7	78.7 90.7	34.9 38.5	36.9 40.8	71.8 79.3	56.6 51.7	57.1 60.1	114.7 121.8	Male Female A statistical study made to correlate the ranges to factors like age, injury, sports ability, interspace dimension, etc.	
Ball and Meijers (1964)	Autopsy segment C2-D1 was loaded in f.e. Radiographs taken in extreme position. Angles measured on radiographs between pins inserted in vertebrae bodies.	A considerable range (65.5–110.5) encountered in healthy specimens. Mobility increased after removal of p.e. Angular mobility greatest between C5–C6.									The horizontal component of movement in flexion-extension was not altered after removal of p.e.	

TABLE XI (Continued)

Investigator	Methodology	Range of Motion									Comment Range of Motion	Pattern of Motion
		Sagittal			Frontal			Horizontal				
		Flexion	Extension	Total	Right Lat.	Left Lat.	Total	Right Rot.	Left Rot.	Total		
Band and Jones (1964)	Cineradiographic study. Each patient received 30 pounds of traction in sitting position to produce approximately 10 degrees of flexion in midcervical spine.	(1) Increased mobility in 16 (out of 20) patients was evident. (2) Slight separation of vertebrae and facets at C4-C5 and C5-C6 levels was observed consistently.										Under traction, increased gliding was demonstrated between the vertebral bodies in all patients.
Colachis and Strohn (1965)	Radiographs of live subjects for neutral, fully extended, and fully flexed positions while seated. Angles calculated by superposition.	24° 21.5 mm 27.5 mm	16° 38.0 mm 18.5 mm	40° 16.5 mm 9.0 mm							Average intervertebral motion. Anterior dist. change. Posterior dist. change.	The difference in anterior and posterior heights of disc is the primary reason for the curve of the cervical spine.
		(1) Greater motion in flexion than in extension. (2) Greatest total motion occurs at C5-C6 interspace and least at C7-T1 interspace.										
Lysell (1969)	Four steel balls were inserted in each body of autopsy cervical segment. Radiographs taken for incremental motion in sagittal, frontal, and horizontal planes.	40 ±6	24 ±24	64 ±10			49° ±14			45° ±18	Large individual variation in all planes. Later segmented motion distribution studied.	Center of motion obtained for two-dimensional motions in all 3 planes. Calculated top (T) angles which are a measure of shape of course of motion of vertebrae.
		The series included various degrees of degeneration.					Combined rotation at 28° ± 8			Combined lat. flex. at 24° ±10		

TABLE XI (Continued)

Investigator	Methodology	Range of Motion									Comment Range of Motion	Pattern of Motion
		Sagittal			Frontal			Horizontal				
		Flexion	Extension	Total	Right Lat.	Left Lat.	Total	Right Rot.	Left Rot.	Total		
Panjabi, White, and Johnson (1975)	Cervical motion segments consisting of 2 adjacent vertebrae and soft tissues were loaded in f.e. using 25% body weight.	Rotation: 7.03° ± 2.28 Translation: 1.61 ± 0.66 mm Rotation: 11.00° ± 2.98 Translation: 3.34 ± 0.93 mm									Initial displacement with intact segment. Prior to failure.	Angular and translatory displacement pattern studies as a function of sequence of transection of connecting components.
Panjabi et al. (1975)	Needles and balls were attached to each vertebra of autopsy cervical specimen. Spine was loaded axially in sagittal plane with load increments. X-rays taken at each load increment. Procedure repeated with one component transected at a time.										Angular change and anterior and posterior distance changes were measured as a function of increasing axial load and transection of connecting components.	

TABLE XI (Continued)

Investigator	Methodology	Range of Motion			Comment on Range of Motion	Pattern of Motion
		Sagittal	Frontal	Horizontal		
White (1969) Two-Dimensional	Each specimen consisted of two vertebrae. Ribs and muscles removed. Under controlled environment, the segment loaded to simulate flexion, extension, lateral bending, and axial rotation under standardized loads. (Thoracic spine.)	Means of combined sagittal motion increases at more caudal levels. Removal of posterior elements causes more extension per unit force.	More frontal motion at the lowest segment than at intermediate levels.	Axial rotation decreases at more caudal levels. Removal of P.E. causes more axial rotation per unit moment.	Range of motion studied at each thoracic level under a force of 6 Kp/cm^2 or a moment of 20 Kp/cm.	1. ICR for all planes were clustered in 0.5 mm circle. 2. Removal of P.E. causes a shift in the clustered set of ICR's. 3. ICR for flexion located below those for extension. 4. ICR for left lateral bending clustered to right of midline and vice versa.
White (1969) Three-Dimensional	Specimen consisted of 6 to 8 vertebrae with ribs and muscles removed. Four steel balls were inserted into each body specimen mounted on apparatus and moved in sagittal, frontal, and horizontal plane in increments. Two x-ray radiographs taken at each increment. (Thoracic spine.)	Total 34.4° A tendency for greater sagittal motion at lower levels.	Total 52.0° No particular pattern for cephalo-caucal variation.	Total 41.1° Less axial rotation at the lower vertebral levels.	Range of motion studied at each thoracic level.	Coupling exists as rotation of body into the concavity of lateral curve. Calculation of helical screw axis of motion demonstrated.
		Summary of results of work on thoracic spine prior to White (1969) is reported in a tabular form in his thesis.				
Loebl (1967)	In vivo study on 176 subjects, age 15-84, using inclinometer. The method is accurate within 10% of total range of movement. (Thoracic and lumbar spines.)	In lumbar spine young males mean flexion-extension total is 66° and in thoracic spine is 35°.			A-P movement at dorso-lumbar junction in young adults averaged 25°.	Mean standing dorsal curvature of young males is 37°. Mean maximal curvature in extension of lumbar spine of young males is 38°.

TABLE XI (Continued)

Investigator	Methodology	Range of Motion			Comment on Range of Motion	Pattern of Motion
		Sagittal	Frontal	Horizontal		
Cassette et al. (1971)	Specimen consisted of L3 to L5 with joints intact. Imbedded in mold from inferior one-half of L4 and below. Torque applied to the free L3 vertebra in horizontal plane. Four guide wires inserted in L3 body horizontally. Pictures taken at each increment of torque.					1. Center of rotation found anterior to facet joint in the region of posterior nucleus and annulus. 2. C.O.R. moved to the side to which rotation was forced. 3. In the whole joint, C.O.R. found to be more posteriorly located than in isolated disc.
Rolander (1960)	Lumbar spine. Specimen consisted of two vertebrae with intermediate disc and ligaments intact. Muscles and fat removed. Bottom half of inferior body put in mold. Loads applied in sagittal, frontal planes. Displacement measured by gauges. Fusion simulated.	Largest change in angle of intact specimen: Flex.: max + 7.5° min + 1.1° Ext.: max - 6.3° min - 1.8°	Largest change in angle of intact specimen: Right: max + 7.6° min + 1.1° Left: max - 6.6° min - 1.2°		1. Posterior fusion provides stabilizing effect on the involved segment. 2. In case of specimens comprising of several segments, effect of fusion is noticeable in adjacent segments. 3. Healthy discs show a concentration of I.C.R. for ventroflexion in dorsal part of disc and vice versa. 4. Maximum horizontal displacement in intact specimen was less than ±2 mm. 5. Rotation in sagittal and frontal plane is nonlinear (s-shaped) function of moment and also a function of vertical force.	

TABLE XII

SUMMARY OF EXISTING MATHEMATICAL APPROACHES FOR KINEMATIC ANALYSIS OF HUMAN SPINE

Investigator	One-, Two-, or Three-Dimensional	Purpose of the Study	Type of Data Required	Methodology	Additional Comments
Schultz and Galante (1970)	Three-dimensional analysis	To study the geometry of three-dimensional motion of the spine in flexion-extension, lateral bending, and axial rotation	Spatial coordinates of six points on grounded vertebrae, body coordinates of twelve points on each moving vertebra, and body coordinates of six points on the last vertebra in the series and the anatomical lengths between point pairs	Any two adjacent vertebrae are connected by six anatomical position lengths. If the spatial description of the bottom vertebra is known and the six lengths between points pairs are specified, the spatial description of the top vertebra can be obtained using the least squared error technique	
McNeice et al. (1975)	Three-dimensional analysis	To describe the three-dimensional geometry of the spine	Three-dimensional coordinates of all vertebrae centroids and reference points. Obtained directly from A-P and lateral radiographs	A cubic spline function is fitted between two adjacent centroids. This provides the continuity requirements of both the first and second derivatives at the two junctions and also only the local sensitivity to coordinate perturbation	Geometric parameters like Cobb spatial angle, spatial kyphotic index, etc. are defined which have clinical significance in treatment of scoliosis
Panjabi and White (1971)	Three-dimensional analysis	To describe the relative motion and translation of each vertebra with respect to subjacent vertebra due to each increment of motion	Four steel balls inserted in each vertebra. The spine is moved in three planes in increments. Coordinates of these reference points in all vertebrae are obtained by two x-rays at each increment	A vector method based on the assumption of infinitesimal rotation is described which is less sensitive to the errors in the experimental data than are other existing methods like Euler's method	Also presented is the concept of screw axis of motion to describe a general body motion which is independent of the body shape or measuring points. This is proposed as a means to compare two spinal motions

TABLE XIII

COMPARISON OF AVAILABLE INSTRUMENTATION TECHNIQUES TO MEASURE IN-VITRO RELATIVE MOTION OF SYNOVIAL JOINTS

Instrumentation Technique	Components of Motion	Accuracy	Cost	Dynamic Motion Measurement	Remarks
Bubble Goniometer [1]	Intersegmental angular measurement, planar, not suitable for 3-D motion component measurement.	Inaccuracy in the method of measurement since the line of reference shifts giving wrong values of flexion, extension.		Not suitable.	
Cineradiography [16]	Qualitative description of the planar motion.	Poor resolution and accuracy in identifying the body points on film.		Can be used for measurement of planar motion.	
Bi-Planar X-rays [4, 5, 6]	Measures all six components of 3-D space motion.	Graphical inaccuracies and distortion errors.	Not economical for measurement of continuous motion where large number of x-rays are needed.	Not suitable.	Needs an elaborate setup.
Externally Applied Electronic Transducer [7, 8]	Total angular rotation only in horizontal plane measured at each pin level--single component of motion measurement.	(1) Accuracy to one degree. (2) Interference with normal mode of motion. (3) Steinmann pins can become loose during lateral bending. (4) Individual effort involved makes the measurement subjective.		Dynamic loads can loosen the Steinmann pins, causing inaccuracies in the measurement of axial rotation.	Pelvic fixation devices necessary.

TABLE XIII (Continued)

Instrumentation Technique	Components of Motion	Accuracy	Cost	Dynamic Motion Measurement	Remarks
Electromechanical Motion Transducer [9]	Measures all six components of motion.	(1) Reported errors due to long-term drift of transducer circuitry. (2) Most susceptible to errors in measurement of axial rotation and A-P displacement.		Not suitable due to inertia of the fluid columns.	Uses large liquid mercury filled tubes as strain elements.
Linkage Transducers [10-16]	Measures all six components of motion.	(1) Repetitive results can be obtained. (2) Accurate to the resolution of rotary potentiometers. (3) Rigid mounting can be achieved with ease. (4) Lightweight and no interference with the normal mode of motion. (5) Continuous data can be obtained on the relative motion.	Less expensive than the x-ray measurements.	Most suitable for dynamic motion measurement. The link-deflections due to dynamic loads are order of magnitude less than the resulting intervertebral displacements.	Needs a multi-channel voltmeter for static measurements and a voltage recorder for dynamic measurement.

TABLE XIV

BRIEF ANALYSIS OF THE MOTION SIMULATION MODELS FOR A SPINE SUBJECTED TO STATIC LOADS

Investigator	Belytschko [52]	Seireg [53]	Hong [54]	Andriacchi [55]	Roberts and Chen [56]
Scope	3-D elasto-static model of thoraco-lumbar spine	3-D model to calculate forces in muscles and reactions at intervertebral joints in static postures	3-D elasto-static model of cervical spine	3-D elasto-static model simulating thoraco-lumbar spine with sacrum, sternum, and ribs	Elasto-static finite element model to include sternum, ribs, costal cartilage, and vertebral column
Data	Each disc: axial, shear, bending and torsion stiffness. Each ligament: axial stiffness	Relative positions of all vertebrae in a given static posture	Eight reference points for 8 vertebrae; 126 spring elements for 8 discs, ligaments, facets	(1) Geometry of vertebrae, sternum, ribs, and location of CT and CV articulations (2) Ligaments and CV articulation--spring element discs, costal cartilage, CT articulation--beam element	(1) Coordinates of 169 nodal points to define thoratic cage (2) cross sectional properties of bones considering elliptic section and ideally elastic, homogeneous, and isotropic material
Simulation Procedure	(1) Equilibrium configuration found using incremental stiffness matrix approach (2) Considers nonlinearities due to large displacements	Equations of equilibrium written in terms of relative position of vertebrae, muscle forces and joint reactions, and solved using linear optimization by minimizing $U=\Sigma^{\text{muscle}}_{\text{forces}} + 4\Sigma^{\text{reaction}}_{\text{moment}} + 2\Sigma^{\text{reaction}}_{\text{forces}}$	Six equations of static equilibrium for each body under the action of external and internal forces, using finite displacement matrices. Group sequential method used	3-D motion of 39 rigid bodies with 234 degrees of freedom is represented by coupled linear equations. Model developed by Belytschko	Equations of equilibrium formulated using stiffness matrix approach. Element stiffness matrix considers axial, bending, and torsional strain energy
Validation/ Simulation Study	(1) Response to lateral loads (2) Stability under compressive loads. Vertebral rotations compared with reported results	Reaction forces at disc L3-L4 calculated for 52° forward tilt and compared with those of Nachemson	Functions of individual cervical muscles analyzed to study their effectiveness in producing specified head motion	(1) Response of rib cage to lateral and compressive loads compared with reported results (2) Additional studies on role of rib cage in bending response and stabilizing the vertebral column	
Remarks	Stiff elements placed at contact points of adjacent vertebrae to prevent motions inconsistent with facet geometry	Model does not consider the role of articular facet joints in controlling the intervertebral motion	Joints between skull-atlas, Atlas-Axis, and Axis-C modeled using nonlinear springs. Assumption of spherical motion made for articular facet joints	Articular facet joints modeled by bilinear spring elements	

APPENDIX B

DERIVATION OF SOME RELATIONSHIPS USED IN CHAPTER V

B.1 Components of a Vector Quantity Along the Axes of the $(XYZ)_{(i-1)}$ Coordinate System

Consider a vector quantity $\vec{V}$ defined in a coordinate System $(XYZ)_i$. Let the direction cosines of the axes O_iX_i, O_iY_i, O_iZ_i referred to the fixed frame of reference $X_oY_oZ_o$ be $(\ell_{o_{x_i}}, m_{o_{x_i}}, n_{o_{x_i}})$, $(\ell_{o_{y_i}}, m_{o_{y_i}}, n_{o_{y_i}})$, $(\ell_{o_{z_i}}, m_{o_{z_i}}, n_{o_{z_i}})$. If X_{i_v}, Y_{i_v}, Z_{i_v} are the components of $\vec{V}$ referred to $(XYZ)_i$, then

$$\vec{V}_i = X_{i_v}\hat{U}_{x_i} + Y_{i_v}\hat{U}_{y_i} + Z_{i_v}\hat{U}_{z_i}$$

$$= X_{i_v}(\ell_{o_{x_i}}\hat{i} + m_{o_{x_i}}\hat{j} + n_{o_{x_i}}\hat{k})$$

$$+ y_{i_v}(\ell_{o_{y_i}}\hat{i} + m_{o_{y_i}}\hat{j} + n_{o_{y_i}}\hat{k})$$

$$+ Z_{i_v}(\ell_{o_{z_i}}\hat{i} + m_{o_{z_i}}\hat{j} + n_{o_{z_i}}\hat{k})$$

where $\hat{i}$, $\hat{j}$, $\hat{k}$ are the unit vectors along the axes O_oX_o, O_oY_o, and O_oZ_o.

If $(\ell_{o_{x_{(i-1)}}}, m_{o_{x_{(i-1)}}}, n_{o_{x_{(i-1)}}})$, $(\ell_{o_{y_{(i-1)}}}, m_{o_{y_{(i-1)}}}, n_{o_{y_{(i-1)}}})$, and $(\ell_{o_{z_{(i-1)}}}, m_{o_{z_{(i-1)}}}, n_{o_{z_{(i-1)}}})$ are the direction cosines of the axes $OX_{(i-1)}$, $OY_{(i-1)}$, and $OZ_{(i-1)}$ referred to the fixed frame of reference $X_oY_oZ_o$, then

$$X_{(i-1)_{v_i}} = \hat{U}_{x_{(i-1)}} \cdot \vec{V}_i$$

$$Y_{(i-1)_{v_i}} = \hat{U}_{y_{(i-1)}} \cdot \vec{V}_i$$

$$Z_{(i-1)_{v_i}} = \hat{U}_{z_{(i-1)}} \cdot \vec{V}_i$$

which yield the following equation:

$$\zeta_{(i-1)_{v_i}} = \ell_{o\zeta_{(i-1)}} (X_{i_v} \ell_{ox_i} + Y_{i_v} \ell_{oy_i} + Z_{i_v} \ell_{oz_i})$$
$$+ m_{o\zeta_{(i-1)}} (X_{i_v} m_{ox_i} + Y_{i_v} m_{oy_i} + Z_{i_v} m_{oz_i})$$
$$+ n_{o\zeta_{(i-1)}} (X_{i_v} n_{ox_i} + Y_{i_v} n_{oy_i} + Z_{i_v} n_{oz_i})$$

where the dummy variable ζ can be replaced by X, Y, and Z successively to obtain the components of the vector quantity $\vec{V}_i$ about the axes of the coordinate system $(XYZ)_{(i-1)}$.

Using the above equation, the quantities appearing in equilibrium Equations (22) through (27) of Chapter V can be expressed in terms of the direction cosines of the axes of coordinate systems $(XYZ)_i$ and $(XYZ)_{(i-1)}$ referred to the fixed frame of reference $X_oY_oZ_o$.

B.2 Relationship Between the Direction Cosines of the Axes of Coordinate Systems $(XYZ)_i$ and $(XYZ)_{(i-1)}$ Referred to the Fixed Reference $X_oY_oZ_o$

Let $\hat{U}_{\zeta_i}$ be a unit vector along the axis ζ_i whose direction cosines referred to the fixed frame of reference are $\ell_{o\zeta_i}$, $m_{o\zeta_i}$, and $n_{o\zeta_i}$. Then,

$$\hat{U}_{\zeta_i} = \ell_{o\zeta_i} \hat{i} + m_{o\zeta_i} \hat{j} + n_{o\zeta_i} \hat{k} \qquad (46)$$

where $\hat{i}$, $\hat{j}$, k are the unit vectors along the axes OX_o, OY_o, OZ_o, respectively. The unit vector U_{ζ_i} can also be represented by its direction cosines along the axes of the coordinate system $(XYZ)_{(i-1)}$ by the following relationship.

$$\hat{U}_{\zeta_i} = \ell_{(i-1)_{\zeta_i}} \hat{U}_{x_{(i-1)}} + m_{(i-1)_{\zeta_i}} \hat{U}_{y_{(i-1)}} + n_{(i-1)_{\zeta_i}} \hat{U}_{z_{(i-1)}} \tag{47}$$

where $\hat{U}_{x_{(i-1)}}$, $\hat{U}_{y_{(i-1)}}$, and $\hat{U}_{z_{(i-1)}}$ are the unit vectors along the axes of the $(XYZ)_{(i-1)}$ reference system and satisfy the following equations.

$$\hat{U}_{x_{(i-1)}} = \ell_{o_{x_{(i-1)}}} \hat{i} + m_{o_{x_{(i-1)}}} \hat{j} + n_{o_{x_{(i-1)}}} \hat{k} \tag{48a}$$

$$\hat{U}_{y_{(i-1)}} = \ell_{o_{y_{(i-1)}}} \hat{i} + m_{o_{y_{(i-1)}}} \hat{j} + n_{o_{y_{(i-1)}}} \hat{k} \tag{48b}$$

$$\hat{U}_{z_{(i-1)}} = \ell_{o_{z_{(i-1)}}} \hat{i} + m_{o_{z_{(i-1)}}} \hat{j} + n_{o_{z_{(i-1)}}} \hat{k} \tag{48c}$$

Equations (46) through (48) yield the following relationship.

$$\ell_{o_{\zeta_i}} = \ell_{(i-1)_{\zeta_i}} \ell_{o_{x_{(i-1)}}} + m_{(i-1)_{\zeta_i}} \ell_{o_{y_{(i-1)}}} + n_{(i-1)_{\zeta_i}} \ell_{o_{z_{(i-1)}}} \tag{49a}$$

$$m_{o_{\zeta_i}} = \ell_{(i-1)_{\zeta_i}} m_{o_{x_{(i-1)}}} + m_{(i-1)_{\zeta_i}} m_{o_{y_{(i-1)}}} + n_{(i-1)_{\zeta_i}} m_{o_{z_{(i-1)}}} \tag{49b}$$

$$n_{o_{\zeta_i}} = \zeta_{(i-1)_{\zeta_i}} n_{o_{x_{(i-1)}}} + m_{(i-1)_{\zeta_i}} n_{o_{y_{(i-1)}}} + n_{(i-1)_{\zeta_i}} n_{o_{z_{(i-1)}}} \tag{49c}$$

The dummy variable ζ in Equation (49) can be replaced successively by X, Y, and Z to obtain the relationshps between the axes of the coordinate system $(XYZ)_i$ and $(XYZ)_{(i-1)}$ referred to the fixed frame of reference $X_oY_oZ_o$.

B.3 Variation in the Direction Cosines of a Line as a Function of Rotation About a Unit Vector $\hat{U}$

Consider a unit vector $\hat{R}(r_x, r_y, r_z)$ passing through the origin of a rectangular coordinate system OXYZ. If vector $\hat{R}$ is rotated through an angle ϕ about another unit vector $\hat{U}(U_x, U_y, U_z)$ which also passes through the origin O, then the components of the resultant vector $\hat{R}'(r'_x, r'_y, r'_z)$ can be expressed as [82]:

$$\begin{bmatrix} r'_x \\ r'_y \\ r'_z \end{bmatrix} = \underset{3 \times 3}{[DISP]} \begin{bmatrix} r_x \\ r_y \\ r_z \end{bmatrix}$$

where the displacement matrix is given by the matrix below. This yields the following relationships:

$$r'_x = [(1 - \cos\phi)\, U_x^2 + \cos\phi]\cdot r_x + [(1 - \cos\phi)\, U_x U_y - U_z \sin\phi]\cdot r_y + [(1 - \cos\phi)\, U_x U_z + U_y \sin\phi]\cdot r_z \tag{50}$$

$$r'_y = [(1 - \cos\phi)\, U_x U_y + U_z \sin\phi]\cdot r_x + [(1 - \cos\phi)\, U_y^2 + \cos\phi]\cdot r_y + [(1 - \cos\phi)\, U_y U_z - U_x \sin\phi]\cdot r_z \tag{51}$$

$$r'_z = [(1 - \cos\phi)\, U_x U_z - U_y \sin\phi]\cdot r_x + [(1 - \cos\phi)\, U_y U_z + U_x \sin\phi]\cdot r_y + [(1 - \cos\phi)\, U_z^2 + \cos\phi]\cdot r_z \tag{52}$$

Taking variations, with respect to ϕ, of the quantities on both sides of the equal sign in Equation (50) yields

$$[DISP] = \begin{bmatrix} \text{vers } \phi \cdot U_x^2 + \cos \phi & \text{vers } \phi \cdot U_x U_y - U_z \text{ Sin } \phi & \text{vers } \phi \, U_x U_z + U_y \sin \phi \\ \text{vers } \phi \, U_x U_y + U_z \sin \phi & \text{vers } \phi \, U_y^2 + \cos \phi & \text{vers } \phi \, U_y U_z - U_x \sin \phi \\ \text{vers } \phi \, U_x U_z - U_y \sin \phi & \text{vers } \phi \, U_y U_z + U_x \sin \phi & \text{vers } \phi \cdot U_z^2 + \cos \phi \end{bmatrix}$$

where vers $\phi = (1 - \cos \phi)$.

$$\Delta r'_x = [\sin\phi \cdot \Delta\phi \cdot U_x^2 - \sin\phi \cdot \Delta\phi] \cdot r_x$$
$$+ [\sin\phi \cdot \Delta\phi \cdot U_x \cdot U_y - U_z \cdot \cos\phi \cdot \Delta\phi]\ r_y$$
$$+ [\sin\phi \cdot \Delta\phi \cdot U_x \cdot U_z + U_y \cdot \cos\phi \cdot \Delta\phi]\ r_z$$

For the limiting case when $\phi \to 0$,

$$\Delta r_x = \Delta r'_x = -U_z \cdot r_y \cdot \Delta\phi + U_y \cdot r_z \cdot \Delta\phi$$

In the same manner, Equations (51) and (52) yield

$$\Delta r_y = U_z \cdot r_x\ \Delta\phi - U_x \cdot r_z\ \Delta\phi$$

$$\Delta r_z = -U_y \cdot r_x\ \Delta\phi + U_x \cdot r_y\ \Delta\phi$$

Since $\hat{R}$ is a unit vector, the components r_x, r_y, and r_z are the direction cosines ℓ, m, and n. Hence,

$$\Delta\ell = (-U_z \cdot m + U_y \cdot n)\ \Delta\phi \tag{53a}$$

$$\Delta m = (U_z \cdot \ell - U_x \cdot n)\ \Delta\phi \tag{53b}$$

$$\Delta n = (-U_y \cdot \ell + U_x \cdot m)\ \Delta\phi \tag{53c}$$

Equation (53) is an expression of the variations in the direction cosines of a line as a function of rotation about a unit vector $\hat{U}$.

B.4 Location of the Apex of a Least Square Cone Fitted to a Set of Screw Axes

Let $\vec{S}_i$, i = 1, n be the set of screw axes to which a least square cone is to be fitted. Let (ℓ_i, m_i, n_i) be the direction cosines of the ith screw axis, and (X_i, Y_i, Z_i) be the coordinates of a point P_i on the ith screw axis. Let P* (X*, Y*, Z*) be the apex of the least square cone. A perpendicular line drawn from point P* to the axis $\vec{S}_i$ will meet

the axis in a point P_i' $(X_i + \ell_i r_i, Y_i + m_i r_i, Z_i + n_i r_i)$, where r_i is the measure $P_i P_i'$. The distance $|\overrightarrow{P^* P_i'}|$ between the apex P^* and the screw axis $\vec{S}_i$ is the shortest distance between the apex and the screw axis. The fitting of the least square cone to the set of screw axes $\vec{S}_i$, $i = 1, n$ is done in such a manner as to minimize the sum (ε) of the squares of the shortest distances $|\overrightarrow{P^* P_i'}|$ for $i = 1, n$. Thus, the criterion for locating the apex of the least square cone is to minimize:

$$\varepsilon = \sum_{i=1}^{n} [(X_i + \ell_i r_i - X^*)^2 + (Y_i + m_i r_i - Y^*)^2 + (Z_i + n_i r_i - Z^*)^2] \qquad (54)$$

Let ℓ_i^*, m_i^*, n_i^* be the direction cosines of the perpendicular $\overrightarrow{P^* P_i'}$ drawn from the apex P^* to the screw axis $\vec{S}_i$. Then

$$\ell_i^* \propto (X_i + \ell_i r_i - X^*)$$

$$m_i^* \propto (Y_i + m_i r_i - Y^*)$$

$$n_i^* \propto (Z_i + n_i r_i - Z^*)$$

Since $\overrightarrow{P^* P_i'}$ is prependicular to the axis $\vec{S}_i$, the direction cosines satisfy the following relationships

$$\ell_i (X_i + \ell_i r_i - X^*) + m_i (Y_i + m_i r_i - Y^*) + n_i (Z_i + n_i r_i - Z^*) = 0 \qquad i = 1, n$$

This yields

$$r_i = \ell_i (X^* - X_i) + m_i (Y^* - Y_i) + n_i (Z^* - Z_i) \qquad (55)$$

The squared error ε, as defined in Equation (54), is a function of the

variables X*, Y*, Z*. In order to minimize the squared error ε, the following conditions must be satisfied.

$$\frac{\partial \varepsilon}{\partial x^*} = 0 \tag{56}$$

$$\frac{\partial \varepsilon}{\partial y^*} = 0 \tag{57}$$

$$\frac{\partial \varepsilon}{\partial z^*} = 0 \tag{58}$$

Equations (54) through (58) yield the following relationships:

$$\begin{aligned} X^* &[(\ell_i^2 - 1)^2 + (\ell_i m_i)^2 + (\ell_i n_i)^2] + Y^*[(\ell_i^2 - 1)(\ell_i m_i) \\ &+ (m_i^2 - 1)\,\ell_i m_i + (\ell_i n_i)(n_i m_i)] + Z^*\,[(\ell_i^2 - 1)(\ell_i n_i) \\ &+ (m_i n_i)(\ell_i m_i) + (n_i^2 - 1)(\ell_i n_i)] - (\ell_i^2 - 1)\,[(\ell_i^2 - 1)\,X_i \\ &+ \ell_i m_i Y_i + \ell_i n_i Z_i] - (\ell_i m_i)\,[\ell_i m_i X_i + (m_i^2 - 1)\,Y_i \\ &+ m_i n_i Z_i] - (\ell_i n_i)\,[\ell_i n_i X_i + m_i n_i Y_i + (n_i^2 - 1)\,Z_i] = 0 \end{aligned} \tag{59}$$

$$\begin{aligned} X^*\,&[(\ell_i^2 - 1)\,\ell_i m_i + \ell_i m_i\,(m_i^2 - 1) + (\ell_i n_i)(n_i m_i)] \\ &+ Y^*\,[(\ell_i m_i)^2 + (m_i^2 - 1)^2 + (n_i m_i)^2] \\ &+ Z^*\,[(\ell_i m_i)(\ell_i n_i) + (m_i n_i)(m_i^2 - 1) + (n_i^2 - 1)(n_i m_i)] \\ &- (\ell_i m_i)\,[(\ell_i^2 - 1)\,X_i + \ell_i m_i Y_i + \ell_i n_i Z_i] \\ &- (m_i^2 - 1)\,[\ell_i m_i X_i + (m_i^2 - 1)\,Y_i + m_i n_i Z_i] \\ &- (n_i m_i)\,[\ell_i n_i X_i + n_i m_i Y_i + (n_i^2 - 1)\,Z_i] = 0 \end{aligned} \tag{60}$$

$$X^* [(\ell_i^2 - 1)(\ell_i n_i) + (m_i \ell_i)(m_i n_i) + (n_i^2 - 1)\ \ell_i n_i]$$

$$+ Y^* [(\ell_i m_i)(\ell_i n_i) + (m_i^2 - 1)(m_i n_i) + (m_i n_i)(n_i^2 - 1)]$$

$$+ Z^* [(\ell_i n_i)^2 + (m_i n_i)^2 + (n_i^2 - 1)^2]$$

$$- (\ell_i n_i) [(\ell_i^2 - 1)\ X_i + \ell_i m_i Y_i + \ell_i n_i Z_i]$$

$$- (m_i n_i) [\ell_i m_i X_i + (m_i^2 - 1)\ Y_i + m_i n_i Z_i]$$

$$- (n_i^2 - 1) [\ell_i n_i X_i + n_i m_i Y_i + (n_i^2 - 1)\ Z_i] = 0 \qquad (61)$$

The coordinates X*, Y*, Z* of the apex P* of the least square cone can be obtained by solving Equations (59) through (61) simultaneously.

APPENDIX C

DEFINITION OF COEFFICIENTS IN THE EQUILIBRIUM EQUATION (42)

The force equilibrium of a body i in contact with bodies (i+1) and (i-1) as described in Chapter V can be expressed in terms of the following six equations.

$$C_{j1_i}\,\Delta R_{1_{(i-1)}} + C_{j2_i}\,\Delta R_{2_{(i-1)}} + C_{j3_i}\,\Delta R_{3_{(i-1)}} + C_{j4_i}\,\Delta R_{4_{(i-1)}}$$
$$+ C_{j5_i}\,\Delta R_{5_{(i-1)}} + C_{j6_i}\,\Delta R_{6_{(i-1)}} + C_{j7_i}\,\Delta q_{r_{(i-1)}}$$
$$+ \sum_k C_{j8_{i_k}}\,\Delta q_{\tau_{(i-1)_k}} = C_{j9_i} \qquad j = 1, 6$$

The subscript i denotes the ith body. The definitions of the coefficients in the above equations are presented below.

Equation 1: $\Sigma F_{x_{(i-1)}} = 0$:

$$\therefore C_{11_i} = 1.0$$

$$C_{12_i} = 0, \quad C_{13_i} = 0, \quad C_{14_i} = 0, \quad C_{15_i} = 0, \quad C_{16_i} = 0$$

$$C_{17_i} = -A_{S_{1_{(i-1)}}} + (-R_{1_i} + S_{1_i})(\ell_{o_{x_{(i-1)}}}\,BB_{o_{x_i}} + m_{o_{x_{(i-1)}}}\,DD_{o_{x_i}}$$
$$+ n_{o_{x_{(i-1)}}}\,FF_{o_{x_i}}) + (-R_{2_i} + S_{2_i})(\ell_{o_{x_{(i-1)}}}\,BB_{o_{y_i}}$$
$$+ m_{o_{x_{(i-1)}}}\,DD_{o_{y_i}} + n_{o_{x_{(i-1)}}}\,FF_{o_{y_i}}$$
$$+ (-R_{3_i} + S_{3_i})(\ell_{o_{x_{(i-1)}}}\,BB_{o_{z_i}} + m_{o_{x_{(i-1)}}}\,DD_{o_{z_i}}$$
$$+ n_{o_{x_{(i-1)}}}\,FF_{o_{z_i}})$$

$$C_{18_{k_i}} = -B_{S_{1_{k_{(i-1)}}}}$$

$$
\begin{aligned}
-C_{19_i} = {} & (\ell_{o_{x_{(i-1)}}} \ell_{o_{x_i}} + m_{o_{x_{(i-1)}}} m_{o_{x_i}} + n_{o_{x_{(i-1)}}} n_{o_{x_i}}) [-R_{1_i} \\
& + (A_{S_{1_i}} \Delta q_{r_i} + \sum_k (B_{S_{1_k}} \Delta q_{\tau_k})_i)] + (\ell_{o_{x_{(i-1)}}} \ell_{o_{y_i}} \\
& + m_{o_{x_{(i-1)}}} m_{o_{y_i}} + n_{o_{x_{(i-1)}}} n_{o_{y_i}}) [-\Delta R_{2_i} + A_{S_{2_i}} \Delta q_{r_i} \\
& + \sum_k (B_{S_{2_k}} \Delta q_{\tau_k})_i] + (\ell_{o_{x_{(i-1)}}} \ell_{o_{z_i}} + m_{o_{x_{(i-1)}}} m_{o_{z_i}} \\
& + n_{o_{x_{(i-1)}}} n_{o_{z_i}}) [-\Delta R_{3_i} + A_{S_{3_i}} \Delta q_{r_i} + \sum_k (B_{S_{3_k}} \Delta q_{\tau_k})_i] \\
& + \sum_k \Delta P_{k_i} [\ell_{o_{x_{(i-1)}}} \ell_{o_{p_{k_i}}} + m_{o_{x_{(i-1)}}} m_{o_{p_{k_i}}} \\
& + n_{o_{x_{(i-1)}}} n_{o_{p_{k_i}}}] + \Delta\ell_{o_{x_{(i-1)}}} [\ell_{o_{x_i}} (-R_{1_i} + S_{1_i}) \\
& + \ell_{o_{y_i}} (-R_{2_i} + S_{2_i}) + \ell_{o_{z_i}} (-R_{3_i} + S_{3_i})] \\
& + \Delta m_{o_{x_{(i-1)}}} [m_{o_{x_i}} (-R_{1_i} + S_{1_i}) + m_{o_{y_i}} (-R_{2_i} + S_{2_i}) \\
& + m_{o_{z_i}} (-R_{3_i} + S_{3_i})] + \Delta n_{o_{x_{(i-1)}}} [n_{o_{x_i}} (-R_{1_i} + S_{1_i}) \\
& + n_{o_{y_i}} (-R_{2_i} + S_{2_i}) + n_{o_{z_i}} (-R_{3_i} + S_{3_i})] \\
& + \Delta\ell_{o_{x_{(i-1)}}} (\sum_k P_k \ell_{o_{p_k}}) + \Delta m_{o_{x_{(i-1)}}} (\sum_k P_k m_{o_{p_k}}) \\
& + \Delta n_{o_{x_{(i-1)}}} (\sum_k P_k n_{o_{p_k}}) + (-R_{1_i} + S_{1_i}) (\ell_{o_{x_{(i-1)}}} AA_{o_{x_i}} \\
& + m_{o_{x_{(i-1)}}} CC_{o_{x_i}} + n_{o_{x_{(i-1)}}} EE_{o_{x_i}}) \\
& + (-R_{2_i} + S_{2_i}) (\ell_{o_{x_{(i-1)}}} AA_{o_{y_i}} + m_{o_{x_{(i-1)}}} CC_{o_{y_i}})
\end{aligned}
$$

$$+ n_{o_{x_{(i-1)}}} EE_{o_{y_i}}) + (-R_{3_i} + S_{3_i})(\ell_{o_{x_{(i-1)}}} AA_{o_{z_i}}$$

$$+ m_{o_{x_{(i-1)}}} CC_{o_{z_i}} + n_{o_{x_{(i-1)}}} EE_{o_{z_i}})$$

Equation 2: $\Sigma F_{y_{(i-1)}} = 0$:

$$C_{21_i} \Delta R_{1_{(i-1)}} + C_{22_i} \Delta R_{2_{(i-1)}} + C_{23_i} \Delta R_{3_{(i-1)}} + C_{24_i} \Delta R_{4_{(i-1)}}$$

$$+ C_{25_i} \Delta R_{5_{(i-1)}} + C_{26_i} \Delta R_{6_{(i-1)}} + C_{27_i} \Delta q_{r_{(i-1)}}$$

$$+ \sum_k (C_{28_{k_i}} \Delta q_{\tau_{k_{(i-1)}}}) = C_{29_i}$$

$$C_{21_i} = 0.0, \quad C_{22_i} = 1.0, \quad C_{23_i} = 0.0,$$

$$C_{24_i} = 0.0, \quad C_{25_i} = 0.0, \quad C_{26_i} = 0.0$$

$$C_{27_i} = -A_{S_{2_{(i-1)}}} + (-R_{1_i} + S_{1_i})(\ell_{o_{y_{(i-1)}}} BB_{o_{x_i}} + m_{o_{y_{(i-1)}}} DD_{o_{x_i}}$$

$$+ n_{o_{y_{(i-1)}}} FF_{o_{x_i}}) + (-R_{2_i} + S_{2_i})(\ell_{o_{y_{(i-1)}}} BB_{o_{y_i}}$$

$$+ m_{o_{y_{(i-1)}}} DD_{o_{y_i}} + n_{o_{y_{(i-1)}}} FF_{o_{y_i}})$$

$$+ (-R_{3_i} + S_{3_i})(\ell_{o_{y_{(i-1)}}} BB_{o_{z_i}} + m_{o_{y_{(i-1)}}} DD_{o_{z_i}}$$

$$+ n_{o_{y_{(i-1)}}} FF_{o_{z_i}})$$

$$C_{28_{k_i}} = -B_{S_{2_{k_{(i-1)}}}}$$

$$
\begin{aligned}
-C_{29_i} = {} & (\ell_{o_{y_{(i-1)}}} \ell_{o_{x_i}} + m_{o_{y_{(i-1)}}} m_{o_{x_i}} \\
& + n_{o_{y_{(i-1)}}} n_{o_{x_i}})(-\Delta R_{1_i} + \Delta S_{1_i}) + (\ell_{o_{y_{(i-1)}}} \ell_{o_{y_i}} \\
& + m_{o_{y_{(i-1)}}} m_{o_{y_i}} + n_{o_{y_{(i-1)}}} n_{o_{y_i}})(-\Delta R_{2_i} + \Delta S_{2_i}) \\
& + (\ell_{o_{y_{(i-1)}}} \ell_{o_{z_i}} + m_{o_{y_{(i-1)}}} m_{o_{z_i}} \\
& + n_{o_{y_{(i-1)}}} n_{o_{z_i}})(-\Delta R_{3_i} + \Delta S_{3_i}) + \sum_k \Delta P_k (\ell_{o_{y_{(i-1)}}} \ell o_{p_k} \\
& + m_{o_{y_{(i-1)}}} m_{o_{p_k}} + n_{o_{y_{(i-1)}}} n_{o_{p_k}}) \\
& + \Delta \ell_{o_{y_{(i-1)}}} [\ell_{o_{x_i}} (-R_{1_i} + S_{1_i}) + \ell_{o_{y_i}} (-R_{2_i} + S_{2_i}) \\
& + \ell_{o_{z_i}} (-R_{3_i} + S_{3_i}) + \Delta m_{o_{y_{(i-1)}}} [m_{o_{x_i}} (-R_{1_i} + S_{1_i}) \\
& + m_{o_{y_i}} (-R_{2_i} + S_{2_i}) + m_{o_{z_i}} (-R_{3_i} + S_{3_i})] \\
& + \Delta n_{o_{y_{(i-1)}}} [n_{o_{x_i}} (-R_{1_i} + S_{1_i}) + n_{o_{y_i}} (-R_{2_i} + S_{2_i}) \\
& + n_{o_{z_i}} (-R_{3_i} + S_{3_i})] + \Delta \ell_{o_{y_{(i-1)}}} (\sum_k P_k \ell_{o_{p_k}}) \\
& + \Delta m_{o_{y_{(i-1)}}} (\sum_k P_k m_{o_{p_k}}) + \Delta n_{o_{y_{(i-1)}}} (\sum_k P_k n_{o_{p_k}}) \\
& + (-R_{1_i} + S_{1_i})(\ell_{o_{y_{(i-1)}}} AA_{o_{x_i}} + m_{o_{y_{(i-1)}}} CC_{o_{x_i}} \\
& + n_{o_{y_{(i-1)}}} EE_{o_{x_i}}) + (-R_{2_i} + S_{2_i})(\ell_{o_{y_{(i-1)}}} AA_{o_{y_i}} \\
& + m_{o_{y_{(i-1)}}} CC_{o_{y_i}} + n_{o_{y_{(i-1)}}} EE_{o_{y_i}})
\end{aligned}
$$

$$+ (-R_{3_i} + S_{3_i})(\ell_{o_{y_{(i-1)}}} AA_{o_{z_i}} + m_{o_{y_{(i-1)}}} CC_{o_{z_i}}$$

$$+ n_{o_{y_{(i-1)}}} EE_{o_{z_i}})$$

Equation 3: $\Sigma F_{z_{(i-1)}} = 0$:

$$C_{31_i} \Delta R_{1_{(i-1)}} + C_{32_i} \Delta R_{2_{(i-1)}} + C_{33_i} \Delta R_{3_{(i-1)}} + C_{34_i} \Delta R_{4_{(i-1)}}$$

$$+ C_{35_i} \Delta R_{5_{(i-1)}} + C_{36_i} \Delta R_{6_{(i-1)}} + C_{37_i} \Delta q_{r_{(i-1)}}$$

$$+ \sum_k (C_{38_{k_i}} \Delta q_{\tau_{k_{(i-1)}}}) = C_{39_i}$$

$$C_{31_i} = 0, \quad C_{32_i} = 0, \quad C_{33_i} = 1.0,$$

$$C_{34_i} = 0, \quad C_{35_i} = 0, \quad C_{36_i} = 0$$

$$C_{37_i} = -A_{S_{3_{(i-1)}}} + (-R_{1_i} + S_{1_i})(\ell_{o_{z_{(i-1)}}} BB_{o_{x_i}} + m_{o_{z_{(i-1)}}} DD_{o_{x_i}}$$

$$+ n_{o_{z_{(i-1)}}} FF_{o_{x_i}}) + (-R_{2_i} + S_{2_i})(\ell_{o_{z_{(i-1)}}} BB_{o_{y_i}}$$

$$+ m_{o_{z_{(i-1)}}} DD_{o_{y_i}} + n_{o_{z_{(i-1)}}} FF_{o_{y_i}})$$

$$+ (-R_{3_i} + S_{3_i})(\ell_{o_{z_{(i-1)}}} BB_{o_{z_i}} + m_{o_{z_{(i-1)}}} DD_{o_{z_i}}$$

$$+ n_{o_{z_{(i-1)}}} FF_{o_{z_i}})$$

$$C_{38_{k_i}} = -B_{S_{3_{k_{(i-1)}}}}$$

$$
\begin{aligned}
-C_{39_i} = {} & (\ell_{o_{z_{(i-1)}}} \ell_{o_{x_i}} + m_{o_{z_{(i-1)}}} m_{o_{x_i}} + n_{o_{z_{(i-1)}}} n_{o_{x_i}})(-\Delta R_{1_i} \\
& + \Delta S_{1_i}) + (\ell_{o_{z_{(i-1)}}} \ell_{o_{y_i}} + m_{o_{z_{(i-1)}}} m_{o_{y_i}} \\
& + n_{o_{z_{(i-1)}}} n_{o_{y_i}})(-\Delta R_{2_i} + \Delta S_{2_i}) + (\ell_{o_{z_{(i-1)}}} \ell_{o_{z_i}} \\
& + m_{o_{z_{(i-1)}}} m_{o_{z_i}} + n_{o_{z_{(i-1)}}} n_{o_{z_i}})(-\Delta R_{3_i} + \Delta S_{3_i}) \\
& + \sum_k \Delta P_k (\ell_{o_{z_{(i-1)}}} \ell_{o_{p_k}} + m_{o_{z_{(i-1)}}} m_{o_{p_k}} + n_{o_{z_{(i-1)}}} n_{o_{p_k}}) \\
& + \Delta \ell_{o_{z_{(i-1)}}} [\ell_{o_{x_i}} (-R_{1_i} + S_{1_i}) + \ell_{o_{y_i}} (-R_{2_i} + S_{2_i}) \\
& + \ell_{o_{z_i}} (-R_{3_i} + S_{3_i})] + \Delta m_{o_{z_{(i-1)}}} [m_{o_{x_i}} (-R_{1_i} + S_{1_i}) \\
& + m_{o_{y_i}} (-R_{2_i} + S_{2_i})] + \Delta m_{o_{z_i}} (-R_{3_i} + S_{3_i}) \\
& + \Delta n_{o_{z_{(i-1)}}} [n_{o_{x_i}} (-R_{1_i} + S_{1_i}) + n_{o_{y_i}} (-R_{2_i} + S_{2_i}) \\
& + n_{o_{z_i}} (-R_{3_i} + S_{3_i})] \\
& + \Delta \ell_{o_{z_{(i-1)}}} (\sum_k P_k \ell_{o_{p_k}}) + \Delta m_{o_{z_{(i-1)}}} (\sum_k P_k m_{o_{p_k}}) \\
& + \Delta n_{o_{z_{(i-1)}}} (\sum_k P_k n_{o_{p_k}}) + (-R_{1_i} + S_{1_i})(\ell_{o_{z_{(i-1)}}} AA_{o_{x_i}} \\
& + m_{o_{z_{(i-1)}}} CC_{o_{x_i}} + n_{o_{z_{(i-1)}}} EE_{o_{x_i}}) \\
& + (-R_{2_i} + S_{2_i})(\ell_{o_{z_{(i-1)}}} AA_{o_{y_i}} + m_{o_{z_{(i-1)}}} CC_{o_{y_i}} \\
& + n_{o_{z_{(i-1)}}} EE_{o_{y_i}}) + (-R_{3_i} + S_{3_i})(\ell_{o_{z_{(i-1)}}} AA_{o_{z_i}}
\end{aligned}
$$

$$+ m_{o_{z_{(i-1)}}} CC_{o_{z_i}} + n_{o_{z_{(i-1)}}} EE_{o_{z_i}})$$

where

$$AA_{o_{\zeta_i}} = \ell_{(i-1)_{\zeta_i}} \Delta\ell_{o_{x_{(i-1)}}} + m_{(i-1)_{\zeta_i}} \Delta\ell_{o_{y_{(i-1)}}}$$

$$+ n_{(i-1)_{\zeta_i}} \Delta\ell_{o_{z_{(i-1)}}}$$

$$BB_{o_{\zeta_i}} = \ell_{o_{x_{(i-1)}}} \cdot A_{(i-1)_{\zeta_i}} + \ell_{o_{y_{(i-1)}}} B_{(i-1)_{\zeta_i}}$$

$$+ \ell_{o_{z_{(i-1)}}} C_{(i-1)_{\zeta_i}}$$

$$CC_{o_{\zeta_i}} = \ell_{(i-1)_{\zeta_i}} \Delta m_{o_{x_{(i-1)}}} + m_{(i-1)_{\zeta_i}} \Delta m_{o_{y_{(i-1)}}}$$

$$+ n_{(i-1)_{\zeta_i}} \Delta m_{o_{z_{(i-1)}}}$$

$$DD_{o_{\zeta_i}} = m_{o_{x_{(i-1)}}} \cdot A_{(i-1)_{\zeta_i}} + m_{o_{y_{(i-1)}}} B_{(i-1)_{\zeta_i}}$$

$$+ m_{o_{z_{(i-1)}}} C_{(i-1)_{\zeta_i}}$$

$$EE_{o_{\zeta_i}} = \ell_{(i-1)_{\zeta_i}} \Delta n_{o_{x_{(i-1)}}} + m_{(i-1)_{\zeta_i}} \Delta n_{o_{y_{(i-1)}}}$$

$$+ n_{(i-1)_i} \Delta n_{o_{z_{(i-1)}}}$$

$$FF_{o_{\zeta_i}} = n_{o_{x_{(i-1)}}} A_{(i-1)_{\zeta_i}} + n_{o_{y_{(i-1)}}} B_{(i-1)_{\zeta_i}}$$

$$+ n_{o_{z_{(i-1)}}} C_{(i-1)_{\zeta_i}}$$

Equation 4: $\Delta M_{x_{(i-1)}} = 0$:

$$C_{41_i} = 0.0$$

$$C_{42_i} = -Z_{(i-1)_{r1_i}}$$

$$C_{43_i} = Y_{(i-1)_{r1_i}}$$

$$C_{44_i} = 1.0$$

$$C_{45_i} = 0.0$$

$$C_{46_i} = 0.0$$

$$C_{47_i} = S_{2_{(i-1)}} BB_{o_{v_{i_z}}} + Z_{(i-1)_{v_i}} A_{S_{2_{(i-1)}}} - S_{3_{(i-1)}} BB_{o_{v_{i_y}}}$$

$$- Y_{(i-1)_{v_i}} A_{S_{3_{(i-1)}}} + \sum_k (P_{i_{k_{z_{(i-1)}}}} BB_{o_{a_{k_{i_y}}}})$$

$$- \sum_k (P_{i_{k_{y_{(i-1)}}}} BB_{o_{a_{k_{i_z}}}}) + R_{3_{(i-1)}} BB_{o_{r1_{i_y}}}$$

$$- R_{2_{(i-1)}} BB_{o_{r1_z}} + R_{i_{z_{(i-1)}}} BB_{o_{r2_{i_y}}} + Y_{(i-1)_{r2_i}} BB_{o_{R_{i_z}}}$$

$$- R_{i_{y_{(i-1)}}} BB_{o_{r2_{i_z}}} - Z_{(i-1)_{r2_i}} BB_{o_{R_{i_y}}} + S_{i_{z_{(i-1)}}} BB_{o_{r_{t_{i_y}}}}$$

$$+ Y_{(i-1)_{r_{t_i}}} BB_{o_{S_{i_z}}} - S_{i_{y_{(i-1)}}} BB_{o_{r_{t_{i_z}}}} - Z_{(i-1)_{r_{t_i}}} BB_{o_{S_{i_y}}}$$

$$- A_{S_{4_{(i-1)}}} + BB_{o_{R_{4_{i_x}}}} + BB_{o_{R_{5_{i_x}}}} + BB_{o_{R_{6_{i_x}}}} + BB_{o_{S_{4_{i_x}}}}$$

$$+ BB_{o_{S_{5_{i_x}}}} + BB_{o_{S_{6_{i_x}}}}$$

$$C_{48_{k_i}} = Z_{(i-1)_{v_i}} B_{S_{2_{(i-1)_k}}} - Y_{(i-1)_{v_i}} B_{S_{3_{(i-1)_k}}} - B_{S_{4_{(i-1)_k}}}$$

$$-C_{49_i} = S_{2_{(i-1)}} AA_{o_{v_{i_z}}} - S_{3_{(i-1)}} AA_{o_{v_{i_y}}}$$

$$+ \sum_k \left(Y_{(i-1)_{a_{k_i}}} \Delta P_{i_{k_{z_{(i-1)}}}} + \sum_k \left(P_{i_{k_{z_{(i-1)}}}} AA_{o_{a_{k_{i_y}}}}\right)\right.$$

$$- \sum_k \left(Z_{(i-1)_{a_{k_i}}} \Delta P_{i_{k_{y_{(i-1)}}}}\right) - \sum_k \left(P_{i_{k_{y_{(i-1)}}}} AA_{o_{a_{k_{i_z}}}}\right)$$

$$+ R_{3_{(i-1)}} AA_{o_{r_{1_{i_y}}}} - R_{2_{(i-1)}} AA_{o_{r_{1_{i_z}}}} + R_{i_{z_{(i-1)}}} AA_{o_{r_{2_{i_y}}}}$$

$$+ Y_{(i-1)_{r_{2_i}}} AA_{o_{R_{i_z}}} - R_{i_{y_{(i-1)}}} AA_{o_{r_{2_{i_z}}}} - Z_{(i-1)_{r_{2_i}}} AA_{o_{R_{i_y}}}$$

$$+ S_{i_{z_{(i-1)}}} AA_{o_{r_{t_{i_y}}}} + Y_{(i-1)_{r_{t_i}}} AA_{o_{S_{i_z}}} - S_{i_{y_{(i-1)}}} AA_{o_{r_{t_{i_z}}}}$$

$$- Z_{(i-1)_{r_{t_i}}} AA_{o_{S_{i_y}}} + \sum_k \Delta T_{i_{k_{x_{(i-1)}}}} + AA_{o_{R_{4_{i_x}}}} + AA_{o_{R_{5_{i_x}}}}$$

$$+ AA_{o_{R_{6_{i_x}}}} + AA_{o_{S_{4_{i_x}}}} + AA_{o_{S_{5_{i_x}}}} + AA_{o_{S_{6_{i_x}}}}$$

Equation 5: $\Sigma M_{y_{(i-1)}} = 0$:

$$C_{51_i} = Z_{(i-1)_{r_{1_i}}}$$

$$C_{52_i} = 0.0$$

$$C_{53_i} = -X_{(i-1)_{r1_i}}$$

$$C_{54_i} = 0.0$$

$$C_{55_i} = 1.0$$

$$C_{56_i} = 0.0$$

$$C_{57_i} = -S1_{(i-1)}\,{}^{BB_o}v_{i_z} - Z_{(i-1)_{v_i}}\,{}^{A}S1_{(i-1)} + S3_{(i-1)}\,{}^{BB_o}v_{i_x}$$
$$+ X_{(i-1)_{v_i}}\,{}^{A}S3_{(i-1)} - \sum_k P_{i_{k_{z_{(i-1)}}}}\,{}^{BB_o}a_{k_{i_x}}$$
$$+ \sum_k P_{i_{k_{x_{(i-1)}}}}\,{}^{BB_o}a_{k_{i_z}} - R3_{(i-1)}\,{}^{BB_o}r1_{i_x}$$
$$+ R1_{(i-1)}\,{}^{BB_o}r1_{i_z} + R_{i_{z_{(i-1)}}}\,{}^{BB_o}r2_{i_x} + X_{(i-1)_{r2_i}}\,{}^{BB_o}R_{i_z}$$
$$+ R_{i_{x_{(i-1)}}}\,{}^{BB_o}r2_{i_z} + Z_{(i-1)_{r2_i}}\,{}^{BB_o}R_{i_x} - X_{(i-1)_{r_{t_i}}}\,{}^{BB_o}S_{i_z}$$
$$- S_{i_{z_{(i-1)}}}\,{}^{BB_o}r_{t_{i_x}} + Z_{(i-1)_{r_{t_i}}}\,{}^{BB_o}S_{i_x} + S_{i_{x_{(i-1)}}}\,{}^{BB_o}r_{t_{i_z}}$$
$$- A_{S5_{(i-1)}} + {}^{BB_o}R4_{i_y} + {}^{BB_o}R5_{i_y} + {}^{BB_o}R6_{i_y} + {}^{BB_o}S4_{i_y}$$
$$+ {}^{BB_o}S5_{i_y} + {}^{BB_o}S6_{i_y}$$

$$C_{58_{k_i}} = -Z_{(i-1)_{v_i}}\,{}^{B}S1_{(i-1)_k} + X_{(i-1)_{v_i}}\,{}^{B}S3_{(i-1)_k} - {}^{B}S5_{(i-1)_k}$$

$$-C_{59_i} = -S_{1_{(i-1)}} {}^{AA_o}v_{i_z} + S_{3_{(i-1)}} {}^{AA_o}v_{i_x}$$

$$- \sum_k X_{(i-1)_{a_{k_i}}} \Delta P_{i_{k_{z_{(i-1)}}}} - \sum_k P_{i_{k_{z_{(i-1)}}}} {}^{AA_o}a_{k_{i_x}}$$

$$+ \sum_k Z_{(i-1)_{a_{k_i}}} \Delta P_{i_{k_{x_{(i-1)}}}} + \sum_k P_{i_{k_{x_{(i-1)}}}} {}^{AA_o}a_{k_{i_z}}$$

$$- R_{3_{(i-1)}} {}^{AA_o}r_{1_{i_x}} + R_{1_{(i-1)}} {}^{AA_o}r_{1_{i_z}} + R_{i_{z_{(i-1)}}} {}^{AA_o}r_{2_{i_x}}$$

$$+ X_{(i-1)_{r_{2_i}}} {}^{AA_o}R_{i_z} + R_{i_{x_{(i-1)}}} {}^{AA_o}r_{2_{i_z}} + Z_{(i-1)_{r_{2_i}}} {}^{AA_o}R_{i_x}$$

$$- X_{(i-1)_{r_{t_i}}} {}^{AA_o}S_{i_z} - S_{i_{z_{(i-1)}}} {}^{AA_o}r_{t_{i_x}} + Z_{(i-1)_{r_{t_i}}} {}^{AA_o}S_{i_x}$$

$$+ S_{i_{x_{(i-1)}}} {}^{AA_o}r_{t_{i_z}} + \sum_k \Delta T_{i_{k_{y_{(i-1)}}}} + {}^{AA_o}R_{4_{i_y}} + {}^{AA_o}R_{5_{i_y}}$$

$$+ {}^{AA_o}R_{6_{i_y}} + {}^{AA_o}S_{4_{i_y}} + {}^{AA_o}S_{5_{i_y}} + {}^{AA_o}S_{6_{i_y}}$$

Equation 6: $\Sigma M_{z_{(i-1)}} = 0$:

$$C_{61_i} = -Y_{(i-1)_{r_{1_i}}}$$

$$C_{62_i} = X_{(i-1)_{r_{1_i}}}$$

$$C_{63_i} = 0.0$$

$$C_{64_i} = 0.0$$

$$C_{65_i} = 0.0$$

$$C_{66_i} = 1.0$$

$$C_{67_i} = S_{1_{(i-1)}} {}^{BB_o v_{i_y}} + Y_{(i-1)_{v_i}} {}^{A_{S_{1_{(i-1)}}}} - S_{2_{(i-1)}} {}^{BB_o v_{i_x}}$$

$$- X_{(i-1)_{v_i}} {}^{A_{S_{2_{(i-1)}}}} + \sum_k P_{i_{k_{y_{(i-1)}}}} {}^{BB_o a_{i_{k_x}}}$$

$$- \sum_k P_{i_{k_{x_{(i-1)}}}} {}^{BB_o a_{i_{k_y}}} + R_{2_{(i-1)}} {}^{BB_o r_{1_{i_x}}}$$

$$- R_{1_{(i-1)}} {}^{BB_o r_{1_{i_y}}} + R_{i_{y_{(i-1)}}} {}^{BB_o r_{2_{i_x}}} + X_{(i-1)_{r_{2_i}}} {}^{BB_o R_{i_y}}$$

$$- R_{i_{x_{(i-1)}}} {}^{BB_o r_{2_{i_y}}} - Y_{(i-1)_{r_{2_i}}} {}^{BB_o R_{i_x}} + X_{(i-1)_{r_{t_i}}} {}^{BB_o S_{i_y}}$$

$$+ S_{i_{y_{(i-1)}}} {}^{BB_o r_{t_{i_x}}} - Y_{(i-1)_{r_{t_i}}} {}^{BB_o S_{i_x}} - S_{i_{x_{(i-1)}}} {}^{BB_o r_{t_{i_y}}}$$

$$- A_{S_{6_{(i-1)}}} + BB_o R_{4_{i_z}} + BB_o R_{5_{i_z}} + BB_o R_{6_{i_z}} + BB_o S_{4_{i_z}}$$

$$+ BB_o S_{5_{i_z}} + BB_o S_{6_{i_z}}$$

$$C_{68_{k_i}} = Y_{(i-1)_{v_i}} {}^{B_{S_{1_{(i-1)_k}}}} - X_{(i-1)_{v_i}} {}^{B_{S_{2_{(i-1)_k}}}} - B_{S_{6_{(i-1)_k}}}$$

$$-C_{69_i} = S_{1_{(i-1)}} {}^{AA_o v_{i_y}} - S_{2_{(i-1)}} {}^{AA_o v_{i_x}} + \sum_k X_{(i-1)_{a_{i_k}}} {}^{\Delta P_{i_{k_{y_{(i-1)}}}}}$$

$$+ \sum_k P_{i_{k_{y_{(i-1)}}}} {}^{AA_o a_{i_{k_x}}} - \sum_k Y_{(i-1)_{a_{i_k}}} {}^{\Delta P_{i_{k_{x_{(i-1)}}}}}$$

$$- \sum_k P_{i_{k_{x(i-1)}}} AA_{o_{a_{i_{k_y}}}} + R_{2_{(i-1)}} AA_{o_{r_{1_{i_x}}}}$$

$$- R_{1_{(i-1)}} AA_{o_{r_{1_{i_y}}}} + R_{i_{y(i-1)}} AA_{o_{r_{2_{i_x}}}} + X_{(i-1)_{r_{2_i}}} AA_{o_{R_{i_y}}}$$

$$- R_{i_{x(i-1)}} AA_{o_{r_{2_{i_y}}}} - Y_{(i-1)_{r_{2_i}}} AA_{o_{R_{i_x}}} + X_{(i-1)_{r_{t_i}}} AA_{o_{S_{i_y}}}$$

$$+ S_{i_{y(i-1)}} AA_{o_{r_{t_{i_x}}}} - Y_{(i-1)_{r_{t_i}}} AA_{o_{S_{i_x}}}$$

$$- S_{i_{x(i-1)}} AA_{o_{r_{t_{i_y}}}} + \sum_k \Delta T_{i_{k_{z(i-1)}}} + AA_{o_{R_{4_{i_z}}}} + AA_{o_{R_{5_{i_z}}}}$$

$$+ AA_{o_{R_{6_{i_z}}}} + AA_{o_{S_{4_{i_z}}}} + AA_{o_{S_{5_{i_z}}}} + AA_{o_{S_{6_{i_z}}}}$$

where

$$A_{S_r} = k_{r_{1_i}} (m_{(i-1)_{u_r}} \cdot Z_{(i-1)_{c_i}}^{(j)} - n_{(i-1)_{u_r}} \cdot Y_{(i-1)_{c_i}}^{(j)})$$

$$+ k_{r_{2_i}} (n_{(i-1)_{u_r}} \cdot X_{(i-1)_{c_i}}^{(j)} - \ell_{(i-1)_{u_r}} \cdot Z_{(i-1)_{c_i}}^{(j)})$$

$$+ k_{r_{3_i}} (\ell_{(i-1)_{u_r}} \cdot Y_{(i-1)_{c_i}}^{(j)} - m_{(i-1)_{u_r}} \cdot X_{(i-1)_{c_i}}^{(j)})$$

$$+ k_{r_{4_i}} (\ell_{(i-1)_{u_r}}) + k_{r_{5_i}} (m_{(i-1)_{u_r}}) + k_{r_{6_i}} (n_{(i-1)_{u_r}})$$

$$B_{S_{r_k}} = k_{r_{1_i}} \ell_{(i-1)_{u_{\tau_k}}} + k_{r_{2_i}} m_{(i-1)_{u_{\tau_k}}} + k_{r_{3_i}} n_{(i-1)_{u_{\tau_k}}}$$

$$X_{(i-1)_{c_i}}^{(j)} = -X_{(i-1)_{r_{l_i}}}^{(j)} + X_{(i-1)_{v_i}}^{(j)}$$

$$Y_{(i-1)_{c_i}}^{(j)} = -Y_{(i-1)_{r_{l_i}}}^{(j)} + Y_{(i-1)_{v_i}}^{(j)}$$

$$Z_{(i-1)_{c_i}}^{(j)} = -Z_{(i-1)_{r_{l_i}}}^{(j)} + Z_{(i-1)_{v_i}}^{(j)}$$

Then

$$\Delta S_{r_{(i-1)}} = \Delta q_r \cdot A_{S_r} + \sum_k \Delta q_{\tau_k} B_{S_{r_k}}$$

$$AA_{o_{v_{i_\zeta}}} = \Delta \ell_{o_{\zeta_{(i-1)}}} (X_{i_v} \ell_{o_{x_i}} + Y_{i_v} \ell_{o_{y_i}} + Z_{i_v} \ell_{o_{z_i}})$$
$$+ \Delta m_{o_{\zeta_{(i-1)}}} (X_{i_v} m_{o_{x_i}} + Y_{i_v} m_{o_{y_i}} + Z_{i_v} m_{o_{z_i}})$$
$$+ \Delta n_{o_{\zeta_{(i-1)}}} (X_{i_v} n_{o_{x_i}} + Y_{i_v} n_{o_{y_i}} + Z_{i_v} n_{o_{z_i}})$$
$$+ \ell_{o_{\zeta_{(i-1)}}} (X_{i_v} AA_{o_{x_i}} + Y_{i_v} AA_{o_{y_i}} + Z_{i_v} AA_{o_{z_i}})$$
$$+ m_{o_{\zeta_{(i-1)}}} (X_{i_v} CC_{o_{x_i}} + Y_{i_v} CC_{o_{y_i}} + Z_{i_v} CC_{o_{z_i}})$$
$$+ n_{o_{\zeta_{(i-1)}}} (X_{i_v} EE_{o_{x_i}} + Y_{i_v} EE_{o_{y_i}} + Z_{i_v} EE_{o_{z_i}})$$

$$BB_{o_{v_i}} = \ell_{o_{\zeta_{(i-1)}}} (X_{i_v} BB_{o_{x_i}} + Y_{i_v} BB_{o_{y_i}} + Z_{i_v} BB_{o_{z_i}})$$
$$+ m_{o_{\zeta_{(i-1)}}} (X_{i_v} DD_{o_{x_i}} + Y_{i_v} DD_{o_{y_i}} + Z_{i_v} DD_{o_{z_i}})$$
$$+ n_{o_{\zeta_{(i-1)}}} (X_{i_v} FF_{o_{x_i}} + Y_{i_v} FF_{o_{y_i}} + Z_{i_v} FF_{o_{z_i}})$$

Then

$$\Delta\zeta_{(i-1)_{v_i}} = AA_{o_{v_{i_\zeta}}} + BB_{o_{v_{i_\zeta}}} \Delta q_r$$

$$\Delta P_{i_{k_{\zeta_{(i-1)}}}} = \Delta P_{i_k} \left[\ell_{o_{p_{i_k}}} \ell_{o_{\zeta_{(i-1)}}} + m_{o_{p_{i_k}}} m_{o_{\zeta_{(i-1)}}} + n_{o_{p_{i_k}}} n_{o_{\zeta_{(i-1)}}} \right] + P_{i_k} \left[\ell_{o_{p_{i_k}}} \Delta\ell_{o_{\zeta_{(i-1)}}} + m_{o_{p_{i_k}}} \Delta m_{o_{\zeta_{(i-1)}}} + n_{o_{p_{i_k}}} \Delta n_{o_{\zeta_{(i-1)}}} \right]$$

The direction cosines of $\vec{P}_{i_k}$, referred to the fixed frame of reference $X_oY_oZ_o$, are assumed to be invariant.

$$AA_{o_{a_{k_\zeta}}} = \Delta\ell_{o_{\zeta_{(i-1)}}} C_{1_{a_{k_i}}} + \Delta m_{o_{\zeta_{(i-1)}}} C_{2_{a_{k_i}}} + \Delta n_{o_{\zeta_{(i-1)}}} C_{3_{a_{k_i}}} + \ell_{o_{\zeta_{(i-1)}}} C_{4_{a_{k_i}}} + m_{o_{\zeta_{(i-1)}}} C_{5_{a_{k_i}}} + n_{o_{\zeta_{(i-1)}}} C_{6_{a_{k_i}}}$$

$$BB_{o_{a_{k_\zeta}}} = \ell_{o_{\zeta_{(i-1)}}} C_{7_{a_{k_i}}} + m_{o_{\zeta_{(i-1)}}} C_{8_{a_{k_i}}} + n_{o_{\zeta_{(i-1)}}} C_{9_{a_{k_i}}}$$

where

$$C_{1_{a_{k_i}}} = X_{i_{a_k}} \ell_{o_{x_i}} + Y_{i_{a_k}} \ell_{o_{y_i}} + Z_{i_{a_k}} \ell_{o_{z_i}}$$

$$C_{2_{a_{k_i}}} = X_{i_{a_k}} m_{o_{x_i}} + Y_{i_{a_k}} m_{o_{y_i}} + Z_{i_{a_k}} m_{o_{z_i}}$$

$$C_{3_{a_{k_i}}} = X_{i_{a_k}} n_{o_{x_i}} + Y_{i_{a_k}} n_{o_{y_i}} + Z_{i_{a_k}} n_{o_{z_i}}$$

$$C_{4_{a_{k_i}}} = X_{i_{a_k}} AA_{o_{x_i}} + Y_{i_{a_k}} AA_{o_{y_i}} + Z_{i_{a_k}} AA_{o_{z_i}}$$

$$C_{5_{a_{k_i}}} = X_{i_{a_k}} CC_{o_{x_i}} + Y_{i_{a_k}} CC_{o_{y_i}} + Z_{i_{a_k}} CC_{o_{z_i}}$$

$$C_{6_{a_{k_i}}} = X_{i_{a_k}} EE_{o_{x_i}} + Y_{i_{a_k}} EE_{o_{y_i}} + Z_{i_{a_k}} EE_{o_{z_i}}$$

$$C_{7_{a_{k_i}}} = X_{i_{a_k}} BB_{o_{x_i}} + Y_{i_{a_k}} BB_{o_{y_i}} + Z_{i_{a_k}} BB_{o_{z_i}}$$

$$C_{8_{a_{k_i}}} = X_{i_{a_k}} DD_{o_{x_i}} + Y_{i_{a_k}} DD_{o_{y_i}} + Z_{i_{a_k}} DD_{o_{z_i}}$$

$$C_{9_{a_{k_i}}} = X_{i_{a_k}} FF_{o_{x_i}} + Y_{i_{a_k}} FF_{o_{y_i}} + Z_{i_{a_k}} FF_{o_{z_i}}$$

Then

$$\Delta\zeta_{(i-1)_{a_{k_i}}} = AA_{o_{a_{k_\zeta}}} + BB_{o_{a_{k_\zeta}}} \cdot \Delta q_r$$

$$AA_{o_{r_{1_\zeta}}} = \Delta\ell_{o_{\zeta_{(i-1)}}} C_{1_{r_{1_i}}} + \Delta m_{o_{\zeta_{(i-1)}}} C_{2_{r_{1_i}}} + \Delta n_{o_{\zeta_{(i-1)}}} C_{3_{r_{1_i}}} + \ell_{o_{\zeta_{(i-1)}}} C_{4_{r_{1_i}}} + m_{o_{\zeta_{(i-1)}}} C_{5_{r_{1_i}}} + n_{o_{\zeta_{(i-1)}}} C_{6_{r_{1_i}}}$$

$$BB_{o_{r_{1_\zeta}}} = \ell_{o_{\zeta_{(i-1)}}} C_{7_{r_{1_i}}} + m_{o_{\zeta_{(i-1)}}} C_{8_{r_{1_i}}} + n_{o_{\zeta_{(i-1)}}} C_{9_{r_{1_i}}}$$

where

$$C_{1_{r_{1_i}}} = X_{i_{r_{1_i}}} \ell_{o_{x_i}} + Y_{i_{r_{1_i}}} \ell_{o_{y_i}} + Z_{i_{r_{1_i}}} \ell_{o_{z_i}}$$

$$C_{2_{r_{1_i}}} = X_{i_{r_{1_i}}} m_{o_{x_i}} + Y_{i_{r_{1_i}}} m_{o_{y_i}} + Z_{i_{r_{1_i}}} m_{o_{z_i}}$$

$$C_{3_{r_{1_i}}} = X_{i_{r_{1_i}}} n_{o_{x_i}} + Y_{i_{r_{1_i}}} n_{o_{y_i}} + Z_{i_{r_{1_i}}} n_{o_{z_i}}$$

$$C_{4_{r_{1_i}}} = X_{i_{r_{1_i}}} AA_{o_{x_i}} + Y_{i_{r_{1_i}}} AA_{o_{y_i}} + Z_{i_{r_{1_i}}} AA_{o_{z_i}}$$

$$C_{5_{r_{1_i}}} = X_{i_{r_{1_i}}} CC_{o_{x_i}} + Y_{i_{r_{1_i}}} CC_{o_{y_i}} + Z_{i_{r_{1_i}}} CC_{o_{z_i}}$$

$$C_{6_{r_{1_i}}} = X_{i_{r_{1_i}}} EE_{o_{x_i}} + Y_{i_{r_{1_i}}} EE_{o_{y_i}} + Z_{i_{r_{1_i}}} EE_{o_{z_i}}$$

$$C_{7_{r_{1_i}}} = X_{i_{r_{1_i}}} BB_{o_{x_i}} + Y_{i_{r_{1_i}}} BB_{o_{y_i}} + Z_{i_{r_{1_i}}} BB_{o_{z_i}}$$

$$C_{8_{r_{1_i}}} = X_{i_{r_{1_i}}} DD_{o_{x_i}} + Y_{i_{r_{1_i}}} DD_{o_{y_i}} + Z_{i_{r_{1_i}}} DD_{o_{z_i}}$$

$$C_{9_{r_{1_i}}} = X_{i_{r_{1_i}}} FF_{o_{x_i}} + Y_{i_{r_{1_i}}} FF_{o_{y_i}} + Z_{i_{r_{1_i}}} FF_{o_{z_i}}$$

Then,

$$\Delta\zeta_{(i-1)_{r_{1_i}}} = AA_{o_{r_{1_\zeta}}} + BB_{o_{r_{1_\zeta}}} \cdot \Delta q_r$$

$$AA_{o_{R_{i_\zeta}}} = \Delta\ell_{o_{\zeta_{(i-1)}}} C_{1_{R_i}} + \Delta m_{o_{\zeta_{(i-1)}}} C_{2_{R_i}} + \Delta n_{o_{\zeta_{(i-1)}}} C_{3_{R_i}}$$

$$+ \ell_{o_{\zeta_{(i-1)}}} C_{4_{R_i}} + m_{o_{\zeta_{(i-1)}}} C_{5_{R_i}} + n_{o_{\zeta_{(i-1)}}} C_{6_{R_i}}$$

$$+ \Delta R_{1_i} C_{10_{R_{i_\zeta}}} + \Delta R_{2_i} C_{11_{R_{i_\zeta}}} + \Delta R_{3_i} C_{12_{R_{i_\zeta}}}$$

$$BB_{o_{R_{i_\zeta}}} = \ell_{o_{\zeta_{(i-1)}}} C_{7_{R_i}} + m_{o_{\zeta_{(i-1)}}} C_{8_{R_i}} + n_{o_{\zeta_{(i-1)}}} C_{9_{R_i}}$$

where

$$C_{1_{R_i}} = -R_{1_i} \ell_{o_{x_i}} - R_{2_i} \ell_{o_{y_i}} - R_{3_i} \ell_{o_{z_i}}$$

$$C_{2_{R_i}} = -R_{1_i} m_{o_{x_i}} - R_{2_i} m_{o_{y_i}} - R_{3_i} m_{o_{z_i}}$$

$$C_{3_{R_i}} = -R_{1_i} n_{o_{x_i}} - R_{2_i} n_{o_{y_i}} - R_{3_i} n_{o_{z_i}}$$

$$C_{4_{R_i}} = -R_{1_i} AA_{o_{x_i}} - R_{2_i} AA_{o_{y_i}} - R_{3_i} AA_{o_{z_i}}$$

$$C_{5_{R_i}} = -R_{1_i} CC_{o_{x_i}} - R_{2_i} CC_{o_{y_i}} - R_{3_i} CC_{o_{z_i}}$$

$$C_{6_{R_i}} = -R_{1_i} EE_{o_{x_i}} - R_{2_i} EE_{o_{y_i}} - R_{3_i} EE_{o_{z_i}}$$

$$C_{7_{R_i}} = -R_{1_i} BB_{o_{x_i}} - R_{2_i} BB_{o_{y_i}} - R_{3_i} BB_{o_{z_i}}$$

$$C_{8_{R_i}} = -R_{1_i} DD_{o_{x_i}} - R_{2_i} DD_{o_{y_i}} - R_{3_i} DD_{o_{z_i}}$$

$$C_{9_{R_i}} = -R_{1_i} FF_{o_{x_i}} - R_{2_i} FF_{o_{y_i}} - R_{3_i} FF_{o_{z_i}}$$

$$C_{10_{R_{i_\zeta}}} = -\ell_{o_{x_i}} \ell_{o_{\zeta_{(i-1)}}} - m_{o_{x_i}} m_{o_{\zeta_{(i-1)}}} - n_{o_{x_i}} n_{o_{\zeta_{(i-1)}}}$$

$$C_{11_{R_{i_\zeta}}} = -\ell_{o_{y_i}} \ell_{o_{\zeta_{(i-1)}}} - m_{o_{y_i}} m_{o_{\zeta_{(i-1)}}} - n_{o_{y_i}} n_{o_{\zeta_{(i-1)}}}$$

$$C_{12_{R_{i_\zeta}}} = -\ell_{o_{z_i}} \ell_{o_{\zeta_{(i-1)}}} - m_{o_{z_i}} m_{o_{\zeta_{(i-1)}}} - n_{o_{z_i}} n_{o_{\zeta_{(i-1)}}}$$

Then,

$$\Delta R_{i_{\zeta(i-1)}} = AA_{o_{R_{i_\zeta}}} + BB_{o_{R_{i_\zeta}}} \cdot \Delta q_r$$

$$AA_{o_{S_{i_\zeta}}} = \Delta \ell_{o_{\zeta(i-1)}} C_{1_{S_i}} + \Delta m_{o_{\zeta(i-1)}} C_{2_{S_i}} + \Delta n_{o_{\zeta(i-1)}} C_{3_{S_i}}$$
$$+ \ell_{o_{\zeta(i-1)}} C_{4_{S_i}} + m_{o_{\zeta(i-1)}} C_{5_{S_i}} + n_{o_{\zeta(i-1)}} C_{6_{S_i}}$$
$$+ \Delta S_{1_i} C_{10_{S_{i_\zeta}}} + \Delta S_{2_i} C_{11_{S_{i_\zeta}}} + \Delta S_{3_i} C_{12_{S_{i_\zeta}}}$$

$$BB_{o_{S_{i_\zeta}}} = \ell_{o_{\zeta(i-1)}} C_{7_{S_i}} + m_{o_{\zeta(i-1)}} C_{8_{S_i}} + n_{o_{\zeta(i-1)}} C_{9_{S_i}}$$

where

$$C_{1_{S_i}} = S_{1_i} \ell_{o_{x_i}} + S_{2_i} \ell_{o_{y_i}} + S_{3_i} \ell_{o_{z_i}}$$

$$C_{2_{S_i}} = S_{1_i} m_{o_{x_i}} + S_{2_i} m_{o_{y_i}} + S_{3_i} m_{o_{z_i}}$$

$$C_{3_{S_i}} = S_{1_i} n_{o_{x_i}} + S_{2_i} n_{o_{y_i}} + S_{3_i} n_{o_{z_i}}$$

$$C_{4_{S_i}} = S_{1_i} AA_{o_{x_i}} + S_{2_i} AA_{o_{y_i}} + S_{3_i} AA_{o_{z_i}}$$

$$C_{5_{S_i}} = S_{1_i} CC_{o_{x_i}} + S_{2_i} CC_{o_{y_i}} + S_{3_i} CC_{o_{z_i}}$$

$$C_{6_{S_i}} = S_{1_i} EE_{o_{x_i}} + S_{2_i} EE_{o_{y_i}} + S_{3_i} EE_{o_{z_i}}$$

$$C_{7_{S_i}} = S_{1_i} BB_{o_{x_i}} + S_{2_i} BB_{o_{y_i}} + S_{3_i} BB_{o_{z_i}}$$

$$C_{8_{S_i}} = S_{1_i} DD_{o_{x_i}} + S_{2_i} DD_{o_{y_i}} + S_{3_i} DD_{o_{z_i}}$$

$$C_{9_{S_i}} = S_{1_i} FF_{o_{x_i}} + S_{2_i} FF_{o_{y_i}} + S_{3_i} FF_{o_{z_i}}$$

$$C_{10_{S_{i_\zeta}}} = \ell_{o_{x_i}} \ell_{o_{\zeta_{(i-1)}}} + m_{o_{x_i}} m_{o_{\zeta_{(i-1)}}} + n_{o_{x_i}} n_{o_{\zeta_{(i-1)}}}$$

$$C_{11_{S_{i_\zeta}}} = \ell_{o_{y_i}} \ell_{o_{\zeta_{(i-1)}}} + m_{o_{y_i}} m_{o_{\zeta_{(i-1)}}} + n_{o_{y_i}} n_{o_{\zeta_{(i-1)}}}$$

$$C_{12_{S_{i_\zeta}}} = \ell_{o_{z_i}} \ell_{o_{\zeta_{(i-1)}}} + m_{o_{z_i}} m_{o_{\zeta_{(i-1)}}} + n_{o_{z_i}} n_{o_{\zeta_{(i-1)}}}$$

Then,

$$\Delta S_{i_{\zeta_{(i-1)}}} = AA_{o_{S_{i_\zeta}}} + BB_{o_{S_{i_\zeta}}} \cdot \Delta q_r$$

$$\Delta T_{i_{k_{\zeta_{(i-1)}}}} = \Delta T_{i_k} [\ell_{o_{T_{i_k}}} \cdot \ell_{o_{\zeta_{(i-1)}}} + m_{o_{T_{i_k}}} m_{o_{\zeta_{(i-1)}}} + n_{o_{T_{i_k}}} n_{o_{\zeta_{(i-1)}}}] + T_{i_k} [\ell_{o_{T_{i_k}}} \cdot \Delta\ell_{o_{\zeta_{(i-1)}}} + m_{o_{T_{i_k}}} \Delta m_{o_{\zeta_{(i-1)}}} + n_{o_{T_{i_k}}} \Delta n_{o_{\zeta_{(i-1)}}}]$$

The direction cosines of $\vec{T}_{i_k}$, referred to the fixed frame of reference $X_o Y_o Z_o$, are assumed to be invariant.

$$AA_{o_{R_{4_{i_\zeta}}}} = -\Delta R_{4_i} C_{1_{R_{4_i}}} - R_{4_i} (\ell_{o_{x_i}} \Delta\ell_{o_{\zeta_{(i-1)}}} + m_{o_{x_i}} \Delta m_{o_{\zeta_{(i-1)}}} + n_{o_{x_i}} \Delta n_{o_{\zeta_{(i-1)}}}) - R_{4_i} (AA_{o_{x_i}} \ell_{o_{\zeta_{(i-1)}}} + CC_{o_{x_i}} m_{o_{\zeta_{(i-1)}}} + EE_{o_{x_i}} n_{o_{\zeta_{(i-1)}}})$$

$$BB_{o_{R_{4_{i_\zeta}}}} = -R_{4_i} (BB_{o_{x_i}} \ell_{o_{\zeta_{(i-1)}}} + DD_{o_{x_i}} m_{o_{\zeta_{(i-1)}}} + FF_{o_{x_i}} n_{o_{\zeta_{(i-1)}}})$$

where

$$C1_{R4_{i_\zeta}} = \ell_{o_{x_i}} \ell_{o_{\zeta_{(i-1)}}} + m_{o_{x_i}} m_{o_{\zeta_{(i-1)}}} + n_{o_{x_i}} n_{o_{\zeta_{(i-1)}}}$$

Then,

$$\Delta R4_{i_{\zeta_{(i-1)}}} = AA_{o_{R4_{i_\zeta}}} + BB_{o_{R4_{i_\zeta}}} \cdot \Delta q_r$$

$$AA_{o_{R5_{i_\zeta}}} = -R5_i \, C1_{R5_{i_\zeta}} - R5_i (\ell_{o_{y_i}} \Delta\ell_{o_{\zeta_{(i-1)}}} + m_{o_{y_i}} \Delta m_{o_{\zeta_{(i-1)}}} + n_{o_{y_i}} \Delta n_{o_{\zeta_{(i-1)}}}) - R5_i (AA_{o_{y_i}} \ell_{o_{\zeta_{(i-1)}}} + CC_{o_{y_i}} m_{o_{\zeta_{(i-1)}}} + EE_{o_{y_i}} n_{o_{\zeta_{(i-1)}}})$$

$$BB_{o_{R5_{i_\zeta}}} = -R5_i (BB_{o_{y_i}} \ell_{o_{\zeta_{(i-1)}}} + DD_{o_{y_i}} m_{o_{\zeta_{(i-1)}}} + FF_{o_{y_i}} n_{o_{\zeta_{(i-1)}}})$$

where

$$C1_{R5_{i_\zeta}} = \ell_{o_{y_i}} \ell_{o_{\zeta_{(i-1)}}} + m_{o_{y_i}} m_{o_{\zeta_{(i-1)}}} + n_{o_{y_i}} n_{o_{\zeta_{(i-1)}}}$$

Then,

$$\Delta R5_{i_{\zeta_{(i-1)}}} = AA_{o_{R5_{i_\zeta}}} + BB_{o_{R5_{i_\zeta}}} \cdot \Delta q_r$$

$$AA_{o_{R6_{i_\zeta}}} = -R6_i \, C1_{R6_{i_\zeta}}$$

$$- R6_i \left(\ell_{o_{\zeta_i}} \Delta\ell_{o_{\zeta(i-1)}} + m_{o_{z_i}} \Delta m_{o_{\zeta(i-1)}} \right.$$

$$\left. + n_{o_{z_i}} \Delta n_{o_{\zeta(i-1)}} \right) - R6_i \left(AA_{o_{z_i}} \ell_{o_{\zeta(i-1)}} \right.$$

$$\left. + CC_{o_{z_i}} m_{o_{\zeta(i-1)}} + EE_{o_{z_i}} n_{o_{z_{\zeta(i-1)}}} \right)$$

$$BB_{o_{R6_{i_\zeta}}} = -R6_i \left(BB_{o_{z_i}} \ell_{o_{\zeta(i-1)}} + DD_{o_{z_i}} m_{o_{\zeta(i-1)}} \right.$$

$$\left. + FF_{o_{z_i}} n_{o_{\zeta(i-1)}} \right)$$

where

$$C_{o_{R6_{i_\zeta}}} = \ell_{o_{z_i}} \ell_{o_{\zeta(i-1)}} + m_{o_{z_i}} m_{o_{\zeta(i-1)}} + n_{o_{z_i}} n_{o_{\zeta(i-1)}}$$

Then,

$$\Delta R6_{i_{\zeta(i-1)}} = AA_{o_{R6_{i_\zeta}}} + BB_{o_{R6_{i_\zeta}}} \cdot \Delta q_r$$

$$AA_{o_{S4_{i_\zeta}}} = \Delta S4_i \cdot C1_{S4_i}$$

$$+ S4_i \left(\ell_{o_{x_i}} \Delta\ell_{o_{\zeta(i-1)}} + m_{o_{x_i}} \Delta m_{o_{\zeta(i-1)}} \right.$$

$$\left. + n_{o_{x_i}} \Delta n_{o_{\zeta(i-1)}} \right) + S4_i \left(AA_{o_{x_i}} \ell_{o_{\zeta(i-1)}} \right.$$

$$\left. + CC_{o_{x_i}} m_{o_{\zeta(i-1)}} + EE_{o_{x_i}} n_{o_{\zeta(i-1)}} \right)$$

$$BB_{o_{S_{4_{i_\zeta}}}} = S_{4_i}\,(BB_{o_{x_i}}\,\ell_{o_{\zeta_{(i-1)}}} + DD_{o_{x_i}}\,m_{o_{\zeta_{(i-1)}}} + FF_{o_{x_i}}\,n_{o_{\zeta_{(i-1)}}})$$

where

$$C_{1_{S_{4_{i_\zeta}}}} = \ell_{o_{x_i}}\,\ell_{o_{\zeta_{(i-1)}}} + m_{o_{x_i}}\,m_{o_{\zeta_{(i-1)}}} + n_{o_{x_i}}\,n_{o_{\zeta_{(i-1)}}}$$

Then,

$$\Delta S_{4_{i_{\zeta_{(i-1)}}}} = AA_{o_{S_{4_{i_\zeta}}}} + BB_{o_{S_{4_{i_\zeta}}}} \cdot \Delta q_r$$

$$AA_{o_{S_{5_{i_\zeta}}}} = \Delta S_{5_i}\,C_{1_{S_{5_{i_\zeta}}}} + S_{5_i}\,(\ell_{o_{y_i}}\,\Delta\ell_{o_{\zeta_{(i-1)}}} + m_{o_{y_i}}\,\Delta m_{o_{\zeta_{(i-1)}}} + n_{o_{y_i}}\,\Delta n_{o_{\zeta_{(i-1)}}}) + S_{5_i}\,(AA_{o_{y_i}}\,\ell_{o_{\zeta_{(i-1)}}} + CC_{o_{y_i}}\,m_{o_{\zeta_{(i-1)}}} + EE_{o_{y_i}}\,n_{o_{\zeta_{(i-1)}}})$$

$$BB_{o_{S_{5_{i_\zeta}}}} = S_{5_i}\,(BB_{o_{y_i}}\,\ell_{o_{\zeta_{(i-1)}}} + DD_{o_{y_i}}\,m_{o_{\zeta_{(i-1)}}} + FF_{o_{y_i}}\,n_{o_{\zeta_{(i-1)}}})$$

where

$$C_{1_{S_{5_{i_\zeta}}}} = \ell_{o_{y_i}}\,\ell_{o_{\zeta_{(i-1)}}} + m_{o_{y_i}}\,m_{o_{\zeta_{(i-1)}}} + n_{o_{y_i}}\,n_{o_{\zeta_{(i-1)}}}$$

Then,

$$\Delta S_{5_{i_{\zeta(i-1)}}} = AA_{o_{S_{5_{i_\zeta}}}} + BB_{o_{S_{5_{i_\zeta}}}} \cdot \Delta q_r$$

$$AA_{o_{S_{6_{i_\zeta}}}} = S_{6_i} \cdot C_{1_{S_{6_{i_\zeta}}}} + S_{6_i} (\ell_{o_{z_i}} \Delta\ell_{o_{\zeta(i-1)}} + m_{o_{z_i}} \Delta m_{o_{\zeta(i-1)}} + n_{o_{z_i}} \Delta n_{o_{\zeta(i-1)}}) + S_{6_i} (AA_{o_{z_i}} \ell_{o_{\zeta(i-1)}} + CC_{o_{z_i}} m_{o_{\zeta(i-1)}} + EE_{o_{z_i}} n_{o_{\zeta(i-1)}})$$

$$BB_{o_{S_{6_{i_\zeta}}}} = S_{6_i} (BB_{o_{z_i}} \ell_{o_{\zeta(i-1)}} + DD_{o_{z_i}} m_{o_{\zeta(i-1)}} + FF_{o_{z_i}} n_{o_{\zeta(i-1)}})$$

where

$$C_{1_{S_{6_{i_\zeta}}}} = \ell_{o_{z_i}} \ell_{o_{\zeta(i-1)}} + m_{o_{z_i}} m_{o_{\zeta(i-1)}} + n_{o_{z_i}} n_{o_{\zeta(i-1)}}$$

Then,

$$\Delta S_{6_{i_{\zeta(i-1)}}} = AA_{o_{S_{6_{i_\zeta}}}} + BB_{o_{S_{6_{i_\zeta}}}} \cdot \Delta q_r$$

$$AA_{o_{r_{2_{i_\zeta}}}} = \Delta\ell_{o_{\zeta(i-1)}} C_{1_{r_{2_i}}} + \Delta m_{o_{\zeta(i-1)}} C_{2_{r_{2_i}}} + \Delta n_{o_{\zeta(i-1)}} C_{3_{r_{2_i}}} + \ell_{o_{\zeta(i-1)}} C_{4_{r_{2_i}}}$$

$$+ m_{o_{\zeta_{(i-1)}}} C_{5_{r_{2_i}}} + n_{o_{\zeta_{(i-1)}}} C_{6_{r_{2_i}}}$$

$$+ \sum_k CC_{o_{r_{2_{i_\zeta}}}} \Delta q_{\tau_{i_k}}$$

$$BB_{o_{r_{2_{i_\zeta}}}} = \ell_{o_{\zeta_{(i-1)}}} C_{7_{r_{2_i}}} + m_{o_{\zeta_{(i-1)}}} C_{8_{r_{2_i}}} + n_{o_{\zeta_{(i-1)}}} C_{9_{r_{2_i}}}$$

$$CC_{o_{r_{2_{i_\zeta}}}} = C_{10_{r_{2_{i_\zeta}}}} \ell_{i_{u_{\tau_{i_k}}}} + C_{11_{r_{2_{i_\zeta}}}} m_{i_{u_{\tau_{i_k}}}} + C_{12_{r_{2_{i_\zeta}}}} n_{i_{u_{\tau_{i_k}}}}$$

where

$$C_{1_{r_{2_i}}} = X_{i_{r_{2_i}}} \ell_{o_{x_i}} + Y_{i_{r_{2_i}}} \ell_{o_{y_i}} + Z_{i_{r_{2_i}}} \ell_{o_{z_i}}$$

$$C_{2_{r_{2_i}}} = X_{i_{r_{2_i}}} m_{o_{x_i}} + Y_{i_{r_{2_i}}} m_{o_{y_i}} + Z_{i_{r_{2_i}}} m_{o_{z_i}}$$

$$C_{3_{r_{2_i}}} = X_{i_{r_{2_i}}} n_{o_{x_i}} + Y_{i_{r_{2_i}}} n_{o_{y_i}} + Z_{i_{r_{2_i}}} n_{o_{z_i}}$$

$$C_{4_{r_{2_i}}} = X_{i_{r_{2_i}}} AA_{o_{x_i}} + Y_{i_{r_{2_i}}} AA_{o_{y_i}} + Z_{i_{r_{2_i}}} AA_{o_{z_i}}$$

$$C_{5_{r_{2_i}}} = X_{i_{r_{2_i}}} CC_{o_{x_i}} + Y_{i_{r_{2_i}}} CC_{o_{y_i}} + Z_{i_{r_{2_i}}} CC_{o_{z_i}}$$

$$C_{6_{r_{2_i}}} = X_{i_{r_{2_i}}} EE_{o_{x_i}} + Y_{i_{r_{2_i}}} EE_{o_{y_i}} + Z_{i_{r_{2_i}}} EE_{o_{z_i}}$$

$$C_{7_{r_{2_i}}} = X_{i_{r_{2_i}}} BB_{o_{x_i}} + Y_{i_{r_{2_i}}} BB_{o_{y_i}} + Z_{i_{r_{2_i}}} BB_{o_{z_i}}$$

$$C_{8_{r_{2_i}}} = X_{i_{r_{2_i}}} DD_{o_{x_i}} + Y_{i_{r_{2_i}}} DD_{o_{y_i}} + Z_{i_{r_{2_i}}} DD_{o_{z_i}}$$

$$C_{9_{r_{2_i}}} = X_{i_{r_{2_i}}} FF_{o_{x_i}} + Y_{i_{r_{2_i}}} FF_{o_{y_i}} + Z_{i_{r_{2_i}}} FF_{o_{z_i}}$$

$$C_{10_{r_{2_i}}} = \ell_{o_{x_i}} \ell_{o_{\zeta_{(i-1)}}} + m_{o_{x_i}} m_{o_{\zeta_{(i-1)}}} + n_{o_{x_i}} n_{o_{\zeta_{(i-1)}}}$$

$$C_{11_{r_{2_i}}} = \ell_{o_{y_i}} \ell_{o_{\zeta_{(i-1)}}} + m_{o_{y_i}} m_{o_{\zeta_{(i-1)}}} + n_{o_{y_i}} n_{o_{\zeta_{(i-1)}}}$$

$$C_{12_{r_{2_i}}} = \ell_{o_{z_i}} \ell_{o_{\zeta_{(i-1)}}} + m_{o_{z_i}} m_{o_{\zeta_{(i-1)}}} + n_{o_{z_i}} n_{o_{\zeta_{(i-1)}}}$$

Then,

$$\Delta\zeta_{(i-1)_{r_{2_i}}} = AA_{o_{r_{2_{i_\zeta}}}} + BB_{o_{r_{2_{i_\zeta}}}} \cdot \Delta q_r$$

$$AA_{o_{r_{t_{i_\zeta}}}} = AA_{o_{r_{2_{i_\zeta}}}} - \Delta\zeta_{(i-1)_{r_{1_{(i+1)}}}} + \Delta\zeta_{(i-1)_{v_{(i+1)}}}$$

$$BB_{o_{r_{t_{i_\zeta}}}} = BB_{o_{r_{2_{i_\zeta}}}}$$

where

$$\Delta\zeta_{(i-1)_{r_{1_{(i+1)}}}} = \Delta\ell_{o_{\zeta_{(i-1)}}} C_{1_{r_{1_{(i+1)}}}} + \Delta m_{o_{\zeta_{(i-1)}}} C_{2_{r_{1_{(i+1)}}}} + \Delta n_{o_{\zeta_{(i-1)}}} C_{3_{r_{1_{(i+1)}}}} + \ell_{o_{\zeta_{(i-1)}}} C_{4_{r_{1_{(i+1)}}}} + m_{o_{\zeta_{(i-1)}}} C_{5_{r_{1_{(i+1)}}}} + n_{o_{\zeta_{(i-1)}}} C_{6_{r_{1_{(i+1)}}}}$$

$$\Delta\zeta_{(i-1)_{v_{(i+1)}}} = \Delta\ell_{o_{\zeta_{(i-1)}}} C_{1_{v_{(i+1)}}} + \Delta m_{o_{\zeta_{(i-1)}}} C_{2_{v_{(i+1)}}}$$

$$+ \Delta n_{o_{\zeta_{(i-1)}}} C_{3_{v_{(i+1)}}} + \ell_{o_{\zeta_{(i-1)}}} C_{4_{v_{(i+1)}}}$$

$$+ m_{o_{\zeta_{(i-1)}}} C_{5_{v_{(i+1)}}} + n_{o_{\zeta_{(i-1)}}} C_{6_{v_{(i+1)}}}$$

The dummy variable ζ in all the above equations can be successively replaced by X, Y, and Z to obtain the X, Y, and Z components, respectively.

VITA

Avinash Gajanan Patwardhan

Candidate for the Degree of

Doctor of Philosophy

Thesis: KINEMATIC ANALYSIS AND SIMULATION STUDIES OF INTERVERTEBRAL MOTION

Major Field: Mechanical Engineering

Biographical:

Personal Data: Born in Nagpur, India, on May 3, 1951, the son of Mr. and Mrs. G. K. Patwardhan; married to Vandana Kesheo on July 31, 1978, the father of Jennifer Patwardhan.

Education: Graduated from Government Multipurpose Higher Secondary School, Nagpur, India, in April, 1967; received the Bachelor of Engineering (Mechanical) degree from Nagpur University, Nagpur, India, in 1972; received the Master of Engineering (Mechanical) degree from the Indian Institute of Science, Bangalore, India, in 1974; completed requirements for the Doctor of Philosophy degree in May, 1980, at Oklahoma State University, Stillwater, Oklahoma.

Professional Experience: Graduate research and teaching assistant, School of Mechanical and Aerospace Engineering, Oklahoma State University, August, 1974, to present.